

AD-A114 735

GEORGIA INST OF TECH. ATLANTA
DYNAMIC STABILITY OF STRUCTURES:
FEB 82 6 J SIMITSES, I SHEINMAN

APPLICATION TO FRAMES, CYLINDR--ETC(U)
F33615-79-C-3221
AFWAL-TR-81-3155

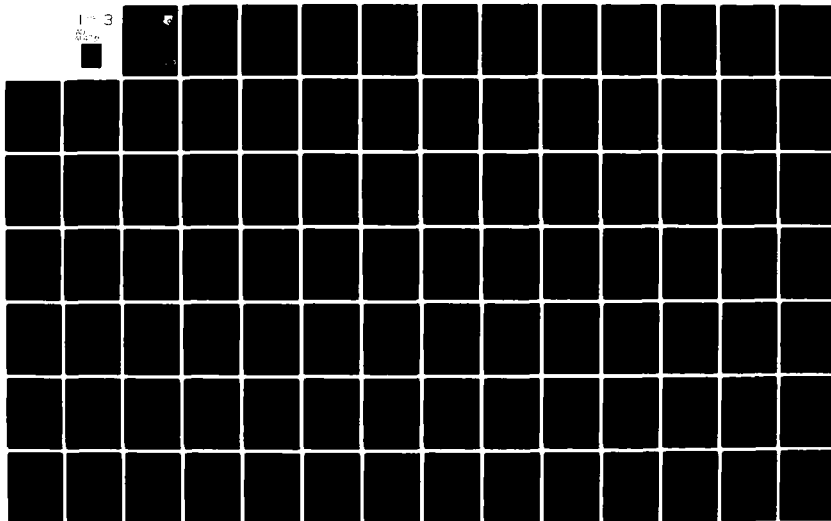
F/6 20/11

NL

UNCLASSIFIED

1-3

02-0



AFWAL-TR-81-3155

DYNAMIC STABILITY OF STRUCTURES: APPLICATION
TO FRAMES, CYLINDRICAL SHELLS AND OTHER SYSTEMS

GEORGE J. SIMITSES
IZHAK SHEINMAN

GEORGIA INSTITUTE OF TECHNOLOGY
ATLANTA, GEORGIA 30332

FEBRUARY 1982

TECHNICAL REPORT AFWAL-TR-81-3155
Final Report for Period May 1980 - April 1981

Approved for public release; distribution unlimited.

Copy available to DTIC does not
permit fully legible reproduction

FLIGHT DYNAMICS LABORATORY
AIR FORCE WRIGHT AERONAUTICAL LABORATORIES
AIR FORCE SYSTEMS COMMAND
WRIGHT-PATTERSON AIR FORCE BASE, OHIO 45433

DTIC
ELECTE
MAY 24 1982
A

DTIC FILE COPY

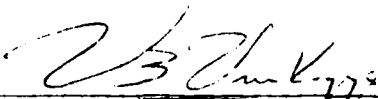
82 05 24 117

NOTICE

When Government drawings, specifications, or other data are used for any purpose other than in connection with a definitely related Government procurement operation, the United States Government thereby incurs no responsibility nor any obligation whatsoever; and the fact that the government may have formulated, furnished, or in any way supplied the said drawings, specifications, or other data, is not to be regarded by implication or otherwise as in any manner licensing the holder or any other person or corporation, or conveying any rights or permission to manufacture use, or sell any patented invention that may in any way be related thereto.


This report has been reviewed by the Office of Public Affairs (ASD/PA) and is releasable to the National Technical Information Service (NTIS). At NTIS, it will be available to the general public, including foreign nations.

This technical report has been reviewed and is approved for publication.


VIPPERLA B. VENKAYYA
Project Engineer


FREDERICK A. PICCHIONI, Lt Col, USAF
Chief, Analysis & Optimization Branch

FOR THE COMMANDER


RALPH L. KUSTER, JR., Col, USAF
Chief, Structures & Dynamics Div.

If your address has changed, if you wish to be removed from our mailing list, or if the addressee is no longer employed by your organization please notify AFWAL/FIBR, W-PAFB, OH 45433 to help us maintain a current mailing list.

Copies of this report should not be returned unless return is required by security considerations, contractual obligations, or notice on a specific document.

DISCLAIMER NOTICE

**THIS DOCUMENT IS BEST QUALITY
PRACTICABLE. THE COPY FURNISHED
TO DTIC CONTAINED A SIGNIFICANT
NUMBER OF PAGES WHICH DO NOT
REPRODUCE LEGIBLY.**

UNCLASSIFIED

SECURITY CLASSIFICATION OF THIS PAGE (When Data Entered)

REPORT DOCUMENTATION PAGE		READ INSTRUCTIONS BEFORE COMPLETING FORM
1. REPORT NUMBER AFWAL-TR-81-3155	2. GOVT ACCESSION NO. AD-A114 735	3. RECIPIENT'S CATALOG NUMBER
4. TITLE (and Subtitle) DYNAMIC STABILITY OF STRUCTURES: APPLICATION TO FRAMES, CYLINDRICAL SHELLS AND OTHER SYSTEMS		5. TYPE OF REPORT & PERIOD COVERED Final Report May 1980 - April 1981
		6. PERFORMING ORG. REPORT NUMBER
7. AUTHOR(s) George J. Simitzes Izhak Sheinman		8. CONTRACT OR GRANT NUMBER(s) F33615-79-C-3221
9. PERFORMING ORGANIZATION NAME AND ADDRESS Georgia Institute of Technology Atlanta, Georgia 30332		10. PROGRAM ELEMENT, PROJECT, TASK AREA & WORK UNIT NUMBERS P.E. 62201F Proj. 2401, Task 240102 Work Unit 24010228
11. CONTROLLING OFFICE NAME AND ADDRESS Flight Dynamics Laboratory (AFWAL/FIBRA) Air Force Wright Aeronautical Laboratories (AFSC) Wright-Patterson AFB, Ohio 45433		12. REPORT DATE February 1982
		13. NUMBER OF PAGES 197
14. MONITORING AGENCY NAME & ADDRESS (if different from Controlling Office)		15. SECURITY CLASS. (of this report) UNCLASSIFIED
		15a. DECLASSIFICATION/DOWNGRADING SCHEDULE
16. DISTRIBUTION STATEMENT (of this Report) Approved for public release; distribution unlimited.		
17. DISTRIBUTION STATEMENT (of the abstract entered in Block 20, if different from Report)		
18. SUPPLEMENTARY NOTES		
19. KEY WORDS (Continue on reverse side if necessary and identify by block number) Dynamic Stability Cylindrical Shells Frames Imperfection Sensitivity Arches		
20. ABSTRACT (Continue on reverse side if necessary and identify by block number) This report deals primarily with extension of the energy-based concepts of dynamic stability, developed earlier for finite-degree-of-freedom systems, to continuous systems. Moreover, the related criteria for dynamic stability are demonstrated through several structural configurations, such as eccentrically loaded simple two-bar frames, geometrically imperfect, thin, cylindrical shells (of stiffened and unstiffened construction) and subjected to uniform axial compression and lateral pressure, and a pinnted, half-sine, shallow arch (CONTINUED ON REVERSE SIDE)		

DD FORM 1 JAN 73 1473

EDITION OF 1 NOV 65 IS OBSOLETE

UNCLASSIFIED

SECURITY CLASSIFICATION OF THIS PAGE (When Data Entered)

UNCLASSIFIED

SECURITY CLASSIFICATION OF THIS PAGE(When Data Entered)

Block 20 (Continued)

loaded transversely. All of these systems are subject to violent buckling under static application of the loads. Moreover, the developed concepts are extended, so as to apply to structural systems, which are either subject to smooth buckling or are not subject to buckling at all under static loading. This extension is clearly demonstrated through several simple examples. Through this extension it is shown that, in a general sense for systems loaded by sudden loads, there is no question of dynamic stability or instability, but only a question of dynamic response in a deflectional space with imposed limitation on the size of the allowable deflections. Finally, in the case of the imperfect cylindrical shell, in order to find critical dynamic conditions, it was necessary to develop a solution scheme that describes completely the behavior of the shell under static loading (including post-limit point behavior). The solution scheme and the related computer program are fully explained.

UNCLASSIFIED

SECURITY CLASSIFICATION OF THIS PAGE(When Data Entered)

FOREWORD

This report was prepared by Professor George J. Simitzes and Dr. Izhak Sheinman, both of the school of Engineering Science and Mechanics at the Georgia Institute of Technology, Atlanta, Georgia. Dr. Sheinman is a visiting scholar, on leave from the Department of Civil Engineering of the Technion-Israel Institute of Technology, Haifa, Israel. This work was performed under Contract No. F33615-79-C-3221 with the U.S.A.F. Aeronautical Systems Division (AFSC), Wright-Patterson Air Force Base, Ohio 45433. This final technical report was released by the authors in June 1981. The report covers work conducted under contract, from May 1980 through April 1981 (end of contract period).



Accession For	
DTIC	<input checked="" type="checkbox"/>
DTIC	<input type="checkbox"/>
Unannounced	<input type="checkbox"/>
Justification	
By	
Distribution/	
Availability Codes	
Dist	Avail and/or Special
A23 9	

TABLE OF CONTENTS

SECTION	PAGE
I. INTRODUCTION	1
II. SIMPLE TWO-BAR FRAMES UNDER SUDDENLY APPLIED LOADS.	7
III. STIFFENED AND UNSTIFFENED, IMPERFECT CYLINDRICAL SHELLS UNDER SUDDENLY APPLIED LOADS.	27
The stability criterion	27
The static solution	29
(i) Solution Methodology	41
(ii) Numerical Results and Discussion	54
The critical conditions for sudden application of the loads	83
IV. THE PINNED HALF-SINE LOW ARCH	90
Geometry and Governing Equations	90
Critical Dynamic Conditions	93
Effect of Static Preloading	96
Effect of Small Damping	111
V. OTHER SYSTEMS	117
The mass-spring system	117
Suddenly-loaded beams	128
The imperfect column	130
APPENDIX A FLOW CHART	141
APPENDIX B COMPUTER PROGRAM	157
REFERENCES	191

SECTION I

INTRODUCTION

This report, in essence, is a continuation of Ref. 1. In this reference, the concept of dynamic stability for suddenly loaded systems was discussed in detail, including criteria and estimates, on the basis of the energy approach. Moreover, they were demonstrated through simple mechanical models, with finite-degrees-of-freedom. These models are characteristic of imperfection sensitive systems, and under static conditions they are subject to either limit-point instability or unstable bifurcational instability (in both cases, violent buckling). The suddenly applied loads are of constant magnitude and, in general, of finite duration. The extreme cases of ideal impulse and constant load of infinite duration were discussed and presented separately, as well, for two reasons: (a) the concepts for these two cases are simpler to present and (b) historically these extreme cases were treated extensively by the initial investigators of dynamic stability of suddenly-loaded structures [2-13]. The methodologies employed by these investigators can be classified into three groups: (i) equations of motion approach (Budiansky-Roth [3]), (ii) the phase plane-total energy approach (Hsu [6]), and (iii) the potential energy approach (Hoff-Simitses [2,11]).

The first approach (a) has had wide acceptance, because it is well suited for computer-type solutions. The equations of motion are solved for various levels of the load parameter. For small levels, the solution is simply oscillatory; as the load level increases, the motion changes to distinctly large amplitude (from the initial undisturbed position) oscillations. The load level at which this change occurs is termed

critical dynamic load. A great advantage of this approach is that it can estimate the critical conditions accurately, and the loading can be, in general, time-dependent. Of course, the obvious disadvantage is that it is extremely difficult and it requires a large amount of computer time to solve the equations of motion for various levels of the applied load (constant or infinite duration). The difficulty and the required time further increase as the load becomes time-dependent.

The other two approaches can estimate conditions under which the motion will remain oscillatory about the near static equilibrium position (lower bound on critical suddenly applied load) or conditions under which the motion will definitely be of large amplitude (upper bound). Hsu termed the former a sufficiency condition for stability and the latter a sufficiency condition for instability. Simitses referred to these two bounds as critical loads and he termed the former minimum possible critical load (MPCL) and the latter minimum guaranteed critical load (MGCL). In many cases considered, the static critical load is coincident with the upper bound. Needless to say, that the emphasis of approaches (b) and (c) is to estimate the lower bound and use this as a basis for design (whenever applicable).

This report deals primarily with extension of the energy concepts discussed in Ref. 1, and application of the related criteria to a number of practical structural configurations, such as frames, imperfect cylindrical shells (of stiffened and unstiffened construction) and shallow arches. These systems also are subject to violent buckling under static application of the loads.

Moreover, in the last chapter of the present report, the developed concepts are applied to structural systems which are not subject to

violent buckling under quasistatic application of the loads. The ensuing discussion provides the necessary clarifications.

All structural configurations, when acted upon by quasi-static loads, respond in a manner described in one of the five figures, Figs. 1.1 - 1.5. These figures characterize equilibrium positions (structural response) as plots of a load parameter, P , versus some characteristic displacement, θ . The solid curves denote the response of systems which are free of imperfections and the dashed-line curves denote the response of the corresponding imperfect configuration.

Fig. 1.1 shows the response of such structural elements as columns, plates, and unbraced portal frames. The perfect configuration is subject to bifurcational buckling, while the imperfect configuration is characterized by stable equilibrium (unique), for elastic material behavior.

Fig. 1.2 typifies the response of some simple trusses and two-bar frames. The perfect configuration is subject to bifurcational buckling, but smooth (stable branch) in one direction of the response and violent (unstable branch) in the other. Correspondingly the response of the imperfect configuration is characterized by stable equilibrium (and unique) for increasing load in one direction, while in the other, the system is subject to limit point instability.

Fig. 1.3 typifies the response of troublesome structural configurations such as cylindrical shells (especially under uniform axial compression and of isotropic construction), pressure-loaded spherical shells and some simple two-bar frames. These systems are imperfection-sensitive systems and are subject to violent buckling under static loading.

A large class of structural elements is subject to limit point instability. In some cases, unstable bifurcation is present in addition

to the limit point. The response of such systems is shown on Fig. 1.4.

Two structural elements that behave in this manner are the shallow spherical cap and the low arch. Both elements have been used extensively.

Finally, there is a very large class of structural elements, which are always in stable equilibrium for elastic behavior and for all levels of the applied loads. These systems are not subject to instability under static conditions. Typical members of this class are beams, and transversely loaded plates. For this class of structural elements, Fig. 1.5 shows a typical load-displacement curve.

The concept of dynamic stability as developed in Ref. 1 and as discussed in Refs. 3 and 6, was always with reference to systems which under static loading are subject to violent buckling. This implies that dynamic buckling has been discussed for systems with static behavior shown in Figs. 1.2 (to the left), 1.3 and 1.4.

In developing concepts and the related criteria and estimates for dynamic buckling (see Ref. 1), it was observed that, even for systems which are subject to violent (static) buckling, critical dynamic loads can be associated with limitations in deflectional response rather than escaping motion through a static unstable point. This is especially applicable to the design of structural members and configurations, which are deflection limited. From this point of view then, the concept of dynamic stability can be extended to all structural systems especially those of Figs. 1.1 (imperfect), 1.2 (imperfect and to the right), and 1.5. Note that from this point of view there is no question of dynamic instability, but strictly a question of dynamic response in a limited deflection space.

This extension of the concept will be amplified in Section 5. The examples and applications chosen clarify the extension. Moreover, the

problem of a suddenly loaded imperfect column is presented, primarily because it represents the only system, other than those which are subject to violent (static) buckling, which has received some attention in the open literature.

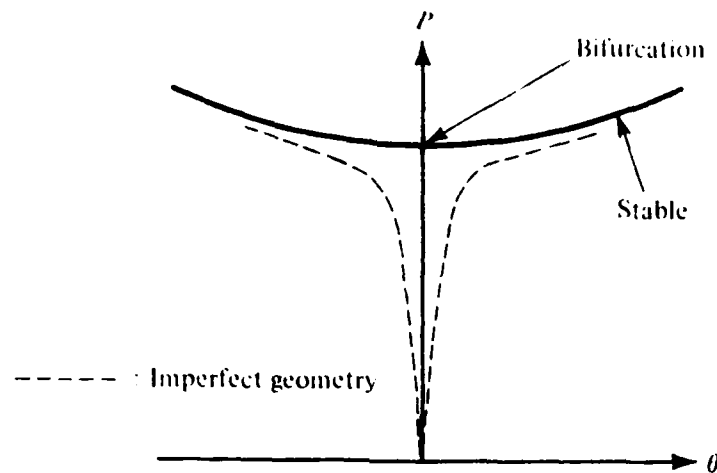


Fig. 1.1. Bifurcated Equilibrium Paths with Stable Branching.

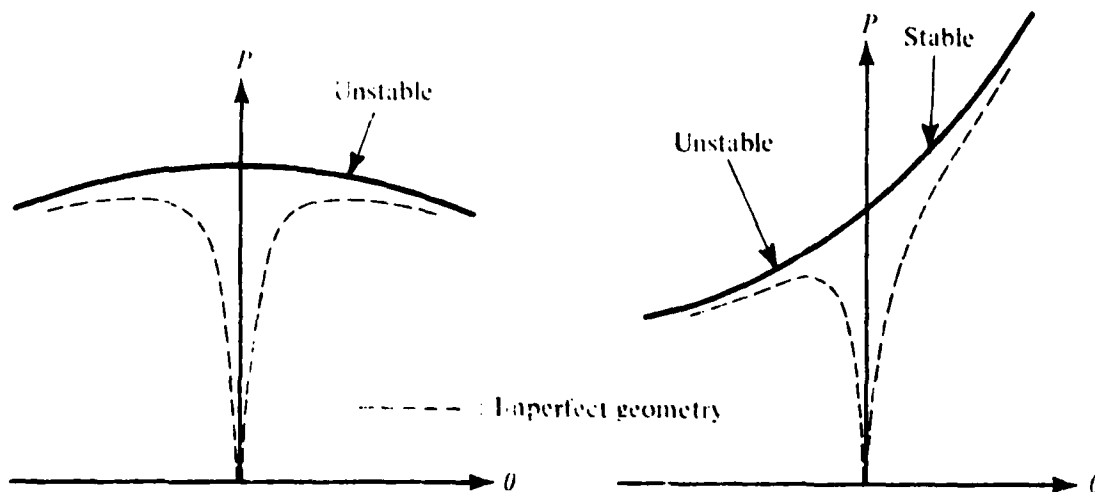


Fig. 1.3. Bifurcated Equilibrium Paths with Unstable Branching.

Fig. 1.2. Bifurcated Equilibrium Paths with Stable and Unstable Branches.

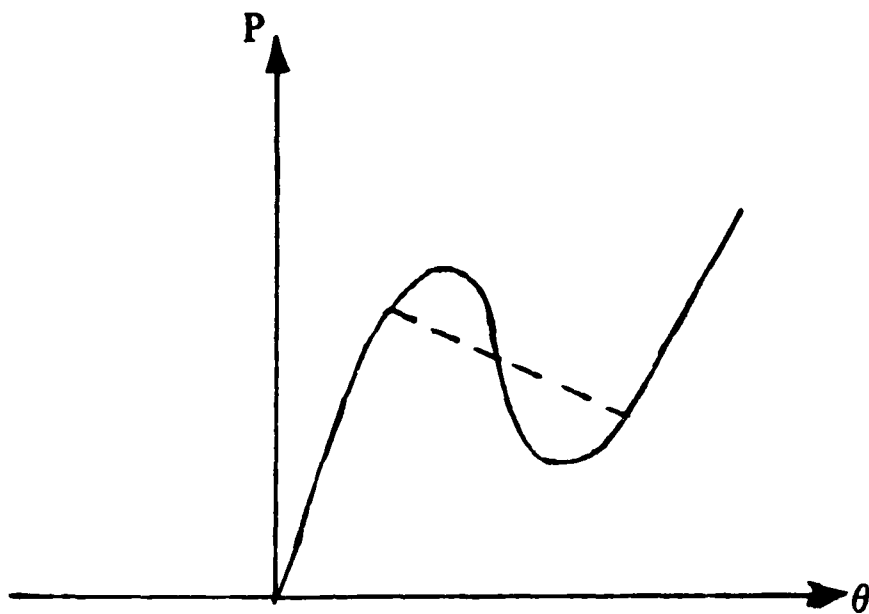


Fig. 1.4. Snap-through Buckling Paths
(Through Limit Point or Unstable Branching).

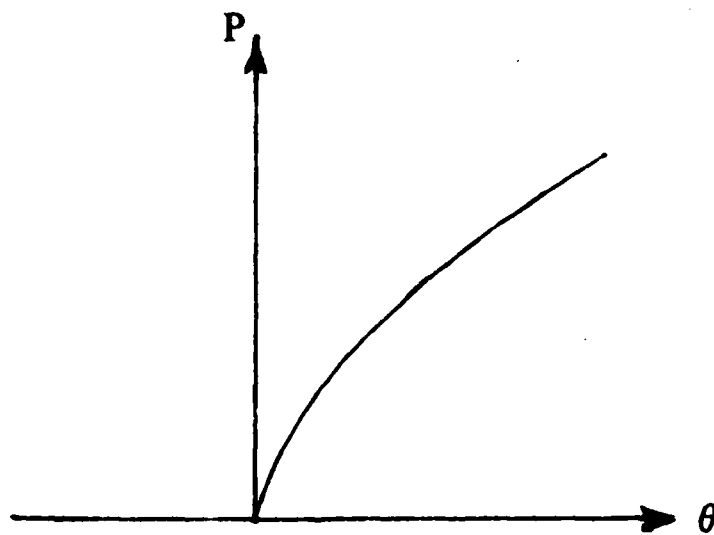


Fig. 1.5. Unique Stable Equilibrium Path.

SECTION II

SIMPLE TWO-BAR FRAMES UNDER SUDDENLY APPLIED LOADS

The Stability Criterion

Consider the simple two-bar frame shown of Fig. 2.1. The two bars are of the same structural geometry (length ℓ , corss-sectional area A , second moment of area I , and Young's modulus E). The vertical bar is supported by an immovable hinge, while the horizontal bar is supported by a hinge with three variations: (a) immovable (Model A), (b) movable in a vertical direction (Model B), and (c) movable in a horizontal direction (Model C). The external load, $P(t) = H(t)P$ [$H(t)$ is the heaviside function], is applied vertically with an eccentricity e , and it represents a constant force, P , suddenly applied, with infinite duration. The transverse and axial displacement components are $w_1(x,t)$ and $\xi(x,t)$, respectively.

By employing Hamilton's principle, one can obtain the equations of motion for the system.

$$\delta \int_{t_1}^{t_2} (T - U_T) dt = 0 \quad (2.1)$$

where the functionals U_T (total potential) and T (kinetic energy) are given by

$$U_T [\xi_1, w_1; P] = \frac{1}{2} \sum_{i=1}^2 \int_0^\ell \left[AE \left(\xi_{i,x} + \frac{1}{2} w_{i,x}^2 \right)^2 + EI w_{i,xx}^2 \right] dx \\ + H(t) [P \xi_1(\ell) + Pe w_{2,x}(\ell)] \quad (2.2)$$

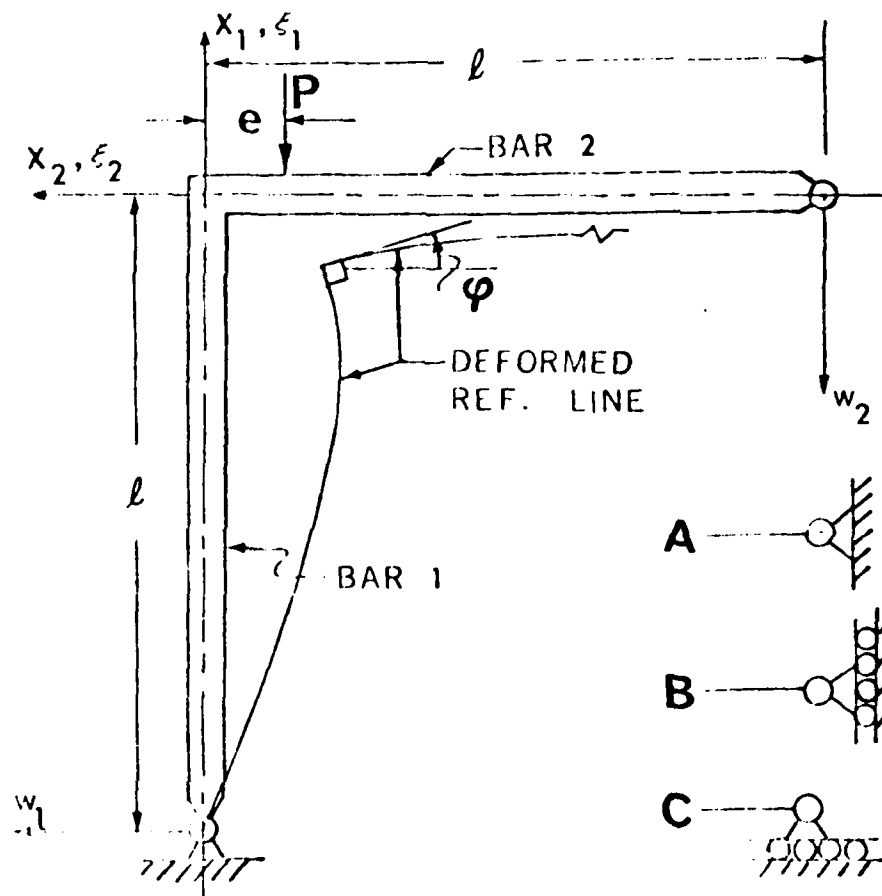


Fig. 2.1 Geometry and Sign Convention of a Two-Bar Frame

$$T[\xi_i, w_i; P] = \frac{1}{2} \sum_{i=1}^2 \int_0^l m (w_{i,t}^2 + \xi_{i,t}^2) dx \quad (2.3)$$

where the indices denote partial derivatives and m is the mass per unit length, the same for both bars. The equations of motion are:

$$EA \left(\xi_{i,x} + \frac{1}{2} w_{i,x}^2 \right)_{,x} - m \xi_{i,tt} = 0$$

$$EI w_{i,xxxx} - EA \left[\left(\xi_{i,x} + \frac{1}{2} w_{i,x}^2 \right) w_{i,x} \right]_{,x} + m w_{i,tt} = 0, \quad i = 1, 2 \quad (2.4)$$

The kinematic continuity conditions at the joint are

$$\begin{aligned} w_1(l,t) &= \xi_2(l,t); \quad w_2(l,t) = -\xi_1(l,t); \\ w_{1,x}(l,t) &= w_{2,x}(l,t) \end{aligned} \quad (2.5)$$

The natural boundary conditions at the joint are obtained from the variational problem and by employing Eqs. (2.5), which are independent of this formulation. These natural boundary (force) conditions are:

$$\begin{aligned} AE \left[\xi_{1,x}(l,t) + \frac{1}{2} w_{1,x}^2(l,t) \right] + EI w_{2,xxx}(l,t) - AE \left[\xi_{2,x}(l,t) \right. \\ \left. + \frac{1}{2} w_{2,x}^2(l,t) \right] w_{2,x}(l,t) + PH(t) = 0 \\ AE \left[\xi_{1,x}(l,t) + \frac{1}{2} w_{1,x}^2(l,t) \right] w_{1,x}(l,t) - EI w_{1,xxx}(l,t) + AE \left[\xi_{2,x}(l,t) \right. \\ \left. + \frac{1}{2} w_{2,x}^2(l,t) \right] = 0 \end{aligned} \quad (2.6)$$

$$EI [w_{1,xx}(l,t) + w_{2,xx}(l,t)] + H(t) Pe = 0$$

Finally, the support conditions for the three models (A,B and C) are listed below, as common to both models and those, which are different

Common

$$\xi_1(0,t) = w_1(0,t) = w_{1,xx}(0,t) = w_{2,xx}(0,t) = 0 \quad (2.7)$$

Model A

$$\xi_2(0,t) = 0, \quad w_2(0,t) = 0 \quad (2.8)$$

Model B

$$\xi_2(0,t) = 0, \quad EI w_{2,xxx}(0,t) - AE \left[\xi_{2,x}(0,t) + \frac{1}{2} w_{2,x}^2(0,t) \right] = 0 \quad (2.9)$$

Model C

$$w_2(0,t) = \xi_{2,x}(0,t) + \frac{1}{2} w_{2,x}^2(0,t) = 0 \quad (2.10)$$

The initial conditions must reflect the fact that, the system is at rest initially ($t = 0$).

$$\xi_i(x,0) = w_i(x,0) = 0 \quad (2.11)$$

$$\xi_{i,t}(x,0) = w_{i,t}(x,0) = 0 \quad i = 1,2$$

The solution of the equations of motion, Eqs. (2.4), a system of coupled nonlinear partial differential equations, subject to the auxiliary, Eqs. (2.5) - (2.7) and (2.8), or (2.9), or (2.10), and initial conditions, Eqs. (2.11), is, at best, extremely difficult. Furthermore, even if the solution is possible, for various magnitudes of the applied force, P , of the eccentricity, e , and slenderness ratio, λ , a criterion for stability is still missing. One possibility, here, is to employ the criterion of Budiansky and Roth [3], which, in this particular case, requires a wise choice for a characteristic displacement response. Another possibility, of course, is to employ this criterion in conjunction with an approximate solution obtained on the basis of either direct variational methods or methods of weighted residuals [14]. In this latter approach, there is an uncertainty with both the direction and the estimation of the error involved in the approximation.

In the light of the above difficulties, a simpler approach, giving accurate results for design purposes, is needed. The analysis, described and employed herein, provides an extension of the energy approach as developed in Ref. 1. This extension is described in the ensuing paragraphs and, in so doing, criteria and estimates are clearly established.

First, by virtue of the initial conditions, Eqs. (2.11), both the kinetic energy, T , and the total potential, U_T , are zero at $t = 0$. From the law of conservation of energy, for this undamped conservative system, initially stress free, the total energy (Hamiltonian) is constant for $t > 0$.

$$U_T[\xi_i, w_i; P] + T[\xi_i, w_i]_{,x} = C \quad (2.12)$$

where U_T and T are given by Eqs. (2.2) and (2.3), respectively, and C is a known constant (this constant can be made zero by properly defining U_T).

Since T is positive definite, Eq. (2.3), for all kinematically admissible trajectories, then motion is possible only when U_T is non-positive, or

$$U_T[\xi_i, w_i; P] \leq 0 \quad (2.13)$$

Next, let us assume that, at some level of the applied load $P = \bar{P}$, the ensuing motion is bounded, for all kinematically admissible trajectories. Then, for each possible trajectory, regardless of whether it corresponds to a true trajectory of motion or not, there is a set of displacement functions of position $[\xi_i^*(x), w_i^*(x)]$, $i = 1, 2$ (because of

bounded motion) such that

$$U_T [\xi_i, w_i ; \bar{P}] = 0 \quad (2.14)$$

The collection of all such sets, corresponding to all conceivable, kinematically admissible trajectories, forms a boundary, which is characterized by $U_T = 0$ and it separates the region of $U_T < 0$ from the region of $U_T > 0$. This boundary is dependent upon the level of the applied load, \bar{P} . Because of Eq. (2.13), it has been established that motion can only take place in the region characterized by $U_T < 0$. At this point, note that, regardless of the trajectory, the velocities $(\xi_{i,t}, w_{i,t})$ are zero and a change in the motion takes place, whenever the system reaches the boundary described above. Furthermore, the region characterized by $U_T < 0$ must contain at least one relative minimum point for U_T , regardless of trajectory and time. It may contain more than one relative minimum and some other stationary points. These stationary points are characterized by sets of displacement magnitudes and shapes, which, by definition, correspond to static equilibrium positions for the particular value of the applied load, P .

By having set, thusly, the stage, we can now define "unbuckled" motion (see also [1]). If the bounded region ($U_T < 0$) contains only one stationary point (a minimum) then the motion for this \bar{P} is called "unbuckled". The physical interpretation of "unbuckled" motion corresponds to the system performing nonlinear oscillations about the corresponding near stable static equilibrium position. This is exactly the case for small levels of the suddenly applied load. The only way the motion can become "buckled" (unbounded in the sense described above) is if the

boundary characterized by the set of $[\xi_1^*(x), w_1^*(x)]$ contains an unstable static equilibrium position for the corresponding value of the applied load. This value of the load represents an upper bound of all loads for which the motion remains "unbuckled", and it is called, herein, critical dynamic load. Incidentally, this level of the load corresponds to Hsu's sufficiency condition for stability and Simitses' minimum possible critical load (MPCL). Note that when damping is present, for loads smaller than this critical dynamic load, the system is asymptotically stable, because it will eventually come to rest at the near static equilibrium position.

For the frame problems, under consideration, one needs only solve the corresponding static problem and compute the value of the total potential U_T , at every static unstable equilibrium point. This static solution is outlined below and it is given in detail in [15, 16]. By dropping the inertia terms, the equations of motion, Eqs. (2.4), become static equilibrium equations. The general solutions, obtained from these equations, for the four displacement components, w_i, ξ_i ($i = 1, 2$), are computed in terms of simple spatial functions and twelve constants. Use of the three kinematic continuity conditions Eqs. (2.5), the three natural boundary conditions at the joint, Eqs. (2.6) and the six support conditions, Eqs. (2.7) - (2.11), yields a system of twelve equations in the twelve constants. The load parameter, the eccentricity and the slenderness ratio appear also in these equations. Some of these constants are zero and the remaining ones, except for two, appear in a linear sense. Elimination of these particular constants finally yields a system of, at most, two non-linear equations that relate two constants to the

given parameters. A methodology is outlined in [15] for solving these two nonlinear equations.

It should be mentioned here that the two constants appearing in the nonlinear equations are measures of the axial force in the two bars (k_i) [the complete solutions are given in the next section]. The given parameters are listed below in nondimensionalized form

$$\beta^2 = \frac{P\ell^2}{EI}; \quad \bar{e} = \frac{e}{\ell}; \quad \lambda = \frac{\ell}{\rho} \quad (2.15)$$

where $\rho^2 = I/A$.

Thus, the total potential, U_T , for the static problem may be expressed solely in terms of k_i , β^2 , \bar{e} and λ , i.e.

$$U_T = U_T(k_i, \beta^2, e, \lambda) \quad (2.16)$$

For any given geometry (e, λ), static equilibrium positions are shown as plots of load parameter, β^2 , versus joint rotations (characteristic displacement - see Fig. 2,2). At every point of this curve, the value of the total potential is computed. The value of β^2 at which U_T changes from negative to positive corresponds to the dynamic critical load, $\beta_{cr_D}^2$. Another possible procedure for finding $\beta_{cr_D}^2$ is the simultaneous solution of the two nonlinear equilibrium equations

$$\frac{\partial U_T}{\partial k_i} = 0, \quad k_i = 1, 2 \quad (2.17)$$

and

$$U_T = 0 \quad (2.18)$$

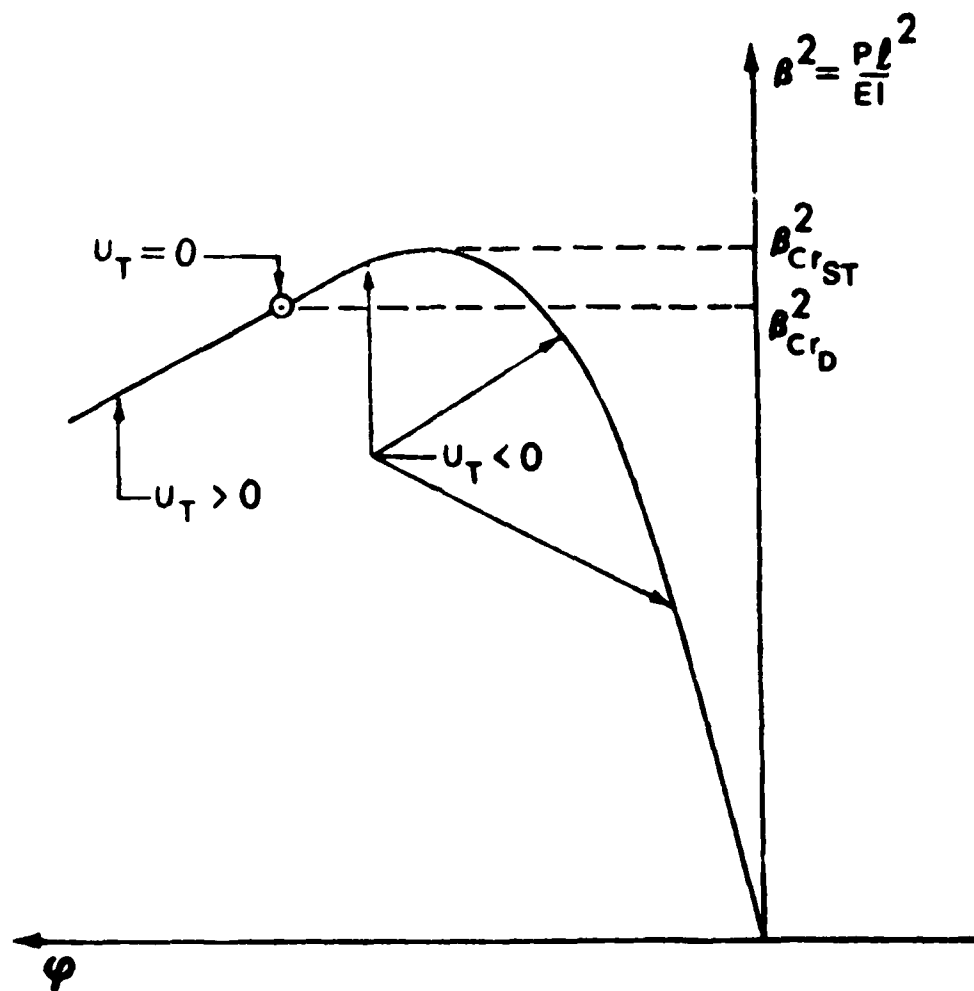


Fig. 2.2. Typical Load versus Characteristic Displacement (Joint Rotation) Curve.

subject to the condition that the static equilibrium position, at which $U_T = 0$, is unstable, or

$$\frac{\partial^2 U_T}{\partial k_i^2} \not> 0 \quad i = 1, 2 \quad (2.19)$$

$$\left(\frac{\partial^2 U_T}{\partial k_1^2} \right) \left(\frac{\partial^2 U_T}{\partial k_2^2} \right) \not> \left(\frac{\partial^2 U_T}{\partial k_1 \partial k_2} \right)^2$$

Note that Eqs. (2.19) imply that, the conditions for static stability are violated.

This alternate procedure needs special attention, because it can easily yield physically unacceptable solutions. These unacceptable solutions arise from the nonlinearity of the problem and do not belong on the load-displacement curve shown on Fig. 2.2 (physically unacceptable).

The numerical results, presented herein, are obtained from the first solution, although the alternate solution was employed for spot checking. Data are generated on the Georgia Tech high speed digital computer CDC-Cyber-70, Model 74-28.

Summary of Static Solution Expressions

In addition to the nondimensionalized parameters given by Eqs. (2.15), the following nondimensionalized parameters are also introduced.

$$X = x/l; \quad w_i = w_i/l; \quad \Xi_i = \xi_i/l$$

$$k_i^2 = \frac{S_i l^2}{EI} \quad i = 1, 2 \quad (2.20)$$

where S_i is the magnitude of the compressive force in the i th bar.

With these parameters the solution to the corresponding static problem and the expression for U_T are given below for each model separately.

Model A

$$\Xi_1(X) = - \frac{k_1^2}{\lambda^2} X - B_1(X)$$

$$W_1(X) = A_{11} \sin k_1 X + A_{13} X \quad (2.21)$$

$$\Xi_2(X) = - \frac{k_2^2}{\lambda^2} X - B_2(X)$$

$$W_2(X) = A_{21} \sin k_2 X + A_{23} X$$

where

$$B_1(X) = \frac{1}{2} \left[A_{13}^2 X + 2A_{11}A_{13} \sin k_1 X + \frac{k_1^2 A_{11}^2}{2} \left(X + \frac{\sin 2k_1 X}{2k_1} \right) \right]$$

$$B_2(X) = \frac{1}{2} \left[A_{23}^2 X + 2A_{21}A_{23} \sin k_2 X + \frac{k_2^2 A_{21}^2}{2} \left(X + \frac{\sin 2k_2 X}{2k_2} \right) \right] \quad (2.22)$$

$$A_{11} = \frac{\beta^2 \bar{e} k_2 \cos k_2 + (k_1^4 + k_2^4 - k_1^2 \beta^2) \sin k_2 / k_1^2}{k_1 k_2 (k_1 \sin k_1 \cos k_2 + k_2 \cos k_1 \sin k_2)} ;$$

$$A_{21} = \frac{\beta^2 \bar{e} k_1 \cos k_2 + (k_1^4 + k_2^4 - k_1^2 \beta^2) \sin k_2 / k_2^2}{k_1 k_2 (k_1 \sin k_1 \cos k_2 + k_2 \cos k_1 \sin k_2)}$$

$$A_{13} = -k_2^2 / k_1^2 ; \quad A_{23} = (k_1^2 - \beta^2) / k_2^2$$

and k_1 , k_2 , for every value of the applied load, β^2 , load eccentricity, \bar{e} , and slenderness ratio, λ , are obtained from the simultaneous solution

of the following two nonlinear equations

$$\begin{aligned} A_{11} \sin k_1 + A_{13} + B_2(1) + \frac{k_2^2}{\lambda^2} &= 0 \\ A_{21} \sin k_2 + A_{23} - B_1(1) - \frac{k_1^2}{\lambda^2} &= 0 \end{aligned} \quad (2.23)$$

The expressions for U_T and joint rotation, φ , are

$$\begin{aligned} U_T = \frac{k_1^4 + k_2^4}{\lambda^2} + \frac{A_{11}^2 k_1^4}{2} \left(1 - \frac{\sin 2k_1}{2k_1}\right) + \frac{A_{21}^2 k_1^4}{2} \left(1 - \frac{\sin 2k_2}{2k_2}\right) \\ + 2B^2 \left[e(A_{21} k_2 \cos k_2 + A_{23}) - (A_{21} \sin k_2 + A_{23}) \right] \end{aligned} \quad (2.24)$$

$$\varphi = W_{1,X}(1) = A_{11} k_1 \cos k_1 + A_{13} \quad (2.25)$$

Model B

$$\Xi_1(X) = -\frac{k_1^2}{\lambda^2} X - B_1(X) \quad ;$$

$$W_1(X) = A_{11} \sin k_1 X + A_{13} X \quad ; \quad (2.26)$$

$$\Xi_2(X) = -\frac{k_2^2}{\lambda^2} X - B_2(X) \quad ; \quad W_2(X) = A_{21} \sin k_2 X + A_{24} X$$

where

$$\begin{aligned} B_1(X) &= \frac{1}{2} A_{13}^2 X + 2A_{11} A_{13} \sin k_1 X + \frac{k_1^2 A_{11}^2}{2} \left(X + \frac{\sin 2k_1 X}{2k_1} \right) \\ B_2(X) &= \frac{k_2^2 A_{21}^2}{4} \left(X + \frac{\sin 2k_2 X}{2k_2} \right) \end{aligned}$$

$$A_{11} = \frac{\beta^2 \bar{e} k_2 \cos k_2 + k_2^4 \sin k_2 / k_1^2}{k_1 k_2 (k_1 \sin k_1 \cos k_2 + k_2 \cos k_1 \sin k_2)} \quad (2.27)$$

$$A_{21} = \frac{\beta^2 \bar{e} k_1 \cos k_1 - k_2^2 \sin k_1}{k_1 k_2 (k_1 \sin k_1 \cos k_2 + k_2 \cos k_1 \sin k_2)}$$

$$A_{13} = -k_2^2 / k_1^2 ; \quad k_1^2 = \beta^2 ; \quad A_{24} = B_1(1) + \frac{k_1^2}{\lambda^2} - A_{21} \sin k_2$$

and k_2 (since for this case $k_1^2 = \beta^2$) for every value of the applied load, β^2 , and structural geometry, \bar{e} , λ , can be found from the solution of the following nonlinear equation:

$$k_2^2 A_{21} \left[A_{21} \frac{\beta^2}{4} \left(1 + \frac{\sin 2k_2}{2k_2} \right) - \sin k_2 \right] + \bar{e} \beta^2 + k_2^2 \left(\frac{\beta^2}{\lambda^2} - 1 \right) = 0 \quad (2.28)$$

The expressions for U_T and joint rotation, φ , are

$$U_T = \frac{k_1^4 + k_2^4}{\lambda^2} + \frac{A_{11}^2 k_1^4}{2} \left(1 - \frac{\sin 2k_1}{2k_1} \right) + \frac{A_{21}^2 k_2^4}{2} \left(1 - \frac{\sin 2k_2}{2k_2} \right) \quad (2.29)$$

$$+ 2\beta^2 \left[\bar{e} (A_{21} k_2 \cos k_2) - (A_{21} \sin k_2 + A_{24}) \right]$$

$$\varphi = A_{11} k_1 \cos k_1 + A_{13} \quad (2.30)$$

Model C

$$\Xi_1 = -\frac{k_1^2}{\lambda^2} X - B_1(X) ; \quad W_1 = A_{11} \sin k_1 X$$

$$\Xi_2 = A_{25} - B_2(X) ; \quad W_2 = A_{21} X^3 + A_{23} X \quad (2.31)$$

where

$$\begin{aligned}
 B_1(X) &= \frac{k_1^2 A_{11}^2}{4} \left(X + \frac{\sin 2k_1 X}{2k_1} \right) \\
 B_2(X) &= \frac{1}{2} \left(\frac{9}{5} A_{21}^2 X^5 + 2A_{21}A_{23}X^3 + A_{23}^2 X \right) \\
 A_{11} &= \frac{k_1^2 + \beta^2(\bar{e} - 1)}{k_1^2 \sin k_1} \\
 A_{21} &= \frac{k_1^2 - \beta^2}{6} \\
 A_{23} &= \frac{k_1^2 + \beta^2(\bar{e} - 1)}{k_1} \cot k_1 + \frac{\beta^2 - k_1^2}{2} \\
 A_{25} &= A_{11} \sin k_1 + B_2(1) ,
 \end{aligned} \tag{2.32}$$

and k_1 is the solution of the following nonlinear equation (for any β^2 , \bar{e} , and λ):

$$\begin{aligned}
 &\frac{\beta^2 - k_1^2}{3} + \frac{k_1^2 + \beta^2(\bar{e} - 1)}{k_1} \cot k_1 - \frac{k_1^2}{\lambda^2} \\
 &- \frac{1}{4} \left[\frac{k_1^2 + \beta^2(\bar{e} - 1)}{k_1 \sin k_1} \right]^2 \left(1 + \frac{\sin 2k_1}{2k_1} \right) = 0
 \end{aligned} \tag{2.33}$$

Finally,

$$\begin{aligned}
 U_T &= \frac{k_1^4}{\lambda^2} + \frac{A_{11}^2 k_1^4}{2} \left(1 - \frac{\sin 2k_1}{2k_1} \right) + 12A_{21}^2 \\
 &+ 2\beta^2 \bar{e} (3A_{21} + A_{23}) - (A_{21} + A_{23})
 \end{aligned} \tag{2.34}$$

$$\varphi = A_{11} k_1 \cos k_1 \quad (2.35)$$

Numerical Results and Discussion

On the basis of the criterion established, critical loads are computed for all three frames and for a large practical range of load eccentricities ($-0.01 \leq \bar{e} \leq 0.01$) and of slenderness ratios ($\lambda = 40, 80, \infty$). The results are presented graphically in Figs. 2.3 - 2.5, and discussed separately for each frame (Model).

Model A: The results for this model are presented graphically on Fig. 2.3 and part of them in a tabular form on Table 2.1. It is observed that, as in the static case, there is a small positive eccentricity, \bar{e}_{cr} , such that for $\bar{e} \leq \bar{e}_{cr}$ there is dynamic instability, while for $\bar{e} > \bar{e}_{cr}$ there is not. This \bar{e}_{cr} is λ -dependent and identical to the corresponding static case. For all λ -values considered, except $\lambda \rightarrow \infty$, the difference between β_{crD}^2 and β_{crst}^2 is the largest at $\bar{e} = \bar{e}_{cr}$ and it diminishes as \bar{e} increases negatively. On the contrary, for $\lambda \rightarrow \infty$ this effect is reversed and more specifically, the difference is close to zero at $\bar{e} = \bar{e}_{cr}$ and it increases as \bar{e} increases negatively. In addition, eccentricity has a destabilizing effect regardless of the value of the slenderness ratio. This effect is less pronounced for the static case.

Finally, dynamic instability, as defined herein, takes place with a trajectory corresponding to a positive joint rotation φ . Because of this, of course, the compressive force in the vertical bar, k_1 , is higher than the applied load, β^2 , at the instant of possible "buckled" motion (trajectory possibly passing through the unstable static equilibrium point).

Note that the experimental results of Thompson ($\lambda = 1275$ [17]) agree very well with the $\lambda \rightarrow \infty$ theoretical prediction. The largest discrepancy between theory and experiment is approximately 1.5%.

Model B: This is the only model, which exhibits bifurcational buckling (through an unstable branch) under static application of the load. The results are presented graphically in Fig. 2.4 and part of them in tabular form on Table 2.1.

It is seen from Fig. 2.4 that the effect of slenderness on the dynamic critical load is appreciable, while its effect on the static critical load (limit point load) is negligible. In addition, for all λ , except $\lambda \rightarrow \infty$, the difference between the static and dynamic critical loads is the largest at $\bar{e} = 0$ and decreases as $|\bar{e}|$ increases. Furthermore, at $\bar{e} = 0$ and for a given λ , except $\lambda \rightarrow \infty$, there are two dynamic critical loads, one corresponding to a negative rotation φ trajectory (the lower) and one corresponding to a positive φ trajectory (the upper). Definitely the system, for $\bar{e} = 0$, buckles in the mode associated with the lower load and it should be designed for this lower dynamic critical load. But the results indicate that a small positive eccentricity, in this case, has a stabilizing effect, because it forces the system to dynamically buckle through a positive rotation φ trajectory and therefore it can carry a higher load. In general, though, eccentricity has a destabilizing effect. This means that as $|\bar{e}|$ increases the dynamic critical load decreases.

Model C: The results for this model are presented graphically in Fig. 2.5 and part of them in tabular form on Table 2.1. The observations for this model are very similar to those corresponding to model A.

Table 21: Critical Conditions for $\lambda = 80$

Model	\bar{c}	k_1	k_2	$\beta_{cr_D}^2$	$\beta_{cr_D}^2 / \beta_{cr_{st}}^2$
A	0.00047288	13.350303	0.701563	12.7054	0.915
	0.0000	13.319785	0.709696	12.6625	0.935
	-0.0013	13.239899	0.732511	12.5486	0.948
	-0.0025	13.170965	0.753974	12.4483	0.954
	-0.0050	13.040181	0.799120	12.2528	0.961
	-0.0070	12.946092	0.834976	12.1081	0.963
	-0.0100	12.819032	0.887372	11.9077	0.965
B	0	8.77116	.37756	8.77116	0.8887058
	.002	8.37378	.42278	8.37378	0.9010594
	.004	7.99803	.46167	7.99803	0.8986994
	.008	7.31164	.52393	7.31164	0.8867721
	.010	7.00021	.54887	7.00021	0.8804564
	0	9.24600	.31035	9.24600	0.9368172
	-.002	9.05455	.34513	9.05455	0.9554539
	-.004	8.88447	.37852	8.88447	0.9606390
	-.008	8.59210	.43900	8.59210	0.9592319
	-.010	8.46421	.46605	8.46421	0.9558657
C	0.0004722	1.37022	0	1.27144	0.895
	0.0000	1.36547	0	1.26421	0.921
	-0.0013	1.35332	0	1.24523	0.939
	-0.0025	1.34319	0	1.22885	0.946
	-0.0050	1.32475	0	1.19771	0.953
	-0.0075	1.30910	0	1.16995	0.955
	-0.0100	1.29550	0	1.14492	0.956

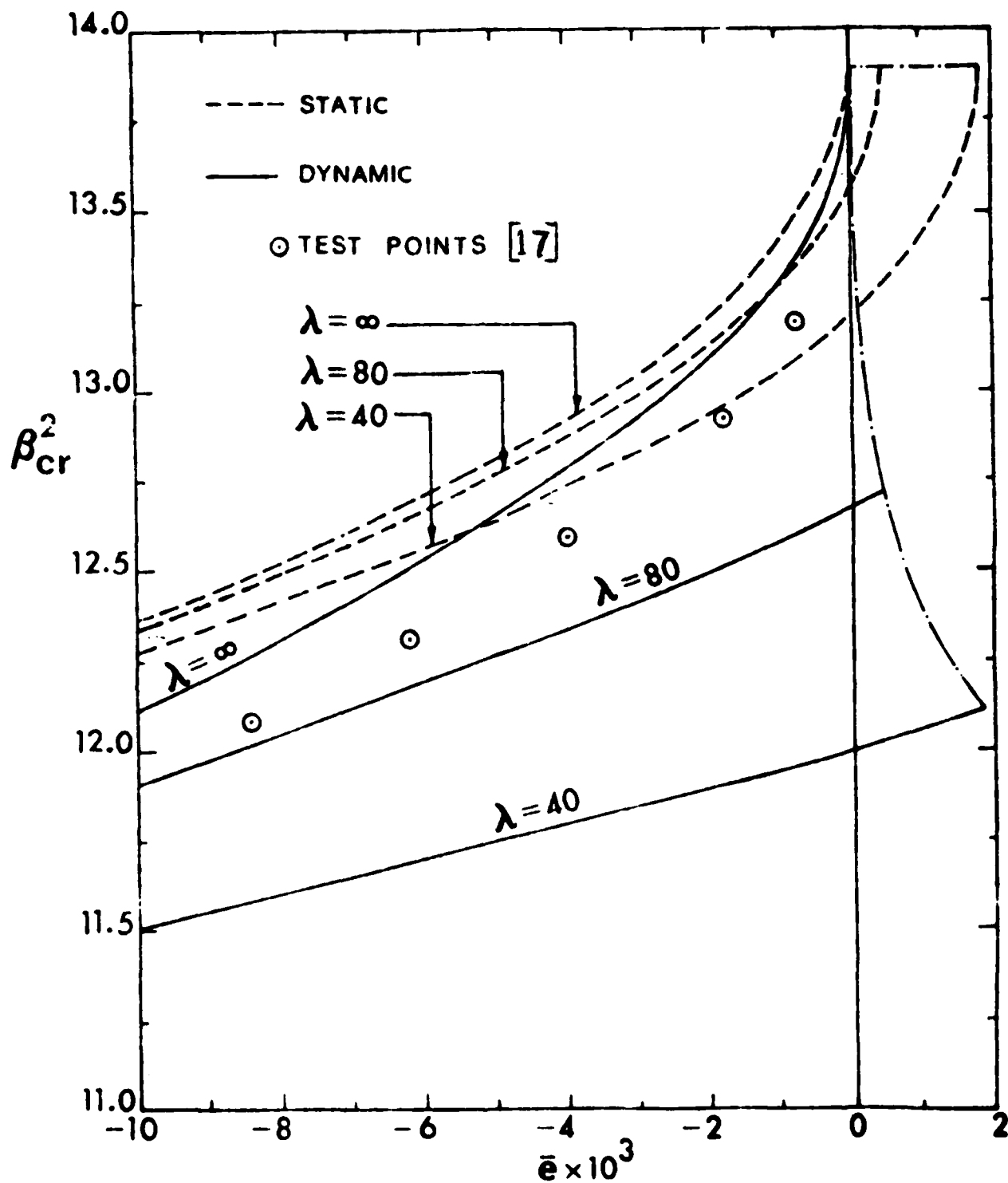


Fig. 2.3 Effect of Eccentricity, \bar{e} , and Slenderness ratio, λ , on the Static and Dynamic Critical Loads, β^2 . (Model A)

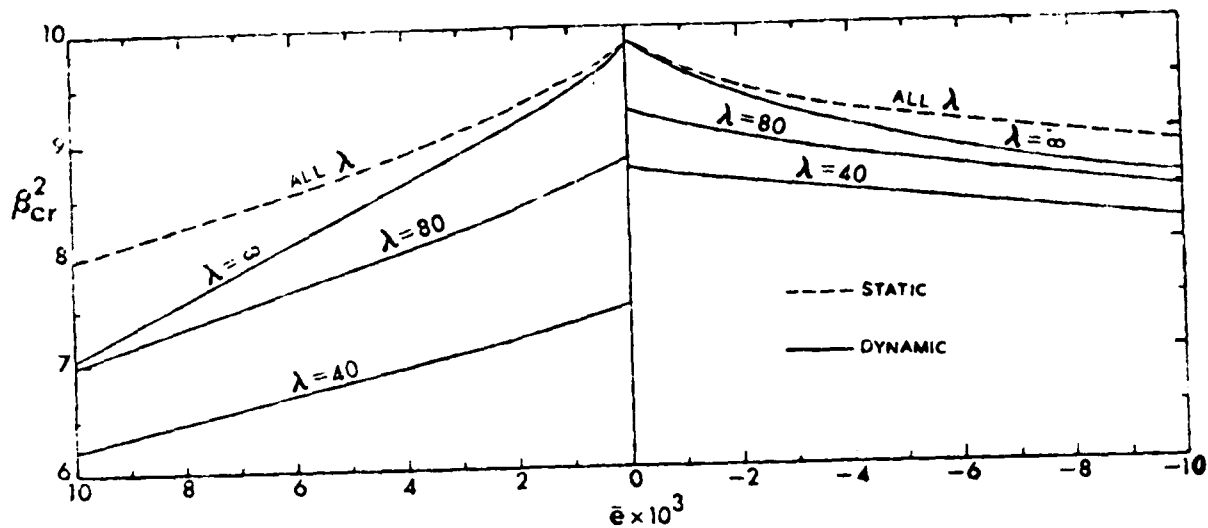


Fig. 2.4. Effect of Eccentricity, \bar{e} , and Slenderness ratio, λ , on the Static and Dynamic Critical Loads, β^2 . (Model B).

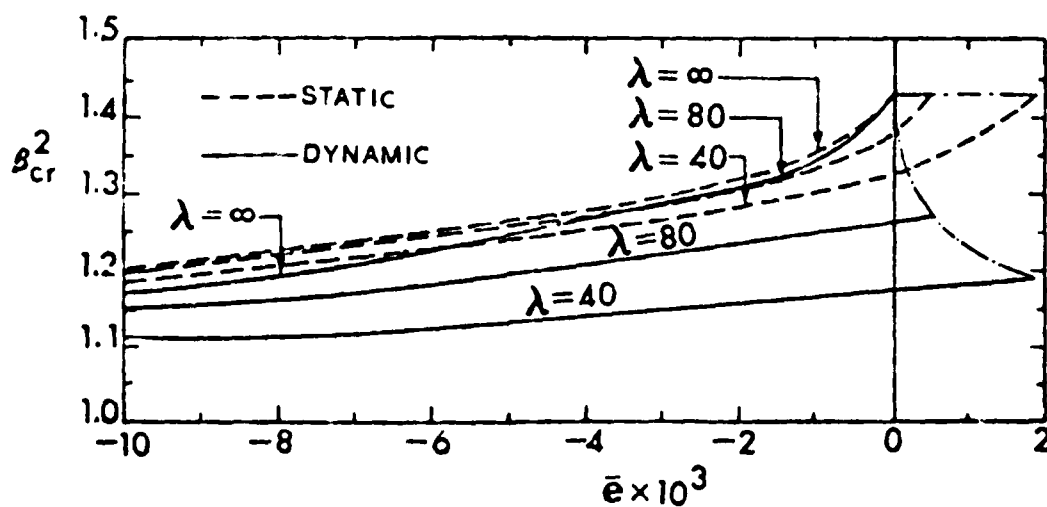


Fig. 2.5. Effect of Eccentricity, \bar{e} , and Slenderness ratio, λ , on the Static and Dynamic Critical Loads, β^2 . (Model C).

In all three models, when the alternate method was employed, Eqs. (2.17) and (2.19), in some cases, the results were physically unacceptable. This is only mentioned here as a word of caution to those who may attempt to use this particular procedure for estimating dynamic critical loads. For the systems investigated herein, a less restrictive definition, related to the boundedness of the motion, may be employed, which is: an unbounded motion takes place for that magnitude of the applied load for which U_T assumes always negative values no matter what combination of kinematically admissible functions w_i , ξ_i can be assigned; Otherwise the motion is bounded.

SECTION III

STIFFENED AND UNSTIFFENED, IMPERFECT CYLINDRICAL SHELLS UNDER SUDDENLY APPLIED LOADS.

There are a few publications dealing with dynamic buckling of shell configurations. Some of them deal with shallow spherical caps (see [12] for a fairly complete review) and even fewer with cylindrical shells [4, 18-22], most of which are based on the Budiansky-Roth approach. In this chapter, the necessary criterion and the related solution methodology are presented, based on the energy approach [1].

The Stability Criterion

Consider a stiffened, geometrically imperfect, circular cylindrical shell, (see Fig. 3.1), supported in various ways (all possible boundary conditions) and loaded suddenly by a set of loads consisting of uniform axial compression and uniform pressure. These loads may be applied individually or in combination, but they will be, in general, represented by a load parameter λ . The case considered, herein, corresponds to suddenly applied loads of infinite duration and constant magnitude. Since the internal and external loads are conservative, the system is conservative.

Let u , v , and w be the reference surface displacement component (see next section) which are, in general, functions of position (x, y, z) and time, t . Then, the total potential is a functional of the displacement components and their space-dependent partial derivatives. Similarly, the kinetic energy is a functional (positive definite) of the time-dependent derivatives. The functional is said to be positive definite if it is positive for all possible values of the functions in the integrand, except zero, in which case the functional is zero.

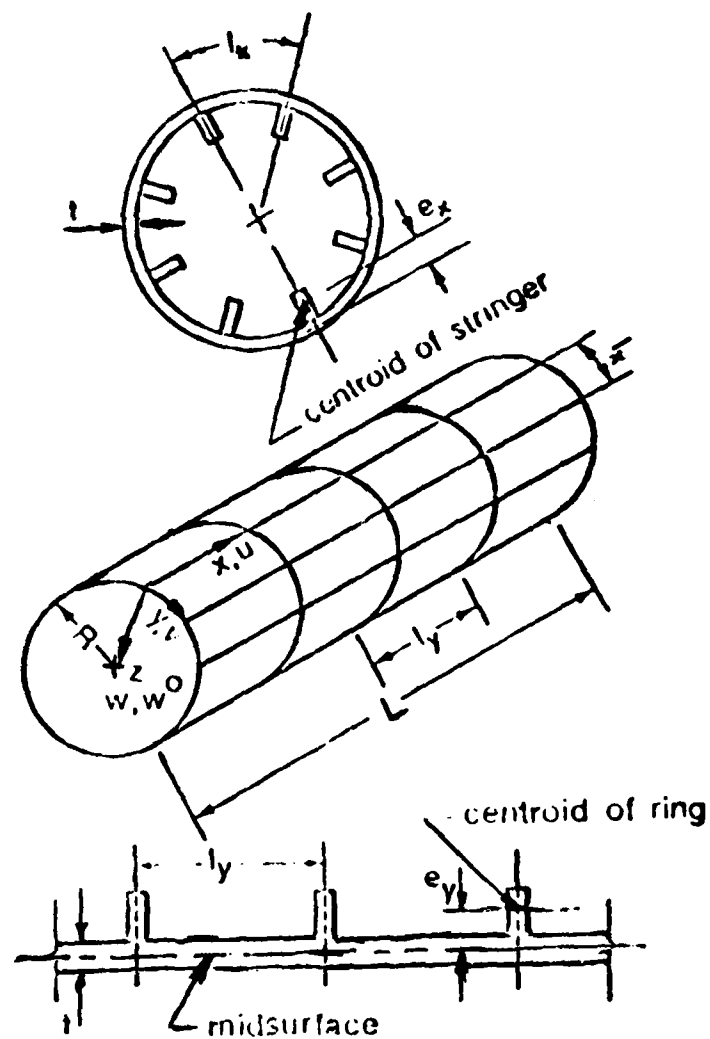


Fig. 3.1 Geometry and Sign Convention

On the basis of the conservation of energy principle, the total energy is a constant, C , or

$$U_T [u, v, w; \lambda] + T [u, {}_t, v, {}_t, w, {}_t] = C \quad (3.1)$$

where U_T and T are the total potential and kinetic energy functionals respectively and C is a constant as far as buckling trajectories are concerned. This means that, in the case of uniform pressure on a cylindrical shell, the breathing mode trajectory cannot possibly be considered as an admissible buckling trajectory. The reason for this lies in the fact that a perfect cylindrical shell with ends free to expand and/or contract when loaded by uniform pressure deforms in the breathing mode primarily (primary path), therefore "buckled" motion cannot possibly occur through this mode. Then, C in Eq. (3.1) will account for the potential of the external forces because of primary path modes. Note that in the case of axial compression C contains the potential of the axial force in connection with the axial mode (the part of u which is not w -dependent). This point is further dealt with in a later section.

Next, define a modified total potential, $U_{T_{\text{mod.}}}$ such that

$$U_{T_{\text{mod.}}} + T = 0 \quad (3.2)$$

where

$$U_{T_{\text{mod.}}} = U_T - C$$

With this modification the criterion becomes identical to that for the frame problem (Section 2).

The Static Solution

It is obvious from the stability criterion as applied to the case of sudden loads of constant magnitude and infinite duration, that a complete

static analysis is needed. This includes pre-limit point behavior, establishment of the limit point and post-limit point behavior. At each equilibrium point, the corresponding value of the modified total potential must be evaluated. According to the criterion, then, the value of the load for which the modified total potential is zero at an unstable equilibrium point (post-limit point) corresponds to a lower bound of the critical dynamic load.

Consider an imperfect, orthogonally stiffened, thin, circular, cylindrical shell (see Fig. 1), loaded by axial compression and/or uniform pressure. Let $w^0(x,y)$ denote the deviation of the shell midsurface (taken as a reference surface) from the corresponding perfectly cylindrical one. Moreover, let u , v , and w denote the displacement components of the material points on the reference surface. The component $w(x,y)$ is measured from the reference surface in the radial direction.

The nonlinear kinematic relations for this configuration are

$$\begin{aligned}\epsilon_{xx}^0 &= u_{,x} + \frac{1}{2} \left(w_{,x}^2 + 2w_{,x} w_{,x}^0 \right) \\ \epsilon_{yy}^0 &= v_{,y} - \frac{w}{R} + \frac{1}{2} \left(w_{,y}^2 + 2w_{,y} w_{,y}^0 \right) \\ \gamma_{xy}^0 &= 2\epsilon_{xy} = u_{,y} + v_{,x} + w_{,x} w_{,y} + w_{,x} w_{,y}^0 + w_{,y} w_{,x}^0 \\ \kappa_{xx} &= w_{,xx} ; \kappa_{yy} = w_{,yy} ; \kappa_{xy} = w_{,xy}\end{aligned}\tag{3.3}$$

and

$$\begin{aligned}\epsilon_{xx} &= \epsilon_{xx}^0 - zw_{,xx} \\ \epsilon_{yy} &= \epsilon_{yy}^0 - zw_{,yy} \\ \gamma_{xy} &= \gamma_{xy}^0 - zz w_{,xy}\end{aligned}\tag{3.4}$$

The relations of the stress and moment resultants to the strains and changes in curvature and torsion are (see Ref. 23):

$$\begin{aligned}
 N_{xx} &= E_{xxp} \left[(1+\lambda_{xx}) \epsilon_{xx}^0 + \nu \epsilon_{yy}^0 - e_x \lambda_{xx} \kappa_{xx} \right] \\
 N_{yy} &= E_{xxp} \left[\nu \epsilon_{xx}^0 + (1+\lambda_{yy}) \epsilon_{yy}^0 - e_y \lambda_{yy} \kappa_{yy} \right] \\
 N_{xy} &= E_{xxp} \left[(1-\nu) \epsilon_{xy}^0 \right] \\
 M_{xx} &= D \left\{ \left[(1+\rho_{xx}) + \frac{12}{t^2} e_x^2 \lambda_{xx} \right] \kappa_{xx} + \nu \kappa_{yy} - \frac{12}{t^2} e_x \lambda_{xx} \epsilon_{xx}^0 \right\} \\
 M_{yy} &= D \left\{ \nu \kappa_{xx} + \left[(1+\rho_{yy}) + \frac{12}{t^2} e_y^2 \lambda_{yy} \right] \kappa_{yy} - \frac{12}{t^2} e_y \lambda_{yy} \epsilon_{yy}^0 \right\} \\
 M_{xy} &= D(1-\nu) \kappa_{xy}
 \end{aligned} \tag{3.5}$$

where

$$\begin{aligned}
 E_{xxp} &= Et/(1-\nu^2); \quad D = Et^3/12(1-\nu^2); \quad \lambda_{xx} = A_x(1-\nu^2)/t l_x \\
 \lambda_{yy} &= A_y(1-\nu^2)/t l_y; \quad \rho_{xx} = EI_{xc}/D l_x; \quad \text{and} \quad \rho_{yy} = EI_{yc}/D l_y.
 \end{aligned}$$

From Eqs. (3.5) one may derive the following expressions for the reference surface strains

$$\begin{aligned}
 \epsilon_{xx}^0 &= a_1 N_{xx} + a_2 N_{yy} + a_3 \kappa_{xx} + a_4 \kappa_{yy} \\
 \epsilon_{yy}^0 &= a_2 N_{xx} + a_1 N_{yy} + b_3 \kappa_{xx} + b_4 \kappa_{yy} \\
 \epsilon_{xy}^0 &= \frac{1}{2} \gamma_{xy} = N_{xy}/(1-\nu) E_{xxp}
 \end{aligned} \tag{3.6}$$

where

$$\begin{aligned}
 a_1 &= (1+\lambda_{yy})/\alpha E_{xxp} ; \quad a_2 = -\nu/\alpha E_{xxp} ; \quad a_3 = (1+\lambda_{yy})e_x \lambda_{xx}/\alpha \\
 a_4 &= -\nu e_y \lambda_{yy}/\alpha ; \quad b_2 = (1+\lambda_{xx})/\alpha E_{xxp} ; \quad b_3 = -\nu e_x \lambda_{xx}/\alpha \\
 b_4 &= (1+\lambda_{xx})e_y \lambda_{yy}/\alpha ; \quad \alpha = [(1+\lambda_{xx})(1+\lambda_{yy}) - \nu^2]
 \end{aligned} \tag{3.7}$$

By employing the principle of the stationary value of the total potential one can derive the following equilibrium equations

$$N_{xx,x} + N_{xy,y} = 0$$

$$N_{xy,x} + N_{yy,y} = 0$$

$$\begin{aligned}
 M_{xx,xx} + 2M_{xy,xy} + M_{yy,yy} &= \frac{N_{yy}}{R} + [N_{yy}(w, {}_y w_y^0)]_{,y} + [N_{xy}(w, {}_x w_x^0)]_{,y} \\
 &+ [N_{xx}(w, {}_x w_x^0)]_{,x} + [N_{xy}(w, {}_y w_y^0)]_{,x} + p
 \end{aligned}$$

By introducing the Airy stress function, as $N_{xx} = -\bar{N}_{xx} + F, {}_{yy}$, $N_{yy} = F, {}_{xx}$ and $N_{xy} = -F, {}_{xy}$ where \bar{N}_{xx} is the level of the applied uniform axial compression, the first two of Eqs. (3.8) are identically satisfied.

Next, by eliminating u and v from the first three of Eqs. (3.3), employing Eqs. (3.6), the Airy stress function and the last three of Eqs. (3.3) one can derive the compatibility equation in terms of the Airy stress function, F and the radial displacement, w . If one expresses the third of Eq. (3.8) in terms of F and w , the governing equations consist of two coupled partial differential equations in F and w . These are:

Equilibrium

$$DL_h[w] - L_q[F] - F_{,xx}/R + \bar{N}_{xx}(w_{,xx} + w_{,xx}^0) - L[F, w + w^0] - p = 0 \quad (3.9)$$

Compatibility

$$L_d[F] + L_q[w] + \frac{1}{2}L[w, w + 2w^0] + w_{,xx}/R = 0 \quad (3.10)$$

where L_d , L_h , and L_q are differential operators defined by L_g ,

$$L_g[S] = g_{11}S_{,xxxx} + 2g_{12}S_{,xxyy} + g_{22}S_{,yyyy} \quad (3.11)$$

with

$$\begin{aligned} d_{11} &= (1 + \lambda_{xx})/\alpha E_{xxp} \\ d_{12} &= [(1 + \lambda_{xx})(1 + \lambda_{yy}) - \nu]/\alpha(1 - \nu)E_{xxp} \end{aligned} \quad (3.12)$$

$$\begin{aligned} d_{22} &= (1 + \lambda_{yy})/\alpha E_{xxp} \\ h_{11} &= 1 + \rho_{xx} = \frac{12}{t^2} \cdot \frac{e_x^2 \lambda_{xx}(1 + \lambda_{yy} - \nu^2)}{\alpha} \\ h_{12} &= 1 + \frac{12}{t^2} \frac{\nu e_x e_y \lambda_{xx} \lambda_{yy}}{\alpha} \\ h_{22} &= 1 + \rho_{yy} + \frac{12}{t^2} \frac{e_y^2 \lambda_{yy}(1 + \lambda_{xx} - \nu^2)}{\alpha} \end{aligned} \quad (3.13)$$

$$\begin{aligned} q_{11} &= -\nu e_x \lambda_{xx}/\alpha \\ q_{12} &= [(1 + \lambda_{yy})e_x \lambda_{xx} + (1 + \lambda_{xx})e_y \lambda_{yy}]/(2\alpha) \\ q_{22} &= -\nu e_y \lambda_{yy}/\alpha \end{aligned} \quad (3.14)$$

and L is a differential operator defined by

$$L[S, T] = S_{,xx} T_{,yy} - 2S_{,xy} T_{,xy} + S_{,yy} T_{,xx} \quad (3.15)$$

The total potential expression, in terms of the Airy stress function and the radial displacement, is given below

$$\begin{aligned} U_T = & \frac{1}{2E_{xxp}} \int_A (\beta_1 F_{,yy}^2 + \beta_2 F_{,xx}^2 + \beta_3 F_{,xx} F_{,yy} + \beta_4 F_{,xy}^2) dA \\ & + \frac{D}{2} \int_A (\alpha_1 w_{,yy}^2 + \alpha_2 w_{,xx}^2 + \alpha_3 w_{,xx} w_{,yy} + \alpha_4 w_{,xy}^2) dA - \int_A p w dA \quad (3.16) \\ & - \frac{\bar{N}_{xx}}{2E_{xxp}} \int_A (2\beta_1 F_{,yy} + \beta_3 F_{,xx}) dA + \frac{\beta_1}{E_{xxp}} \pi R L \bar{N}_{xx}^2 - \bar{N}_{xx}^2 \pi R L e_{AV} \end{aligned}$$

where e_{AV} (average end shortening) is given by

$$e_{AV} = - \int_A u_{,x} dA / 2\pi R L \quad (3.17)$$

and

$$\begin{aligned} \beta_1 &= d_{22} E_{xxp}; \quad \beta_2 = d_{11} E_{xxp}; \quad \beta_3 = -2\nu/\alpha; \quad \beta_4 = 2/(1-\nu) \\ \alpha_1 &= h_{22}; \quad \alpha_2 = h_{11}; \quad \alpha_3 = 2\nu \left[1 + \frac{12}{t^2} \frac{e_x e_y \lambda_{xx} \lambda_{yy}}{\alpha} \right] \alpha_4 = 2(1-\nu) \end{aligned} \quad (3.18)$$

Similarly, the expressions for the average end shortening and "unit end shortening" at $y = 0$ are given by

$$\begin{aligned} e_{AV} = & a_1 \bar{N}_{xx} - \frac{1}{2\pi R L} \int_0^{2\pi R} \int_0^L [a_1 F_{,yy} + a_2 F_{,xx} + a_3 w_{,xx} + a_4 w_{,yy} \\ & - \frac{1}{2} w_{,x} (w_{,x} + 2w_{,x}^0)] dx dy \end{aligned} \quad (3.19)$$

$$e = a_1 \bar{N}_{xx} - \frac{1}{L} \int_0^L [a_1 F_{,yy} + a_2 F_{,xx} + a_3 w_{,xx} + a_4 w_{,yy} - \frac{1}{2} F_{,x} (w_{,x} + 2w_{,x}^0)]_{y=0} dx \quad (3.20)$$

Note that e measures the amount of end shortening per unit of cylinder length, L .

The associated boundary conditions are either kinematic or natural. Thus, one must prescribe the values of either u , v , w and $w_{,x}$ or N_{xx} , N_{xy} , Q_x^* and M_{xx} .

Before listing the various boundary conditions, the expressions for M_{xx} and Q_x^* in terms of F and w are given. Moreover, a few explanatory remarks are presented for certain boundary conditions.

First, the expressions for M_{xx} and Q_x^* are:

$$\begin{aligned} M_{xx} &= \gamma_1 w_{,xx} + \gamma_2 w_{,yy} + \gamma_3 (F_{,yy} - \bar{N}_{xx}) + \gamma_4 F_{,xx} \\ Q_x^* &= (F_{,yy} - \bar{N}_{xx}) (w_{,x} + w_{,x}^0) + F_{,xy} (w_{,y} + w_{,y}^0) - M_{xx,x} - 2M_{xy,y} \end{aligned} \quad (3.21)$$

where

$$\gamma_1 = Dh_{11}; \quad \gamma_2 = \frac{D}{2} \alpha_3; \quad \gamma_3 = -a_3; \quad \gamma_4 = -b_3 \quad (3.22)$$

As far as the in-plane boundary condition at either end one may write

$$\begin{array}{cc} \text{either} & \text{or} \\ N_{xx} = -\bar{N}_{xx} & \delta u = 0 \\ & (u = \text{prescribed}) \end{array} \quad (3.23)$$

but in terms of the Airy stress function one may write

$$\begin{array}{cc} \text{either} & \text{or} \\ F_{,yy} = 0 & u = \text{prescribed} \end{array} \quad (3.23a)$$

From the above it is clear that the true in-plane condition (at one of the two ends) must be $F_{,yy} = 0$. At the other end it could be $u = 0$. Note that if one assigns various values to u at a boundary, the corresponding load (\bar{N}_{xx}) is unknown. This approach is not covered in this report.

Finally, if the applied load, \bar{N}_{xx} , passes through the reference surface and the reference surface is hinged (for the simply supported case), then in this case one may write $M_{xx} = 0$. On the other hand if the load is applied in an eccentric manner then $M_{xx} \neq 0$ but $M_{xx} = \pm e\bar{N}_{xx}$, where e is the load eccentricity (if $e = 0$, one has the usual simply supported condition).

All possible (extreme) boundary conditions are included in the analysis and the related solution methodology (including the computer program). These are, simply supported (SS), free (FF) and clamped (CC) for all possible combinations of in-plane boundary conditions ($i=1,2,3,4$).

SS-1; $w = 0$; $M_{xx} = \pm e\bar{N}_{xx}$	1. $F_{,xy} = F_{,yy} = 0$	
	2. $F_{,xy} = 0$; $u = 0$	
CC-1; $w = w_{,x} = 0$	3. $v = F_{,yy} = 0$	(3.24)
FF-1; $Q_x^* = 0$; $M_{xx} = \pm e\bar{N}_{xx}$	4. $v = 0$; $u = C$	
	where $C = \text{constant}$	

The conditions in u and v can be expressed in terms of w and F as in Ref. 24. For example, the condition $u = C$ in SS -2 can be replaced by a condition expressed solely in terms of w , w^0 , F and their gradients. This is accomplished by the following procedure:

This boundary condition, SS=2, at $x = 0$ or L is given by $w = 0$; $F_{,xy} = 0$, $M_{xx} = \pm e\bar{N}_{xx}$ and $u = C$. The first two are in terms of w and F . The third one, $M_{xx} = \pm e\bar{N}_{xx}$, from the first of Eqs. (3.21) is expressed in terms of w , F , and their gradients. For the last one, one

notes that [see Eqs. (3.3) and (3.5)]

$$\epsilon_{xy} = \frac{1}{2} [u_{,y} + v_{,x} + w_{,x} w_{,y} + w_{,y} w_{,x}^0 + w_{,x} w_{,y}^0] = -F_{,xy} / (1-\nu) E_{xx} p \quad (3.25)$$

since $F_{,xy} = 0$, $w_{,y} = 0$ because $w(0,y) = 0$, and $u_{,y} = 0$ because $u(0,y) = C$, Eq. (3.25) becomes

$$v_{,x} + w_{,x} w_{,y}^0 = 0 \quad (3.26)$$

Similarly, from Eqs. (3.3) and (3.5) one may write

$$\begin{aligned} \epsilon_{yy} &= v_{,y} + \frac{1}{2} [w_{,y} (w_{,y} + 2w_{,y}^0)] - \frac{w}{R} \\ &= a_2 N_{xx} + b_2 N_{yy} + b_3 \kappa_{xx} + b_4 \kappa_{yy} \end{aligned} \quad (3.27)$$

This equation, Eq. (3.27), is valid at any point along the shell, therefore differentiation with respect to x does not violate its validity. If this is done and if the N 's and κ 's are expressed in terms of w , F , and their gradients, one may write

$$\begin{aligned} v_{,yx} + \frac{1}{2} [w_{,xy} (w_{,y} + 2w_{,y}^0) + w_{,y} (w_{,xy} + 2w_{,xy}^0)] - \frac{w_{,x}}{R} \\ = a_2 F_{,yyx} + b_2 F_{,xxx} + b_3 w_{,xxx} + b_4 w_{,yyx} \end{aligned} \quad (3.28)$$

Evaluation of Eq. (3.28) at $x = 0$ or L , and use of the fact that $w_{,y}(0,y) = 0$ yields

$$v_{,yx} + w_{,xy} w_{,y}^0 - w_{,x}/R = a_2 F_{,yyx} + b_2 F_{,xxy} + b_3 w_{,xxx} + b_4 w_{,yyx} \quad (3.29)$$

Differentiation of Eq. (3.26) with respect to y , yields

$$v_{,xy} + w_{,xy} w_{,y}^0 + w_{,x} w_{,yy}^0 = 0 \quad (3.30)$$

Substitution of Eq. (3.30) into Eq. (3.29) yields a boundary condition equivalent to $u = C$, or

$$b_2 F_{,xxx} + b_3 w_{,xxx} + b_4 w_{,yyx} + w_{,x} \left(\frac{1}{R} + w_{,yy}^0 \right) = 0 \quad (3.31)$$

Similar steps may be followed to express all possible boundary conditions in terms of w , F , and their gradients. In order to save space, only the final expression for all possible boundary conditions, Eqs. (3.24), are given below, which have been incorporated into the computer program (see Appendix A). The condition, shown below, corresponds to uniform application of \bar{N}_{xx} across the cross-section ($M_{xx} = a_2 \bar{N}_{xx}$).

$$\text{SS-1 } w = \gamma_1 w_{,xx} + \gamma_4 F_{,xx} = F_{,xy} = F_{,yy} = 0$$

$$\text{SS-2 } w = \gamma_1 w_{,xx} + \gamma_3 F_{,yy} + \gamma_4 F_{,xx} = F_{,xy} = 0$$

$$b_2 F_{,xxx} + b_3 w_{,xxx} + b_4 w_{,yyx} + w_{,x} \left(\frac{1}{R} + w_{,yy}^0 \right) = 0$$

$$\text{SS-3 } w = \gamma_1 w_{,xx} + \gamma_4 F_{,xx} = F_{,yy} = 0, b_2 F_{,xx} + b_3 w_{,xx} = a_2 \bar{N}_{xx} \quad (3.32)$$

$$\text{SS-4 } w = \gamma_1 w_{,xx} + \gamma_3 F_{,yy} + \gamma_4 F_{,xx} = a_2 (F_{,yy} - \bar{N}_{xx}) + b_2 F_{,xx}$$

$$+ b_3 w_{,xx} = 0$$

$$\left[a_2 + 2/(1-\nu) \bar{E}_{xxp} \right] F_{,xyy} + b_2 F_{,xxx} + b_3 w_{,xxx} + b_4 w_{,xyy}$$

$$+ w_{,x} \left(\frac{1}{R} + w_{,yy}^0 \right) = 0$$

$$\text{CC-1 } w = w_{,x} = F_{,xy} = F_{,yy} = 0$$

$$\text{CC-2 } w = w_{,x} = F_{,xy} = 0 \quad b_2 F_{,xxx} + b_3 w_{,xxx} = 0$$

$$\text{CC-3 } w = w_{,x} = F_{,yy} = 0 \quad b_2 F_{,xx} + b_3 w_{,xx} = a_2 \bar{N}_{xx}$$

$$\begin{aligned}
\text{CC-4 } w = w_{,x} &= a_2 \left(F_{,yy} - \bar{N}_{xx} \right) + b_2 F_{,xx} + b_3 w_{,xx} = 0 \\
\left[a_2 + 2/(1-\nu) E_{xx} \right] F_{,yyx} &+ b_2 F_{,xxx} + b_3 w_{,xxx} = 0
\end{aligned} \tag{3.33}$$

Similarly the FF-1 condition and the symmetry and antisymmetry conditions at $x = L/2$ are

$$\begin{aligned}
\text{FF-1 } \gamma_1 w_{,xx} + \gamma_2 w_{,yy} + \gamma_4 F_{,xx} &= F_{,yy} = F_{,xy} = 0 \\
\gamma_4 F_{,xxx} + \gamma_1 w_{,xxx} + \left[\gamma_2 + 2D(1-\nu) \right] w_{,xyy} &+ \bar{N}_{xx} (w_{,x} - w_{,x}^0) = 0
\end{aligned} \tag{3.34}$$

$$\text{Symmetry } (w_{,x} = Q^* = N_{xy} = u = 0)$$

$$w_{,x} = \gamma_1 w_{,xxx} + \gamma_4 F_{,xxx} - (F_{,yy} - \bar{N}_{xx}) w_{,x}^0 = 0 \tag{3.35}$$

$$F_{,xy} = b_2 F_{,xxx} + b_3 w_{,xxx} + w_{,x}^0 w_{,yy} = 0$$

$$\text{Antisymmetry } (w = M_{xx} = v = F_{,yy} = 0)$$

$$w = \gamma_1 w_{,xx} + \gamma_4 F_{,xx} = 0 \tag{3.36}$$

$$F_{,yy} = 0, b_2 F_{,xx} + b_3 w_{,xx} = a_2 \bar{N}_{xx}$$

For the case of zero load eccentricity the various boundary conditions become

$$\text{SS-1 } w = \gamma_1 w_{,xx} + \gamma_4 F_{,xx} = F_{,xy} = F_{,yy} = 0$$

$$\text{SS-2 } w = \gamma_1 w_{,xx} + \gamma_3 (F_{,yy} - \bar{N}_{xx}) + \gamma_4 F_{,xx} = F_{,xy} = 0$$

$$b_2 F_{,xxx} + b_3 w_{,xxx} + b_4 w_{,yyx} + w_{,x} \left(\frac{1}{R} + w_{,yy}^0 \right) = 0$$

$$\text{SS-3 } w = \gamma_1 w_{,xx} + \gamma_4 F_{,xx} = F_{,yy} = b_2 F_{,xx} + b_3 w_{,xx} = a_2 \bar{N}_{xx}$$

$$\begin{aligned}
\text{SS-4 } w &= \gamma_1 w_{,xx} + \gamma_3 (F_{,yy} - \bar{N}_{xx}) + \gamma_4 F_{,xx} = a_2 (F_{,yy} - \bar{N}_{xx}) \\
&+ b_2 F_{,xx} + b_3 w_{,xx} = 0 \\
&[a_2 + 2/(1-\nu)E_{xx,p}] F_{,xyy} + b_2 F_{,xxx} + b_3 w_{,xxx} + b_4 w_{,xyy} \\
&+ w_{,x} \left(\frac{1}{R} + w_{,yy}^0 \right) = 0
\end{aligned} \tag{3.37}$$

$$\text{CC-1 } w = w_{,x} = F_{,xy} = F_{,yy} = 0$$

$$\text{CC-2 } w = w_{,x} = F_{,xy} = 0 \quad b_2 F_{,xxx} + b_3 w_{,xxx} = 0$$

$$\text{CC-3 } w = w_{,x} = F_{,yy} = 0 \quad b_2 F_{,xx} + b_3 w_{,xx} = a_2 \bar{N}_{xx} \tag{3.38}$$

$$\text{CC-4 } w = w_{,x} = a_2 (F_{,yy} - \bar{N}_{xx}) + b_2 F_{,xx} + b_3 w_{,xx} = 0$$

$$[a_2 + 2/(1-\nu)E_{xx,p}] F_{,yyx} + b_2 F_{,xxx} + b_3 w_{,xxx} = 0$$

Similarly the FF-1 conditions are

$$\text{FF-1 } \gamma_1 w_{,xx} + \gamma_2 w_{,yy} + \gamma_4 F_{,xx} = F_{,yy} = F_{,xy} = 0 \tag{3.39}$$

$$\gamma_4 F_{,xxx} + \gamma_1 w_{,xxx} + [\gamma_2 + 2D(1-\nu)] w_{,xyy} + N_{xx} (w_{,x} - w_{,x}^0) = 0$$

The problem, as formulated herein, is to find the complete nonlinear response of the shell to externally applied pressure and compression. This response includes post-limit point behavior or postbuckling behavior, whichever is applicable. Thus, all equilibrium positions may be presented as plots of applied load parameter versus some characteristic displacement (the average end shortening is one possibility). Moreover, at each equilibrium point, the values of the total potential and modified total potential are recorded, in order to establish critical dynamic conditions.

Solution Methodology

The solution methodology described, herein, is an extension of the procedure outlined in [25]. Therefore, some duplication is unavoidable, especially in the interest of making this section self-contained.

As seen from Eqs. (3.9) and (3.10), the field equations consist of two coupled, nonlinear, partial differential equations in terms of the transverse displacement component, w , and the Airy stress function F .

A separated solution of the form shown below (see [24]), is used in order to reduce the system of partial differential equations to one of ordinary differential equations.

$$\begin{aligned} w(x,y) &= \sum_{i=0}^K W_i(x) \cos \frac{iny}{R} \\ F(x,y) &= \sum_{i=0}^{2K} f_i(x) \cos \frac{iny}{R} \end{aligned} \quad (3.40)$$

where n denotes the number of full waves around the circumference.

The initial geometric imperfection is also expressed in a similar form

$$W^0(x,y) = \sum_{i=0}^K W_i^0(x) \cos \frac{iny}{R} \quad (3.41)$$

where $W_i^0(x)$ denotes known functions of position x .

The following steps are employed in order to accomplish the reduction to a system of ordinary differential equations. First, Eqs. (3.40) and (3.41) are substituted into the compatibility equation [Eq. (3.10)]. Next, by employing trigonometric identities of double Fourier series involving products (as in [26]), the compatibility equation reduces to a trigonometric

series in $\frac{iny}{R}$. The coefficient of each term involves differential operations on W_i , f_i , and W_i^0 . Use of the orthogonality of the trigonometric functions reduces the compatibility equation into $2K + 1$ ordinary, nonlinear, differential equations.

Next, the Galerkin procedure is employed (in the circumferential direction) in connection with the equilibrium equation [Eq. (3.9)]. This leads to the vanishing of $(K + 1)$ Galerkin integrals, which results into a system of $(K + 1)$ nonlinear ordinary differential equations in W_i and f_i .

These equations are:

(a) Compatibility $(2K + 1)$

for $i = 0$

$$f_o'' = \frac{1}{d_{11}} \left[-q_{11} W_o'' - W_o/R + \frac{n^2}{4R^2} \sum_{j=1}^K j^2 (W_j + 2W_j^0) W_j + a_2 \bar{N}_{xx} \right] \quad (3.42)$$

The above equation is obtained from the first (fourth order) compatibility equation, with the continuity condition on v at zero and 2π satisfied.

for $i = 1, 2, \dots, 2K$

$$\begin{aligned} d_{11} f_i'''' - 2 \left(\frac{in}{R} \right)^2 d_{12} f_i'' + \left(\frac{in}{R} \right)^4 d_{22} f_i \\ + \delta_{i1} \left[q_{11} W_i'''' - 2 \left(\frac{in}{R} \right)^2 q_{12} W_i'' + \left(\frac{in}{R} \right)^4 q_{22} W_i + W_i''/R \right] \\ - \frac{n^2}{4R^2} \sum_{j=0}^K \left\{ [(i+j)^2 \delta_{i+j} (W_{i+j} + 2W_{i+j}^0) \right. \\ \left. + (2 - \eta_{j-1}^2)(i-j)^2 \delta_{|i-j|} (W_{|i-j|} + 2W_{|i-j|}^0)] W_j'' \right. \\ \left. + [\delta_{i+j} (W_{i+j}'' + 2W_{i+j}^{0''}) + (2 - \eta_{j-1}^2) \delta_{|i-j|} (W_{|i-j|}'' + 2W_{|i-j|}^{0''})] \right\} \end{aligned} \quad (3.43)$$

$$\begin{aligned}
& + 2w_{|i-j|}^{o''})] j^2 w_j + 2[(i+j)\delta_{i+j}(w_{i+j}' + 2w_{i+j}^{o'}) \\
& - \eta_{i-j}|i-j|\delta_{i-j}(w_{i-j}' + 2w_{i-j}^{o'})] j w_j \} = 0
\end{aligned}$$

where

$$\delta_l = \begin{cases} 0 & l > K \\ 1 & l \leq K \end{cases} \quad \eta_l = \begin{cases} -1 & l < 0 \\ 0 & l = 0 \\ 1 & l > 0 \end{cases}$$

and

$$()' = \frac{d}{dx} .$$

(b) Equilibrium $(K + 1)$

for $i = 0$

$$\begin{aligned}
& w_0'''' [Dh_{11} + q_{11}^2/d_{11}] + w_0'' [2q_{11}/R \cdot d_{11}] + w_0 [1/R^2 \cdot d_{11}] + \bar{N}_{xx}(w_0'' + w_0^{o''}) \\
& - \frac{n^2}{4R^2} \sum_{j=1}^K j^2 \left\{ \frac{q_{11}}{d_{11}} [(w_j' + 2w_j^{o'})w_j'' + (w_j'' + 2w_j^{o''})w_j] \right. \\
& \quad + 2(w_j' + 2w_j^{o'})w_j' + \frac{1}{Rd_{11}} [(w_j' + 2w_j^{o'})w_j] - 2[(w_j' + w_j^{o'})f_j'' \\
& \quad \left. + (w_j'' + w_j^{o''})f_j + 2(w_j' + w_j^{o'})f_j'] \right\} - \frac{a_2 \bar{N}_{xx}}{Rd_{11}} = 0
\end{aligned} \tag{3.44}$$

for $i = 1, 2, \dots, K$

$$\begin{aligned}
& D \left[h_{11} w_i'''' - 2 \left(\frac{in}{R} \right)^2 h_{12} w_i'' + \left(\frac{in}{R} \right)^4 h_{22} w_i \right] \\
& - \left[q_{11} f_i'''' - 2 \left(\frac{in}{R} \right)^2 q_{12} f_i'' + \left(\frac{in}{R} \right)^4 q_{22} f_i + f_i''/R \right]
\end{aligned}$$

$$\begin{aligned}
& + \bar{N}_{xx} (W_i'' + W_i^{o''}) - W_i' \left[\frac{q_{11}}{d_{11}} \left(\frac{in}{R} \right)^2 \right] (W_i + W_i^o) - W_i \left[\frac{1}{\alpha R d_{11}} \left(\frac{in}{R} \right)^2 \right] (W_i \\
& + W_i^o) + \frac{n^4}{4R^4} \frac{i^2}{d_{11}} (W_i + W_i^o) \sum_{j=1}^K j^2 (W_j + 2W_j^o) W_j \\
& + \frac{n^2 i^2}{R^2} (W_i + W_i^o) \frac{a_2 \bar{N}_{xx}}{d_{11}} + \frac{n^2}{2R^2} \sum_{j=1}^{2K} \left\{ [(i+j)^2 \delta_{i+j} (W_{i+j} + W_{i+j}^o) \right. \\
& + (2 - \eta_{j-i}^2) (i-j)^2 \delta_{|i-j|} (W_{|i-j|} + W_{|i-j|}^o)] f_j'' \\
& + [\delta_{i+j} (W_{i+j}'' + W_{i+j}^{o''}) + (2 - \eta_{j-i}^2) \delta_{|i-j|} (W_{|i-j|}'' + W_{|i-j|}^{o''})] j^2 f_j \\
& + 2[(i+j) \delta_{i+j} (W_{i+j}' + W_{i+j}^{o'}) \\
& \left. - \eta_{i-j} |i-j| \delta_{|i-j|} (W_{|i-j|}' + W_{|i-j|}^{o'})] j f_j' \right\} = 0
\end{aligned} \tag{3.45}$$

For a given imperfection and value of the applied load, \bar{N}_{xx} , Eqs. (3.42)-(3.45) represent a system of $(3K + 2)$ coupled nonlinear differential equations in $(3K + 2)$ unknowns, f_i with $i = 0, 1, 2, \dots, 2K$ and W_i with $i = 0, 1, 2, \dots, K$.

Note that by setting $n=0$, Eqs. (3.42)-(3.45) reduce to the linearized version of the equations of compatibility and equilibrium. Moreover, it is seen from Eqs. (3.40) that regardless of the value of n ($=1, 2, \dots$ any integer) the axisymmetric mode (W_0, f_0) is represented because the summation on i starts from zero.

In addition, it is seen from Eq. (3.41) that the imperfection expression is suitable for the case when the imperfection shape is similar to the buckling mode, as well as for any arbitrary axisymmetric imperfection and for any arbitrary symmetric (with respect to y) imperfection.

In this last case, a solution can be accomplished by setting $n=1$, [see Eqs. (3.40)], and by taking K sufficiently large in order to achieve a convergent solution and have an accurate representation for the imperfection.

Next, the boundary conditions (at $x = \text{constant}$), for two cases of simple supports are presented below.

$$\underline{\text{SS-1}} \quad (M_{xx} = 0)$$

$$W_0 = 0; \quad W_0'' = -\gamma_4 a_2 \bar{N}_{xx} / (\gamma_1 d_{11} - \gamma_4 q_{11})$$

$$W_i = \gamma_1 W_i'' + \gamma_4 f_i'' = 0; \quad i = 1, 2, 3, \dots, K \quad (3.46a)$$

$$f_i = f_i' = 0; \quad i = 1, 2, 3, \dots, 2K$$

$$\underline{\text{SS-1}} \quad (M_{xx} = a_3 \bar{N}_{xx})$$

$$W_0 = 0; \quad W_0'' = -\gamma_4 a_2 \bar{N}_{xx} / (\gamma_1 d_{11} - \gamma_4 q_{11})$$

$$W_i = \gamma_1 W_i'' + \gamma_4 f_i'' = 0; \quad i = 1, 2, 3, \dots, K \quad (3.46b)$$

$$f_i = f_i' = 0; \quad i = 1, 2, 3, \dots, 2K$$

$$\underline{\text{SS-2}} \quad (M_{xx} = 0)$$

$$W_0 = 0; \quad W_0'' = -\gamma_4 a_2 \bar{N}_{xx} / (\gamma_1 d_{11} - \gamma_4 q_{11}) + \gamma_3 \bar{N}_{xx}$$

$$W_i = \gamma_1 W_i'' - \gamma_3 \left[\bar{N}_{xx} + \left(\frac{in}{R} \right)^2 f_i \right] + \gamma_4 f_i'' = 0; \quad i = 1, 2, \dots, K$$

$$f_i' = 0; \quad i = 1, 2, 3, \dots, 2K$$

$$b_2 f_i''' + b_3 w_i''' - \left(\frac{in}{R}\right)^2 b_4 w_i' + \frac{1}{R} w_i' - \frac{n^2}{2R^2} \sum_{j=0}^K [(i+j)^2 w_{i+j}^o] \quad (3.47a)$$

$$+ (1 - \eta_{j-i}^2 + \eta_i) (i-j)^2 w_{|i-j|}^o \Big] w_j' = 0; \quad i = 1, 2, \dots, 2K$$

$$\underline{SS-2} \quad (M_x = a_3 \bar{N}_{xx})$$

$$w_o = 0; \quad w_o'' = -\gamma_4 a_2 \bar{N}_{xx} / (\gamma_1 d_{11} - \gamma_4 q_{11})$$

$$w_i = \gamma_1 w_i'' - \gamma_3 \left(\frac{in}{R}\right)^2 f_i + \gamma_4 f_i'' = 0; \quad i = 1, 2, \dots, K$$

$$f_i' = 0; \quad i = 1, 2, 3, \dots, 2K \quad (3.47b)$$

$$b_2 f_i''' + b_3 w_i''' - \left(\frac{in}{R}\right)^2 b_4 w_i' + \frac{1}{R} w_i' - \frac{n^2}{2R^2} \sum_{j=0}^K [(i+j)^2 w_{i+j}^o]$$

$$+ (1 - \eta_{j-i}^2 + \eta_i) (i-j)^2 w_{|i-j|}^o \Big] w_j' = 0; \quad i = 1, 2, \dots, 2K$$

$$\underline{SS-3} \quad (M_{xx} = 0)$$

$$w_o = 0; \quad w_o'' = -\gamma_4 a_2 \bar{N}_{xx} / (\gamma_1 d_{11} - \gamma_4 q_{11})$$

$$w_i = \gamma_1 w_i'' + \gamma_4 f_i'' = 0; \quad i = 1, 2, \dots, K \quad (3.48a)$$

$$f_i = b_2 f_i'' + b_3 w_i'' = 0; \quad i = 1, 2, \dots, 2K$$

$$\underline{\text{SS-3}} \quad (M_{xx} = a_3 \bar{N}_{xx})$$

$$W_0 = 0; \quad W_0'' = -\gamma_4 a_2 \bar{N}_{xx} / (\gamma_1 d_{11} - \gamma_4 q_{11})$$

$$W_i = \gamma_1 W_i'' + \gamma_4 f_i'' = 0; \quad i = 1, 2, \dots, K \quad (3.48b)$$

$$f_i = b_2 f_i'' + b_3 W_i'' = 0; \quad i = 1, 2, \dots, 2K$$

$$\underline{\text{SS-4}} \quad (M_{xx} = 0)$$

$$W_0 = 0; \quad W_0'' = -\gamma_4 a_2 \bar{N}_{xx} / (\gamma_1 d_{11} - \gamma_4 q_{11}) + \gamma_3 \bar{N}_{xx}$$

$$W_i = \gamma_1 W_i'' - \gamma_3 \left[\bar{N}_{xx} + \left(\frac{in}{R} \right)^2 f_i \right] + \gamma_4 f_i'' = 0; \quad i = 1, 2, \dots, K$$

$$- a_2 \bar{N}_{xx} + \left(\frac{in}{R} \right)^2 f_i + b_2 f_i'' + b_3 W_i'' = 0; \quad i = 1, 2, \dots, 2K$$

$$- \left[a_2 + 2/(1-\nu) E_{xxp} \right] \left(\frac{in}{R} \right)^2 f_i' + b_2 f_i''' + b_3 W_i''' \quad (3.49a)$$

$$- b_4 \left(\frac{in}{R} \right)^2 W_i' + \frac{1}{R} W_i' - \frac{n^2}{2R^2} \sum_{j=0}^K \left[(i+j)^2 W_{i+j}^0 + (1-\eta_{j-i}^2 \right.$$

$$\left. + \eta_i \right) W_{|i-j|}^0 \left. \right] W_j' = 0; \quad i = 1, 2, \dots, 2K$$

$$\underline{\text{SS-4}} \quad (M_{xx} = a_3 \bar{N}_{xx})$$

$$W_0 = 0; \quad W_0'' = -\gamma_4 a_2 \bar{N}_{xx} / (\gamma_1 d_{11} - \gamma_4 q_{11})$$

$$W_i = \gamma_1 W_i'' - \gamma_3 \left(\frac{in}{R} \right)^2 f_i + \gamma_4 f_i'' = 0; \quad i = 1, 2, \dots, K$$

$$- a_2 \left(\frac{in}{R} \right)^2 f_i'' + b_2 f_i'' + b_3 W_i'' = 0; \quad i = 1, 2, \dots, 2K$$

$$- \left[a_2 + 2/(1-\nu) E_{xxp} \right] \left(\frac{in}{R} \right)^2 f_i' + b_2 f_i''' + b_3 W_i''' - b_4 \left(\frac{in}{R} \right)^2 W_i' \\ + \frac{1}{R} W_i' - \frac{n^2}{2R^2} \sum_{j=0}^K [(i+j)^2 W_{i+j}^0 + (1 - \eta_{j-1}^2 \\ + \eta_i) W_{|i-j|}^0] W_j' = 0; \quad i = 1, 2, \dots, 2K \quad (3.49b)$$

$$\underline{CC-1} \quad W_i = W_i' = 0; \quad i = 0, 1, \dots, K \quad (3.50) \\ (j=1,2,3,4)$$

and

$$\underline{CC-1} \quad f_i = f_i' = 0; \quad i = 1, 2, \dots, 2K \quad (3.50a)$$

$$\underline{CC-2} \quad f_i' = b_2 f_i''' + b_3 W_i''' = 0; \quad i = 1, 2, \dots, 2K \quad (3.50b)$$

$$\underline{CC-3} \quad f_i = b_2 f_i'' + b_3 W_i'' = 0; \quad i = 1, 2, \dots, 2K \quad (3.50c)$$

$$\underline{CC-4} \quad - a_2 \left(\frac{in}{R} \right)^2 f_i + b_2 f_i'' + b_3 W_i'' = 0; \quad i = 1, 2, \dots, 2K \\ - \left[a_2 + 2/(1-\nu) E_{xxp} \right] \left(\frac{in}{R} \right)^2 f_i' + b_2 f_i''' + b_3 W_i''' = 0, \quad (3.50d)$$

$$i = 1, 2, \dots, 2K$$

Note that Eq. (3.42) is employed to eliminate f_0'' from the remaining equations, and there are no boundary conditions with reference to (f_0'') . Thus, the number of boundary conditions, at the $x = \text{constant}$ boundaries, is equal to $(6K + 2)$ instead of $(6K + 4)$.

Similarly, the expressions for the total potential, U_T , average end shortening, e_{AV} , and "unit end shortening", e , can be written in terms of f_i ($i = 1, 2, \dots, 2K$) and W_i ($i = 0, 1, 2, \dots, K$).

$$\begin{aligned}
 U_T = \pi R \int_0^L \left[\frac{1}{E_{xxp}} \left\{ \frac{\beta_2}{d_{11}^2} \left[-\frac{W_0}{R} - q_{11} W_0'' + a_2 \bar{N}_{xx} \right. \right. \right. \\
 + \frac{n^2}{4R^2} \sum_{i=1}^K i^2 (W_i + 2W_i^0) W_i \left. \right]^2 + \frac{1}{2} \sum_{i=1}^{2K} \left[\beta_1 \left(\frac{in}{R} \right)^4 f_i^2 \right. \\
 + \beta_2 f_i'^2 - \beta_3 \left(\frac{in}{R} \right)^2 f_i f_i'' + \beta_4 \left(\frac{in}{R} \right)^2 f_i'^2 \left. \right] \Big\} + D \left\{ \alpha_2 W_0''^2 \right. \\
 \left. + \frac{1}{2} \sum_{i=1}^K \left[\alpha_1 \left(\frac{in}{R} \right)^4 W_i^2 + \alpha_2 W_i''^2 - \alpha_3 \left(\frac{in}{R} \right)^2 W_i' W_i' \right. \right. \\
 \left. \left. + \alpha_4 \left(\frac{in}{R} \right)^2 W_i'^2 \right] \right\} - \bar{N}_{xx} \left\{ W_0' (W_0' + 2W_0^{0'}) \right. \\
 \left. + \frac{1}{2} \sum_{i=1}^K \left[W_i' (W_i' + 2W_i^{0'}) \right] \right\} \Big] dx \\
 + 2\pi R a_3 \bar{N}_{xx} \int_0^L W_0'' dx - \bar{N}_{xx}^2 \frac{\pi R L \beta_1}{E_{xxp}}
 \end{aligned} \tag{3.51}$$

$$\begin{aligned}
 e_{AV} = a_1 \bar{N}_{xx} + \frac{1}{L} \int_0^L \left\{ \frac{a_2}{d_{11}} \left[\frac{W_0}{R} + q_{11} W_0'' + a_2 \bar{N}_{xx} \right. \right. \\
 - \frac{n^2}{4R^2} \sum_{i=1}^K i^2 (W_i + 2W_i^0) W_i \left. \right] - a_3 W_0'' \\
 \left. + \frac{1}{2} W_0' (W_0' + W_0^{0'}) + \frac{1}{4} \sum_{i=1}^K W_i' (W_i' + W_i^{0'}) \right\} dx
 \end{aligned} \tag{3.52}$$

$$\begin{aligned}
e = & a_1 N_{xx} + \frac{1}{L} \int_0^L \left[\frac{a_2}{d_{11}} \left[\frac{w_0}{R} + q_{11} w_0'' + a_2 \bar{N}_{xx} \right. \right. \\
& - \frac{n^2}{4R^2} \sum_{i=1}^K i^2 (w_i + 2w_i^0) w_i \left. \right] + \sum_{i=1}^{2K} \left[q_1 \left(\frac{in}{R} \right)^2 f_i \right. \\
& - a_2 f_i'' - a_3 \sum_{i=0}^K w_i'' + a_4 \sum_{i=1}^K \left(\frac{in}{R} \right)^2 w_i \\
& \left. + \frac{1}{2} \left[\sum_{i=0}^K w_i' \right] \sum_{i=0}^K (w_i' + 2w_i^{0'}) \right] dx
\end{aligned} \tag{3.53}$$

The solution methodology employed is described below, and it involves two solution schemes, one for finding equilibrium positions up to the limit point and one past the limit point.

First, a generalization of Newton's method [27,28], applicable to differential equations, is employed to reduce the nonlinear field equations, Eqs. (3.42)-(3.45) and appropriate boundary conditions to a sequence of linearized systems. In this method, the iteration equations (linearized system) are derived by assuming that the solution can be achieved by a small correction to an approximate solution.

For finding pre-limit point equilibrium positions, the applied load level, \bar{N}_{xx} , is taken as known, the linear ($n=0$) solution is taken to be the approximate solution, and the small corrections (in w_i 's, and f_i 's) are obtained through the solution of the linearized (with respect to the corrections) differential equations. Note that, in this range, the stiffness matrix is positive definite.

For finding post-limit point equilibrium positions (in a range of negative stiffness matrix), the numerical scheme is modified. The load

parameter, \bar{N}_{xx} , is taken to be unknown, and one of the displacement parameters W_i replaces it as a known parameter. Great care must be exercised in choosing this W_i . This is done by observing how the various W_i 's change with \bar{N}_{xx} changes in the pre-limit point range, and choosing a W_i that tends to increase in a smooth and continuous manner, but most importantly is one of the most dominant displacement terms. In this post-limit point range, the linear solution cannot be taken as the initial estimate for the needed iterations. Therefore, the last converged, pre-limit point solution is used as an initial estimate for finding the first post-limit point solution. From there on, in this same range, the previous solution is utilized as an initial estimate. Needless to say that this latter procedure may also be used in the pre-limit point range, starting near the undeformed position. Unfortunately, this procedure is not very economical with regard to computer time and, therefore, it is very inefficient in this range.

It is decided to increase the number of dependent variables from $(3K + 1) (W_0, W_1, \dots, W_K, f_1, f_{2K})$ to $(6K + 2) (W_0, W_1, \dots, W_K, f_1, \dots, f_{2K}, \eta_0, \eta_1, \dots, \eta_K, \xi_1, \dots, \xi_{2K})$

where

$$\eta_i = W_i'' \quad i = 0, 1, 2, \dots, K$$

and

$$\xi_j = f_j'' \quad j = 1, 2, \dots, 2K$$

(3.54)

The reason for this reduction of the order of the field equations, but increase of the number of the field equations, is related to the solution scheme, which is based on the finite difference procedure. In finite differences, it is convenient to keep the order of differential equations as low as possible (first and second order preferably). Then, the

linearized (in the increments) field equations, Eqs. (3.43)-(3.45), the transformation equations, Eqs. (3.54), and boundary terms, can be written in matrix form, as shown below:

Field Equations

$$[R] [Z''] + [S] [Z'] + [T] [Z] = \{g\} \quad (3.55)$$

Boundary Terms

$$[\bar{S}] [Z'] + [\bar{T}] [Z] = \{\bar{g}\} \quad (3.56)$$

where $\{Z\}$ is the vector of the $(6K + 2)$ unknowns. Note that when the load parameter is considered as a known term, then

$$\{Z\}^T = \{W_0, W_1, \dots, W_K, f_1, f_2, \dots, f_{2K}, \eta_0, \eta_1, \dots, \eta_K, \xi_1, \xi_2, \dots, \xi_{2K}\} \quad (3.57)$$

On the other hand, if a certain W_j (chosen dominant term) is considered as a known term, this W_j is removed from vector $\{Z\}$, Eq. (3.61), and it is replaced by the load parameter.

Also, note that $[R]$, $[S]$, $[T]$, $[\bar{S}]$, $[\bar{T}]$, $\{g\}$, and $\{\bar{g}\}$ in Eqs. (3.55) and (3.56) contain known terms (associated with initial approximate solution and applied known increments). The ordinary differential equations are next cast into the form of finite difference equations. Thus, the linear differential equations, Eqs. (3.55) and (3.56) are changed into a system of linear algebraic equations. The usual central difference formula is used at all mesh points, l , i.e.,

$$\begin{aligned} Z'_l &= (Z_{l+1} - Z_{l-1})/2\Delta \\ Z''_l &= (Z_{l+1} - 2Z_l + Z_{l-1})/\Delta^2 \end{aligned} \quad (3.58)$$

Note that, since the second derivatives in W_i and f_i are taken as independent variables, Eqs. (3.54), the second of Eqs. (3.58) is only applied to the fourth derivatives of W_i and f_i .

By using one fictitious point outside the cylinder at each end, one obtains a system of $(6K + 2) \times (NP + 2)$ linear difference equations. (Note that NP stands for number of mesh points.) These equations are solved by an algorithm which is a modification of the one described in [29]. A computer program has been written for the Georgia Tech high speed digital computer CDC-CYBER-70, Model 74-28. The listing and flow chart are given in the Appendices B and A respectively.

In generating data, in order to investigate pre- and post-limit point behavioral response of axially loaded cylindrical shells, the solution procedure goes as follows: first, the system of equations is solved for a small level of the applied load, \bar{N}_{xx} , (taken as known). Then, solutions are sought for step increases in \bar{N}_{xx} , until the process fails to converge. The load level at which the solution fails to converge is a measure of the limit point or critical load (see [25]). As explained in [25], when approaching the critical load, the increment in the applied load must be small and the sign of the determinant of the coefficients of the response must be checked. If convergence fails, the load level is over the limit point. But if convergence does not fail and the sign of the determinant changes from what it was at the previous load level, then the load level is also over the limit point. Desired accuracy can be achieved by taking smaller and smaller increments in \bar{N}_{xx} . Note that a cost penalty must be paid for improving the accuracy in \bar{N}_{xx} or by this approach. It is also observed that by employing this procedure (algorithm in which \bar{N}_{xx} is known and the response, W_i, f_i , is unknown), no solution can be obtained

past the limit point. Because of this, the new algorithm is employed at this point of the solution procedure. The new algorithm, as already explained, simply changes the role of one of the displacement terms with that of the applied load \bar{N}_{xx} . While the first procedure is followed, the most dominant displacement term is identified (or a group of terms). At some level before the limit point, the procedure is switched and a solution is formed that corresponds to an increment in the chosen dominant displacement parameter. To this end, the previous solution is used as an initial solution. The procedure is continued until the entire post-limit point response is obtained. During this phase of the solution procedure, some convergence failures can also occur. These failures can be attributed to one of two reasons: (a) either the increment in the dominant displacement parameter is too large or (b) the NP (number of mesh points) is too small for an accurate description of the response. Both of these can easily be corrected. In this second phase, large increments are purposely used in order to save computer time. If the solution fails to converge, then the increment is automatically reduced.

Numerical integration is used to find the total potential and end shortening. By this solution procedure, the entire load-displacement or load-end shortening curves can be obtained for a given imperfection and each wave number n .

Numerical Results and Discussion

Numerical results are obtained for two geometries, one unstiffened and one stiffened, for axially loaded cylindrical shells.

The geometry for both is described below:

(a) Unstiffened Cylindrical Shell

$R = 4 \text{ in.}, t = 0.004 \text{ in.}, 0.008 \text{ in.}, 0.016 \text{ in.}, 0.050 \text{ in.};$

$$L = 4 \text{ in.}, 12 \text{ in.}, 20 \text{ in.}, 40 \text{ in.};$$

$$E = 10.5 \times 10^6 \text{ psi}; \nu = 0.3; \text{ with} \quad (3.59)$$

$$W^0(x,y) = t\xi \left[-\cos \frac{2\pi x}{L} + 0.1 \sin \frac{\pi x}{L} \cos \frac{\pi y}{R} \right]$$

and SS-3 Boundary Conditions, Eqs. (3.32)

(b) Ring and Stringer-Stiffened Cylindrical Shell

$$R = 4 \text{ in.}; t = 0.04 \text{ in.}; L = 4 \text{ in.},$$

$$e_x = \pm 0.24 \text{ in.}; e_y = \pm 0.12 \text{ in.}; (+ \text{ for internal stiffeners})$$

$$E = 10.5 \times 10^6 \text{ psi}; \nu = 0.3; \quad (3.60)$$

$$\lambda_{xx} = 0.910; \lambda_{yy} = 0.455; \rho_{xx} = 100; \rho_{yy} = 20; \text{ with}$$

$$W^0_{(x,y)} = h\xi \sin \frac{\pi x}{L} \cos \frac{\pi y}{R}; \text{ SS-3 Boundary Conditions, Eqs. (3.32)}$$

Before discussing the results, a few more clarifying remarks about the geometry are needed. The unstiffened geometry is taken from [25] and [30]. Note that in these references only the critical load is given and not the complete behavior. This geometry employs, virtually, an axisymmetric imperfection. Note that the non-axisymmetric amplitude is 10% of the axisymmetric amplitude. A smaller value was tried (1% for the non-axisymmetric amplitude) and the response (see Fig. 3.2; $R/t = 500$) is, for all purposes, identical to that of geometry (a). The only difference is the value for $\bar{N}_{xx_{cr}}$ (limit-point load). This difference only reflects the effect of imperfection amplitude, i.e., for $\xi = 1$, $N_{xx_{cr}} = 12.24 \text{ lbs/in.}$ for 1% non-axisymmetric amplitude, while $N_{xx_{cr}} = 11.44 \text{ lbs/in.}$ for 10% non-axisymmetric amplitude. Note that, in the former case, the maximum imperfection amplitude is $1.01h$ while in the latter it is $1.10h$. The

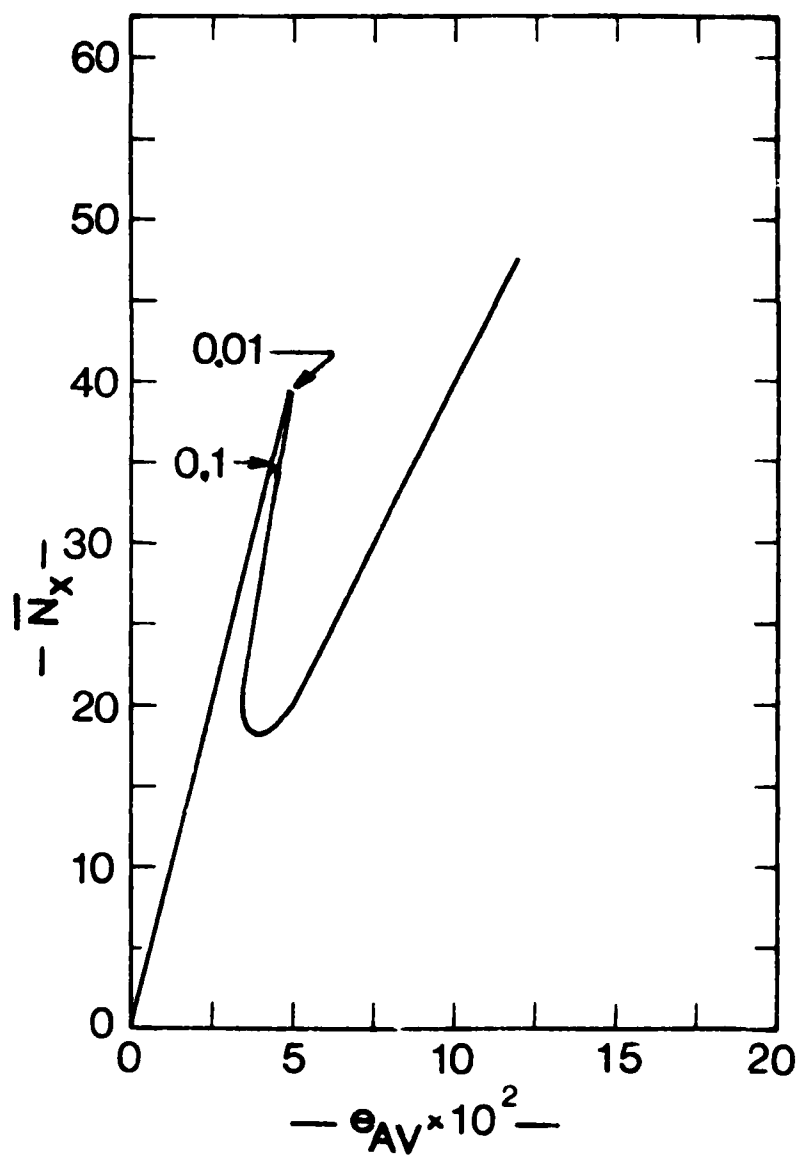


Fig. 3.2 Effect of the Asymmetric Imperfection Amplitude ($R/t = 500$; $L/R = 1$; $n = 10$).

classical load for this case is 25.42 lbs/in. The reason that the 10% amplitude is used in the numerical results obtained is that the higher the non-axisymmetric amplitude, the faster the solution. Moreover, in this geometry, ξ is varied from zero to four, in order to study the effect of imperfection amplitude. Note that for the chosen imperfection,

$$w_{\max}^0/h = 1.1\xi \quad (3.61)$$

Finally, results are generated for several values of n (number of circumferential full waves). This is needed in order to obtain a clear picture of the complete response.

The stiffened geometry corresponds to examples 14, 16, 18, 19, and 21 of [25]. Again, note that in [25], only limit-point loads were obtained. Moreover, in [25], SS-3 boundary conditions are used, but with $M_{xx} = 0$ [see Eqs. (3.37)]. In the present work, SS-3 with $M_{xx} = a_3 \bar{N}_{xx}$ boundary conditions are employed [see Eqs. (3.32)]. In addition to the difference in SS-3 boundary conditions, difference in response for the stiffened geometries lies in the fact that a term ($a_2 \bar{N}_{xx}$) is missing from Eq. (20a) of [25]. This omission has been corrected in the present work [see Eq. (3.42)]. The most important results are presented in graphical form and tabular form. In the ensuing discussion, including conclusions, the statements are based on all generated data.

Tables 3.1 and 3.2 present the various unstiffened geometries for which results are obtained (axial compression). Table 3.1 also gives values of critical static and dynamic loads, as well as minimum post-limit point loads and the linear theory (classical) static critical loads. Finally, for each example, it gives the number of mesh points used in the finite difference scheme and the value of n . Table 3.2 summarizes

TABLE 3.1 Axially-Loaded Unstiffened Cylindrical Shells

SS-3; R = 4.; E = 10.5 × 10⁶; ν = 0.3

$$w^0(x,y) = -\xi t \cos \frac{2\pi x}{L} + 0.15t \sin \frac{\pi x}{L} \cos \frac{\pi y}{R}$$

No	L in.	t in.	L/R	R/t	ξ	classical N _{xx} lbs/in	N _{xx} ^L lbs/in	N _{xx} ^m lbs/in	N _{xx} ^d lbs/in	n	No. mesh pts.	λ ^L	λ ^m	λ ^d
1	4.0	0.004	1.0	1,000	0.5	25.42	24.44	1.174	20.420	8	55	0.961	0.046	0.803
2							24.13	0.524	17.740	9	55	0.949	0.021	0.698
3							23.46	1.027	14.920	10	55	0.922	0.040	0.587
4							20.71	2.050	13.199	11	35	0.815	0.081	0.519
5							17.55	3.456	11.059	12	35	0.690	0.136	0.435
6							16.61	4.804	10.199	13	35	0.653	0.189	0.401
7							17.17	6.025	10.142	14	35	0.675	0.237	0.399
8	4.0	0.004			1.0		24.21	0.977	19.460	8	55	0.952	0.038	0.766
9							23.44	0.565	16.139	9	55	0.922	0.022	0.635
10							19.22	1.310	12.550	10	35	0.756	0.052	0.494
11							14.16	2.521	9.538	11	35	0.557	0.099	0.375
12							11.86	3.860	8.110	12	35	0.467	0.152	0.319
13							11.34	5.169	7.789	13	35	0.446	0.203	0.306
14	4.0	0.004			4.0		20.98	2.083	15.770	7	35	0.825	0.082	0.620
15							8.47	1.780	6.944	8	35	0.333	0.070	0.273
16							3.30	2.000	2.874	9	35	0.130	0.078	0.113
17							2.10*	---	---	10	35	0.083	---	---
18							2.30*	---	---	11	35	0.091	---	---
19							3.40*	---	---	12	35	0.134	---	---
20							4.50*	---	---	13	35	0.177	---	---
21							5.85*	---	---	14	35	0.230	---	---

TABLE 3.1 Axially-Loaded Unstiffened Cylindrical Shells (Cont'd.)

No	L in.	t in.	L/R	R/t	ξ	classical N_{xx} lbs/in	N_{xx}^d lbs/in	N_{xx}^m lbs/in	N_{xx}^d lbs/in	n	No. mesh pts.	λ^d	λ^m	λ^d
22	4.0	0.008	1.0	500	1.0	101.81	98.75	19.01	89.46	6	65	0.970	0.187	0.879
23							91.84	10.90	68.95	7	65	0.902	0.107	0.677
24							65.33	7.80	46.09	8	35	0.642	0.077	0.453
25							43.24	12.29	31.17	9	35	0.425	0.121	0.306
26							35.00	17.98	26.09	10	35	0.344	0.177	0.256
27							35.17	24.10	26.46	11	35	0.345	0.237	0.260
28							39.18	29.97	---	12	35	0.385	0.295	---
29							45.30	34.89	---	13	35	0.445	0.343	---
30	4.0	0.016	1.0	250	1.0	407.23	406.00	---	---	4	35	0.997	---	---
31							362.50	---	291.21	5	35	0.890	---	0.715
32							257.90	42.89	187.42	6	35	0.633	0.105	0.460
33							138.30	51.55	106.41	7	35	0.340	0.127	0.261
34							101.10	72.15	80.61	8	35	0.248	0.177	0.198
35							104.90	97.79	---	9	35	0.258	0.240	---
36							129.00	126.30	---	10	35	0.313	0.310	---
37	4.0	0.05	1.0	80	1.0	3977.00	3500.00	2509.00	2894.00	3	35	0.880	0.631	0.728
38							1356.00	683.80	1103.20	4	35	0.341	0.172	0.277
39							623.80	599.70	---	5	35	0.157	0.151	---
40							675.00*	---	---	6	35	0.169	---	---
41	20.0	0.016	5.0	250	1.0	407.23	621.40	108.40	382.04	3	35	1.526	0.266	0.938
42							292.80	47.79	174.16	4	35	0.719	0.117	0.428
43							353.20	137.00	188.48	5	35	0.867	0.336	0.463
44	32.0		8.0				355.80	132.90	190.00	3	65	0.873	0.326	0.466
45							408.60	178.90	212.12	4	65	1.003	0.439	0.521

TABLE 3.1 Axially-Loaded Unstiffened Cylindrical Shells (Cont'd.)

No	L in.	t in.	L/R	R/t	ξ	classical N_{xx} lbs/in	N_{xx}^f lbs/in	N_{xx}^m lbs/in	N_{xx}^d lbs/in	n	No. mesh pts.	λ^d	λ^m	λ^d
46	40.0	0.016	10.0	250	1.0	407.23	910.20	---	545.18	2	65	2.235	---	1.339
47	→	→	→	→	→	→	356.30	159.60	193.21	3	65	0.875	0.392	0.474
48	→	→	→	→	→	→	537.80	175.30	214.39	4	65	1.321	0.430	0.526
49	→	→	→	→	→	→	402.30	---	---	5	65	0.988	---	---
50	4.0	0.05	1.0	80	0.08	3977.00	3287.00	---	---	5	35	0.826	---	---
51	→	0.008	1.0	500	1.0	101.81	39.38	18.08	27.42	10	35	0.387	0.178	0.269
52	→	0.05	1.0	80	0.32	3977.00	2234.00	766.70	1595.43	5	35	0.562	0.193	0.401
53	12.0	0.016	3.0	250	1.0	407.23	416.20	46.00	---	4	35	1.020	0.113	---
54	→	→	→	→	→	→	242.40	53.05	162.05	5	35	0.595	0.130	0.398
55	→	→	→	→	→	→	265.00	---	---	6	35	0.651	---	---
56	→	→	→	→	→	→	315.00	---	---	7	35	0.774	---	---
57	→	→	→	→	→	→	361.10	---	---	8	35	0.887	---	---

*Change of slope (not a critical load); see Fig. 3.5.

TABLE 3.2 Summary of Results for Axially-Loaded Unstiffened Shells

R/t	L/R	ξ	classical \bar{N}_{xx} lbs/in	\bar{N}_{xx}^l lbs/in	\bar{N}_{xx}^m lbs/in	\bar{N}_{xx}^d lbs/in	n	λ^l	λ^m	λ^d	n^l	n^m
1000	1	0.5	25.42	16.61	0.5244	10.1996	8-13	0.653	0.0206	0.401	13	9
1000	1	1.0	25.42	11.34	0.5649	7.7890	8-13	0.446	0.0222	0.306	13	9
1000	1	4	25.42	2.10*	1.7800	2.8740	7-10	0.096	0.0700	0.113	10	8
250	1	1	407.23	101.10	42.89	80.61	6-8	0.248	0.1053	0.198	8	6
250	3	1	407.23	242.40	46.00	162.05	4-5	0.595	0.1130	0.398	5	5
250	5	1	407.23	292.80	47.79	174.16	3-5	0.719	0.1174	0.428	4	4
250	8	1	407.23	355.80	132.90	190.00	3-4	0.873	0.326	0.466	3	3
250	10	1	407.23	356.30	159.60	193.21	3-5	0.875	0.3919	0.474	3	3
1000	1	1	25.42	11.34	0.5649	7.7890	8-13	0.446	0.0222	0.306	13	9
500	1	1	101.81	35.00	7.80	26.09	7-11	0.344	0.0766	0.256	10	8
250	1	1	407.23	101.10	42.890	80.61	6-8	0.248	0.105	0.198	8	6
80	1	1	3977.00	623.08	599.700	---	4-6	0.157	0.151	---	5	5
80	1	0.08	3977.00	3287.00	---	---	5	0.826	---	---	5	5
80	1	0.32	3977.00	2234.00	766.70	1595.43	5	0.562	0.193	0.401	5	5

* change of slope (not a critical load); see Fig. 3.5.

the most important results of the study for axially-loaded unstiffened geometries.

The generated data, appearing in Tables 3.1 and 3.2, are also presented in graphical form and a discussion of the various effects is presented. First the results corresponding to $R/t = 1000$ are presented and discussed. For this group, L/R is equal to one.

Fig. 3.3 is a plot of \bar{N}_{xx} versus average end shortening for $\xi = 0.5$ (unstiffened geometry). These data are generated for several values of full waves, n , around the circumference. From this figure, it is clear that, as the system is loaded quasi-statically from zero, the load deflection curve is the same and independent of n . The limit-point load, $\bar{N}_{xx_{cr}}$ is definitely n -dependent. It is observed that the value of the total potential corresponding to the lowest limit load and associated n is the smallest of all values corresponding to the same load and different n 's (at an equilibrium position). For this value of ξ (which corresponds to $W_{max}^0 = 0.55 h$), the limit point occurs at $\bar{N}_{xx} = 16.61 \text{ lbs/in.}$ [$\lambda^L = (\bar{N}_{xx_{cr}} / \bar{N}_{xx_{cl}}) = 0.653$]. In the post-limit point region, the unstable branch shows several changes from $n = 13$ to $n = 12$ to $n = 11$. These changes occur at the unstable portion of the curve. The change from $n = 11$ to $n = 10$, etc., to $n = 8$, occur at the stable portion of the curves. This implies that if one can transverse the post-limit point branches, he would move along the $n = 13$ (with decreasing load) curve, then along the $n = 12$ and $n = 11$ curves (with decreasing load). Then, along the $n = 11$ curve, the system moves with increasing load until it reaches the $n = 10$ curve. Then it moves along the $n = 10$ curve until it intersects the $n = 9$ curve, etc. In reality, though, under dead weight loading, the system reaches the limit point, and then it snaps-through (violent buckling) towards

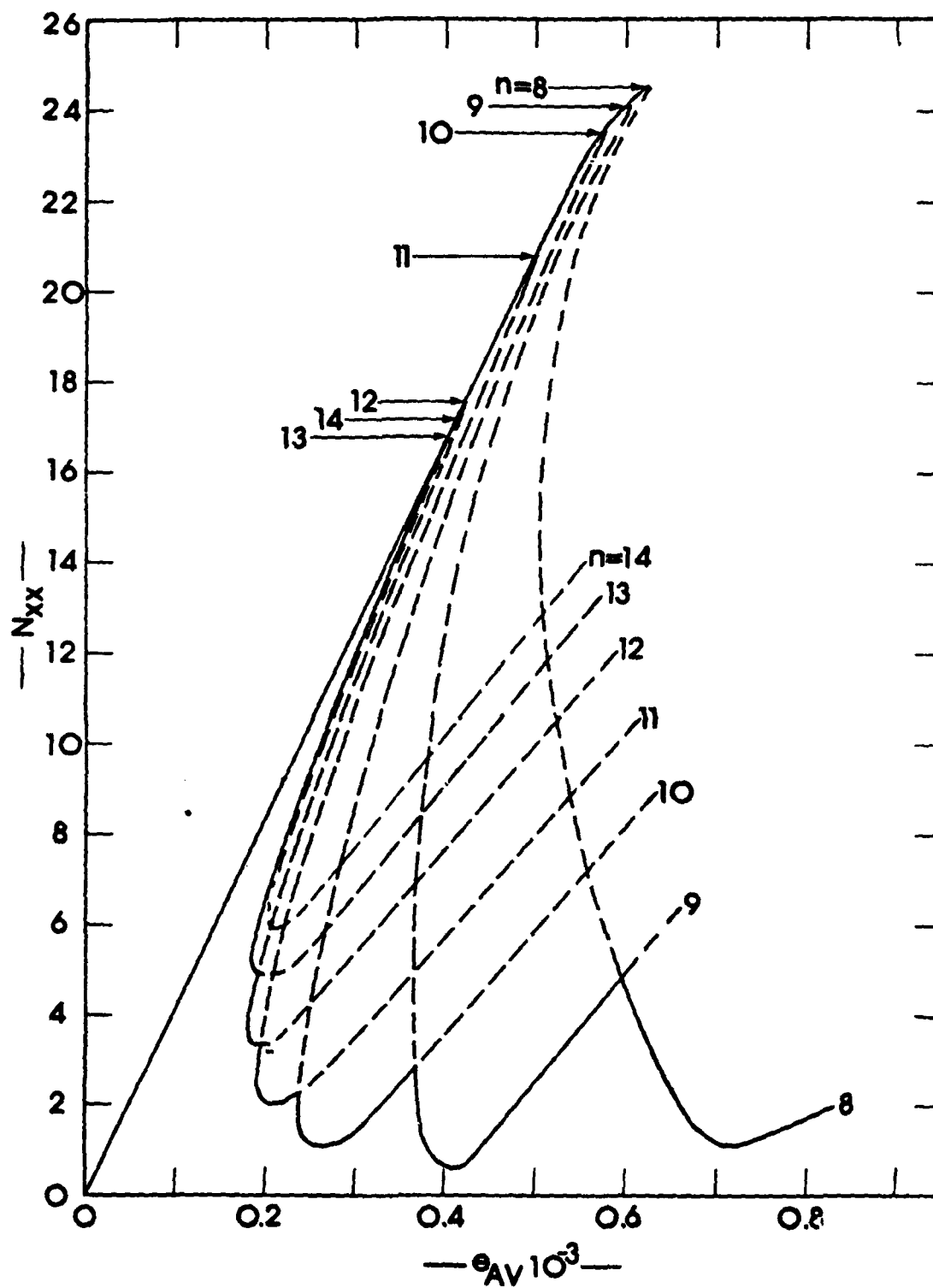


Fig. 3.3 Response of Unstiffened Geometry
($R/t = 1,000$; $L/R = 1$; $\xi = 0.5$)

far stable equilibrium positions. During the snapping process, it is clear from this figure that the shell experiences changes in the circumferential mode, corresponding to various n -values. This phenomenon has been observed experimentally through high-speed photography for very thin and relatively short cylindrical shells.

Fig. 3.4 presents similar data (as Fig. 3.3), but for $\xi = 1$. The behavior is very similar to that corresponding to $\xi = 0.5$. Note that curves corresponding to $n = 13, \dots, 8$ are shown. Data are generated for $n = 14$ and 15 but are not shown on the figure. No data are generated for $n < 8$, because the minimum load (in the post-limit point region) positions correspond to $n = 9$ for both ξ -values (Figs. 3.3 and 3.4). Clearly, the same observations are made concerning violent buckling with changing circumferential mode. Moreover, data are generated for $\xi = 4$ and plotted on Fig. 3.5. Note that for $n \geq 10$, there is no limit point instability, but for $n = 9, 8$, and 7 there exist limit points. The response, though, as the system is loaded quasi-statically from zero, is along the $n = 10$ path and snapping takes place at the load level corresponding to unstable bifurcation (the $n = 10$ and $n = 9$ paths cross). Even for this imperfection amplitude ($\xi = 4$), violent buckling is predicted with change in circumferential mode. Finally, for the unstiffened geometry, Fig. 3.6 presents the effect of the imperfection amplitude, ξ , on the limit-point load, $\lambda^L = \bar{N}_{xx_{cr}} / \bar{N}_{xx_{cl}}$, and on the minimum load, $\lambda^m = \bar{N}_{xx_{min}} / \bar{N}_{xx_{cl}}$. It also presents the effect of imperfection amplitude on the dynamic critical load, λ^d , for the case of constant load of infinite duration. This effect is discussed in a later section. Note that $\bar{N}_{xx_{min}}$ corresponds to the minimum equilibrium load in the post-limit point region. As it can be seen from Fig. 3.6, the shell is extremely sensitive to initial geometric imperfections

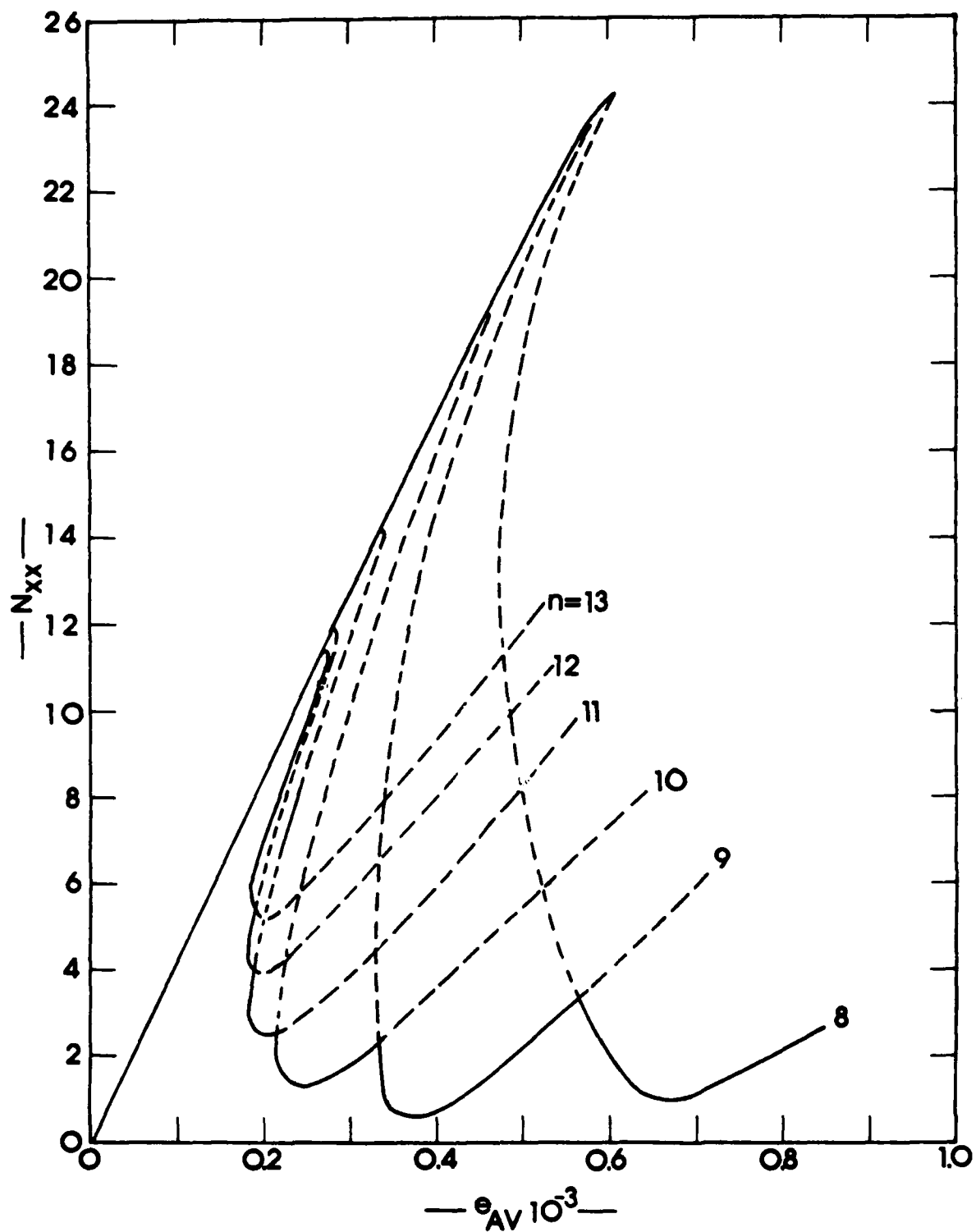


Fig. 3.4 Response of Unstiffened Geometry
($R/t = 1,000$; $L/R = 1$; $\xi = 1.0$)

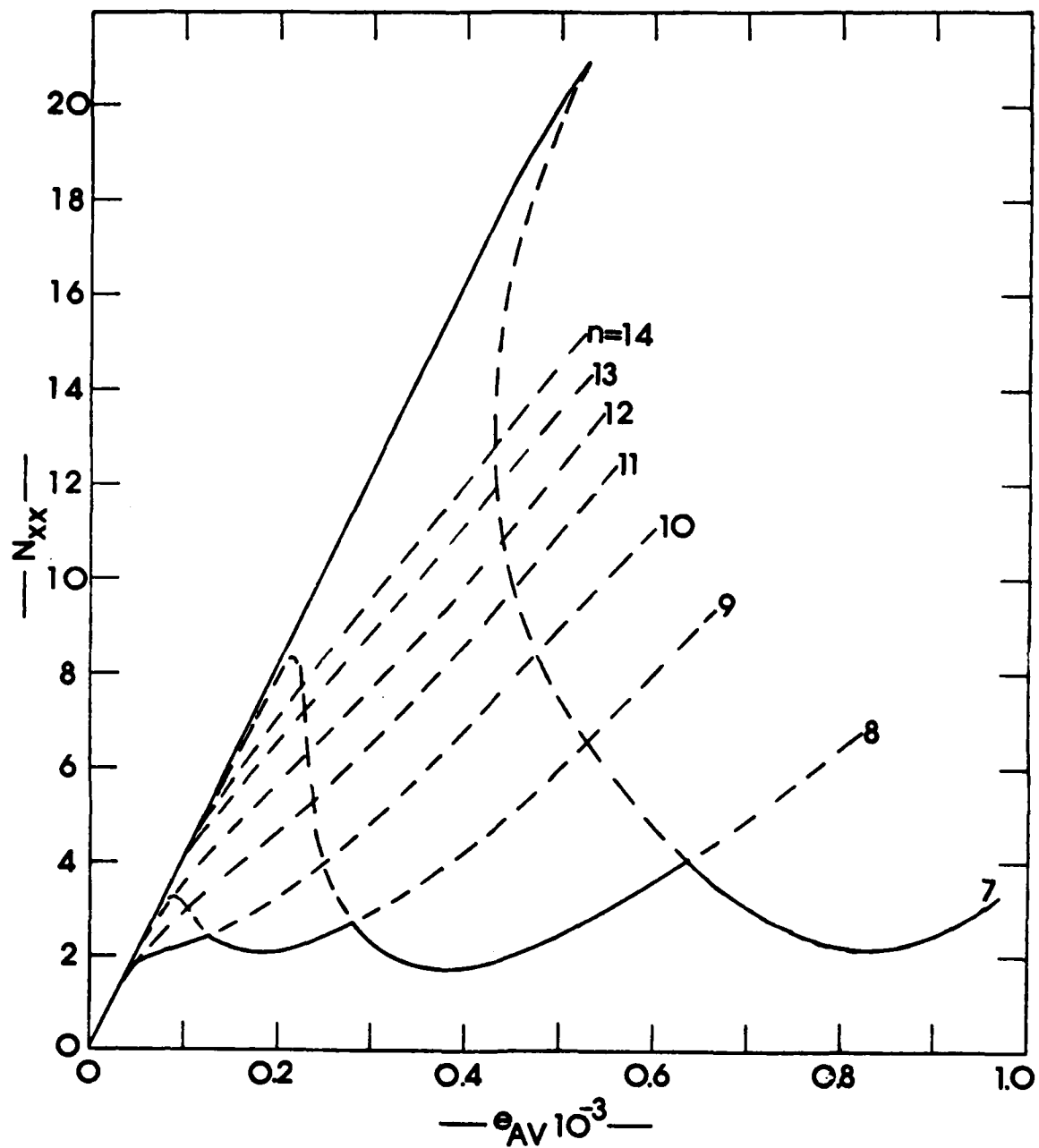


Fig. 3.5 Response of Unstiffened Geometry
($R/t = 1,000$; $L/R = 1$; $\xi = 4.0$)

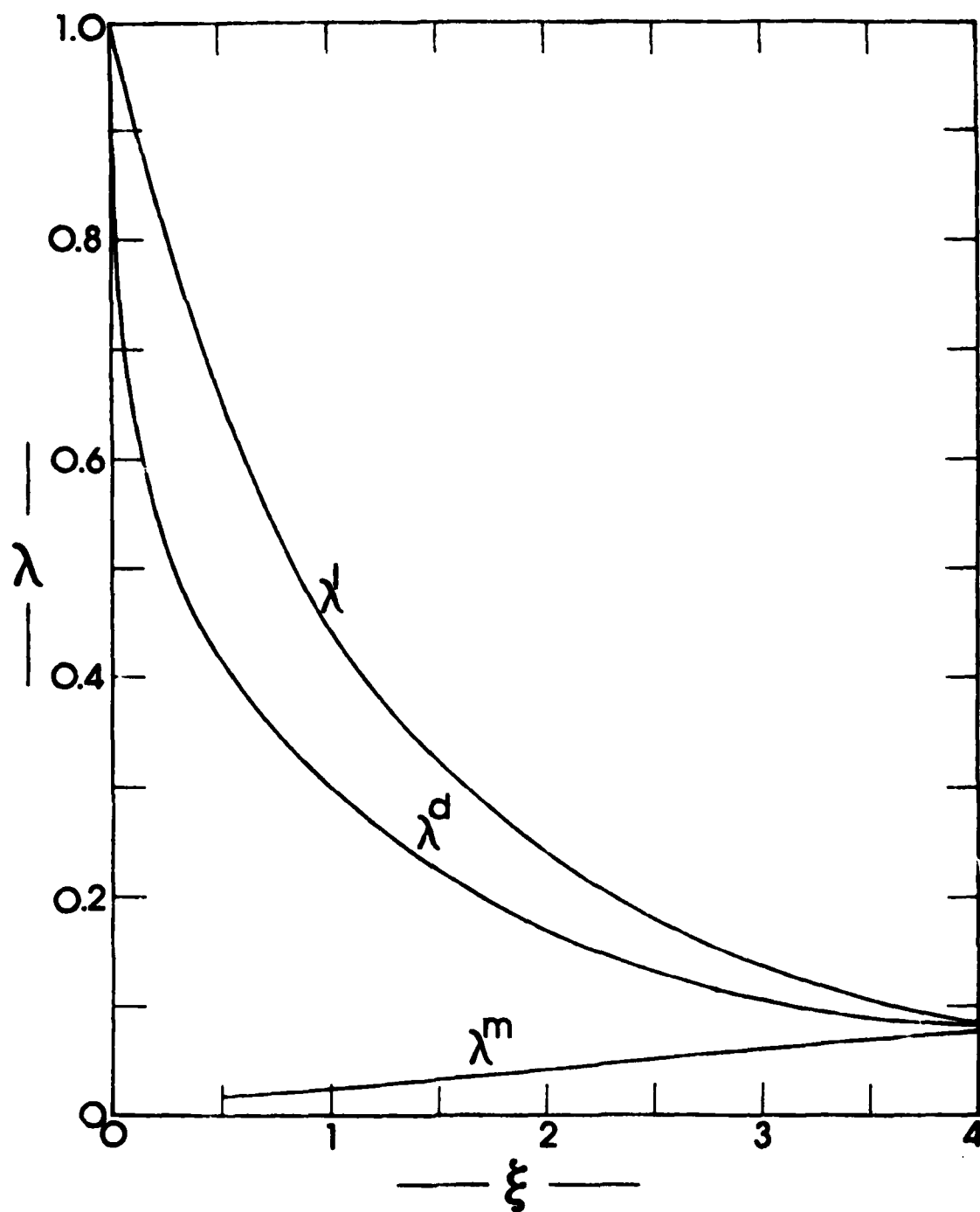


Fig. 3.6 Plots of Load Parameters (λ^l : limit point; λ^d : critical dynamic; λ^m : minimum post-limit point) versus Imperfection Amplitude Parameter.

(of virtually axisymmetric shape). Note that at $\xi = 0.84$, λ^L is equal to one half. Since $W_{\max}^0 = 1.1\xi h$, then $\lambda^L = 0.5$, when $W_{\max}^0 = 0.924 h$. At $\xi = 3.5$, $\lambda^L = 0.1$, and at $\xi = 4$ the values of λ^L and λ^M are almost the same. This means that for $\xi \geq 4$, there is no possibility of snap-through buckling. The cylindrical shell simply deforms, with bending, from the initial application of the load. Finally, Fig. 3.7 presents a composite of Figs. 3.3-3.5, and it includes pre-limit and post-limit point behavior for $\xi = 0.5$, 1.0 and 4.0.

Fig. 3.8 is similar to Fig. 3.4 but for $R/t = 500$. Moreover, Figs. 3.9 and 3.10 fall in the same category. These geometries correspond to Examples 22-40, which along with Examples 8-13 serve to study the effect of R/t on the shell response characteristics. Note that for all of these examples, $\xi = 1.0$ and $L/R = 1$.

Clearly, from Fig. 3.8, it is seen that the response characteristics of the shell are very similar to those corresponding to $R/t = 1000$ (Fig. 3.4). The only difference is that the wave number n corresponding to both the limit point ($n = 11$) and the minimum post-limit point equilibrium load ($n = 8$) are smaller than the ones for $R/t = 1000$. According to Fig. 3.4 these wave numbers are $n = 13$ and $n = 9$ respectively. Note from Figs. 3.9 and 3.10 that this trend continues as R/t decreases, and for $R/t = 80$ $n = 5$ corresponds to both loads. The composite response is shown on Fig. 3.11.

Next, the effect of L/R is examined through examples 30-36, 41-49, and 53-57 (see Table 3.1). All of these geometries correspond to $\xi = 1$ and $R/t = 250$, and L/R varies from one to ten. The results of this study are presented graphically on Figs. 3.9, 3.12, 3.13 and in the composite of Fig. 3.14. It is seen from these figures that as L/R increases, the

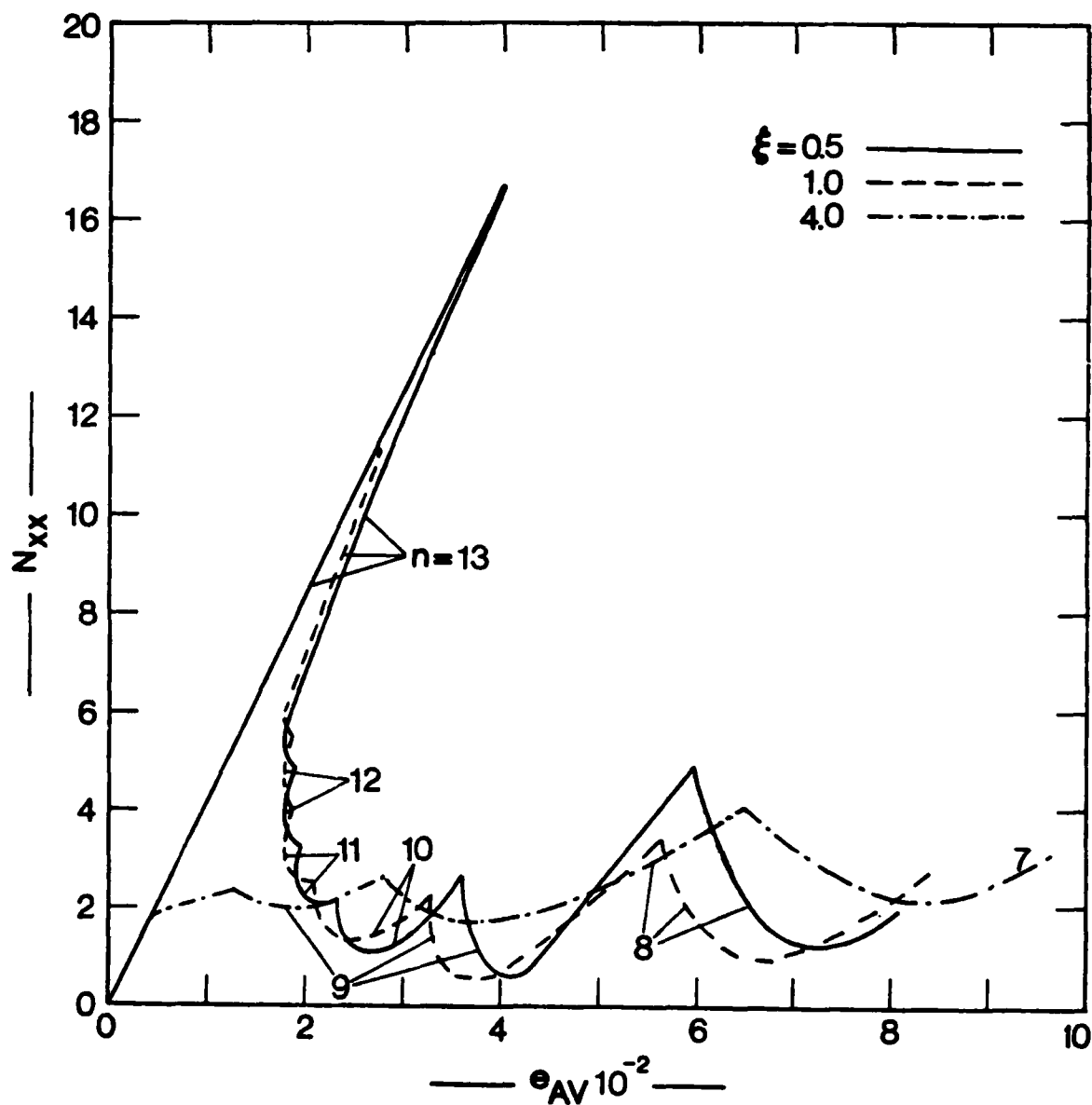


Fig. 3.7 Pre- and Post-Limit Point Response of Unstiffened Geometry ($R/t = 1,000$; $L/R = 1$)

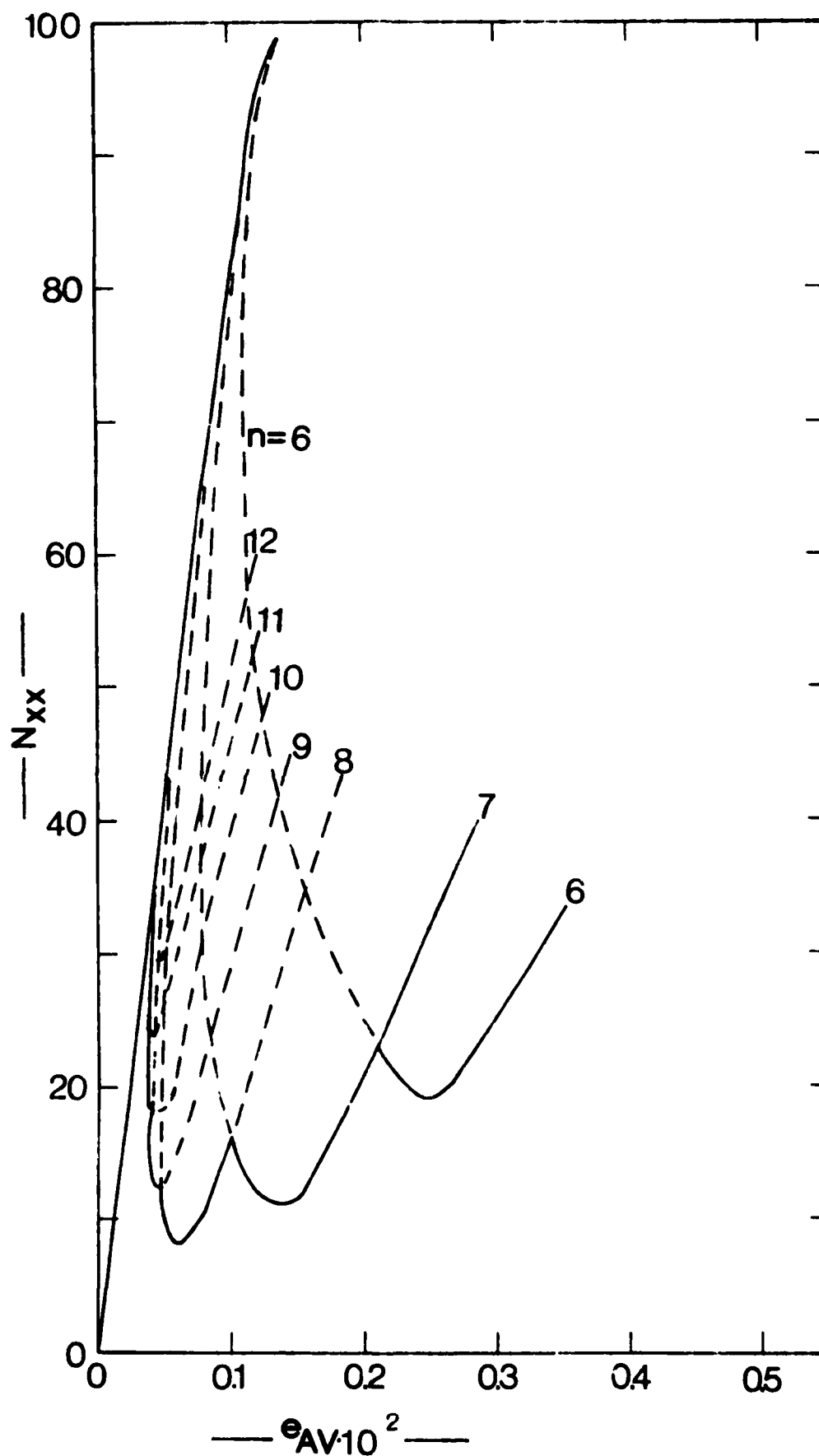


Fig. 3.8 Response of Unstiffened Geometry ($R/t = 500$; $L/R = 1$, $\xi = 1.0$)

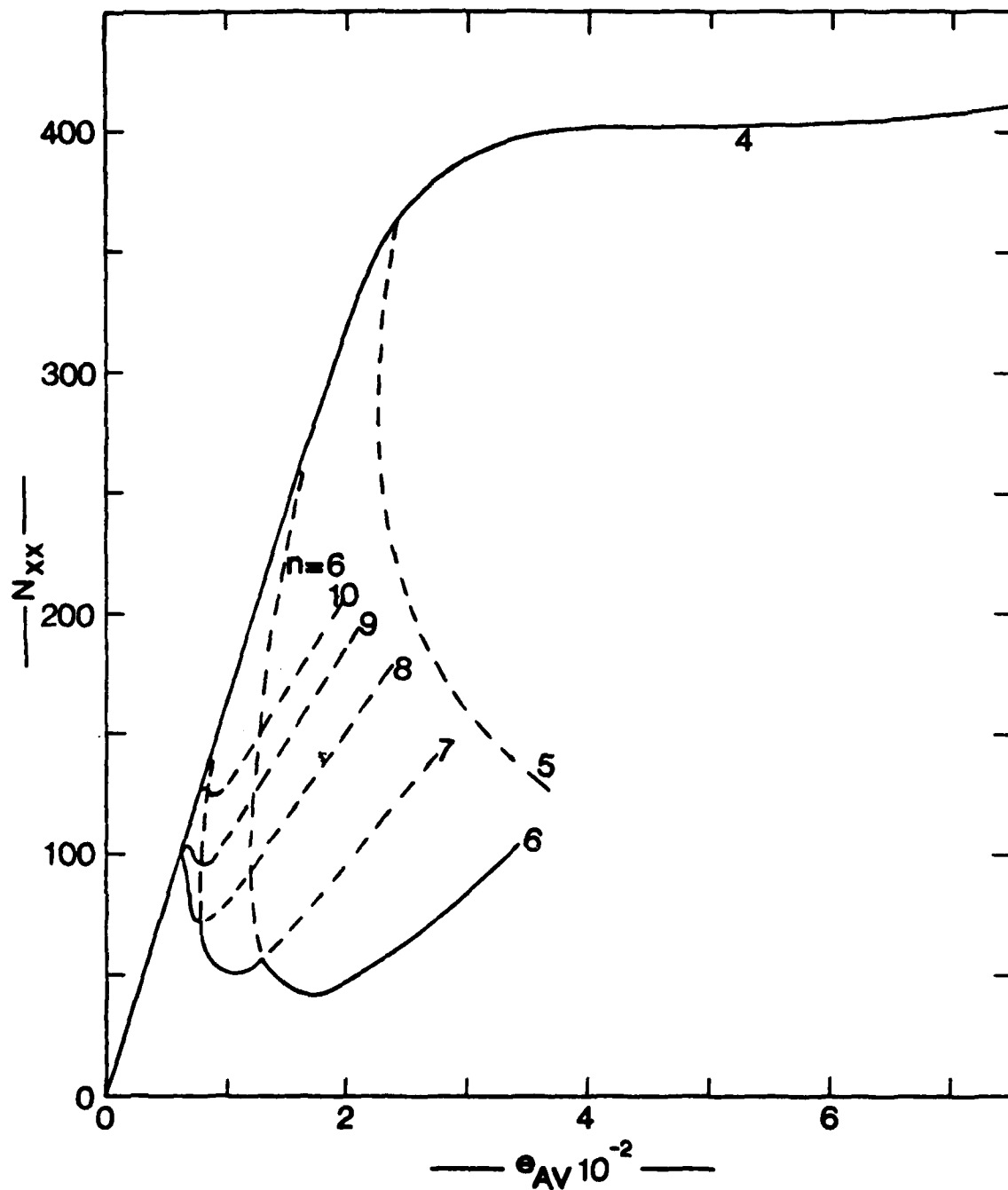


Fig. 3.9 Response of Unstiffened Geometry
($R/t = 250$; $L/R = 1$; $\xi = 1.0$)

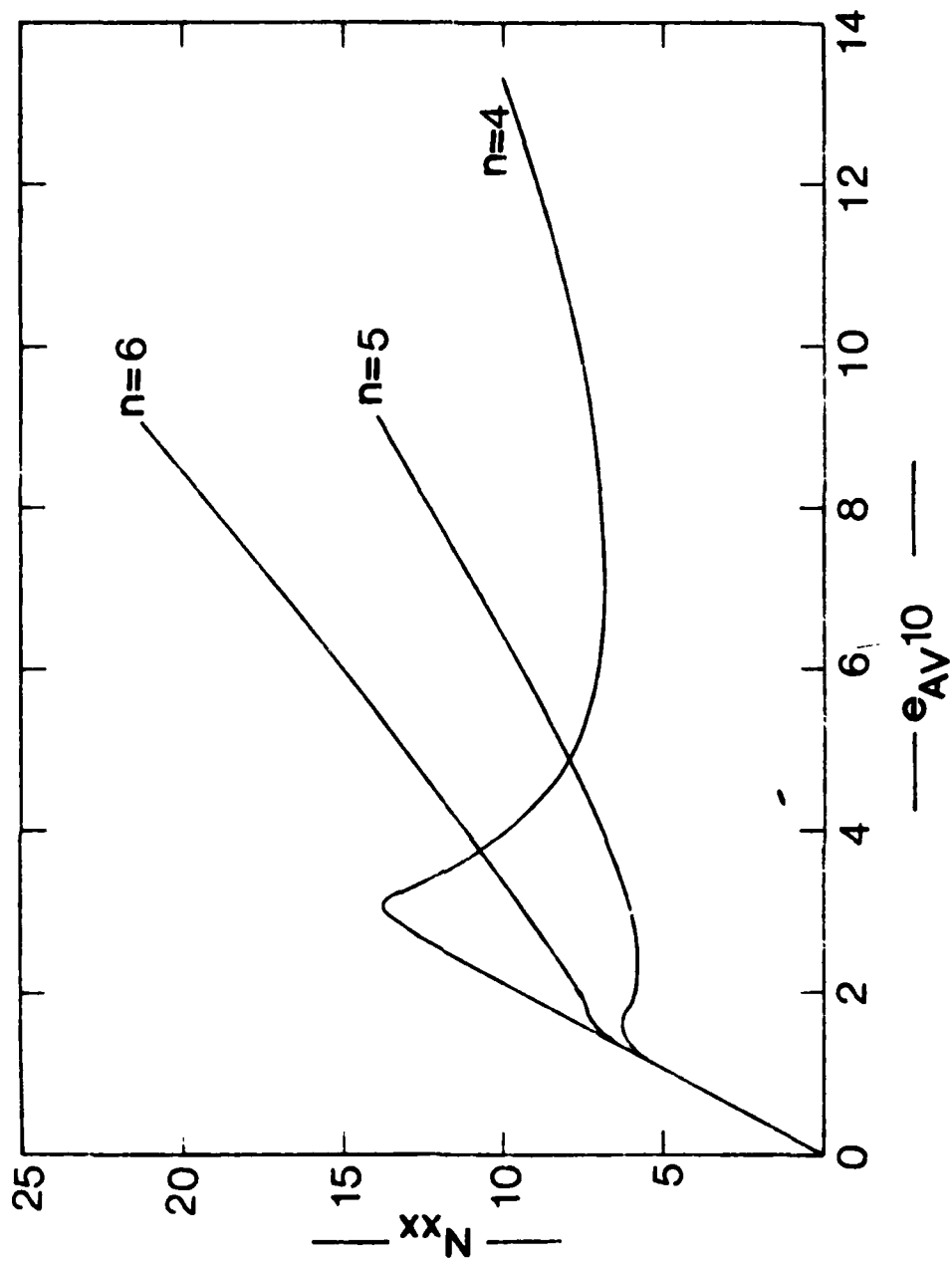


Fig. 3.10 Response of Unstiffened Geometry
($R/t = 80$; $L/R = 1$; $\xi = 1.0$)

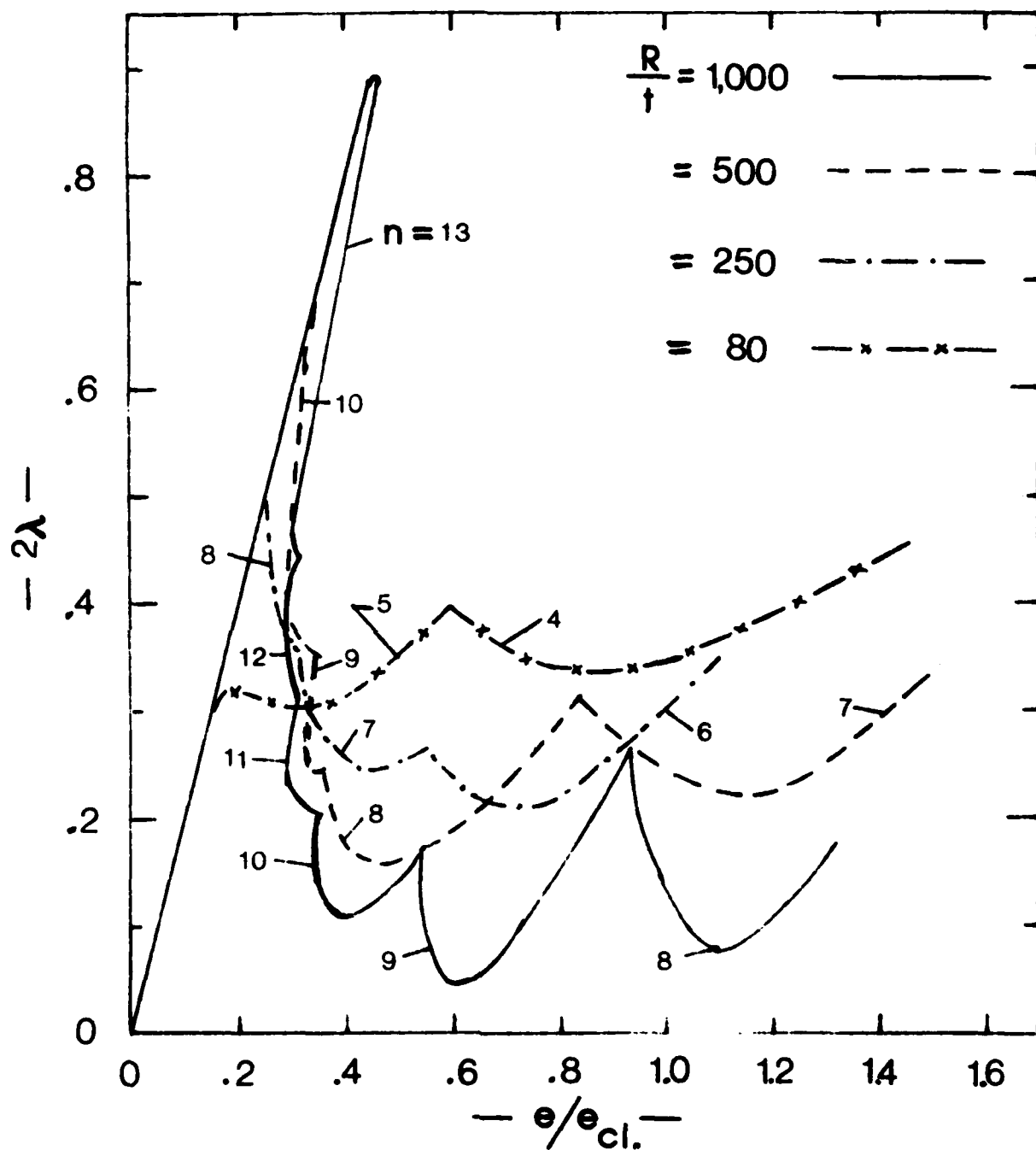


Fig. 3.11 Effect of R/t on the Response of Unstiffened Geometry ($L/R = 1$; $\xi = 1.0$)

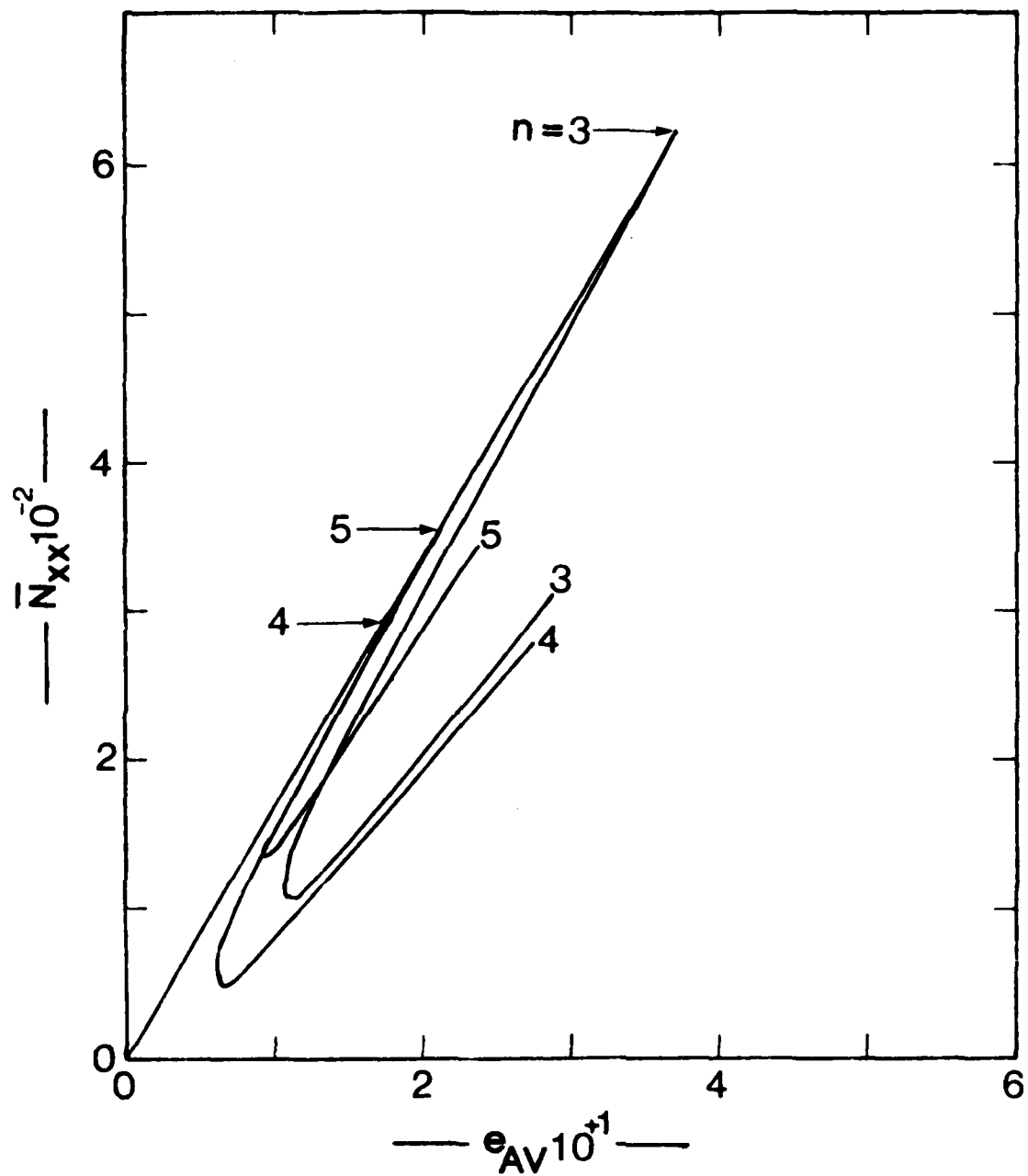


Fig. 3.12 Response of Unstiffened Geometry
($R/t = 250$; $L/R = 5$; $\xi = 1.0$)

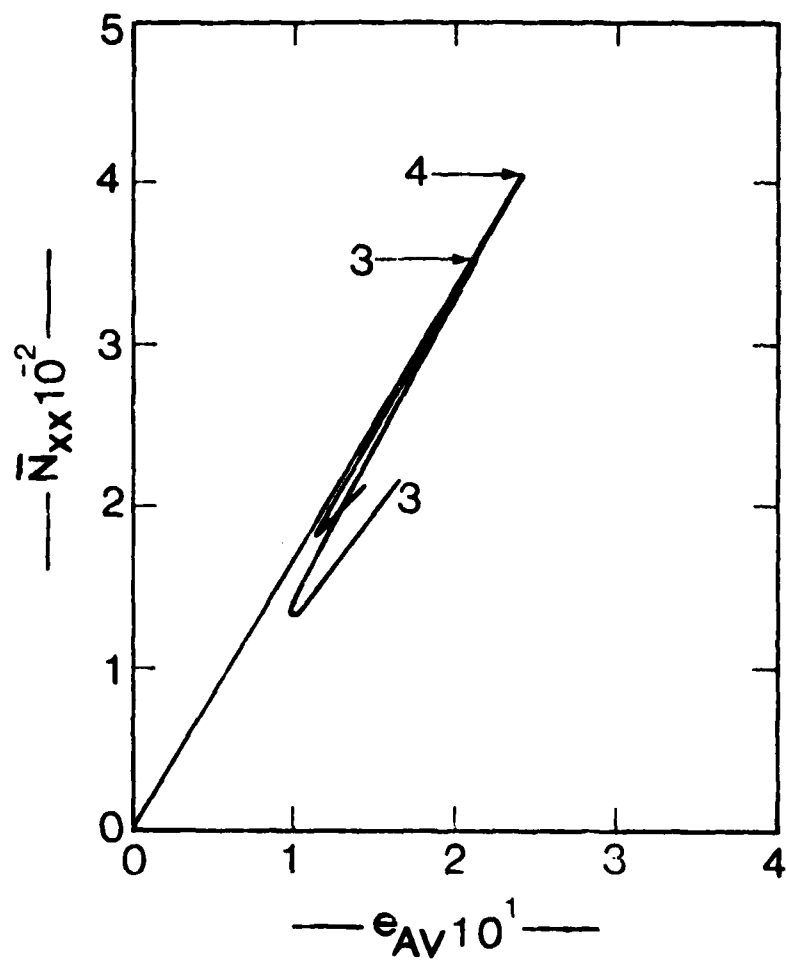


Fig. 3.13 Response of Unstiffened Geometry
($R/t = 250$; $L/R = 8$; $\xi = 1.0$)

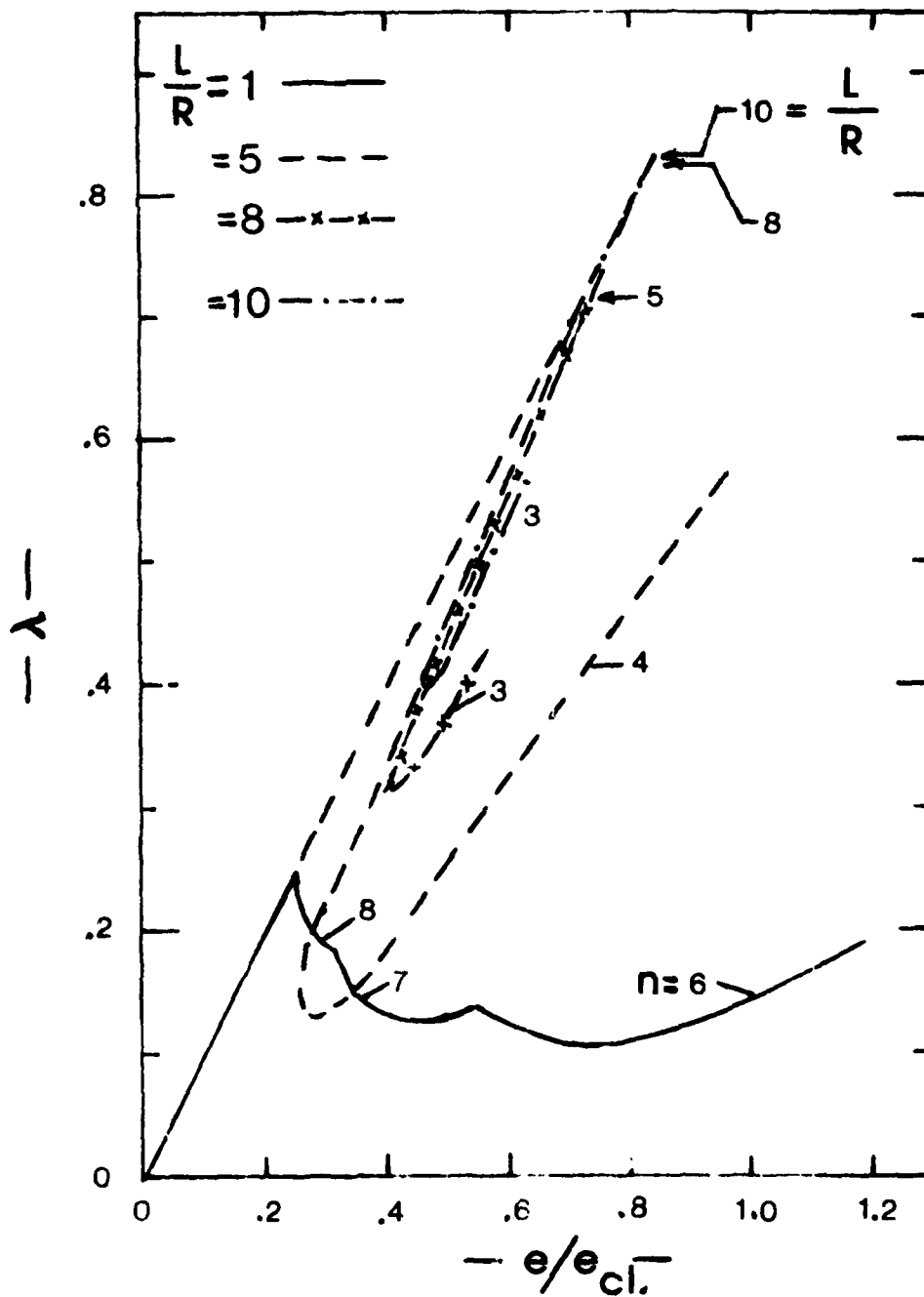


Fig. 3.14 Effect of L/R on the Response of Unstiffened Geometry ($R/t = 250$; $\xi = 1.0$)

entire static equilibrium response corresponds to one wave number ($n = 4$ for $L/R = 5$, $n = 3$ for $L/R = 8$ and 10). Note also that the n -value decreases as L/R increases. This result seems reasonable. In addition, the sensitivity of the shell decreases as L/R increases. This latter effect is better shown on Fig. 3.15. The dynamic results are discussed in a later section.

Finally, Fig. 3.16 presents the effect of R/t on the limit point load, minimum post-limit point load and dynamic critical load. There are two sets of curves, one solid and one dashed. The solid curves correspond to $\xi = 1$ and they imply change in the imperfection amplitude as R/t changes, since the data are generated for a constant R value (4 in.). The dashed line set corresponds to the same imperfection amplitude regardless of the value of the thickness. Note that, when $R/t = 1000$, $t = .004$ in. since $R = 4$ in. From the amplitude of the imperfection, one may relate the solid curve to $\xi = 1$ and the dashed curve to $\xi = 0.016/0.004 = 4$. Thus, it is very reasonable that λ^L corresponding to $\xi = 4$ is much smaller than λ^L corresponding to $\xi = 1$. On the other end of the curve, say $R/t = 100$, the opposite is true. For this value of R/t , $t = 0.04$ in. Then the dashed line curve corresponds to $\xi = \frac{.016}{.040}$, or $\xi = 0.4$, and λ^L corresponding to $\xi = 0.4$ is expected and is larger than λ^L corresponding to $\xi = 1.0$ (solid curve).

For the stiffened geometries, the results are presented on Figs. 3.17-3.19.

The classical values for \bar{N}_{xx} are 35,220 lbs/in. for external positioning of the stiffeners and 19,790 lbs/in. for internal. The geometric imperfection for the stiffened geometries is not axisymmetric but symmetric with respect to y [see Eqs. (3.64)]. This shape is similar to the classical buckling mode, provided that $n = 4$.

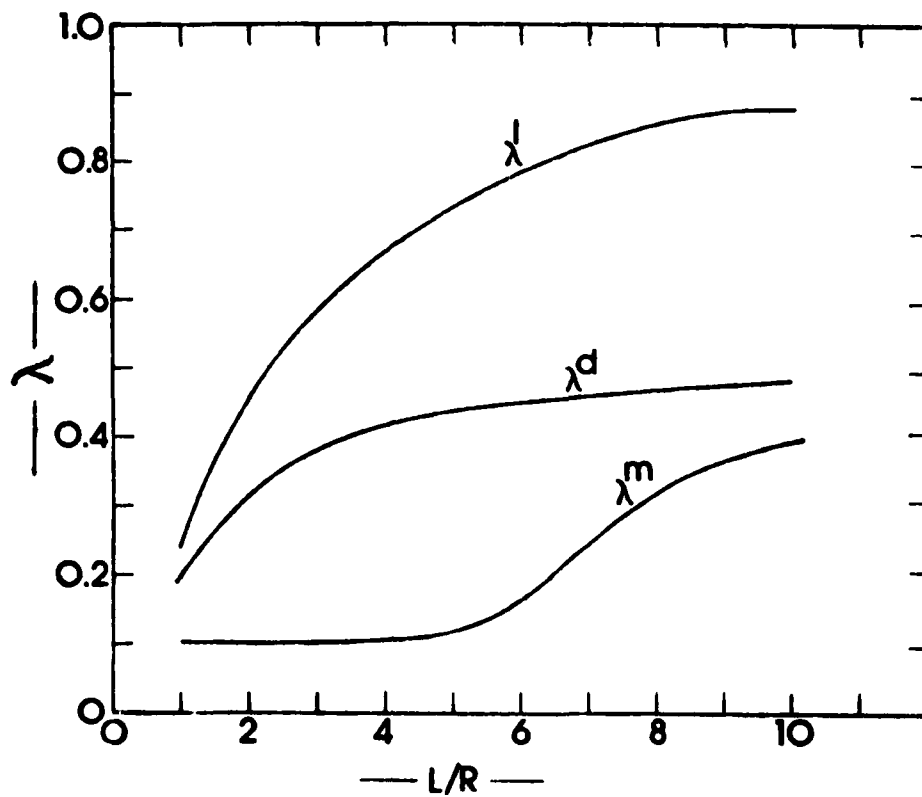


Fig. 3.15 Plots of Load Parameters (λ^l ; λ^d ; λ^m) versus L/R ($R/t = 250$; $\xi = 1$)

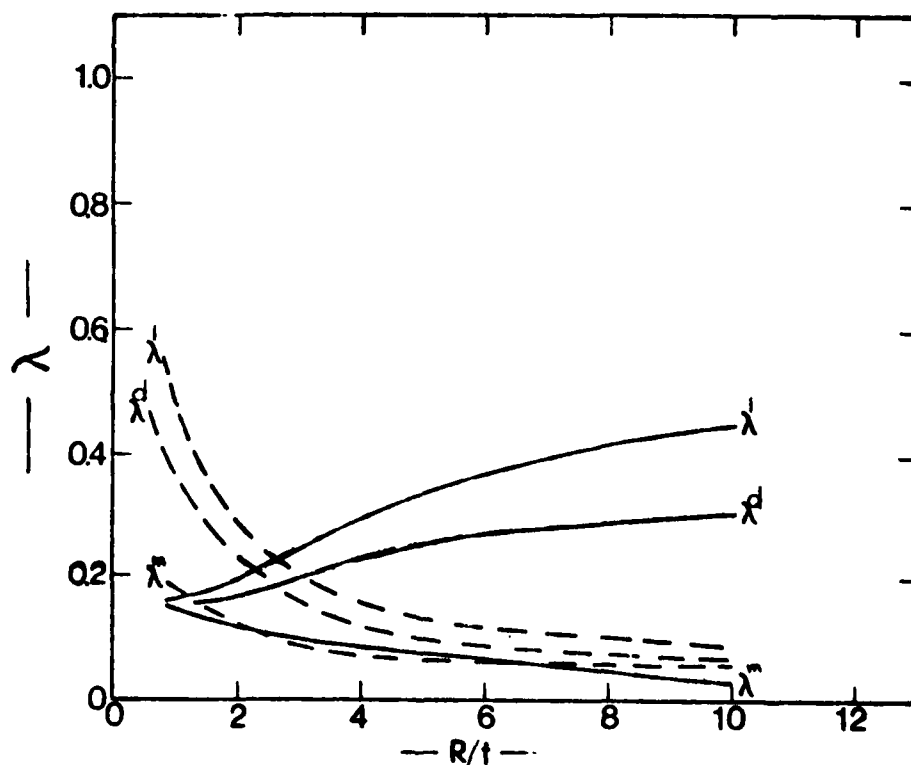


Fig. 3.16 Plots of Load Parameters (λ^l ; λ^d ; λ^m) versus R/t ($L/R = 1$; solid curve $\xi = 1$; dashed line constant imperfection amplitude, $\xi = 0.016/t$).

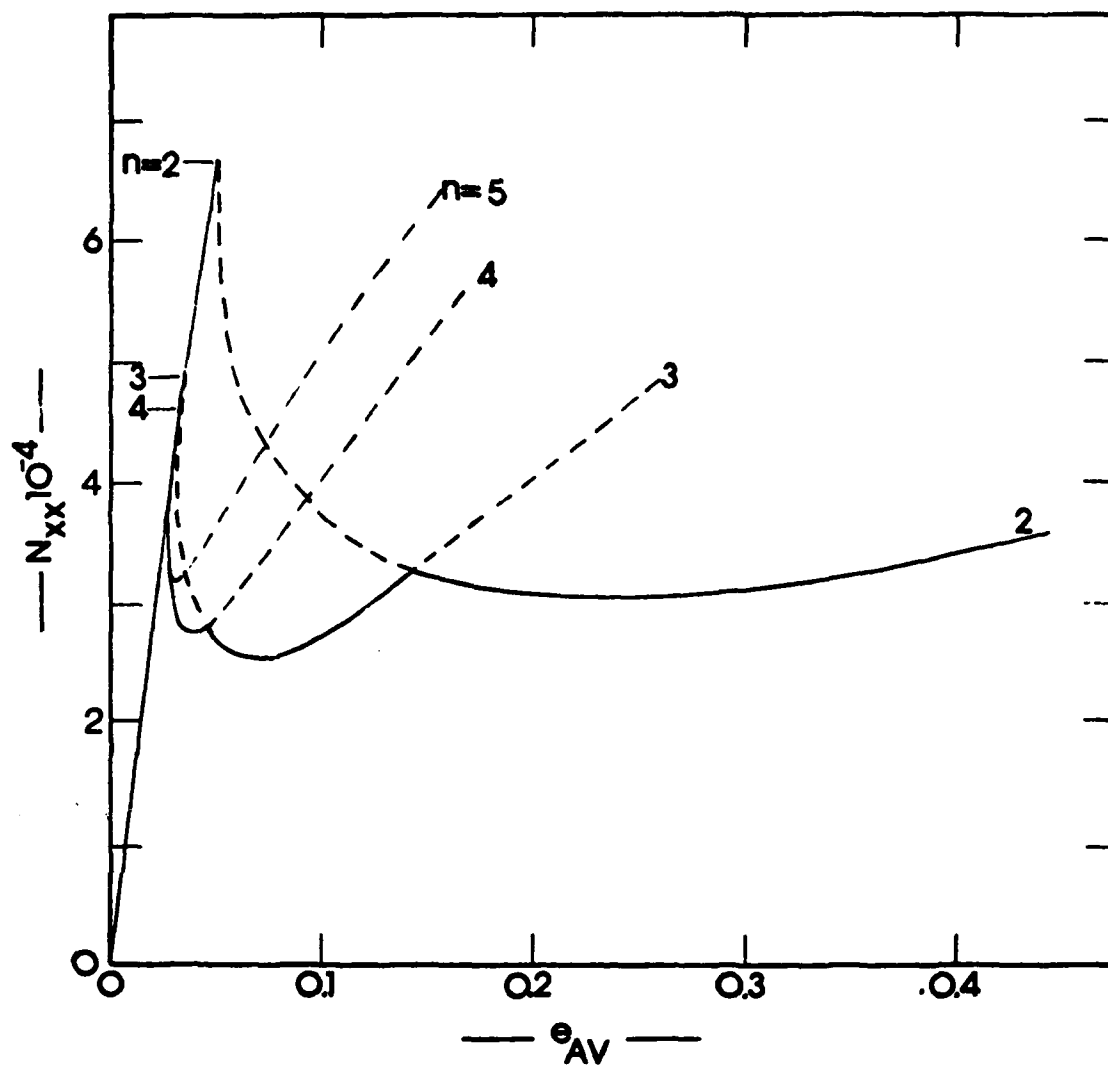


Fig. 3.17 Response of Externally Stiffened Geometry ($\xi = 1$; Axial Load)

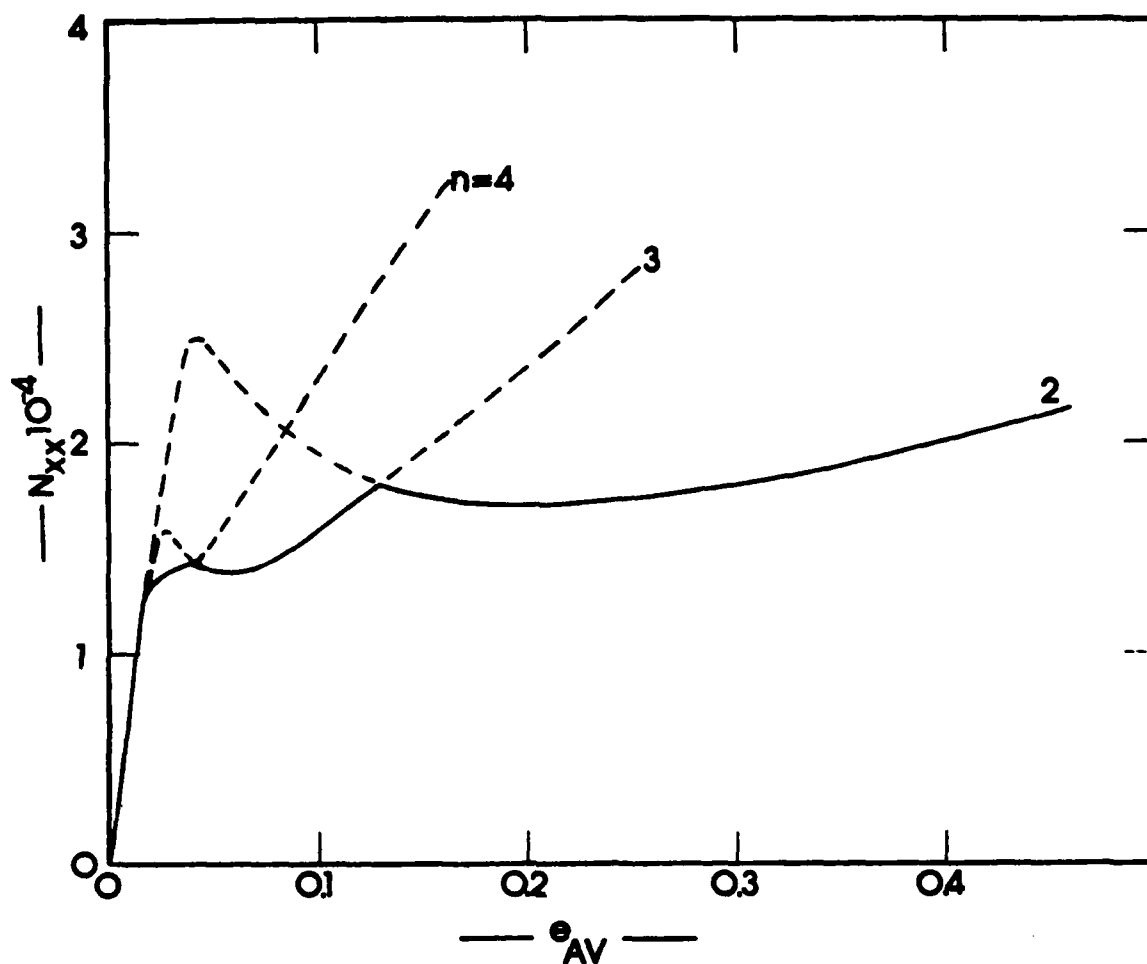


Fig. 3.18 Response of Externally Stiffened Geometry ($\xi = 4$; Axial Load)

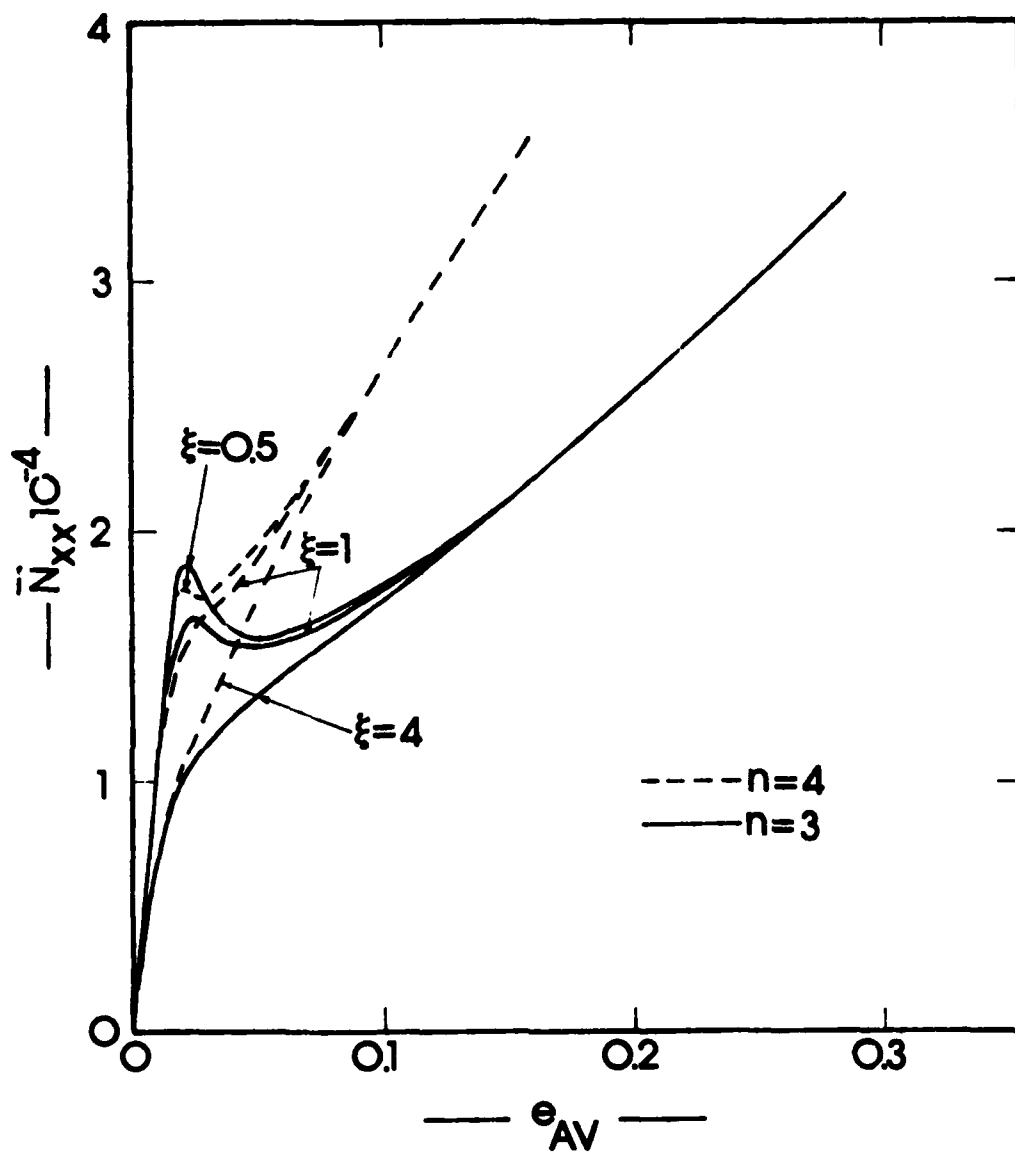


Fig. 3.19 Response of Internally Stiffened Geometry (Axial Load)

The results for the external positioning of the stiffeners are presented on Figs. 3.17 and 3.18 for ξ equal to one and four respectively. It is seen from these two figures that the response is similar to the unstiffened geometry (Figs. 3.3-3.5), but the number of full circumferential waves is smaller (this is an effectively much thicker thin shell). Note that the lowest limit point corresponds to $n = 4$ for $\xi = 1$. On the other hand, for $\xi = 4$, the mode changes from $n = 4$ to $n = 3$ and snapping occurs, because of the existence of an unstable bifurcational branch. In this case also, a change in mode is observed during snap-through buckling. Another important similarity to the unstiffened shell behavior is that this configuration is sensitive to initial geometric imperfections. Note that when $\xi = 1$ (which means that $W_{\max}^0 = h$), $\bar{N}_{xx_{cr}} = 26,200$ lbs/in. or $\lambda^L = 0.46$. The externally stiffened shell is not as sensitive as the unstiffened thinner shell, but it is sensitive to initial geometric imperfections.

The results for the internally stiffened configuration are shown in Fig. 3.19. The dashed lines correspond to $n = 4$ and the solid lines to $n = 3$. Data for other n -values need not be shown on this figure. The three sets of curves correspond to $\xi = 0.5, 1$, and 4 . Note that, for $\xi = 0.5$, limit point instability occurs at $\bar{N}_{xx} = 17,800$ lbs/in. with $n = 4$. Also note that during snap-through buckling, a change of circumferential mode occurs (to $n = 3$). The minimum equilibrium load in the post-limit point region corresponds to $n = 3$. On the other hand for $\xi = 1$, snap-through buckling occurs at $\bar{N}_{xx} = 16,400$ lbs/in. because of the existence of an unstable bifurcated branch (corresponding to $n = 3$). The minimum equilibrium load for $\xi = 1$ also corresponds to $n = 3$. Finally, there is no possibility of a snapping phenomenon for $\xi = 4$, neither through the

existence of a limit point nor through the existence of an unstable bifurcated branch. It is observed that this configuration is not very sensitive to initial geometric imperfections. For $\xi = 0.5$, $\lambda^L = 0.9$ and for $\xi = 1.0$, $\lambda^L = 0.84$. This is attributed to two reasons: (a) internally stiffened configurations are less sensitive than externally stiffened ones and stiffened configurations are less sensitive than unstiffened ones, and (b) for this reported case, SS-3 with $M_{xx} = a_3 \bar{N}_{xx}$ boundary conditions are used, which has a stabilizing effect. The primary reason, though, is the former.

Numerical results are also obtained for a ring-stiffened geometry under pressure. This is the same as Example 1 of Ref. 31.

(c) Ring-Stiffened Cylindrical Shell

$$L = R = 4 \text{ in.}; \quad t = 0.04 \text{ in.}; \quad E = 10.5 \times 10^6 \text{ psi}$$

$$\nu = 0.3; \quad e_x = \lambda_{xx} = 0; \quad \lambda_{yy} = 0.91; \quad \rho_{yy} = 100;$$

(3.62)

$$e_y = 0.24 \text{ in.}; \quad \text{classical } p_{cr} = 4827 \text{ psi}$$

$$w^0(x,y) = \xi t \left(\sin \frac{\pi x}{L} + 0.1 \sin \frac{\pi x}{L} \cos \frac{\pi y}{R} \right);$$

$$\xi = 0.1, 1.0 \text{ and } 4.0.$$

The results of this study are presented in graphical form on Figs. 3.20-3.22.

Fig. 3.20 shows a plot of the pressure, p , versus the average end shortening for $\xi = 1$ and $n = 3$. There are three plots shown on this figure which serve to check the effect of K [see Eq. (3.40)] and the number of mesh points, N.P., on the convergence of the solution. This effect, as characterized by Fig. 3.20, is typical for all ξ and n values.

Clearly, neither effect is significant for pre-limit point behavior and post-limit point behavior up to the minimum load. Beyond this range, the effect of NP is very small, while the effect of K can be significant. Therefore, if one is interested in the response characteristic up to the minimum post-limit point load, both effects are insignificant. In this particular study, one is interested in establishing limit-point loads (critical static loads) and dynamic critical loads which depend on accurately predicting the response in the unstable portion of the post-limit point behavior. (The value of the modified total potential goes to zero in this range if a critical dynamic load exists.) The conclusion is that $K = 1$ and $NP = 35$ suffice for this study, since the cpu time increases rapidly with increases in both K and NP.

Fig. 3.21 shows the effect of n for $\xi = 1$. This effect is the same for the other ξ values, and $n = 3$ characterizes the true response of the ring-stiffened shell. Fig. 3.22 shows the response of the shell for all three values of ξ (and $n = 3$). Note that for $\xi = 0.1$ and 1.0 , the shell expands in the axial direction (negative end shortening) up to the limit point and then it starts to contract. For $\xi = 4$, initially there is an expansion, but contraction commences before reaching the limit point. Note also that this configuration is rather sensitive to initial geometric imperfection (for $\xi = 0.1$, $\lambda^L = .94$; for $\xi = 1.0$, $\lambda^L = 0.80$; for $\xi = 4.0$, $\lambda^L = 0.59$). Note also that the agreement between the value reported in Ref. 31 for λ^L and $\xi = 1$ and the present one is very good. Moreover, the value of n ($=3$) is the same for both.

Critical Conditions for Sudden Application of the Loads.

As stated previously, a critical dynamic condition exists if the modified total potential, $U_{T_{mod}}$, becomes zero at an unstable static equili-

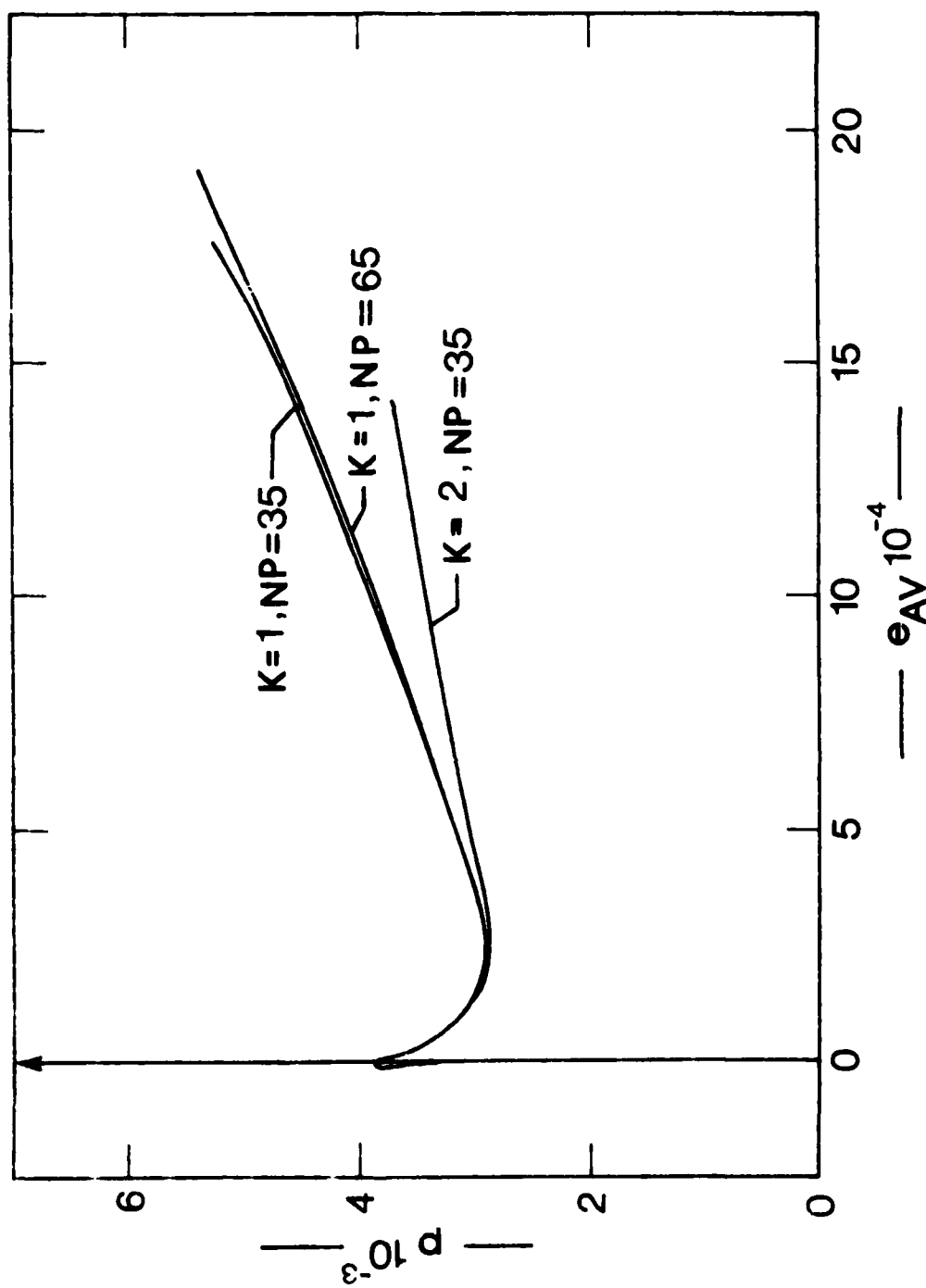


Fig. 3.20 Effect of K and NP (Fourier terms and Mesh Points) on the Response of the Ring-Stiffened Geometry ($n = 3$; $\xi = 1$; pressure load)

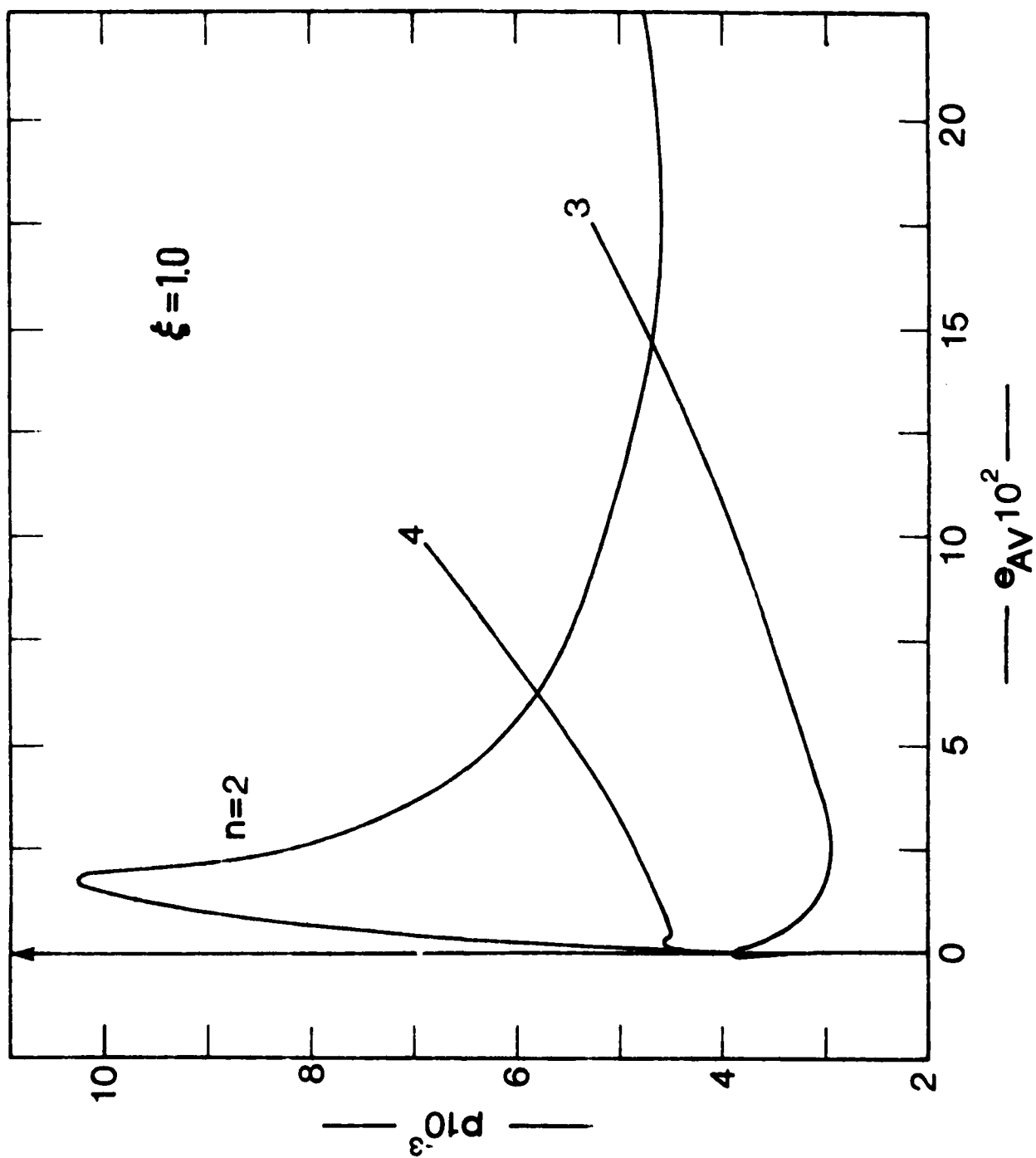


Fig. 3.21 Response of Ring-Stiffened Geometry (pressure load; $\xi = 1$)

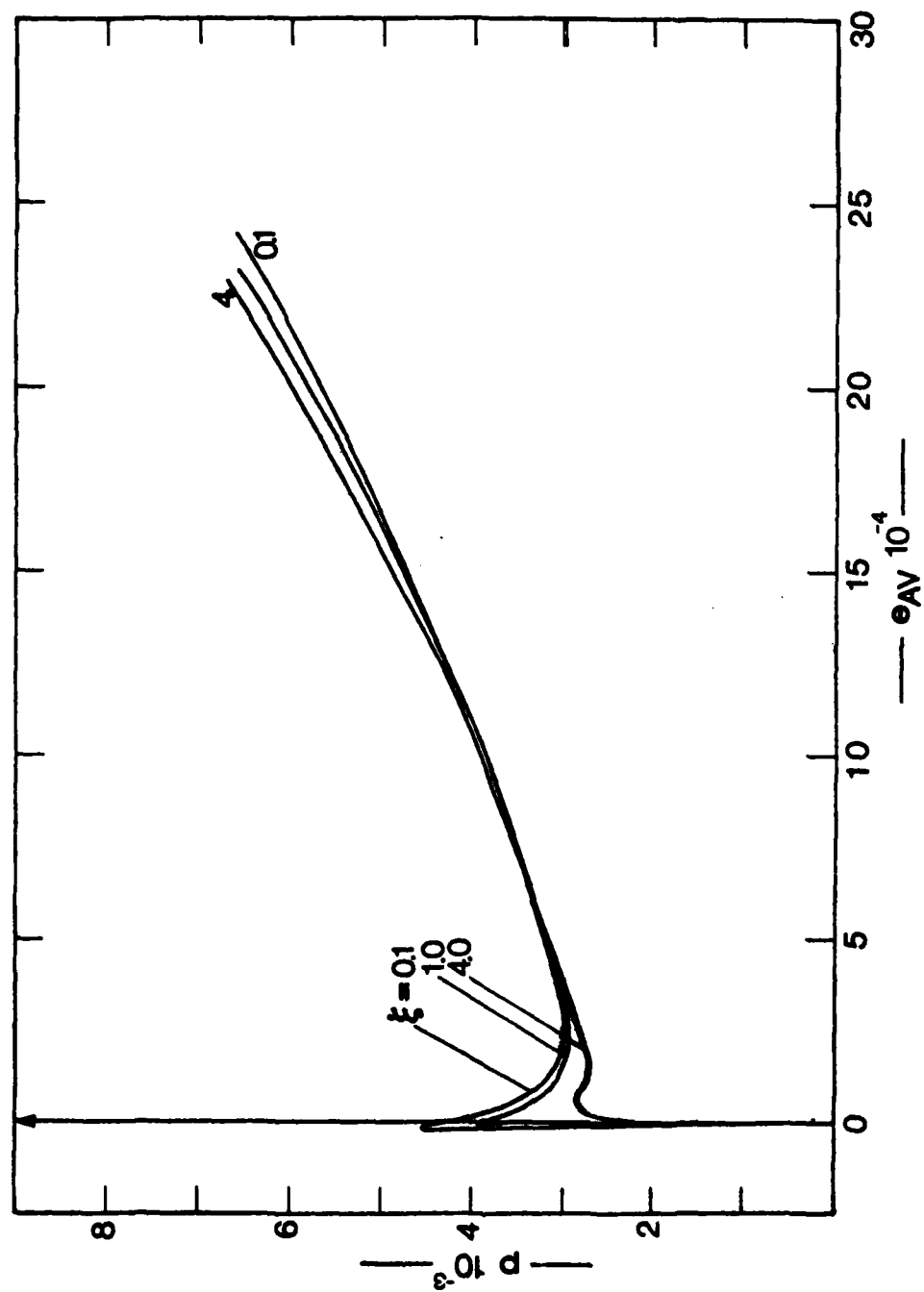


Fig. 3.22 Response of Ring-Stiffened Geometry (pressure load; $n = 3$)

brium point and motion can escape through this point. (A trajectory can possibly exist for "buckled" motion.)

For the axially-loaded unstiffened geometry, the results are presented both in tabular form (Tables 3.1 and 3.2) and in graphical form (Figs. 3.6, 3.15 and 3.16).

The critical dynamic load is obtained from the static solution. It corresponds to a load (static) for which the unstable (post-limit point curve) equilibrium point yields a value zero for the modified total potential. The expression for the modified total potential is given by [see Eqs. (3.16) and (3.19)]

$$\begin{aligned} U_{T_{\text{mod}}} &= U_T - \frac{\beta_1}{E_{xx_p}} \pi R L N_{xx}^2 + 2\pi R L a_1 \bar{N}_{xx}^2 \\ &= U_T + \pi R L a_1 \bar{N}_{xx}^2 \end{aligned} \quad (3.69)$$

It is seen from Tables 1 and 2 that when a limit point exists and the difference between the limit point load and the minimum post-limit point load is distinct, then a clear dynamic critical load exists. On the other hand, if there is no limit point (Examples 17-21 of Table 3.1), there is no critical dynamic load. Similarly, if the value of the limit point load is very close to that of the minimum post-limit point load, it is difficult to have a critical dynamic load (see Examples 35, 36, and 39 of Table 3.1). Fig. 3.6, among others, shows a plot of λ^d versus the imperfection amplitude parameter, ξ . On the basis of the definition of critical dynamic load, λ^d starts from one and decreases to the common value of λ^l and λ^m at $\xi = 4$. Since the static behavior for $\xi > 4$, is not one of limit point instability, then there is no critical dynamic load for these ξ values, according to the concept and criterion discussed at the

beginning of the chapter [see Eq. (3.2)]. On the other hand, if the dynamic response is limited in the space of the displacement components, then a critical load can be defined. This point is discussed in Ref. 1 and in Chapter 5 of the present report.

The effect of L/R is shown on Fig. 3.15. The value of λ^d is very low for L/R equal to one ($\lambda^d = 0.2$) and it increases rapidly with increasing L/R values to $\lambda^d = .48$ at $L/R = 10$. This, of course, holds true only for $\xi = 1.0$, but a similar behavior is observed for ξ -values for which the static behavior is the same as for $\xi = 1.0$ (see Figs. 3.3 and 3.4; but not 3.5).

For the axially-loaded stiffened configuration, the results are presented on Fig. 3.23. It is seen from this figure that the internally stiffened geometry (under static conditions) is not as sensitive as the externally stiffened one. Moreover, the ratio of the dynamic load to the static (λ^d / λ^s) is higher for the internally stiffened geometry. Note that the results for the internally stiffened geometry do not extend past $\xi = 1.0$. This is so because the static behavior will soon ($\xi = 1.5$ or so) cease to be of the limit point instability. On the other hand, the results for external stiffening extend to $\xi = 4$.

It is seen that the largest difference (or smallest ratio λ^d / λ^s) between the static and dynamic critical loads occurs at $\xi \approx 1.0$ (see Figs. 3.6 and 3.23), for axially loaded geometries.

For the pressure-loaded ring-stiffened geometry, critical dynamic loads are obtained by setting the modified potential equal to zero [see Eq. (3.2)]. For this case, C , for a given load, denotes the potential associated with the static primary path mode. This means that the corresponding static problem must be solved (without allowing static buckling)

AD-A114 735

GEORGIA INST OF TECH ATLANTA

F/G 20/11

DYNAMIC STABILITY OF STRUCTURES: APPLICATION TO FRAMES, CYLINDER--ETC(U)

FEB 82 G J SIMITSES, I SHEINMAN

F33615-79-C-3221

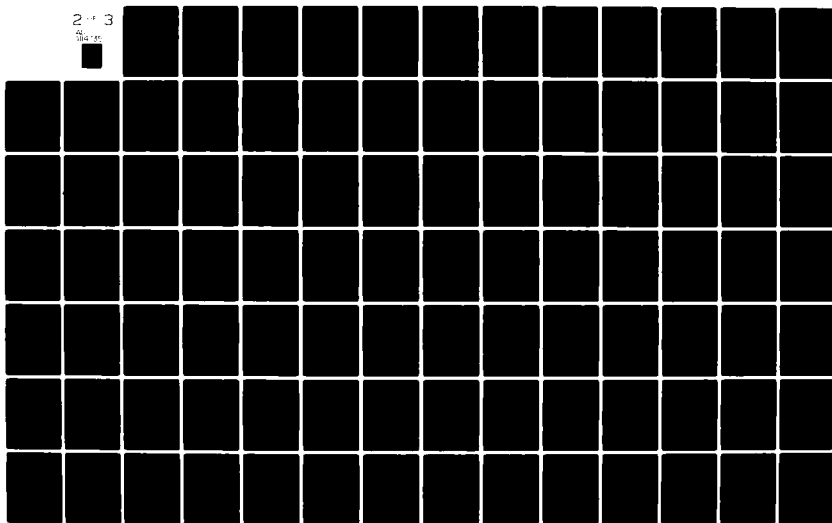
NL

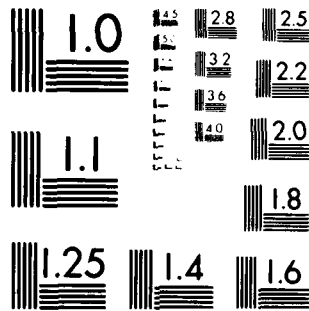
UNCLASSIFIED

AFWAL-TR-81-3155

2-3

2-3





MICROCOPY RESOLUTION TEST CHART
NATIONAL BUREAU OF STANDARDS-1963-A

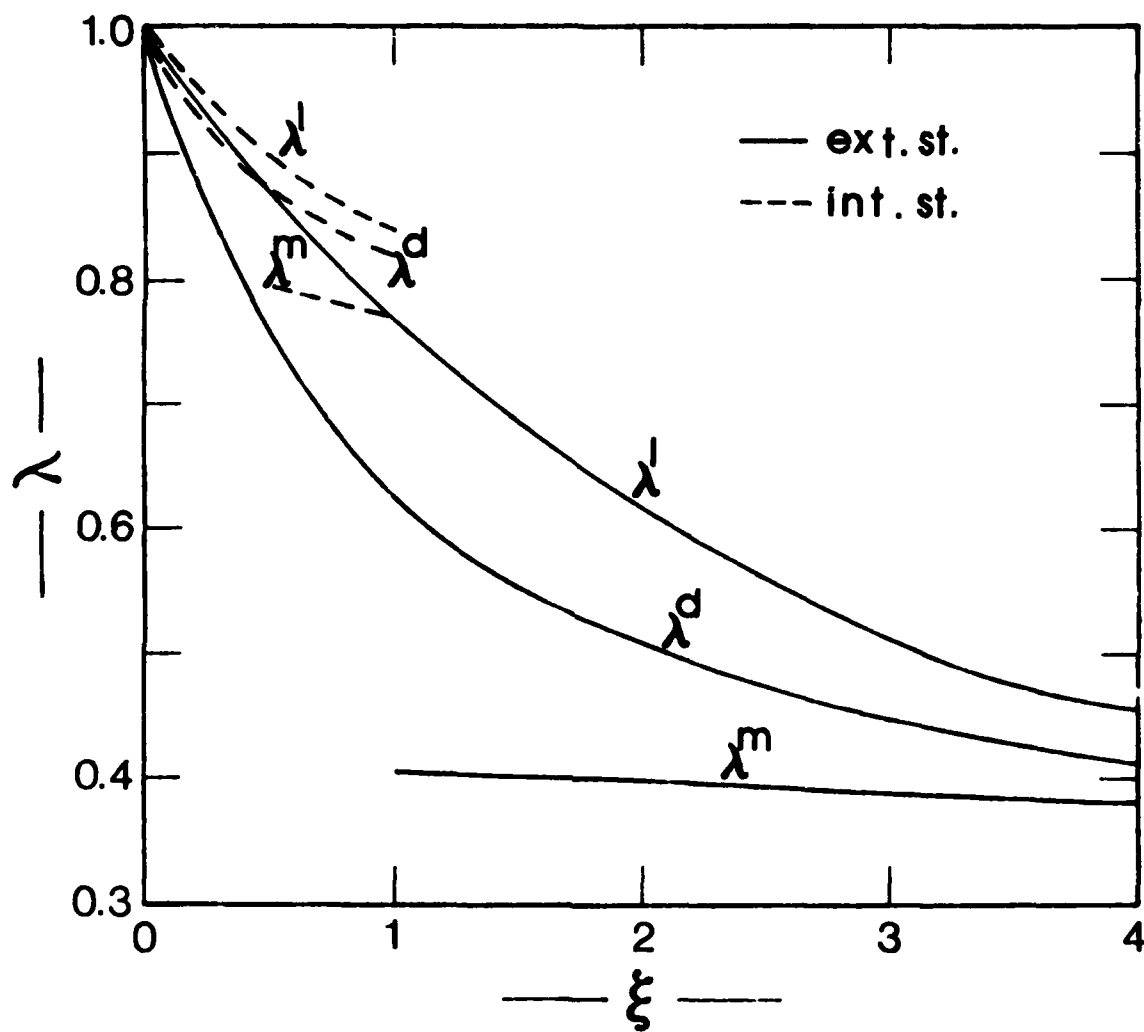


Fig. 3.23 Plots of Load Parameters (λ^l ; λ^d ; λ^m) versus ξ for the Stiffened Geometries (axial load)

with regard to static application of the pressure and by finding the corresponding axisymmetric displacement (breathing mode). Then at each level of the pressure, the corresponding total potential is calculated and for each value of p this corresponds to the value of C in Eq. (3.2).

The estimated results for dynamic critical pressure along with the limit-point values and the minimum post-limit point values are shown on Table 3.3. Only results corresponding to $n = 3$ are shown, because this value of n governs static and dynamic buckling.

Table 3.3 Pressure-Loaded, Ring-Stiffened Cylindrical Shell.

n	ξ	P^L psi	P^d psi	P^m psi	P^d/P^L
3	0.1	4,500	4,470	3,000	0.9933
3	1.0	3,845	3,790	2,970	0.9857
3	4.0	2,830	2,755	2,740	0.9735

It is seen from these results that the reduction in critical pressure, because of the sudden application (dynamic versus static), is very small. This should not be considered as a general conclusion, but more data need to be generated.

SECTION IV

THE PINNED HALF-SINE ARCH

In this particular chapter the concepts of dynamic stability are applied to a half-sine low arch, subjected to a transverse load with a half-sine spatial distribution. The static analysis of such an arch may be found in Ref. 32. Some dynamic stability aspects of this or similar geometries may be found in Refs. 2, 11, 33, 34 and 35. In this chapter some of these studies are summarized, particularly those of Refs. 2, 11, and 35. These studies include loads of constant magnitude and finite durations (as well as the extreme cases of the duration time approaching zero and infinity), and the study of various effect, all of which are presented in Ref. 1. These include, the effect of static pre-loading and small damping.

Geometry and Governing Equations

Consider a slender arch of small initial curvature and symmetric cross section. Furthermore, $w_0(x)$ denotes the initial shape of the middle line, $w(x)$ the shape of the middle line after deformation, and $u(x)$ the horizontal displacement of any point of the midplane (see Fig. 4.1). The following nondimensionalization is introduced

$$\begin{aligned}
 x &= \frac{L}{\pi} \xi \\
 w(x,t) &= \rho \eta(\xi,t) \text{ where } \rho^2 = \frac{I}{A} \\
 t &= \tau \frac{L/\pi}{\sqrt{\frac{E}{\rho}}} \text{ where } \epsilon_E = (\pi \rho/L)^2
 \end{aligned} \tag{4.1}$$

and E is the Young Modulus and $q(\xi,t) = \frac{\rho}{AE\epsilon_E^2} Q^*(x,t)$

where $Q^*(x,t)$ denotes the external force per unit length.

The specific problem to be considered in this section consists of a low pinned arch for which $w_0(x)$ and consequently $\eta_0(\xi)$ is a half-sine-wave. The distributed load, which is applied suddenly with constant magnitude for a finite duration, τ_0 , is also a half-sine-wave. The initial shape is given by

$$\eta_0(\xi) = e \sin \xi \quad 0 < \xi < \pi \quad (4.2)$$

where e is the initial rise parameter. Since $(w_0)_{\max} = \rho e$ and $e =$

$\frac{(w_0)_{\max}}{\rho}$, and if the cross section is rectangular of width b and thickness h , then $\rho = \frac{h}{2/3}$ and $e = 2/3 \frac{(w_0)_{\max}}{h}$, which clearly shows that e is a measure of the ratio of the initial maximum rise to the thickness of the arch.

The expression for the loading is given by

$$q(\xi, \tau) = q_1(\tau) \sin \xi \quad (4.3)$$

The response of the arch, $\eta(\xi, t)$ is represented by

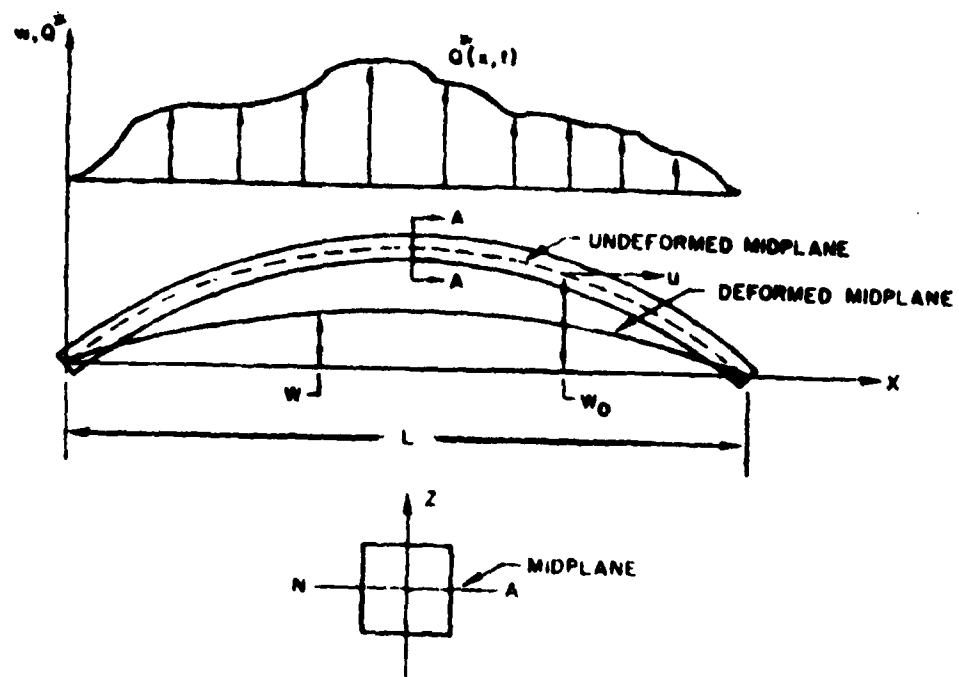
$$\eta(\xi, t) = \eta_0(\xi) + \sum_{n=1}^2 a_n(t) \sin n\xi, \quad 0 < \xi < \pi, \quad t > 0 \quad (4.4)$$

Complete analysis of the problem is given by Simitses in references 11 and 32.

A more convenient set of equations may be obtained by introducing the following new parameters

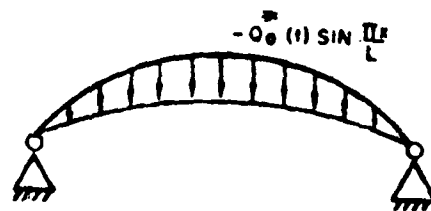
$$r = a_1 + e \quad \text{and} \quad p = q_1 + e \quad (4.5)$$

the expression for the nondimensionalized total potential under p



Section A-A

(a) Geometry



(b) The Pinned Arch

Fig. 4.1. The Low Arch; Geometry and Sign Convention

$\left(\bar{U}_T^P = \frac{4U_T^{q_1}}{P_E \epsilon_E L} \right.$ where $U_T^{q_1}$ the total potential under the load q_1 and $P_E =$

$\frac{\pi^2 EI}{L^2}$ denoting the first Euler load) is given by

$$\bar{U}_T^P = \frac{1}{8}(r^2 - e^2 + 4a_2^2)^2 + r^2 - e^2 + 16a_2^2 + 2p(e-r) \quad (4.6)$$

which is quite similar to the potential energy for the two-degree of freedom model (Model C) discussed in Ref. 1.

Furthermore, neglecting the rotatory and in-plane kinetic energies, the following expression for the nondimensionalized kinetic energy (T is the kinetic energy) is obtained.

$$\bar{T} = \frac{2}{\pi} \int_0^\pi \dot{\eta}^2 d\xi \quad (4.7)$$

Use of Eq. (4.4) in Eq. (4.7) yields the following expression for \bar{T}

$$\bar{T} = \dot{r}^2 + \dot{a}_2^2 = (1 + a_2'^2) \dot{r}^2 \quad (4.8)$$

where $(\dot{}) = \frac{\partial}{\partial \tau}$ and $()^{\circ} = \frac{d}{d\tau}$

Critical Dynamic Conditions

Dynamic Stability under constant load of finite duration has been discussed in Ref. 1 and through simple mechanical models, criteria and estimates for critical conditions were presented. The same problem is posed here, but applied to a pinned low arch.

The expression for the "zero load" total potential is given by

$$\bar{U}_T^0 = \frac{(r-e)^2}{8} (r^2 + 2er + e^2 + 8) + a_2^2 (2a_2^2 + r^2 + 16 - e^2) \quad (4.9)$$

Through a static stability analysis, the following stationary points on the "zero load total potential" are obtained:

Pt. 1 at $[e, 0]$ Stable (Relative min.)

Pt. 2 at $[\frac{1}{2}(-e + \sqrt{e^2 - 16}), 0]$ Unstable (Relative max.)

Pt. 3 at $[\frac{1}{2}(e + \sqrt{e^2 - 16}), 0]$ Stable (Relative min.)

Pt. 4 at $[\frac{e}{3}, \sqrt{\frac{2e^2}{9} - 4}]$ Unstable (Saddle point)

Pt. 5 at $[\frac{e}{3}, \sqrt{\frac{2e^2}{9} - 4}]$ Unstable (Saddle point)

It is proven (Ref. 11) that saddle points exist for $e > 4$. For this range of e -values, the "zero load" total potential value at the saddle points, pts. 4 and 5 is smaller than the corresponding value at the relative maximum, pt. 2. On the basis of this observation the motion can possibly become "buckled" through the saddle points, pts. 4 and 5. The corresponding condition for this case is a "possible critical condition". On the other hand, if the imparted energy, by the applied force at the release time, is sufficient to reach the relative maximum (unstable) static equilibrium point, pt. 2, "buckled" motion is guaranteed and the corresponding critical condition is a "minimum guaranteed one". The former is termed sufficient condition for dynamic stability while the latter sufficient condition for dynamic instability by Hsu [6 - 10].

Next, the computational procedure for finding the possible critical condition is outlined.

The stability criterion for this case (see Ref. 1) is expressed by

$$\bar{U}_T^0(\tau_0) - \bar{U}_T^P(\tau_0) \leq \bar{U}_T^0(L_u^0) \quad (4.10)$$

where L_u^0 is the unstable static equilibrium point under zero load and τ_0 the release time. The equality sign refers to a critical condition, while the inequality sign refers to a dynamically stable condition.

Use of Eq. (4.10) for this geometry yields

$$r \Big|_{\tau = \tau_{o_{cr}}} = e - \frac{8 \left(\frac{e}{3} - 2 \right)}{e - p} \quad (4.11)$$

where $\tau_{o_{cr}}$ is the critical release time.

Moreover, for $0 < \tau < \tau_o$ conservation of energy yields (during this time the system is loaded)

$$\bar{U}_T^P + \bar{T}^P = 0 \quad (4.12)$$

For a given path of motion, integration of Eq. (4.12), yields a relation between the time of release and the position at that instant. Note, that the problem has been cast in the following terms: for a given load, p , find the smallest release time, $\tau_{o_{cr}}$, such that the system may reach an unstable point (saddle point for the minimum possible critical condition) with zero velocity, Eq. (4.11). Since one is interested in obtaining the smallest release time, $\tau_{o_{cr}}$, and since the position at the time of release is path dependent, one can solve the problem by considering the associated brachistochrone problem. The brachistochrone problem makes use of Eq. (4.12) for this system, and through its solution one obtains the relation between the smallest release time, $\tau_{o_{cr}}$, the position at the instant of release, as well as the path that yields $\tau_{o_{cr}}$. The details of the solution to this brachistochrone problem are similar to the ones presented in Ref. 1. for the two-degree-of-freedom model, Model C. The solution to the brachistochrone problem yields that the minimizing path is characterized by $a_2 \equiv 0$ (symmetric path) and the relation between $\tau_{o_{cr}}$ and the position of the system, r_{cr} , at $\tau_{o_{cr}}$ is

$$\tau_{o\ cr} = \int_{\sqrt{e}}^{r_{cr}} \frac{dr}{\sqrt{2p(r - e) + e^2 - r^2 - \frac{1}{8}(r^2 - e^2)^2}} \quad (4.13)$$

Computationally, it is simpler for one to assign values of r_{cr} (starting with values close to the initial position, $r = \sqrt{e}$ and $a_2 = 0$), solve for p through Eq. (4.11) and then for $\tau_{o\ cr}$ through Eq. (4.13).

Note that for the case of the minimum guaranteed critical condition Eq. (4.11) is replaced by a comparable equation which employs the value of the "zero load" total potential at the relative maximum unstable static point.

Numerical results are presented graphically on Figs. 4.2 and 4.3, for the minimum possible critical condition only, and various values of e . The curves of Fig. 4.2 depict critical conditions in terms of applied load, p , versus critical release time, $\tau_{o\ cr}$. One may observe that as the $\tau_{o\ cr}$ increases, the corresponding load approaches, asymptotically, the value of p_{cr} for the infinite duration time. Fig. 4.3 presents the same results as Fig. 4.2, but in terms of $(p\tau_o)_{cr}$ versus critical release time $\tau_{o\ cr}$. Note that as $\tau_{o\ cr}$ approaches zero, the value of $(p\tau_o)_{cr}$ approaches that of the critical ideal impulse (see Ref. 11).

Effect of Static Preloading

In evaluating the effect of static preloading, three values are chosen ($e = 5.0, 6.0, 8.0$), and for each e -value the system is initially loaded quasi-statically with a p_o -load smaller than the p_{cr} -static. Then, the system is loaded dynamically. The following values are used in the dynamic analysis.

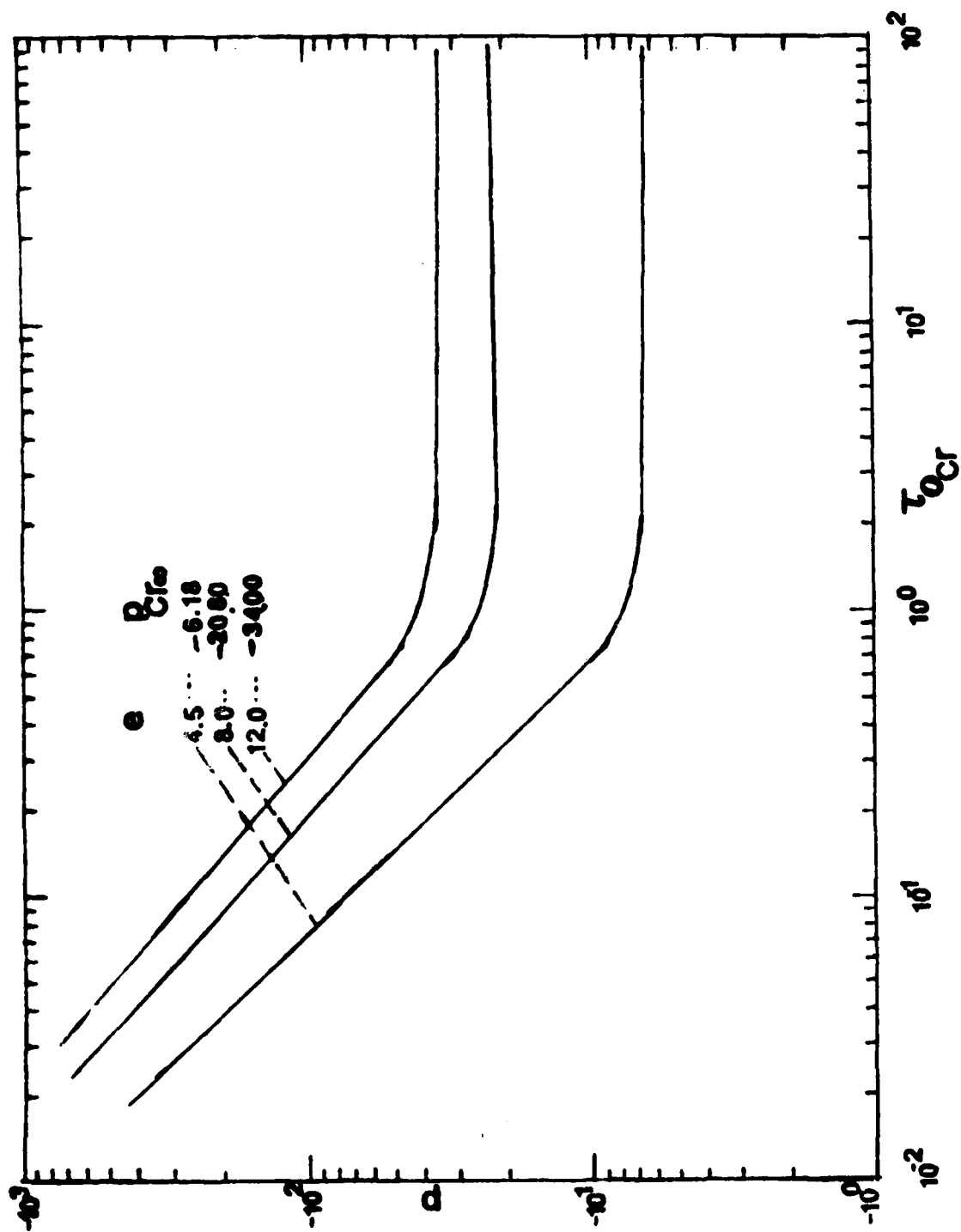


Fig. 4.2. Constant Load, P , versus Critical Duration Time, τ_{ocr} , pinned Arch.

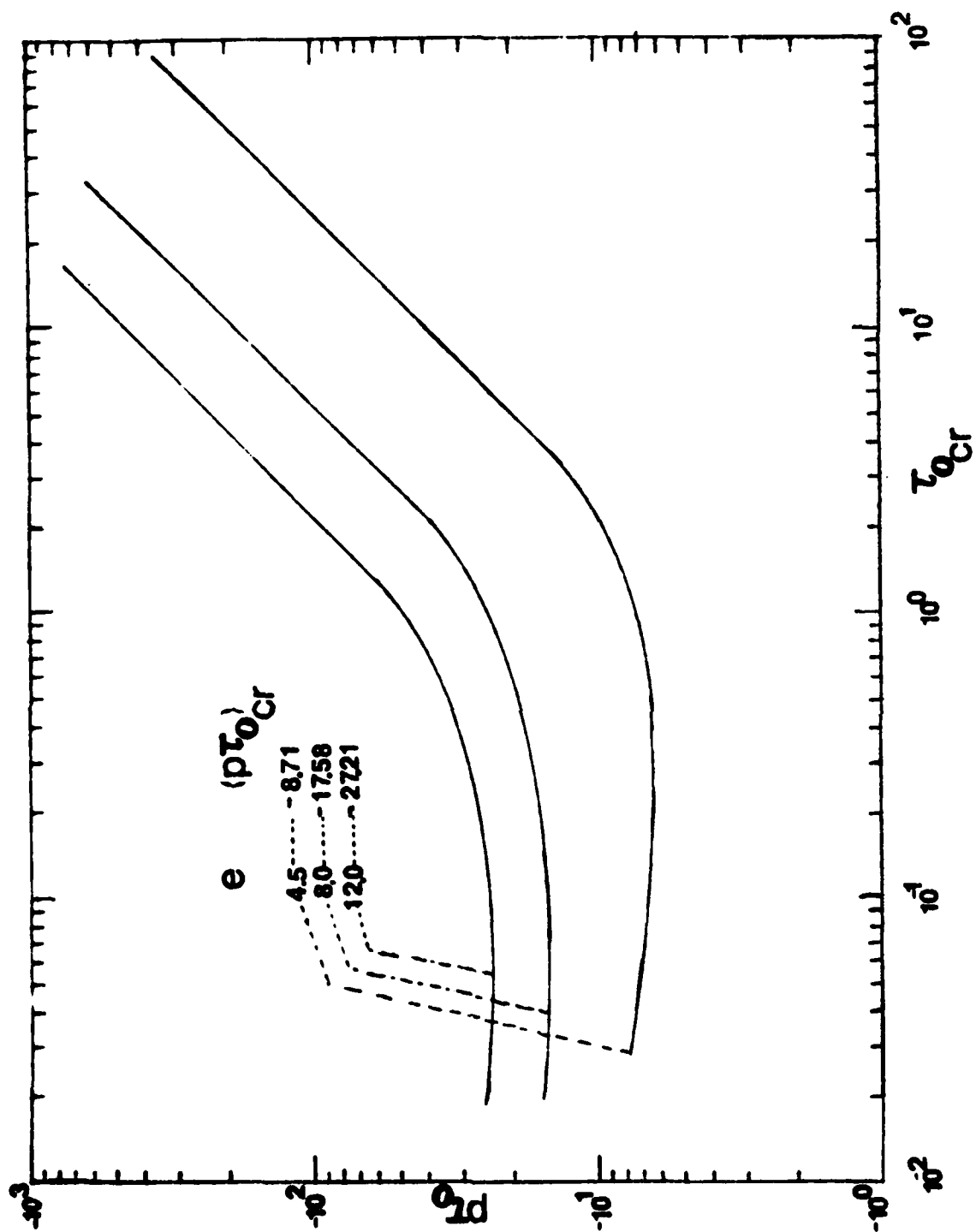


Fig. 4.3. Impulse, $(p\tau_0)_e$, versus Critical Duration Time, τ_{0cr} , pinned Arch.

$$e = 4.5 \quad ; \quad p_{st_{cr}} = -6.18 \quad ; \quad p_o = -1.0, -3.0, -5.0$$

$$e = 5.0 \quad ; \quad p_{st_{cr}} = -9.0 \quad ; \quad p_o = -2.0, -4.0, -6.0$$

$$e = 6.0 \quad ; \quad p_{st_{cr}} = -13.41 \quad ; \quad p_o = -3.0, -4.0, -6.0$$

First, the extreme cases ($\tau_o \rightarrow 0$ and $\tau_o \rightarrow \infty$) are analyzed by employing the proper energy equations (see Ref. 1, Section 6).

For example, for the ideal impulse case, the impulse is related to an initial kinetic energy, $\bar{T}_i^{P_o}$ (the impulse is imparted into the system as initial velocity) and from conservation of energy (for the preloaded system)

$$\bar{U}_T^{P_o} + \bar{T}_T^{P_o} = \bar{U}_T^{P_o}(L_s^{P_o}) + \bar{T}_i^{P_o} \quad (4.14)$$

where $L_s^{P_o}$ is the near static (stable) equilibrium position under P_o (static preloading). Then $\bar{T}_i^{P_o}$ is critical (and the corresponding ideal impulse) if the system can reach the unstable static equilibrium point, $L_u^{P_o}$ with zero kinetic energy, or

$$\bar{T}_i^{P_o} = \bar{U}_T^{P_o}(L_u^{P_o}) - \bar{U}_T^{P_o}(L_s^{P_o}) \quad (4.15)$$

For the second extreme case ($\tau_o \rightarrow \infty$), p_{cr} may also be obtained from energy consideration and the criteria developed in Ref. 1. The characteristic equation for this case is obtained from

$$\bar{U}_T^{P_o} + P \left(L_u^{P_o} + P \right) = \bar{U}_T^{P_o} + P \left(L_s^{P_o} \right) \quad (4.16)$$

The ideal impulse, $(p\tau_o)$ may be related to the initial kinetic energy $\bar{T}_i^{P_o}$ (in the nondimensionalized form - see Refs. 2 and 11) by the expression

$$(p\tau_o) = - [\bar{T}_1^{P_o} (r_s^{P_o})]^{1/2} \quad (4.17)$$

where $r_s^{P_o}$ is the near static (stable) equilibrium position under load P_o .

The critical ideal impulse, through Eqs. (4.17) and (4.15), is obtained by

$$(p\tau_o)_{cr} = - [\bar{U}_T^{P_o} (r_u^{P_o}) - \bar{U}_T^{P_o} (r_s^{P_o})]^{1/2} \quad (4.18)$$

Note that the negative sign on the right hand side of Eqs. (4.17) and (4.18) is present because of the sign convention on the load p (see Fig. 4.1). The expression for the total potential is given by Eq. (4.6).

The numerical results are presented on Table 4. 1.

Table 4.1 - Critical Ideal Impulse, $(p\tau_o)_{cr}$.

$e = 4.5$		$e = 5.0$		$e = 6.0$	
P_o	$(p\tau_o)_{cr}$	P_o	$(p\tau_o)_{cr}$	P_o	$(p\tau_o)_{cr}$
0	-8.71	0	-10.06	0	-12.64
-1.0	-5.11	-2.0	- 4.95	-3.0	- 7.95
-3.0	-3.53	-4.0	- 3.64	-4.0	- 6.80
-5.0	-1.93	-6.0	- 2.28	-6.0	- 5.31
-6.18	0	-9.00	0	-13.41	0

Note that the first row gives the ideal impulse without static pre-loading. Note also that, as the value of p_o approaches the value of the static critical load, the additionally imposed critical impulse tends to zero. This is reflected by the results of the last row (Table 4.1).

The critical load for the case of infinite duration, p_{cr_∞} , is obtained by the following steps, for a given e, p_o combination.

- a) Solve the symmetric response equilibrium equation (see Refs. 2, 11, 32), given below, for $r_s^{p_o}$ (near stable position)

$$(r_s^{p_o})^3 - (e^2 - 4) r_s^{p_o} = 4 p_o \quad (4.19)$$

- b) The static unstable (saddle) equilibrium positions are characterized by (see Ref. 32)

$$r = - \frac{p_o + p}{3}$$

$$\text{and} \quad a_2^2 = \frac{1}{4} \left[e^2 - \frac{(p + p_o)}{9} - 16 \right] \quad (4.20)$$

- c) Eq. (4.16) for this system becomes

$$\begin{aligned} & \frac{1}{8} (r^2 + 4a_2^2 - e^2)^2 + r^2 - e^2 + 16a_2^2 + 2(p_o + p)(e - r) \\ &= \frac{1}{8} (r_s^{p_o} - e^2)^2 + r_s^{p_o} - e^2 + 2(p_o + p)(e - r_s^{p_o}) \end{aligned} \quad (4.21)$$

The simultaneous solution of Eqs. (4.20) and (4.21) yields $r_u^{p_o + p}$ and p_{cr_∞} .

The numerical results for all e , p_o combinations are presented in tabular form on Table 4.2.

Table 4.2 - Critical Dynamic Loads, p_{cr_∞} , (Infinite Duration)

$e = 4.5$			$e = 5.0$			$e = 6.0$		
p_o	p_{cr_∞}	$p_o + p_{cr_\infty}$	p_o	p_{cr_∞}	$p_o + p_{cr_\infty}$	p_o	p_{cr_∞}	$p_o + p_{cr_\infty}$
0	-3.7	-3.7	0	-5.20	-5.20	0	-8.8	-8.7
-1.0	-4.05	-5.05	-2.0	-5.54	-7.54	-3.0	-8.61	-11.61
-3.0	-2.54	-5.54	-4.0	-3.90	-7.90	-4.0	-8.02	-12.02
-5.0	-0.99	-5.99	-6.0	-2.24	-8.24	-6.0	-6.77	-12.77
-6.18	0	-6.18	-9.0	0	-9.00	-13.41	0	-13.41

Note that the first row results of Table 4.2 are taken from Ref. 11. The results of the last row reflect the fact that if the system is loaded quasistatically up to the limit point, then the additional suddenly applied load that the system can withstand tends to zero.

Finally, for the case of constant load, p , applied suddenly for a finite duration, τ_o , critical conditions are obtained from the following steps:

- From the static stability analysis obtain r_s^o , r_u^o , and a_{2u}^o , for each p_o .
- Use of the energy balance for this model and load case [see Eq. (6.9) of Ref. 1] yields

$$\begin{aligned}
2p (r_{ocr} - r_s^o) &= \frac{1}{8} (r_u^o - e^2 + 4a_{2u}^o)^2 \\
&+ r_u^o + 16a_{2u}^o - \frac{1}{8} (r_s^o - e^2)^2 - r_s^o + 2p_o (r_s^o - r_u^o) \quad (4.22)
\end{aligned}$$

where r_{cr} is the position r at the instant of release of the load p ($\tau = \tau_o$). In Eq. (4.22), for a given geometry, e , and static load, P_o , everything is known (p_o , e , r_s^o , r_u^o and a_{2u}^o) except for p and r_{cr} . Therefore, Eq. (4.22) relates p and r_{cr} at the critical condition.

c) Since $\bar{T}^{P+P_o} = (1 + a_2'^2) \left(\frac{dr}{d\tau} \right)^2$, then from Eq. (6.4) of Ref. 1, one may write

$$d\tau = \left[\bar{U}_T^{P_o+P} (r_s^o) - \bar{U}_T^{P_o+P} (r, a_2) \right]^{-\frac{1}{2}} dr \quad (4.23)$$

Invoking the same techniques as the ones used for the same problem but without static preloading in the previous case, the critical time τ_o is computed on the symmetric path $a_2 \equiv 0$.

Integration from $\tau = 0$ to $\tau = \tau_o$ and use of the expression for the total potential [see Eq. (4.6)] yields

$$\begin{aligned}
\tau_{ocr} &= \int_{r_s^o}^{r_{ocr}} \left[\frac{1}{8} (r_s^o - e^2)^2 + r_s^o - \frac{1}{8} (r^2 - e^2)^2 - r^2 \right. \\
&\quad \left. + 2(p + p_o) (r - r_s^o) \right]^{-\frac{1}{2}} dr \quad (4.24)
\end{aligned}$$

Note that Eq. (4.28) also relates r_{cr} to p .

A critical condition is characterized by (p, τ_o) that satisfies both equations, Eqs. (4.22) and (4.24). This means that for a given release time, τ_o , find p_{cr} or for a given p find $\tau_{o_{cr}}$. Computationally, though, it is easier to assign values of r_{cr} , solve for p from Eq. (4.22) and then for the corresponding τ_o from Eq. (4.24).

A computer program has been written for these computations. Values of r_{cr} are assigned, starting with $r_s^o + \delta r$, where δr is very small, and computing the corresponding values of p and $\tau_{o_{cr}}$ for each δr .

The results are presented graphically on Figs. 4.4 - 4.9 for the three values of e . On the first three figures, critical conditions appear as plots of p versus duration time, $\tau_{o_{cr}}$. Note that as $\tau_{o_{cr}}$ become larger and larger, the corresponding value of p approaches p_{cr_∞} (see Table 4.2). On the last three figures (4.7 - 4.9) critical conditions appear as plots of $(p\tau_o)_{cr}$ versus duration time, $\tau_{o_{cr}}$. On these figures, as $\tau_{o_{cr}} \rightarrow 0$, the corresponding value of $(p\tau_o)_{cr}$ approaches the critical ideal impulse (see Table 4.1).

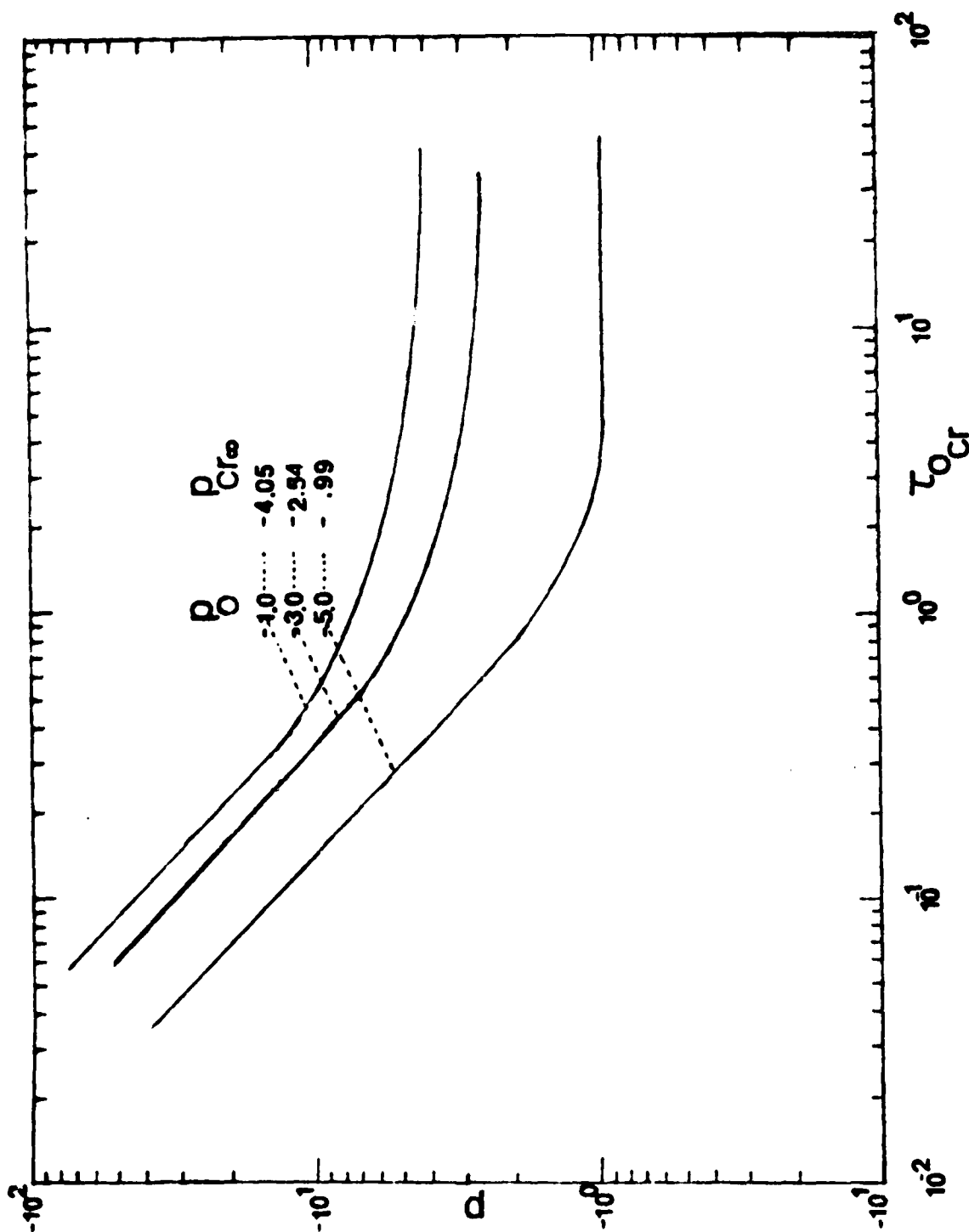


Fig. 4.4 Constant load, P , versus critical duration time, τ_{cr} ; Preloaded pinned Arch, $e = 4.5$

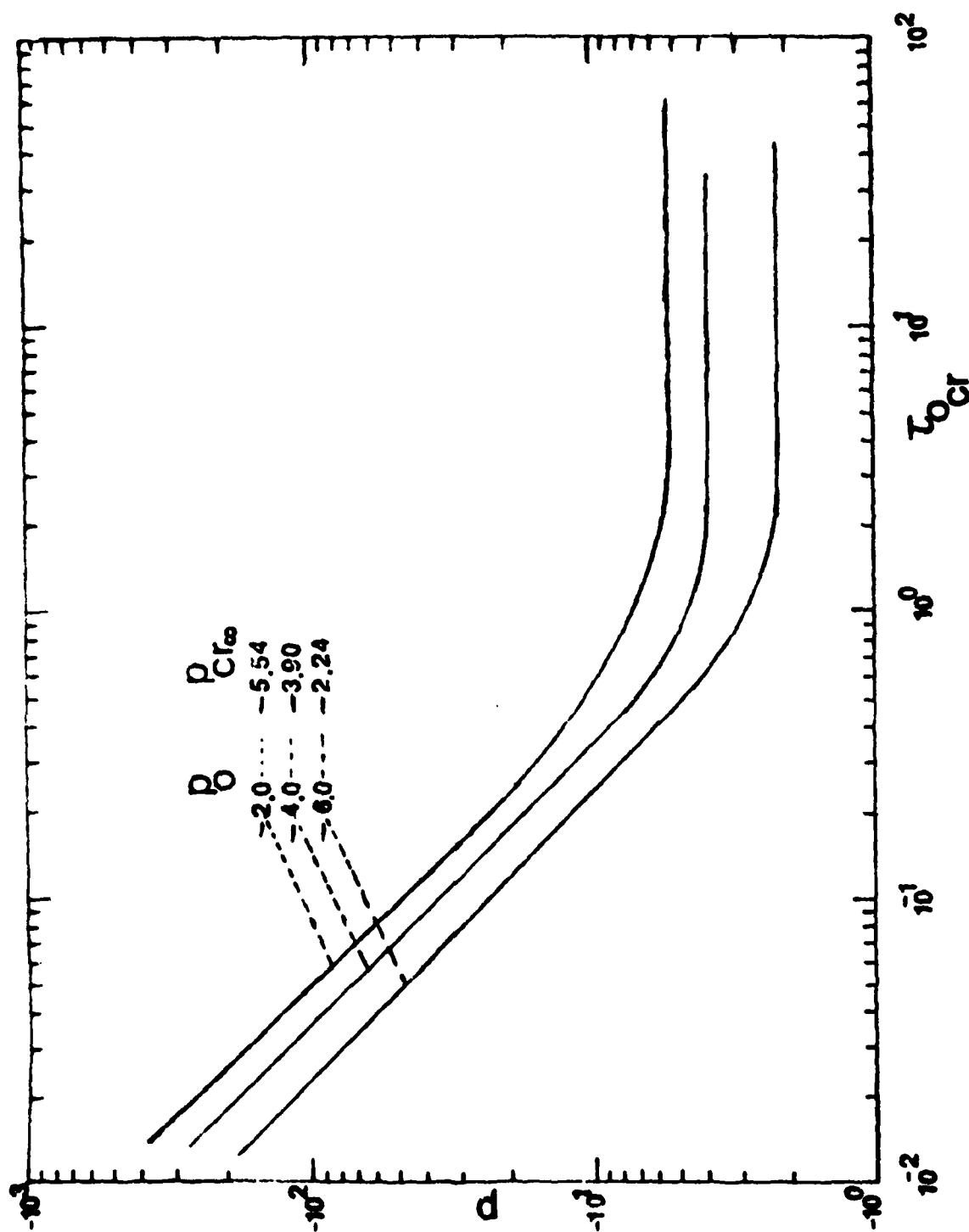


Fig. 4.5. Constant load, p , versus critical Duration Time, τ_{ocr} ; Preloaded pinned Arch, $e=5.0$

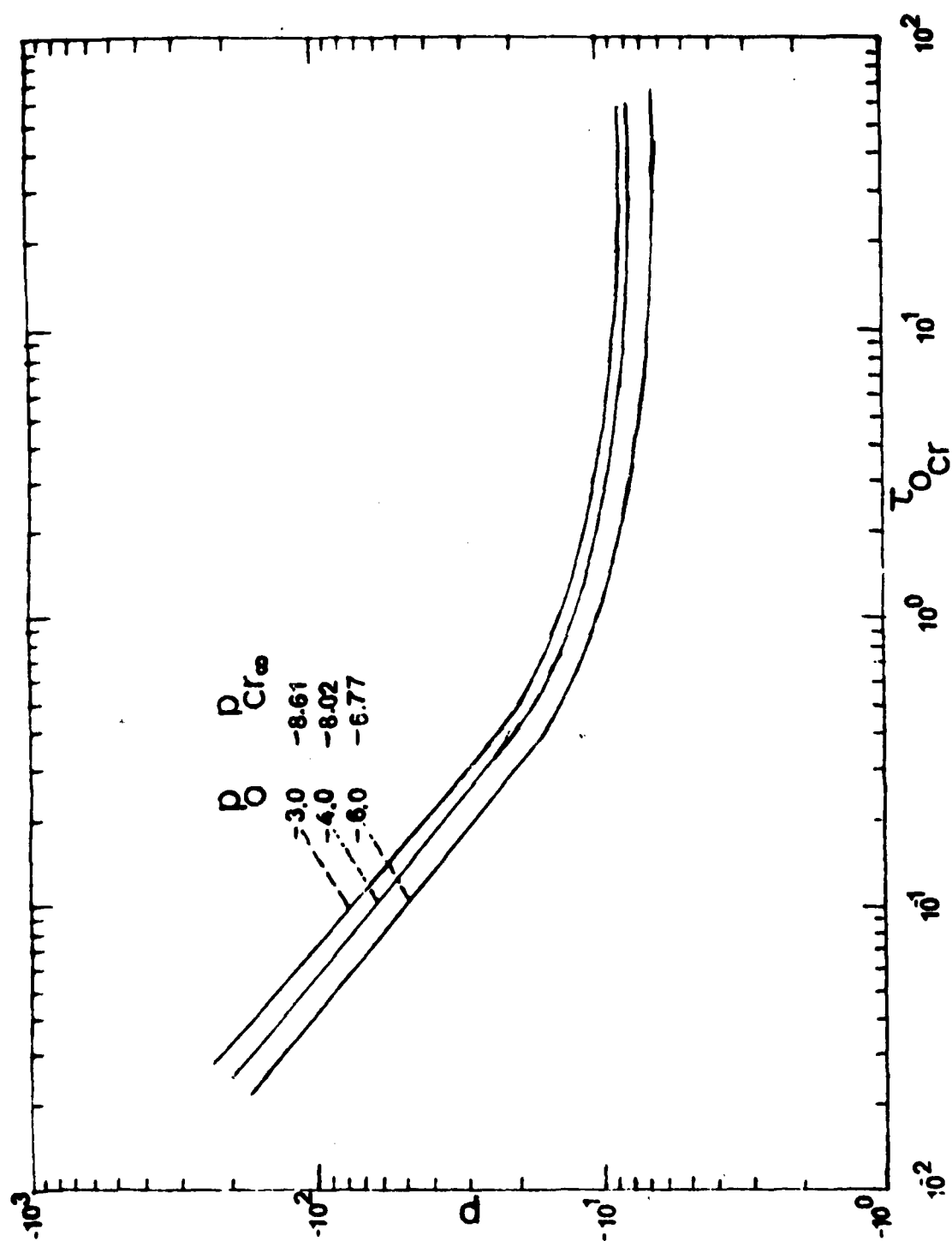


Fig. 4.6. Constant load, p , versus critical Duration Time, τ_{ocr} ; Preloaded pinned Arch, $e=6.0$

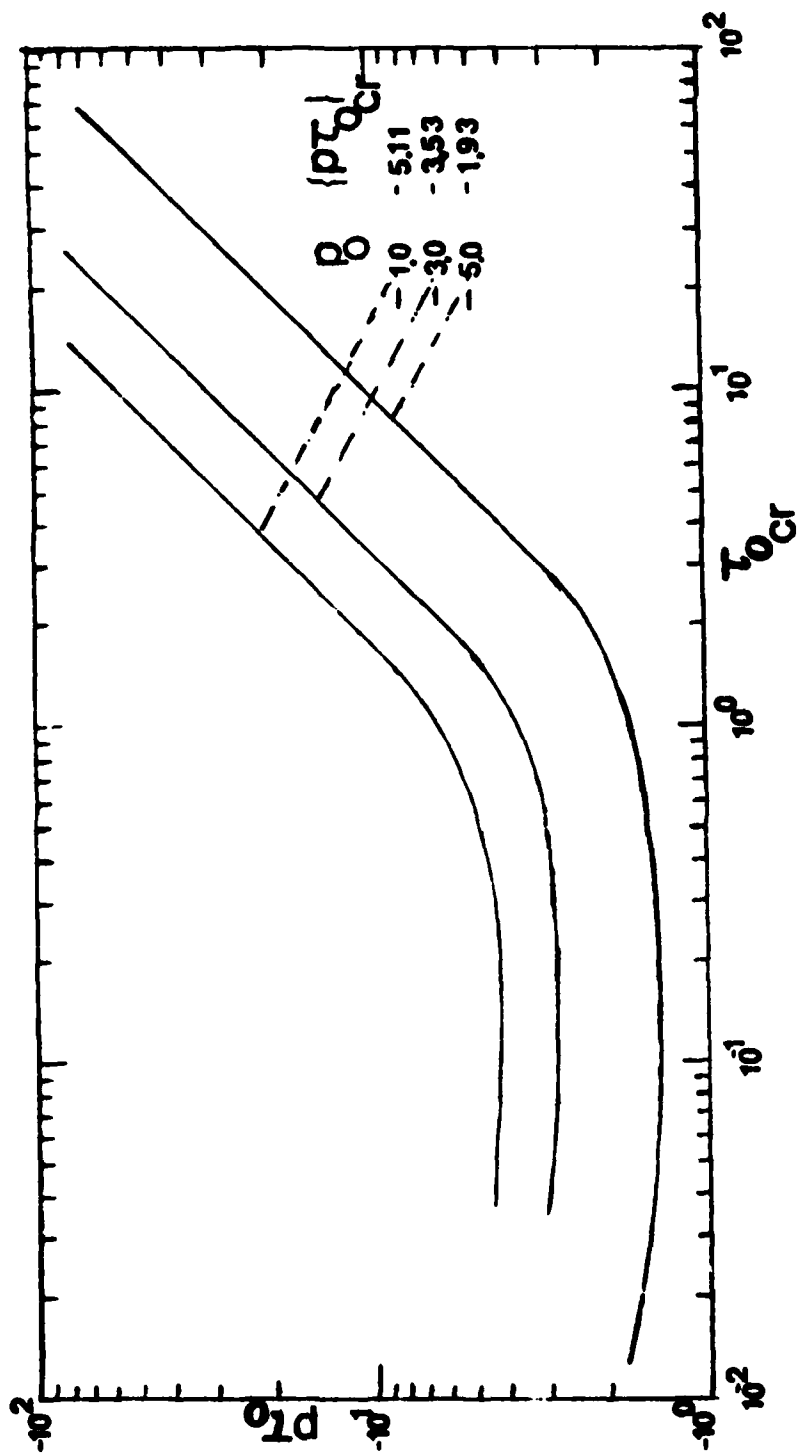


Fig. 4.7. Impulse, $(p\tau_0)$, versus critical Duration Time, τ_{0cr} ; Preloaded pinned Arch, $e = 4.5$.

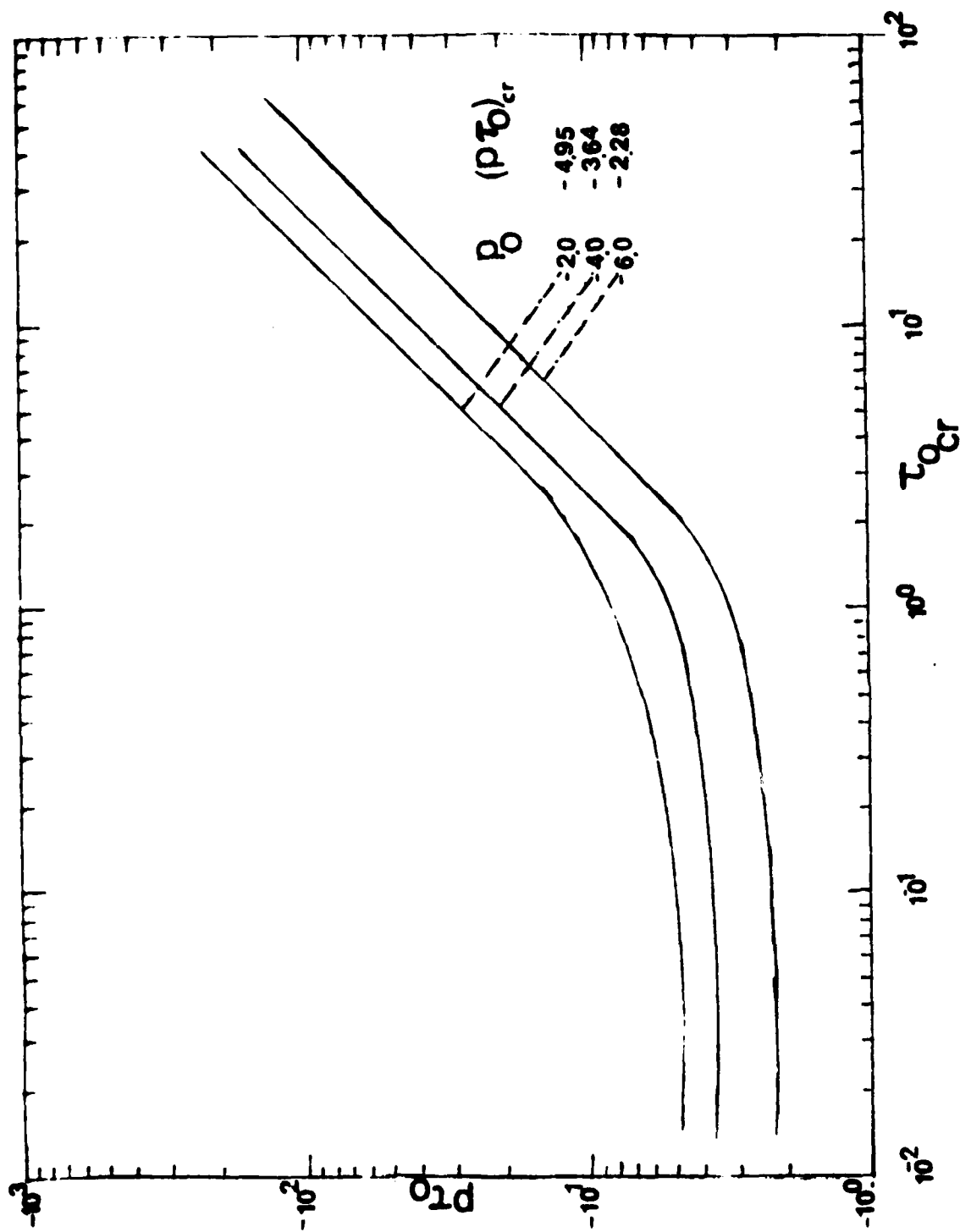


Fig. 4.8. Impulse, (p_0) versus critical Duration Time, τ_{0cr} ; Preloaded pinned Arch, $e=5.0$

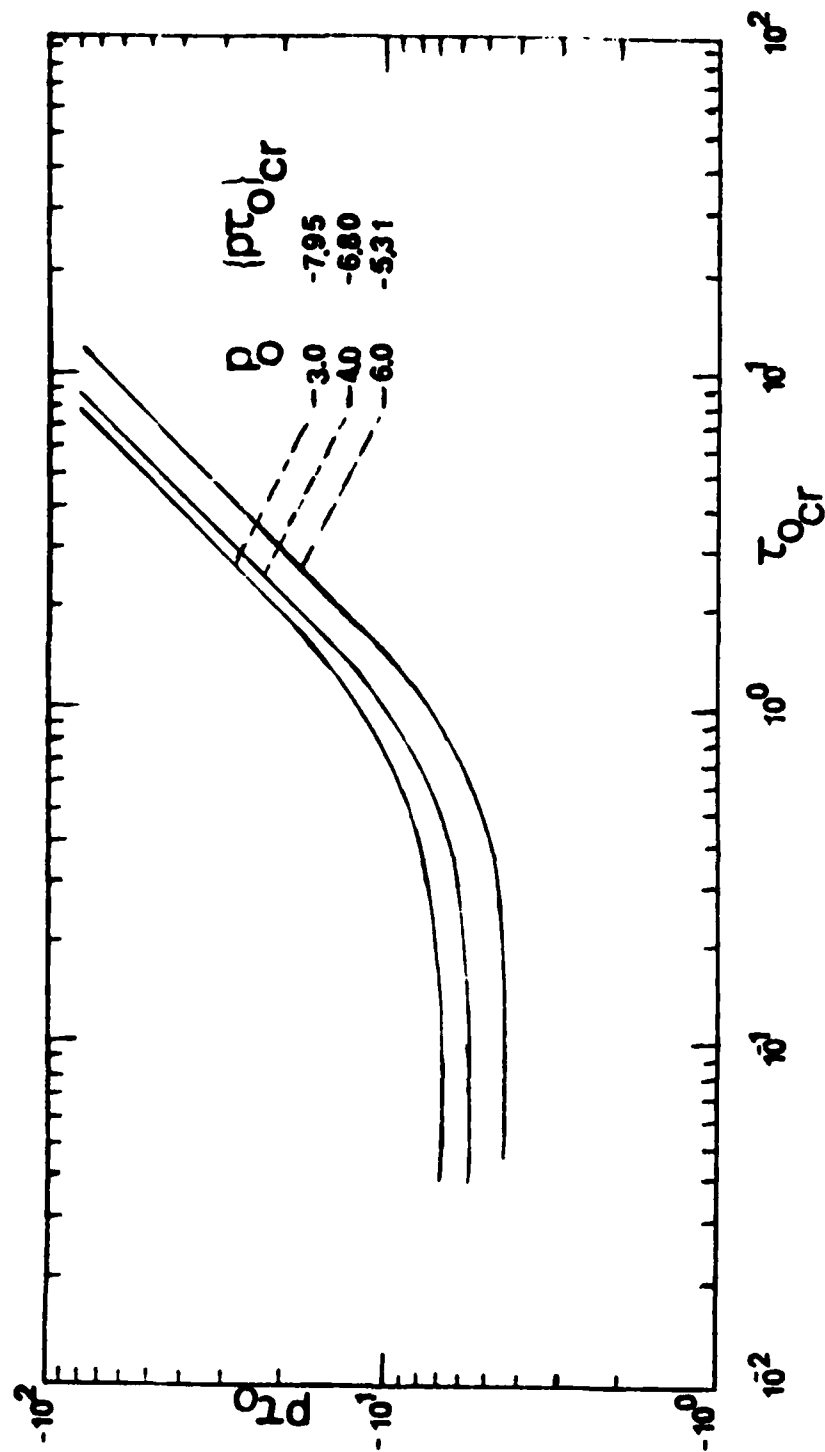


Fig. 4.9. Impulse, (P_0) , versus critical Duration Time, τ_{ocr} ; Preloaded pinned Arch, $e = 6.0$.

Effect of Small Damping

In this section, the effect of small damping on the dynamic stability of the arch (subjected to a constant load of finite duration) is investigated. If μ indicates the damping coefficient, the dissipated energy D , because of damping, is given by [see Section VII of Ref. 1 for concepts and details]

$$D = \mu \int_v \int_w \frac{\partial w}{\partial t} dw dA dx = \mu A \int_0^L \int_w \frac{\partial w}{\partial t} dw dx \quad (4.25)$$

where v stands for volume.

Recalling that $w = \rho \{ \eta_0(\xi) + r(\tau) \sin \xi + a_2(\tau) \sin 2\xi \}$, where $\rho^2 = \frac{I}{A}$ and $x = \frac{L}{\pi} \xi$, then Eq. (4.25) becomes

$$D = \frac{\mu \rho^2 L}{\pi} A \int_0^\pi \oint_{r, a_2} (\dot{r} \sin \xi + \dot{a}_2 \sin 2\xi) (dr \sin \xi + da_2 \sin 2\xi) d\xi \quad (4.26)$$

Since the symmetric path ($a_2 \equiv 0$) is the solution to the undamped system, and since the integrand in Eq. (4.26) must contain only functions of the undamped system, then D reduces to

$$D = \frac{\mu \rho^2 L}{\pi} A \int_e^{r_{cr}} \dot{r} r dr \int_0^\pi \sin^2 \xi d\xi = \frac{\mu \rho^2 L A}{2} \int_e^{r_{cr}} \dot{r} r dr \quad (4.27)$$

The nondimensionalization of D is given by

$$\bar{D} = \frac{4D}{P_E \epsilon_E L} = \bar{\mu} \int_e^{r_{cr}^P} \dot{r} r dr$$

where $\bar{\mu} = \frac{2\mu \rho^2 A \sqrt{\epsilon_E \frac{\epsilon_E}{\sigma}}}{P_E \epsilon_E \frac{L}{\pi}}$ indicates the nondimensionalized damping coefficient,

and $(^0) = \frac{\partial}{\partial \tau}$ with τ given in Eqs. (4.1).

Since r_{cr}^P is expanded in Taylor's series of $\bar{\mu}$ as

$$r_{cr}^P = {}_0r_{cr}^P + \bar{\mu} {}_1r_{cr}^P + O(\bar{\mu}^2) \quad (4.28)$$

and ${}_0r_{cr}^P$ stands for the critical r -coordinate for the undamped system. Then Eq. (4.10) yields

$${}_0r_{cr}^P = e - \frac{8\left(\frac{e^2}{3} - 2\right)}{e - p} \quad (4.29)$$

However, the trajectory that the system follows, from the time of release of the load until it reaches the unstable saddle point $\left[r = -\frac{e}{3}, a_2 = \pm \left(\frac{2e^2}{9} - 4\right)^{\frac{1}{2}}\right]$, is unknown. Since Eq. (4.25) gives the dissipated energy during this period of time as

$$\bar{D} = \bar{\mu} \int_{{}_0r_{cr}}^{-\frac{e}{3}} \int_w (\sin^2 \xi + a_2' \sin^2 2\xi) \frac{0}{r} dr d\xi$$

then by following the same procedure as in Section VII of Ref. 1 for Model C, a conservative estimate for the critical condition is obtained by assuming a symmetric path ($a_2 \equiv 0$).

Then, from Eq. (7.10) of Ref. 1

$${}_1r_{cr}^P = - \frac{\int_e^{-\frac{e}{3}} \frac{0}{r} dr}{2(e - p)} \quad (4.30)$$

Moreover, assuming zero initial conditions, through the equation of motion, Eq. (4.23), along the symmetric path ($a_2 \equiv 0$) for the undamped system, one obtains

$$\dot{r} = - \sqrt{-2p(e - \hat{r}) + \frac{r^2}{8}(2e - r^2 - 8) - \frac{e^2}{8}(e^2 - 8)} \quad (4.31)$$

where $\hat{r} = r$ if $r \leq r_{cr}$ and $\hat{r} = r_{cr}$ if $r > r_{cr}$. From Eq. (4.30)

$$1\tau_{cr}^p = - \frac{\int_e^{\frac{e}{3}} \sqrt{-2p(e - \hat{r}) + \frac{r^2}{8}(2e - r^2 - 8) - \frac{e^2}{8}(e^2 - 8)} dr}{2(e - p)} \quad (4.32)$$

In addition, the critical time $\tau_{o_{cr}}$ may be found through Eq. (7.2) of Ref.

1. Recalling that the kinetic energy is given by Eq. (4.8), the critical time $\tau_{o_{cr}}$ is given by

$$\tau_{o_{cr}} = \int_e^{r_{cr}} \frac{dr}{\sqrt{-2p(e - r) + \frac{r^2}{8}(2e - r^2 - 8) - \frac{e^2}{8}(e^2 - 8) - \bar{\mu} \int_e^r x x dx}} \quad (4.33)$$

Expanding $\tau_{o_{cr}}$ in Taylor's series of $\bar{\mu}$ ($\bar{\mu} < 1$) one may write

$$\tau_{o_{cr}} = {}^o\tau_{o_{cr}} + \bar{\mu} 1\tau_{o_{cr}} + O(\mu^2)$$

Note that ${}^o\tau_{o_{cr}}$ is the critical time for the undamped system and it is given by

$${}^o\tau_{o_{cr}} = \tau_{o_{cr}} \mu = 0 = \int_e^{r_{cr}} \frac{dr}{\sqrt{-2p(e - r) + \frac{r^2}{8}(2e^2 - r^2 - 8) - \frac{e^2}{8}(e^2 - 8)}} \quad (4.34)$$

Moreover, from Eq. (4.33), one may find the expression for $1\tau_{o_{cr}}$, or

$$1\tau_{o_{cr}} = \frac{\partial \tau_{o_{cr}}}{\partial \bar{\mu}} \Big|_{\bar{\mu} = 0} = \frac{1}{2} \int_e^{\tau_{o_{cr}}} \frac{0}{x} dx - \frac{1}{[-2p(e - r) + \frac{r^2}{8} (2e^2 - r^2 - 8) - \frac{e^2}{8} (e - 8)]^{3/2}} \quad (4.35)$$

$$- \frac{1\tau_{cr}}{[-2p(e - r_{cr}^P) + \frac{r_{cr}^P}{8} (2e^2 - r_{cr}^P - 8) - \frac{e^2}{8} (e^2 - 8)]^{1/2}}$$

where corrections $1\tau_{cr}$ and $1\tau_{o_{cr}}$ depend only on undamped system parameters.

The governing equations for finding critical conditions in the presence of small damping ($\bar{\mu} \ll 1$) are Eqs. (4.29), (4.32), (4.34) and (4.35).

These four equations relate the given small damping coefficient $\bar{\mu}$, the applied load p , the time parameters $o\tau_{o_{cr}}$ and $1\tau_{o_{cr}}$, and the position parameters $o r_{cr}^P$ and $1 r_{cr}^P$. A critical condition is expressed in terms of a load level p and the corresponding time $\tau_{o_{cr}} = o\tau_{o_{cr}} + \bar{\mu} 1\tau_{o_{cr}}$. Thus, a critical condition may be found by posing the problem as follows: for a given small damping coefficient $\bar{\mu}$ and load level p , find (through the simultaneous solution of the four governing equations) the corresponding critical time parameters, $o\tau_{o_{cr}}$ and $1\tau_{o_{cr}}$, and position parameters, $o r_{cr}^P$ and $1 r_{cr}^P$. Note that the range of p -values (assigned) must be greater than dynamic critical load for the case of a suddenly applied constant load of infinite duration, without damping. The computational procedure involves the following steps: (a) assign a p -value and compute $o r_{cr}^P$ from Eq. (4.29), (b) employ Eq. (4.32) and solve for $1 r_{cr}^P$, (c) from Eq. (4.34) solve for $o\tau_{o_{cr}}$, and finally (d) employ Eq. (4.35) and solve for $1\tau_{o_{cr}}$.

A computer program is written to accomplish the solution and numerical results are generated for three values of the arch rise parameter e ($e = 4.5, 8.0, 12.0$). These results are presented on Table 4.3.

Note that, since a critical condition corresponds to a set of $p, \tau_{o_{cr}}$ values, a small damping coefficient $\bar{\mu}$ has a stabilizing effect. This effect, though, is very small. For instance, at the high values of the load p (say for $e = 4.5, p = -119.00$) the corresponding value for $\tau_{o_{cr}}$ (if $\bar{\mu} = 0.04$) is $0.098 + 0.0015 = 0.0995$. Remember that the $p - \tau_{o_{cr}}$ curve for the undamped system (see Fig. 4.2) is very steep at the high p -value and virtually flat at the low values of p . On the other hand, when $p = -7.21$ (a value close to $p_{cr_{\infty}} = -6.18$) the corresponding critical time is $\tau_{o_{cr}} = 0.59 + 0.04 = 0.63$. Since the curve is very flat at this load p -value, one may conclude that the effect of small damping is virtually negligible.

Table 4.3. Incremental Critical Time $1\tau_{o_{cr}}$ ($\bar{\mu} = 1$) for several Finite Duration Loads, p. (pinned shallow Arch).

e	p	$\sigma_{o_{cr}}^T$	$1\tau_{o_{cr}}$
4.50	-119.00	0.098	.337
	- 57.00	0.134	.379
	- 30.00	0.210	.446
	- 20.00	0.250	.517
	- 7.21	0.590	.970
8.00	-658.00	0.032	.450
	-214.00	0.089	.514
	-103.00	0.215	.620
	- 75.00	0.293	.706
	- 39.00	0.607	1.203
12.00	-561.00	0.053	.717
	-274.00	0.092	.840
	-179.00	0.183	.990
	-115.00	0.527	1.380

SECTION V

OTHER SYSTEMS

As explained in Chapter 1, it is possible to extend the concept of dynamic buckling to all structural systems regardless of their behavior under static application of the loads (see Figs. 1.1 - 1.5). This extension is presented in Ref. 1, and it is based on limiting the deflectional response of a structure (when loaded suddenly), which is in agreement with requiring boundedness of deflectional response. One should observe that in limiting the deflectional response, boundedness is automatically satisfied (in some cases enforced), while the reverse is not true.

Some examples are presented in this chapter, in order to clarify this extension of the concept of dynamic stability.

The Mass-Spring System

Consider the mass-spring (linear) system shown on Fig. 5.1. Consider a suddenly applied load, $P(t)$, applied at $t = 0$. This load may, in general, include the weight (mg). In the case of finite duration, consider the weight to be negligible.

First, the problem of constant load suddenly applied with infinite duration is considered.

For this case, one may write the equation of motion and solve for the response by imposing the proper initial conditions.

$$\ddot{x} + \frac{k}{m} x = \frac{P}{m} \quad (5.1)$$

subject to

$$\dot{x}(0) = x(0) = 0 \quad (5.2)$$

where the dot denotes differentiation with respect to time.

By changing the dependent variable to

$$y = x + C \quad (5.3)$$

where C is a constant,

the equation of motion and initial conditions become

$$\ddot{y} + \frac{k}{m} y = 0 \quad (5.4)$$

$$y(0) = -\frac{P}{k} \quad \text{and} \quad \dot{y}(0) = 0 \quad (5.5)$$

The solution is

$$y = -\frac{P}{k} \cos \sqrt{\frac{k}{m}} t \quad (5.6)$$

and

$$x = \frac{P}{k} \left(1 - \cos \sqrt{\frac{k}{m}} t \right)$$

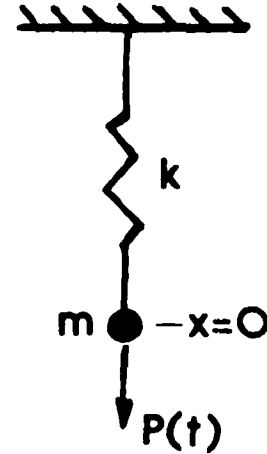


Fig. 5.1 The Mass-Spring System

Note that

$$x_{\max} = \frac{2P}{k} \quad (5.7)$$

and it occurs at

$$\sqrt{\frac{k}{m}} t = \pi \text{ or at } t = \pi \sqrt{\frac{m}{k}} = T/2 \quad (5.8)$$

where T is the period of vibration.

Note that if the load is applied quasistatically, then

$$P_{st} = kx_{st} \quad (5.9)$$

From Eqs. (5.7) and (5.9), it is clear that if the maximum dynamic response, x_{\max} and maximum static deflection $x_{st_{\max}}$ are to be equal and no larger than a specified value X (deflection limited response) then,

$$P_{st} = 2P_{dyn} \quad (5.10)$$

Because of this, many systems for which the design loads are dynamic in nature (suddenly applied of constant magnitude and infinite duration) are designed in terms of static considerations but with design (static) loads twice as large as the dynamic loads, Eq. (5.10). Note that both loads (P_{st} , P_{dyn}) correspond to the same maximum deflection X .

Next, this same problem is viewed from energy considerations.

First, the total potential, U_T , for the system is given by

$$U_T = \frac{1}{2} kx^2 - Px \quad (5.11)$$

and the kinetic energy, T , by

$$T = \frac{1}{2} m(\dot{x})^2 \quad (5.12)$$

Note that the system is conservative, the kinetic energy is a positive definite function of the velocity (for all t), and that $U_T = 0$ when $x = 0$. Then,

$$U_T + T = 0 \quad (5.13)$$

and motion is possible only in the range of x -values for which U_T is non-positive (see shaded area of Fig. 5.2).

It is also seen from Eq. (5.11) that the maximum x -value corresponds to $2P/k$.

Note that the static deflection is equal to P/k [Eq. (5.9) and pt A on Fig. 5.2]. Therefore, if the maximum dynamic response and maximum static deflection are to be equal to X , then Eq. (5.10) must hold.

Now, one may develop a different viewpoint for this same problem. Suppose that a load P is to be applied suddenly to the mass-spring system with the condition that the maximum deflectional response cannot be larger than a specified value X . If the magnitude of the load is such that

$$\frac{2P}{k} < X \quad (5.14)$$

we shall call the load dynamically subcritical.

When the inequality becomes an equality, we shall call the corresponding load dynamically critical (see Ref. 1). This implies that the system cannot withstand a dynamic load $P > \frac{kX}{2}$ without violating the kinematic constraint. Therefore,

$$P_{\text{dyn}_{\text{cr}}} = \frac{kX}{2} \quad (5.15)$$

This extension of the energy concept of dynamic stability was first introduced and discussed in Ref. 1.

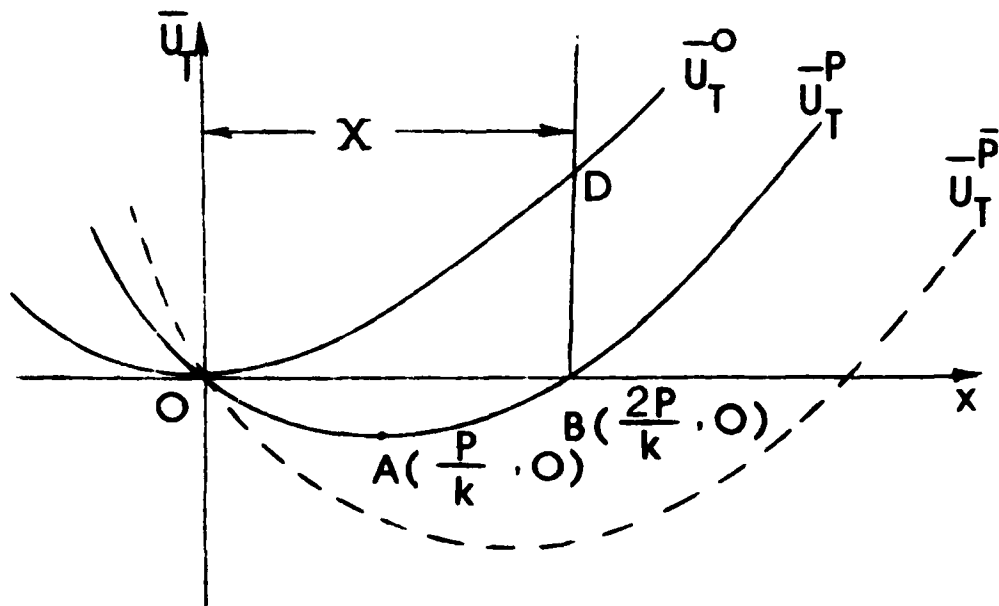


Fig. 5.2 Total Potential Curves
(Suddenly Loaded Mass-Spring
System).

Moreover, on the basis of this concept, one may find a critical ideal impulse. The question, in this load case, is to find the ideal impulse such that the system response does not exceed a prescribed value X . From Fig. 5.2 and conservation of energy

$$U_T^0 + T = T_i \quad (5.16)$$

and T_i is critical if the system can reach position D with zero velocity (kinetic energy). Thus,

$$T_{i_{cr}} = U_T^0(D) = U_T^0(X) \quad (5.17)$$

From the impulse-momentum theorem, the ideal impulse, Imp , is related to the initial velocity and consequently to the initial kinetic energy.

$$Imp = \lim_{t_0 \rightarrow 0} (Pt_0) = m\dot{x}_i \quad (5.18)$$

where \dot{x}_i is the initial velocity magnitude (unidirectional case) and t_0 is the duration time of a square pulse.

From Eq. (5.18)

$$\dot{x}_i = \frac{Imp}{m} \quad (5.19)$$

and use of Eqs. (5.12) yields

$$\dot{x}_i = \left(\frac{2T_i}{m} \right)^{1/2} \quad (5.20)$$

Since the critical initial kinetic energy is given by Eq. (5.17), then

$$Imp_{cr} = (mk)^{1/2} X \quad (5.21)$$

Next, the following nondimensionalized parameters are introduced

$$p = \frac{2P}{kX} ; \quad \xi = \frac{x}{X} ; \quad \tau = t \sqrt{\frac{k}{m}} \quad (5.23)$$

$$\bar{U}_T = \frac{2U_T}{kX^2} ; \quad \bar{T} = \frac{2T}{kX^2} ; \quad \bar{I}_{mp} = \frac{2I_{mp}}{X \sqrt{km}}$$

On the basis of this Eq. (5.21) becomes

$$\bar{I}_{mp_{cr}} = 2 \quad (5.24)$$

Finally, the concept of dynamic stability is next applied to the general case of a suddenly applied load of constant magnitude but finite duration, t_0 . The precise statement of the problem is: find the load, P , for a given duration time, t_0 (or vice versa) such that the maximum deflection is no larger than a prescribed value, X . Note that the extreme cases of $t_0 \rightarrow 0$ and ∞ have been dealt with separately, and that for this case, P must be greater than $P_{dyn_{cr}}$ [see Eq. (5.15)].

For this load case and system, conservation of energy yields

$$U_T^P + T^P = 0 \quad 0 \leq t \leq t_0 \quad (5.25)$$

and

$$U_T^0 + T^0 = C \quad t \geq t_0 \quad (5.26)$$

where C is a constant. This constant can be expressed in terms of U_T^P and U_T^0 values at the instant of release, t_0 . Since there exists kinematic continuity at t_0 , $T^P(t_0) = T^0(t_0)$ then

$$C = U_T^0(t_0) - U_T^P(t_0) \quad (5.27)$$

and

$$U_T^0 + T^0 = U_T^0(t_0) - U_T^P(t_0) \quad (5.28)$$

A critical condition exists if position X can be reached with zero velocity (kinetic energy). Thus, from Eqs. (5.28) and (5.11)

$$\frac{1}{2} kx^2 = Px(t_0) = Px_{cr} \quad (5.29)$$

where x_{cr} is the x -position at the instant of release.

From Eqs. (5.25), (5.11), and (5.12) one may write

$$\frac{1}{2} kx^2 - Px + \frac{1}{2} m(\dot{x})^2 = 0 \quad 0 \leq t \leq t_0 \quad (5.30)$$

or

$$\dot{x} = \left(\frac{2P}{m} x - \frac{k}{m} x^2 \right)^{1/2} \quad (5.31)$$

From this one may write

$$dt = \frac{dx}{\left(\frac{2P}{m} x - \frac{k}{m} x^2 \right)^{1/2}} \quad (5.32)$$

Integration from zero to t_0 yields an equation that relates t_0 , $x(t_0)$ and P .

$$t_0 = \int_0^{x_{cr}} \frac{dx}{\left(\frac{2P}{m} x - \frac{k}{m} x^2 \right)^{1/2}} \quad (5.33)$$

Eqs. (5.23) and (5.29) are two equations that relate P , x_{cr} , and t_0 . A critical condition is expressed in terms of either P_{cr} for a given t_0 or t_{0cr} for a given P -value.

Computationally, it is simpler to assign values of x_{cr} from zero up to X and solve for the corresponding P from Eq. (5.29) and for t_0 from Eq. (5.33).

Use of the nondimensionalized parameters, Eqs. (5.23), yields the following system of governing equations

$$p\xi_{cr} = 1$$

and

(5.34)

$$\tau_o = \int_0^{\xi_{cr}} \frac{d\xi}{(p\xi - \xi^2)^{1/2}}$$

Note that the first of Eqs. (5.34) corresponds to Eq. (5.29) and the second to Eq. (5.33). Moreover, the value of ξ_{cr} varies from zero to one.

The simultaneous solution of Eqs. (5.34) yields

$$p = 1/\xi_{cr} \quad \text{and} \quad \tau_{o_{cr}} = \cos^{-1}(1 - 2\xi_{cr}^2) \quad (5.35)$$

Note that as ξ_{cr} approaches one, $\tau_{o_{cr}}$ is equal to half the period of oscillations and $p = 1$, which is the value that corresponds to the case of constant load suddenly applied, with infinite duration [see Eq. (5.15)].

The results are shown graphically on Fig. 5.3, as plots of p versus t_o/T or $\tau_o/2\pi$.

Parenthesis

Eq. (5.29) may be interpreted in a different way. For instance, one may write

$$kx_{cr}^2 = 2Px_{cr} \quad (5.36)$$

where x_{cr} is the position of the mass at the instant of release of the force, P , and X is the maximum amplitude of oscillations (maximum dynamic response). Moreover, P/k is a measure of the maximum static displacement, $x_{st \max}$ (if P were applied quasi-statically). Then, Eq. (5.36) may be

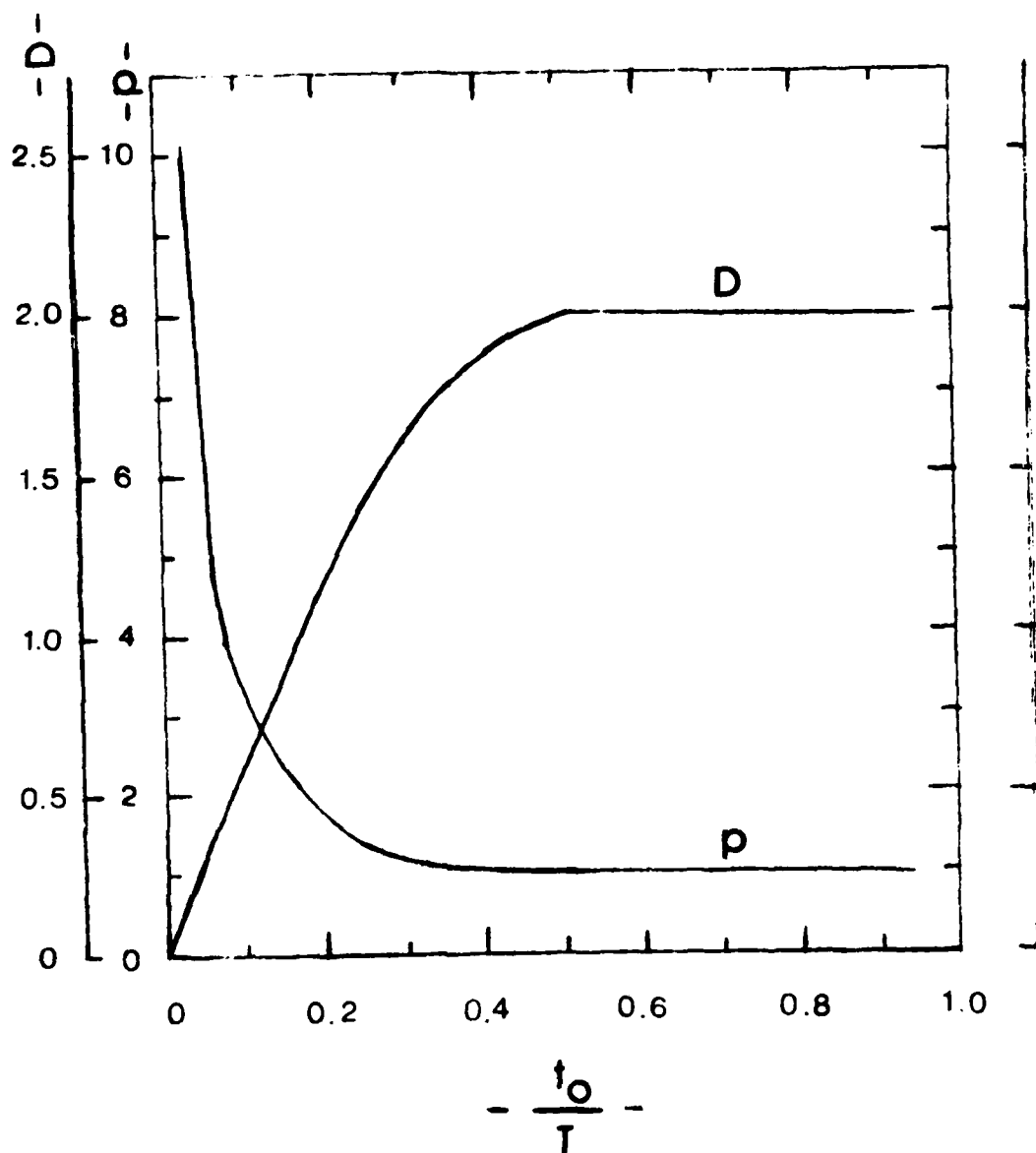


Fig. 5.3 Critical Load and Dynamic Magnification Factor
versus Duration time $\left(\frac{t_o}{T} \text{ or } \frac{\tau_o}{2\pi}\right)$.

written as

$$2 \frac{x_{st_{max}}}{X} \cdot \frac{x_{cr}}{X} = 1 \quad (5.37)$$

Next, $\frac{X}{x_{st_{max}}} = D$ is the dynamic magnification factor and $x_{cr}/X = \xi_{cr}$.

Therefore, Eq. (5.37) becomes

$$2\xi_{cr}/D = 1 \quad \text{or} \quad (5.38)$$

$$\xi_{cr} = \frac{D}{2}$$

Finally, the relation between t_o/T ($= \tau_o/2\pi$) and the magnification factor, D , is obtained from the second of Eqs. (5.35), or

$$\tau_o/2\pi = \frac{t_o}{T} = \frac{1}{2\pi} \cos^{-1} \left(1 - \frac{D^2}{2} \right) \quad (5.39)$$

from which

$$D = 2 \sin \left(\frac{\tau_o}{2} \right) = 2 \sin \frac{\pi t_o}{T} \quad (5.40)$$

The dynamic magnification factor D , (see p. 94 of Ref. 36) is also plotted on Fig. 5.3 and it is identical to that shown on Fig. 6-6 of Ref. 36.

Note that the parameters plotted on Fig. 5.3 represent two different points of view. The plot of p versus t_o/T depicts the amount of a sudden load with finite duration t_o that corresponds to a maximum amplitude X . On the other hand, the plot of D versus t_o/T shows the magnification of the maximum amplitude (compared to the static one) due to sudden application of the load with duration time, t_o . Note that in both cases, t_o need not be larger than half the period of oscillation or $t_o/T < 2$.

Finally, before closing this section, one can see that the extreme cases of $t_0 \rightarrow \infty$ and $t_0 \rightarrow 0$ are special cases of the finite duration case.

From Fig. 5.3, one sees that as $\frac{t_0}{T} \rightarrow \infty$ $p \rightarrow 1$ which is in agreement with Eq. (5.15). The other extreme case is obtained from Eqs. (5.34).

If $t_0 \rightarrow 0$, then ξ_{cr} is an extremely small number and since $0 < \xi \leq \xi_{cr}$ then the second of Eqs. (5.34) becomes

$$\tau_0 = \int_0^{\xi_{cr}} \frac{d\xi}{(\xi/\xi_{cr} - \xi^2)^{1/2}} \approx \int_0^{\xi_{cr}} \frac{d\xi}{(\xi/\xi_{cr})^{1/2}} = 2\xi_{cr} \quad (5.41)$$

Then

$$(\text{Imp})_{cr} = (p\tau_0)_{cr} = \frac{1}{\xi_{cr}} \cdot 2\xi_{cr} = 2$$

which is identical to the result of Eq. (5.24).

Suddenly Loaded Beams

A large class of structural problems, that may be treated in a similar manner as the mass-spring system, is that of Euler-Bernoulli beams. Under static application of the loads, these configurations exhibit unique stable equilibrium positions at each load level (see Fig. 1.5).

Consider, as an example, the cantilever shown on Fig. 5.4. The load $P(t)$ represents a sudden load with finite duration, in general.

If one assumes that the amplitude of the beam, at any point, is given by the static deflection curve multiplied by a time dependent coefficient, $y(t)$,

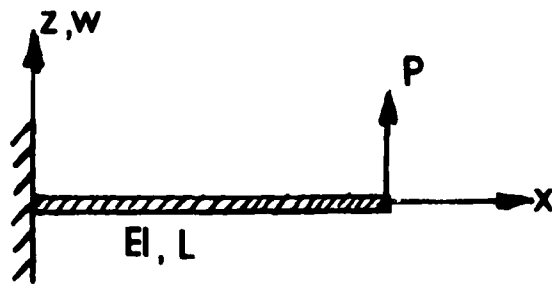


Fig. 5.4 The Cantilever Beam

then

$$w(x,t) = \frac{1}{2} y(t) \left[3\left(\frac{x}{L}\right)^2 - \left(\frac{x}{L}\right)^3 \right] \quad (5.42)$$

Note that under static application of the load P , y is the maximum (tip) deflection and it is related to the load by

$$y = \frac{PL^3}{3EI} \quad (5.43)$$

The total potential for this case is

$$U_T = \frac{EI}{2} \int_0^L \left(\frac{\partial^2 w}{\partial x^2} \right)^2 dx - PW(L,t) \quad (5.44)$$

or

$$U_T = \frac{3EI}{2L} y^2 - Py \quad (5.45)$$

Note that the stiffness, k , at the free end becomes $k = 3EI/L^3$. With this value for the stiffness, k , Eq. (5.45) is identical to Eq. (5.11) or

$$U_T = \frac{1}{2} ky^2 - Py \quad (5.46)$$

Moreover, the kinetic energy for the cantilever problem is

$$T = \frac{1}{2} \int_0^L \rho \left(\frac{\partial w}{\partial t} \right)^2 dx \quad (5.47)$$

where ρ is the linear mass density. Substitution of Eq. (5.42) into Eq. (5.47) yields

$$T = \frac{1}{2} \left(\frac{33\rho L}{140} \right) \dot{y}^2 \quad (5.48)$$

which is similar to Eq. (5.12), provided that $m = 33\rho L/140$. Eq. (5.48) indicates that for the assumed deflection curve, the continuous beam is equivalent to a spring-mass system with k and m given by

$$k = 3EI/L^3 \quad \text{and} \quad m = 33\rho L/140 \quad (5.49)$$

Moreover, the continuous beam is equivalent to a weightless beam with a concentrated mass of m units at the end (see Example 1.5-3 of p. 19 of Ref. 37).

On the basis of the above analogy, the results of the spring-mass system are applicable to the cantilever. In summary, for a prescribed maximum tip deflection, Y , the various critical conditions are given by

$$Imp_{cr} = \lim_{t_o \rightarrow 0} (Pt_o) = (mk)^{1/2} Y \quad (5.49)$$

$$= \left[0.70714 \frac{EI}{L^2 \rho} \right]^{1/2} Y$$

$$P_{dyn_{cr}} = \frac{kY}{2} = \frac{3EI}{2L^3} Y \quad (5.50)$$

Finally, for the case of suddenly applied loads of constant magnitude and finite duration, the results of Fig. 5.3 are applicable provided that the proper expression for p is used.

According to Eqs. (5.23), p may be defined as

$$p = \frac{2P}{kY} = \frac{2PL^3}{3EIY} = \frac{P}{P_{dyn_{cr}}} \quad (5.51)$$

Note also that the magnification factor, D , in this case is the maximum dynamic amplitude (\bar{Y}) divided by the maximum static response.

The Imperfect Column

The imperfect column, under sudden application of an axial load, typifies structural systems with static behavior shown on Fig. 1.1. Note that such a system, when of perfect geometry, is subject to bifurcational

buckling with stable post-buckling behavior (smooth buckling). On the other hand, if there exists an initial geometric imperfection (small initial curvature), the system exhibits a unique stable equilibrium path. Moreover, this system has received the most attention, as far as dynamic buckling is concerned when loaded axially either by sudden loads or by time-dependent loads. Two complete reviews (with respect to their date of publication) of this problem may be found in Refs. 38 and 39. As mentioned in these references, the problem dates back to 1933 with the pioneering work of Koning and Taub (Ref. 40), who considered a simply supported, imperfect (half-sine wave) column subjected to an axial sudden load of specified duration. In their analysis, they neglected the effects of longitudinal inertia, and they showed that for loads higher than the static (Euler load) the lateral deflection increases exponentially, while the column is loaded, and after the release of the load, the column simply oscillates freely with an amplitude equal to the maximum deflection. Many investigations followed this work with several variations. Some included inertia effects, others added effect of transverse shear, etc. The real difficulty of the problem, though, lies in the fact that there was no clear understanding by some investigators of the concept of dynamic stability and the related criteria.

According to Ref. 39, definition of a dynamic buckling load is possible only if there are initial small lateral imperfections in the column. Instability stems then from the growth of these imperfections. "Buckling occurs when the dynamic load reaches a critical value, associated with a maximum acceptable deformation, the magnitude of which is defined in most studies quite arbitrarily." There is some truth to this, primarily because the elastic column does not exhibit limit point instability or any

other violent type of buckling under static application of the load. There is need for a cautioning remark to the above statement, though. Analytically it has been shown (see Ref. 50) that, if a perfect column is suddenly loaded in the axial direction, the fundamental state is one of axial wave propagation (longitudinal oscillations). For some combination of the structural parameters, this state can become unstable and transverse vibrations of increasing amplitude are possible. Therefore, for this perfect column, there exists a possibility of parametric resonance, which is one form of dynamic instability. In spite of this, mostly all columns are geometrically imperfect and therefore, it is reasonable to investigate the dynamic behavior of imperfect columns including all variations of different effects as reported in Refs. 38-49. These effects include: axial inertia, rotatory inertia, transverse shear, and various loading mechanisms. Moreover, experimental results have been generated to test the various theories and effects.

Finally, the criterion employed in Ref. 39, is the one developed by Budiansky and Roth (Ref. 3), and it is applicable only to imperfection sensitive structural systems, such as shallow arches, shallow spherical caps, and axially-loaded, imperfect, cylindrical shells. The reason that the application of the Budiansky-Roth criterion can possibly yield reasonable results for imperfect columns lies in the fact that the corresponding perfect configuration (column) possesses a very flat post-buckling branch. This means that the corresponding imperfect column can experience, at some level of the sudden load or impulse, very large amplitude oscillations (change from small to large amplitude oscillations). Note that the static curve for the imperfect column (static equilibrium), if the load is plotted versus the maximum lateral deflection, yields small values

for the maximum deflection for small levels of the load. As the load approaches the Euler load, the value of the corresponding maximum deflection increases rapidly. On the other hand, if the criterion were to be applied to an imperfect flat plate, it is rather doubtful that reasonable, or any, answers could be obtained. This is so because the slope of the static postbuckling curve, for the perfect plate, is positive, and the imperfect plate exhibits a continuous bending response with smoothly increasing amplitude.

Next, the concept of dynamic stability, as developed in Ref. 1 and discussed in Chapter 1, is applied to an imperfect column. Consider the column shown on Fig. 5.5. The length of the column is L (distance between supports), the bending and extensional stiffnesses are uniform, EI and EA , and the sudden load, $P(t)$, is acting along the horizontal, x , direction. Let u be the horizontal displacement component and $w-w^0$ the vertical (transverse) displacement component. For the analysis presented herein, the initial geometric imperfection, w^0 , is a half-sine wave, or

$$w^0(x) = w_0 \sin \frac{\pi x}{L} \quad (5.52)$$

The kinematic relations and the relations between the axial force, P , and bending moment, M , on one hand and the reference axis strain, ϵ^0 , and change in curvature, κ , on the other are

$$\epsilon = \epsilon^0 + z\kappa \quad (5.53)$$

$$\epsilon^0 = \frac{du}{dx} + \frac{1}{2} \left(\frac{dw}{dx} \right)^2 - \frac{1}{2} \left(\frac{dw^0}{dx} \right)^2$$

$$\kappa = - \left(\frac{d^2 w}{dx^2} - \frac{d^2 w^0}{dx^2} \right) \quad (5.54)$$

$$P = EA\epsilon^0 ; \quad M = EI\kappa \quad (5.55)$$

Moreover, the total potential, U_T^* , expression for the system, is given by (for details, see Ch. 7 of Ref. 32)

$$U_T^* = \int_0^L \left[\frac{P^2}{2EA} + \frac{M^{*2}}{2EI} \right] dx + \bar{P}u(L) \quad (5.56)$$

Furthermore, the same nondimensionalization as in Ref. 32 is employed, or

$$\begin{aligned} \xi &= \frac{\pi x}{L}; \quad \eta(\xi) = \frac{w(x)}{\rho}; \quad v(\xi) = \frac{u(x)}{\rho}; \\ p &= \frac{P}{P_E}; \quad M = \frac{M^*}{\rho P_E}; \quad U_T = \frac{4U_T^*}{P_E \bar{\epsilon}_E L} \end{aligned} \quad (5.57)$$

where

$$\rho^2 = \frac{I}{A}; \quad P_E = \frac{\pi^2 EI}{L^2}; \quad \text{and} \quad \bar{\epsilon}_E = \left(\frac{\pi \rho}{L} \right)^2 \quad (5.58)$$

With these nondimensionalized parameters, one may write

$$p = \frac{1}{2} \left[2 \frac{v'}{\bar{\epsilon}_E^{1/2}} + (\eta')^2 - (\eta_o')^2 \right] \quad (5.59)$$

$$M = - (\eta'' - \eta_o'') \quad (5.60)$$

$$\begin{aligned} U_T &= \frac{1}{\pi} \int_0^\pi \left[\frac{1}{2} \left\{ 2 \frac{v'}{\bar{\epsilon}_E^{1/2}} + (\eta')^2 - (\eta_o')^2 \right\} + 2(\eta'' - \eta_o'')^2 \right] \\ &\quad + \frac{4}{\pi \bar{\epsilon}_E^{1/2}} \bar{P} v(\pi) \end{aligned} \quad (5.61)$$

where $()' = \frac{d}{d\xi}$

From Eq. (5.59), one may write

$$v' = - \bar{\epsilon}_E^{1/2} \left[\frac{1}{2} \{ (\eta')^2 - (\eta_o')^2 \} + \bar{P} \right] \quad (5.62)$$

and

$$\int_0^\pi v' d\xi = v(\pi) = -\bar{\epsilon}_E^{1/2} \left[\frac{1}{2} \int_0^\pi \left[(\eta')^2 - (\eta'_0)^2 \right] d\xi + \bar{p}\pi \right] \quad (5.63)$$

Use of Eq. (5.63) yields the following expression for the total potential,

$$\begin{aligned} U_T = & \frac{1}{\pi} \int_0^\pi 2\bar{p}^2 d\xi + \frac{2}{\pi} \int_0^\pi (\eta'' - \eta''_0)^2 d\xi \\ & - \frac{4\bar{p}}{\pi} \left[\frac{1}{2} \int_0^\pi \left[(\eta')^2 - (\eta'_0)^2 \right] d\xi + \bar{p}\pi \right] \end{aligned} \quad (5.64)$$

Note that in obtaining Eqs. (5.62) and (5.64), use of in-plane static equilibrium is made, or

$$p = \text{const} = -\bar{p} \quad (5.65)$$

For the dynamic case, this implies that the effect of in-plane inertia is being neglected.

Next, let us consider the case of a suddenly loaded (by an axial force) half-sine (imperfect) column. Then

$$w^0 = w_0 \sin \frac{\pi x}{L} \quad \eta_0 = \frac{w_0}{\rho} \sin \xi = e \sin \xi \quad (5.66)$$

Let the response, η , be the form

$$\eta = [A(\tau) + e] \sin \xi \quad (5.67)$$

The implication here is that at time $t = 0$ $\eta = e \sin \xi$.

Use of Eqs. (5.66) and (5.67) into the expression for the total potential, Eq. (5.64), yields

$$\bar{U}_T = -2\bar{p}^2 + A^2 - \bar{p}(A^2 + 2eA) \quad (5.68)$$

A modified potential, $\bar{U}_{T_{\text{mod}}}$, is introduced, such that, regardless of the level of the applied load, the total potential is zero (modified) when $t = 0$ or when $A(0) = 0$. From Eq. (5.68), it is clear that

$$\bar{U}_{T_{\text{mod}}} = \bar{U}_T + 2\bar{p}^2 = A^2 - \bar{p}(A^2 + 2eA) \quad (5.69)$$

The modified total potential is shown graphically on Fig. 5.6 for $\bar{p} = 0$ and $\bar{p} = \text{specified value}$.

As in the case of mass-spring system (note the similarity), critical dynamic conditions can be established, if the maximum allowable amplitude is specified as X .

Only the case of a suddenly applied load of constant magnitude and infinite duration is presented herein. From Fig. 5.6, it is clear that $\bar{p}_{cr_{\infty}}$ (load for which the system will not exceed the maximum allowable displacement, $A(t) \leq X$) is given by

$$X = \frac{2e\bar{p}_{cr_{\infty}}}{1 - \bar{p}_{cr_{\infty}}} \quad \text{or} \quad \bar{p}_{cr_{\infty}} = \frac{X}{X+2e} \quad (5.70)$$

On the other hand, the static load required, such that the maximum static deflection does not exceed the value X , is

$$\bar{p}_{cr_{st}} = \frac{X}{X+e} \quad (5.71)$$

Note that the above expressions, Eqs. (5.70) and (5.71) hold for $e \neq 0$.

The ratio, ρ^d , of $\bar{p}_{cr_{\infty}}$ to $\bar{p}_{cr_{st}}$ is given by

$$\rho^d = \frac{\bar{p}_{cr_{\infty}}}{\bar{p}_{cr_{st}}} = \frac{X+e}{X+2e} = \frac{1+(e/X)}{1+2(e/X)} \quad (5.72)$$

This result is shown graphically on Fig. 5.7.

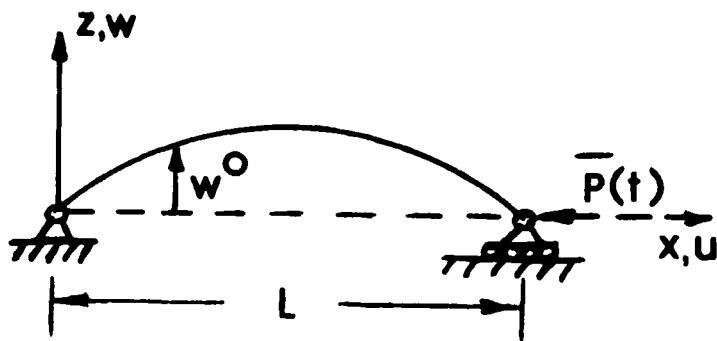


Fig. 5.5 The Imperfect Column

Note that, for very small values of e/X , the ratio ρ^d , is close to 1. For e/X equal to one, $\rho^d = 2/3$. Finally, as e/X becomes very large, then ρ^d approaches the value of one-half.

Parenthesis

If load \bar{p} is applied quasi-statically the maximum deflection, $A_{st_{max}}$, is

$$A_{st_{max}} = \frac{e\bar{p}}{1-\bar{p}} \quad (5.73)$$

If load \bar{p} is applied suddenly the maximum amplitude, $A_{d_{max}}$, is given by

$$A_{d_{max}} = \frac{2e\bar{p}}{1-\bar{p}} \quad (5.74)$$

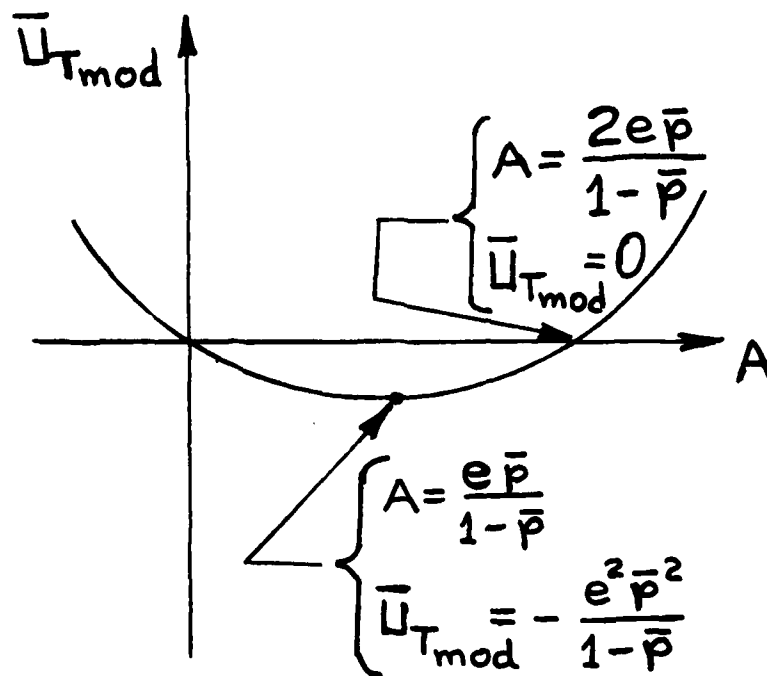


Fig. 5.6 Total Potential for a Suddenly-Loaded Half-Sine Column.

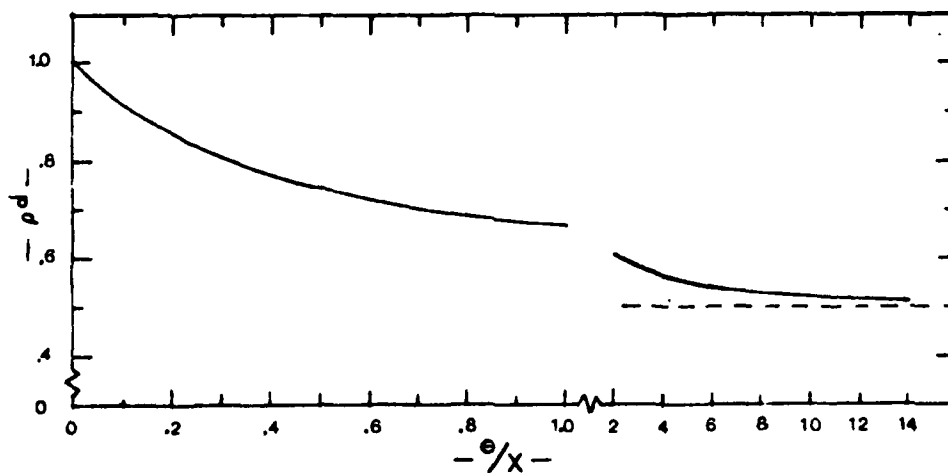


Fig. 5.7 Ratio of Dynamic to Static Load versus ratio of imperfection parameter to maximum allowable displacement (for the imperfect column).

On the basis of the above, the dynamic magnification factor, for this case, is

$$D = A_{d_{\max}} / A_{st_{\max}} = 2 \quad (5.75)$$

regardless of the value of e .

ACKNOWLEDGEMENT

The authors wish to thank the U.S. Air Force Aeronautical Systems Division (AFSC), Patterson Air Force Base, for financially supporting the reported research. Moreover, they wish to thank Dr. V. B. Venkayya for his encouragement and support during the course of the investigation. Furthermore, the authors are grateful to Mr. Andreas Vlahinos for performing some of the calculation and for the artwork. Finally, the authors wish to thank Mrs. Nancy Starkey and Mrs. Betty Mitchell for typing the manuscript and particularly for showing patience and understanding. Mrs. Peggy Varalla's help is also gratefully acknowledged.

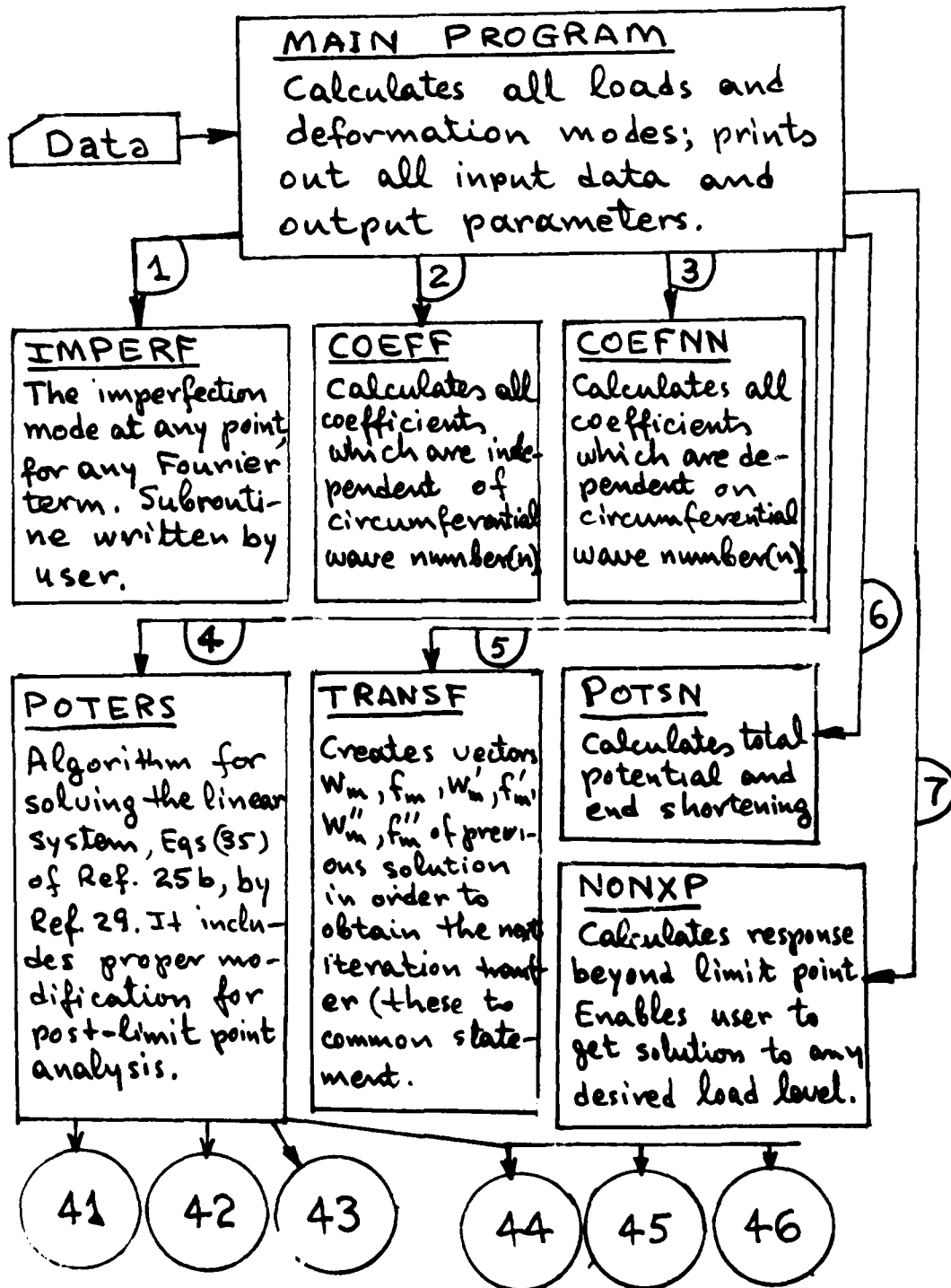
APPENDIX A

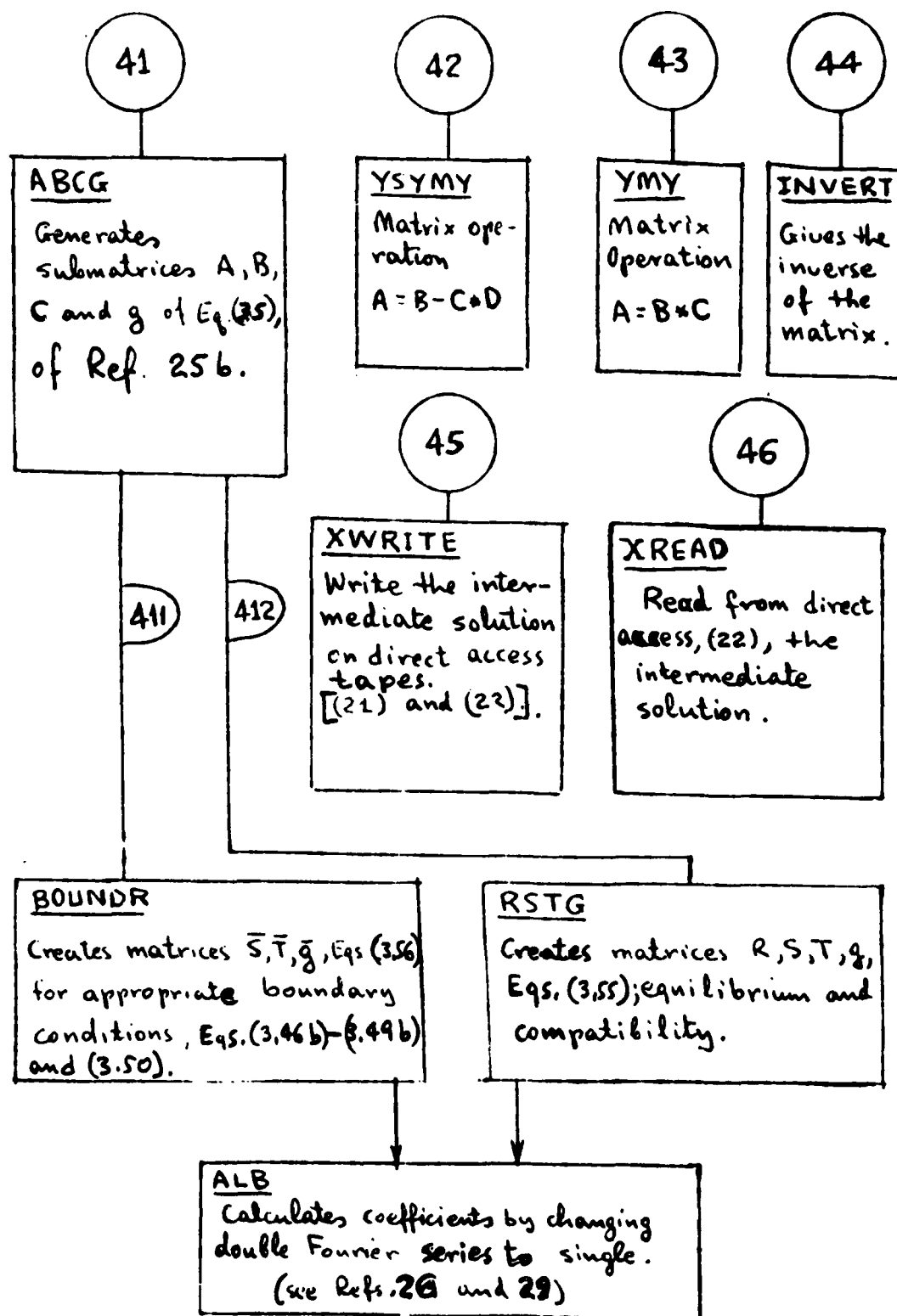
FLOW CHART

(CYLINDRICAL SHELL ANALYSIS)

PRECEDING PAGE BLANK-NOT FILMED

I. BLOCK DIAGRAM





COMMON CARDS

1) Common/CINTG/NEQPOT, MI(500)

NEQPOT - Number of points in axial direction

MI(500) - The order of Eq. I, MI(I) [according to Ref. 29].

2) COMMON/BOUND/LS1, LSN

Definition of boundary condition at the first point (LS1), and at the last point (LSN) of the shell.

3) COMMON/FIDFR/DELTA, AL1, GA1, AL2, BT2, GA2.

Coefficients of finite difference form, Δ , $\alpha^1 = -1/2\Delta$, $\gamma^1 = 1/2\Delta$, $\alpha^2 = \gamma^2 = 1/\Delta^2$, $\beta^2 = -2/\Delta^2$.

4) COMMON/FOURIR/KFOUR, K6, K4, K3, K2, K1.

Fourier series limit ($K = KFOUR$) and parameters dependent on K .

5) COMMON/GEOM/RR, DD, H₁₁, H₁₂, H₂₂, Q₁₁, Q₁₂, Q₂₂, D₁₁, D₁₂, D₂₂

Shell geometric parameters, $R, D, R_{ij}, q_{ij}, d_{ij}$ [Eqs. (3.12) - (3.14)].

6) COMMON/FACTOR/C1, C2, C12.

Coefficients which are dependent on circumferential wave number.

7) COMMON/FACT2/DL1-DL4, DA1-DA4, DB2, DB3, DB4, XNI, E_{exp}.

Coefficients $\gamma_1, \gamma_2, \gamma_3, \gamma_4, a_1, a_2, a_3, a_4, b_2, b_3, b_4, \nu, E_{exp}$.

8) COMMON/CDISK/I21(501),I22(501)

Direct access data set 21 and 22.

9) COMMON/FACT3/DLS,XL,XH.

parameter, $XL=L$, $XH=t$.

10) COMMON/PRES1/WM(200,5),ETM(200,5),WMP(200,5)

The vector of previous solution W_m , W_m'' , and W_m' at point \underline{l} for Fourier term \underline{i} .

11) COMMON/PRES2/WZ(200,5),WZP(200,5),WZPP(200,5)

Imperfection mode W^0 , $W^{0'}$, $W^{0''}$ at point \underline{l} for Fourier term \underline{i} .

12) COMMON/PRES3/FM(200,8),XFM(200,8),FMP(200,8)

The vector of previous solution f_m , f_m'' , and f_m' at point \underline{l} for Fourier term \underline{i} .

13) COMMON/XXLOAD/XPRES

XPRES - hydrostatic pressure.

14) COMMON/NEWPT/JPS, INXXPX

JPS - The Fourier (+1) Number for which the unknown displacement is replaced by the load factor (and treated as known).

INXXPX - See user's manual

15) COMMON/SHEINN/VOLT (12,130), VPOT (7,130),

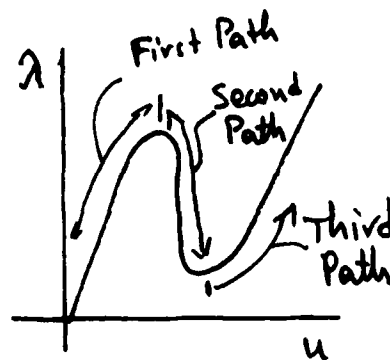
IVOLT

Arrays for printout

16) COMMON/XXNNPP/XNP1, XNP3

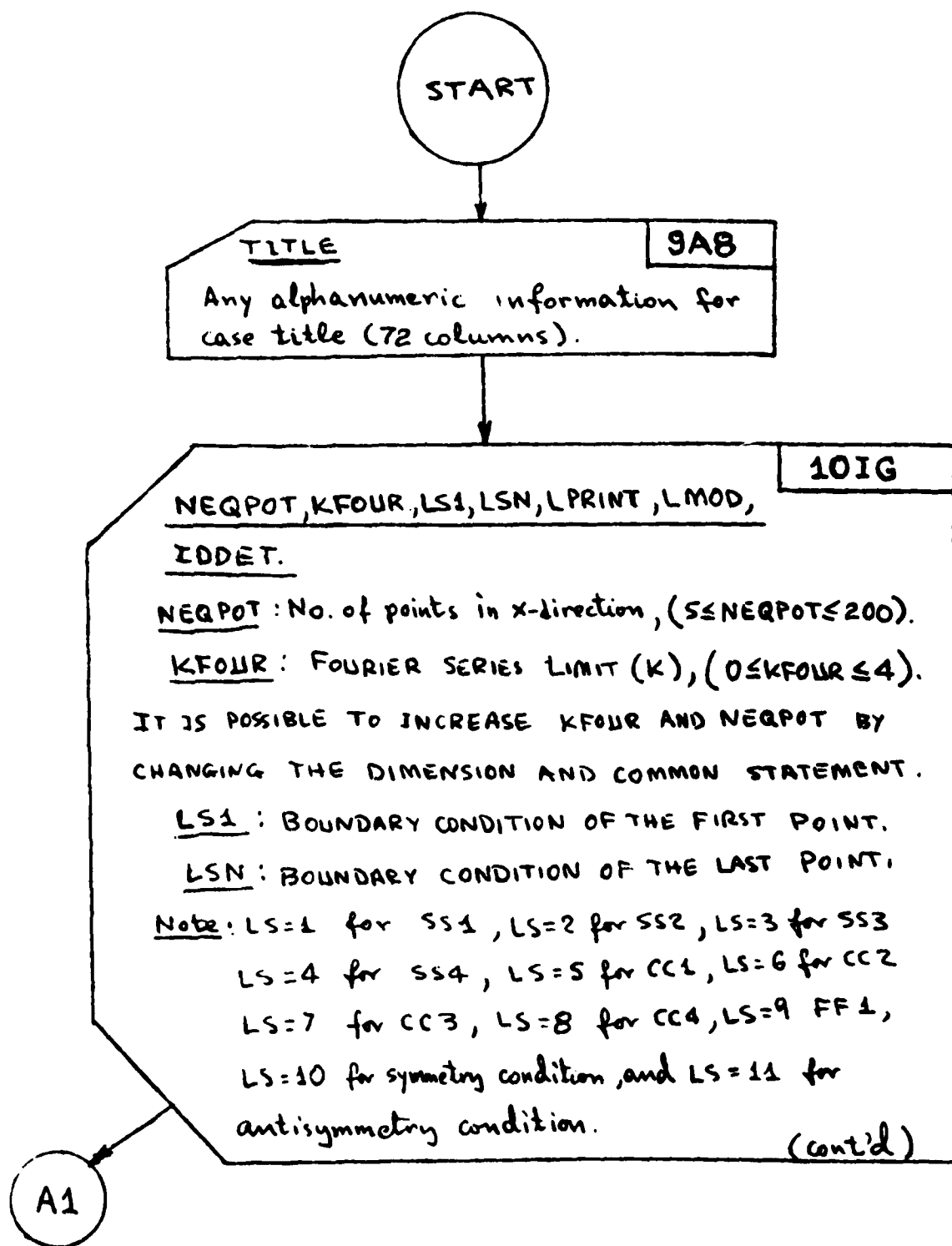
XNP1 - the limit for the first path

XNP3 - the limit for the third path.



USER'S MANUAL

II. FLOW CHART FOR DATA PREPARATION



A1

(cont'd)

LPRINT 0 = minimum printout ; 1 = maximum printout

LMOD 0 = does not print modes, 1 = prints modes

IDDET 0 = does not calculate determinant
1 = calculates determinant and prints it.

AP(12K+4,12K+4), BP(12K+4,12K+4), CP(12K+4,12K+4)
PR(12K+4,12K+4), GP(12K+4,1), XP(12K+4,1), T1(12K+4), C(12K+4),
MT(12K+4), V1((12K+4)*(12K+4)).

COMMON/PRES1/WM(NEQPOT,K+1), ETA(NEQPOT,K+1), WMP(NEQPOT,K+1).

COMMON/PRES2/WZ(NEQPOT,K+1), WZP(NEQPOT,K+1), WZPP(NEQPOT,K+1).

COMMON/PRES3/FM(NEQPOT,2K), XFM(NEQPOT,2K), FMP(NEQPOT,2K).

RR, XL, XH, ELAS, XNI

6E12.4

RR : Radius of the cylinder

XL : Length of the cylinder

XH : Thickness of the cylinder

ELAS : Modulus of Elasticity

XNI : Poisson's ratio.

A2

A2

XLAMD, YLAM, EX, EY, RHOX, RHOY

6E12.4

$$XLAMD = \lambda_{xx} = (1-v^2)A_x/tl_x$$

$$YLAM = \lambda_{yy} = (1-v^2)A_y/tl_y$$

EX = Stringer eccentricity parameter (positive inward)

EY = Ring eccentricity parameter (positive inward)

$$RHOX = \rho_{xx} = EI_{xc}/Dl_x$$

$$RHOY = \rho_{yy} = EI_{yc}/Dl_y$$

The user must write subroutine IMPERF for the definition of the imperfection and the derivatives.

$$WZ(I,J) = W^0 \quad (\text{positive inward})$$

$$WZP(I,J) = W^{0'}$$

$$WZPP(I,J) = W^{0''}$$

I = 1, NEQPOT mesh point

J = 1, KFOUR+1 for all Fourier terms

Note that since $W^0 = \sum_{i=0}^K W_i^0(x) \cos \frac{iny}{2}$

then

J=1 for i=0, and J=KFOUR+1 for i=KFOUR

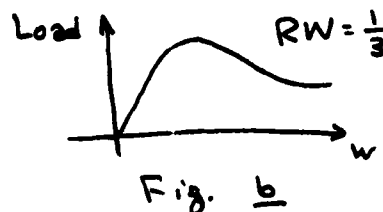
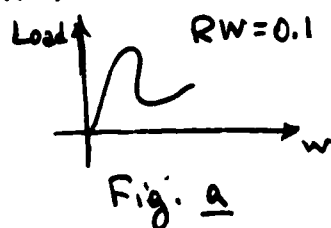
A3

INXXPX, LNXXPX, JPS, LP, RW

- INXXPX = 1 for \bar{N}_{xx} and p as known
- INXXPX = 2 for \bar{N}_{xx} as unknown instead of $W(LP, JPS)$ (the initial solution $\bar{N}_{xx}^m = 0$).
- INXXPX = 3 for \bar{N}_{xx} as unknown instead of $W(LP, JPS)$. (the initial soln for \bar{N}_{xx} is the previous one).
- INXXPX = 4 for p as unknown instead of $W(LP, JPS)$.
- LNXXPX = 1 (used for INXXPX $\neq 1$) \bar{N}_{xx} or p are unknown from the second step. The first step is for getting an initial solution (for the second step).
- LNXXPX = 2 (used for INXXPX $\neq 1$) \bar{N}_{xx} and p are taken as unknowns, one step before limit pt.
- JPS The Fourier number(s) on which $W(LP, JPS)$ is replaced by load as known parameter.
- LP The mesh point on which $W(LP, JPS)$ is replaced by load as known parameter.
- RW (for INXXPX $\neq 1$) The increment of $W(LP, JPS)$. $DW(LP, JPS) = RW * W(LP, JPS)$, where $W(LP, JPS)$ is the last solution before it is replaced by the load as known (parameter). For the next step, the known displacement will be
- $$W^{m+1}(LP, JPS) = W^m(LP, JPS) + DW(LP, JPS).$$

cont'd

After running a few examples, the user can easily select an effective RW. Figs. a and b suggest values for RW, depending on the shell behavior.



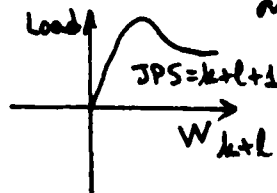
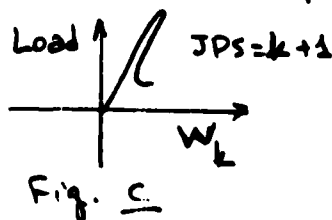
In order to save computer time, run examples by taking the load as known up to the limit pt. ($LN \times PX = Z$).

Note that $LP = \text{no. of mesh points}$, and $JPS =$

Fourier No. $+ 1$ on which $w(LP, JPS)$ is treated as a known parameter.

If LP and JPS are set to zero, the program finds automatically their proper value by identifying the most dominant displ. parameter.

Sometimes the solution does not converge because the chosen dominant parameter behaves as the ones shown on Fig. c. In this case, the user should make another choice (one for which the behavior in the post limit pt. range is similar to that of Fig. d).



The user can give only one of (LP, JPS) or both, or none (by setting them to zero).

A31

DLND, XNXX, XPRESS, DNXP, ACCUR, RI,
XNP1, XNP3.

GE12.4

DLND = 1 For fixed lateral pressure p find \bar{N}_{xx} cr.

DLND = 2 For fixed axial compression \bar{N}_{xx} , find p cr.

DLND = 3 Axial load and pressure are related by the factor XNXX ($\bar{N}_{xx} = XNXX * XPRESS$).

XNXX For DLND=1, is the initial axial load
For DLND=2, is the fixed axial load
For DLND=3, is the factor that relates \bar{N}_{xx} and p (positive XNXX means compression)

XPRESS For DLND=1, is the fixed pressure
For DLND=2,3, is the initial press. (+ inward)

DNXP For DLND=1, is the increment in axial load
For DLND=2,3, is the increment in pressure.

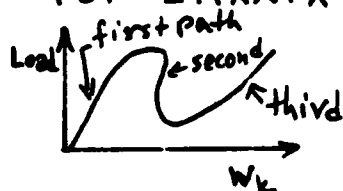
ACCUR The required load accuracy in percent.

RI Maximum number of load points

$$\bar{N}_{xx} = XNXX + RI * DNXP \text{ (for DLND = 1)}$$

$$p = XPRESS + RI * DNXP \text{ (for DLND = 2,3)}$$

For $INXXPX = 2, 3, 4$; $W(LP, JPS) = W^m(LP, JPS) + DW(LP, JPS)$.



XNP1 : The upper limit of first path

XNP3 : The upper limit of third path

The program stops automatically if XNP1 and XNP3 have been exceeded.

A4

A4

INON, INON1, INON2, INON3

1016

INON = 1 The initial solution is the linear solution

INON = 2 The initial solution (at $XNXX + DNXP$ or $XPRES + DNXP$) is the solution at previous step ($XNXX$ or $XPRES$).

INON1 same as INON but for the path on which the load is unknown.

(It is recommended to take $INON = 1$ & $INON1 = 2$).

INON2 = 2 : The results (values) of WM, ETM, WMP, FM, XFM, and FMP for the last step (last run) are put on tape (16) and on permanent file. These values may be used as an initial solution for the next (restart) run of same case.

INON3 = 2 The initial solution is given. (otherwise the program should start from point just before the limit point). In this case, INON2 = 2 (for the previous run).

Note that INON2 & INON3 exist for $LNXXPX = 1$ and $INXXPX \neq 1$.

A5

A5

NNN, LNNN, ILNW

1016

NNN - The circumferential wave number, n . The program finds the limit pt for this n .

LNNN=0 : The program does not check which n gives minimum potential energy.

LNNN=1 : The program finds the limit point for NNN and calculates the total potential for values surrounding NNN at load levels lower than the (NNN) limit point.

LNNN=2 : The program calculates the total potential only for the given load XNXX. In this case, set XNXX close to estimated limit pt.

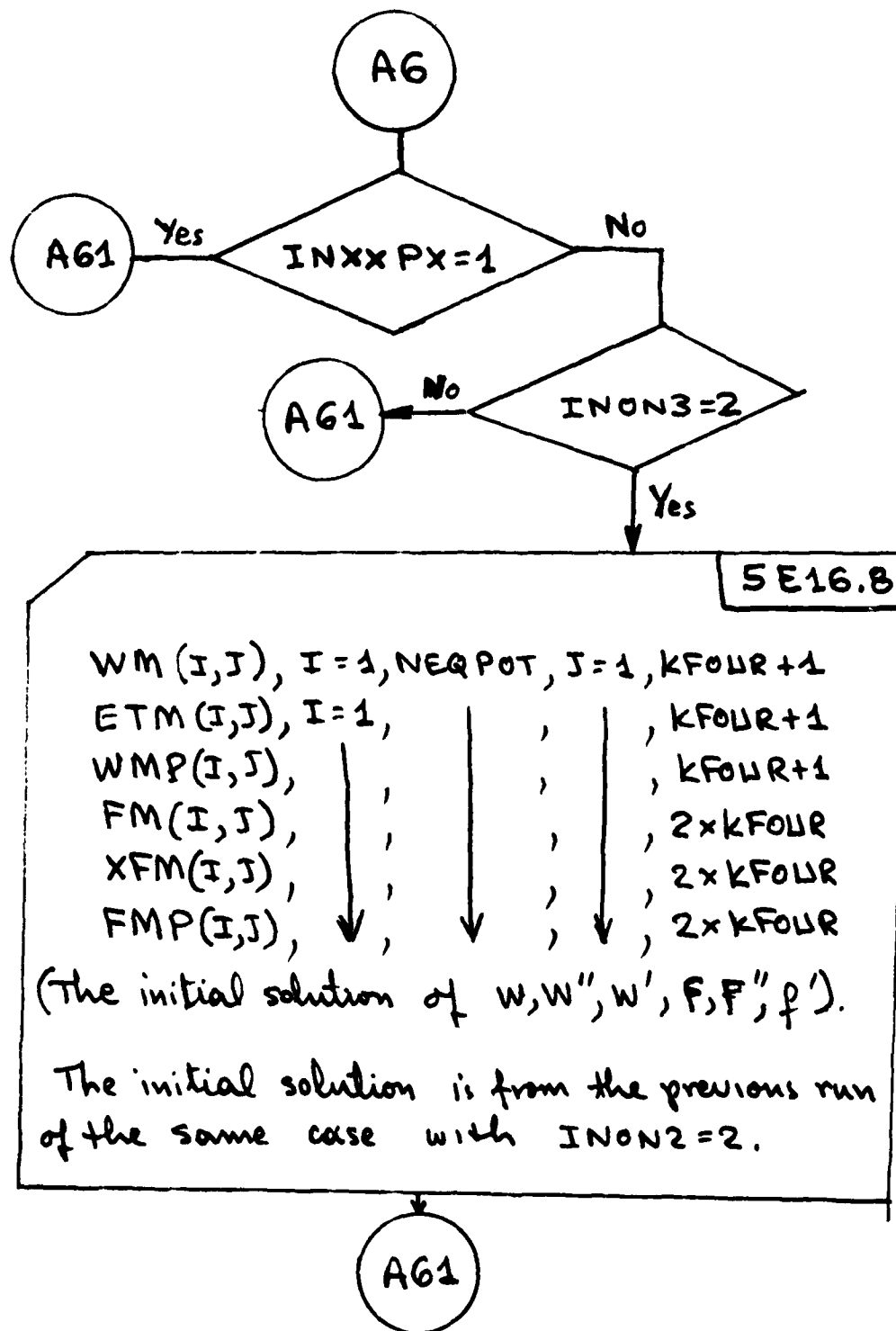
ILNW ≤ 10 : Ten is the maximum number of n -values for which the program calculates the total potential, in order to find the minimum and minimizing n .

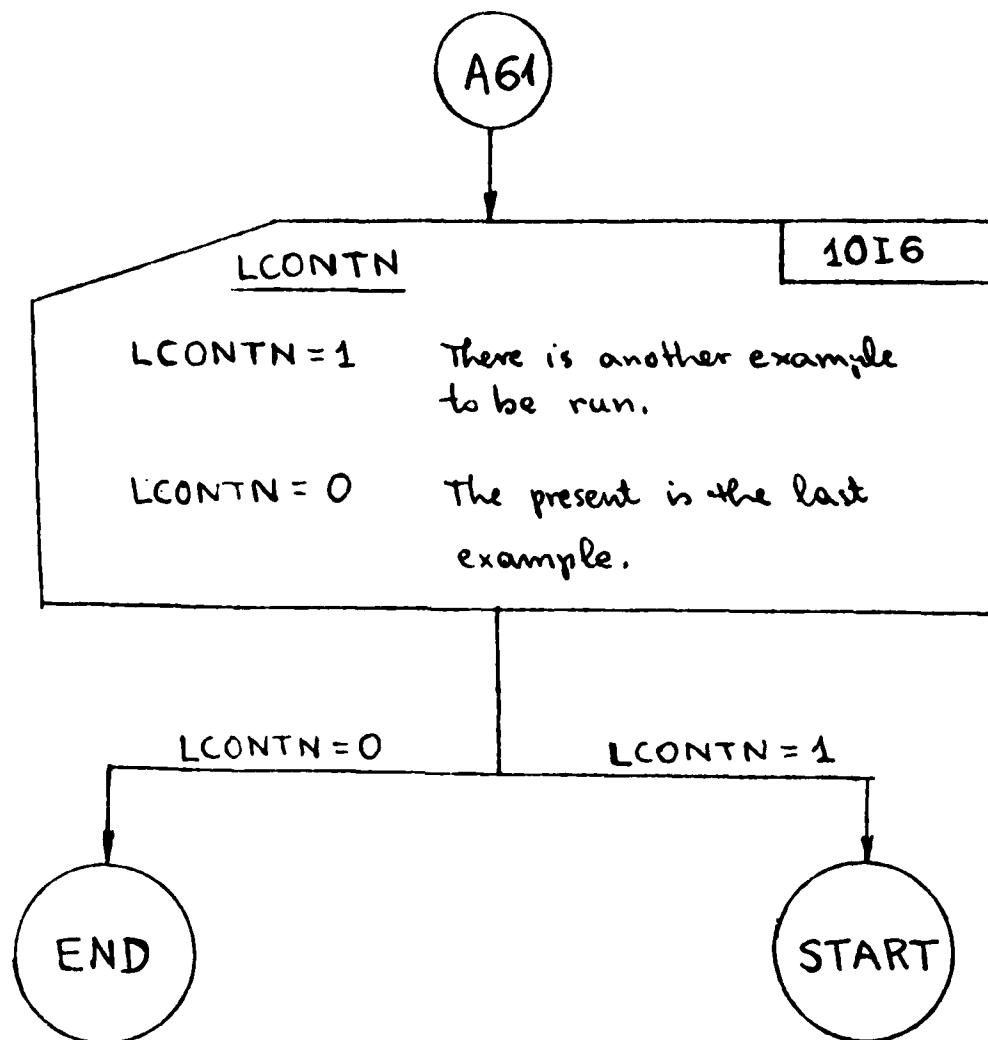
For example, if $n=5$ and ILNW=2 the program calculates the total potential for $n=5$ & 6.

If $U_T(n=6) < U_T(n=5)$ then it calculates $U_T(n=7)$; if not it calculates $U_T(n=5)$.

Note that for INXXPX $\neq 1$ LNNN should be 0

A6





APPENDIX B

COMPUTER PROGRAM

(CYLINDRICAL SHELL ANALYSIS)

```

/JOB
/NOSED
NIRIT,CM160000,T1500.
USER.
FTN,OPT=2.
LGO,INPUT,OUTPUT,DFIL,PL=99999.
REPLACE,DFIL.
/EOB

PROGRAM MAIN(INPUT,OUTPUT,DFIL,TAPES=INPUT,TAPE6=OUTPUT,
1TAPE16=DFIL,TAPE20,TAPE21,TAPE22,TAPE23)
C POST BUCKLING OF STIFFENED CYLINDRICAL SHELLS UNDER UNIFORM AXIAL 3
C COMPRESSION (NONLINEAR THEORY) 4
C AN EXTENSION OF THE PROGRAM FOR LOAD LEVEL OVER THE LIMIT
C POINT HAS BEEN DONE ON NOVEMBER 1960 IN GEORGIA TECH BY
C SHEINMAN
COMMON/XXLOAD/XFRES 5
COMMON/COINTG/NEOPT,MI(500) 6
COMMON/BOUNDO/LS1,LSH 7
COMMON/FIDFR/DELTA,AL1,GA1,AL2,GT2,GA2 8
COMMON/FOURIR/KFOUR,K0,K4,K3,K2,K1 9
COMMON/SEGM/R0,00,H11,H12,H22,Q11,Q12,Q22,D11,D12,D22 10
COMMON/FACTOR/C1,C2,C3,C4,C5,C6,C7,C8,C9,C10,C11,C12 11
COMMON/FACT2/DL1,DL2,DL3,DL4,DA1,DA2,DA3,DA4,DB2,DB3,DB4,XNI,EXXP 12
COMMON/CDISK/I21(501),I22(501),I23(501) 13
COMMON/FACT3/DL5,XL,XH 14
COMMON/PRES1/WM(100,5),ETM(100,5),4MP(100,5) 15
COMMON/PRES2/WZ(100,5),WZF(100,5),WZPP(100,5) 16
COMMON/PRES3/FM(100,8),XFM(100,3),FMP(100,8) 17
COMMON/NEWPT/JPS,INXXPX
COMMON/SHEINN/VCUT(12,130),VPOT(7,130),IVCOT
COMMON/XXNMPP/XNP1,XNP3
COMMON/RVKA/XIMPS
DIMENSION WHM(5),FFM(6) 18
DIMENSION TI(10) 19
DIMENSION WF(2,5),XWF(2,5),FF(2,8),XFF(2,5) 20
DIMENSION AP(52,52),BP(52,52),CP(52,52),FR(52,52),GP(52,1) 21
DIMENSION XP(52,1),T1(52),CC(52),MT(52),V1(2704) 22
DIMENSION DP(52,1)
C 2704=52*52 23
DIMENSION WCON(20,5),FCON(20,6) 24
C ALL THE CARDS WITH SIGN ** IN COLUMNS 73,74 DEPEND ON NUMBER 25
C OF POINTS AND KFOUR 26
EQUIVALENCE (AP(1,1),V1(1)) 27
CALL OPENMS(21,I21,501,0) 28
CALL OPENMS(22,I22,501,0) 29
CALL OPENMS(23,I23,501,0)
ECONV=0.001 30
ECONN=0.001
MAXN=52 31
MAX2=MAXN*MAXN 32
NRHS=1 33
NJ=100 34
NW=5 35
NF=8 36
REWIND 16
C NJ,NW,NF - FOR DIMENSION -- NJ=MAXIMUM POINTS IN AXIAL DIRECTION 37
C NW= MAXIMUM KFOUR+1 , NF= MAXIMUM 2*KFOUR , MAXN=12*KFOUR+4 38
C IN ORDER TO INCREASE THE CAPABILITY OF THE PROGRAM FOR MANY POINTS IN 39
C DIRECTION AND HIGHER LIMIT OF FOURIER SERIES THE USER HAS TO CHANGE 40
C ALL THE CARDS WITH THE SIGN ** IN COLUMNS 73 AND 74 41
1111 WRITE(6,20) 42
READ(5,10) (TI(I),I=1,9) 43
WRITE(6,00) 44
WRITE(6,10) (TI(I),I=1,9) 45

```

READ(5,*)NEQPT,KFOUR,LS1,LSN,LPRINT,LMOD,IODET	46
IF(LPRINT.EQ.1)LMOD=1	47
READ(5,*)RR,XL,XH,ELAS,XNI,XMPS	48
READ(5,*)XLAMD,YLAMC,XX,EYY,RHOX,RHOY	49
IOVER=0	
JPR=0	
IVOUT=0	
EX=-EXX	50
EY=-EYY	51
C *****	52
CALL COEFF(EX,EY,XLAMC,YLAMC,RHOX,RHOY,ELAS)	53
C *****	54
WRITE(6,500)NEQPT,KFOUR,LS1,LSN	55
WRITE(6,501)RR,XL,XH,ELAS,XNI,DC,EXXP	56
WRITE(6,573)XLAMD,YLAMC,EXX,EYY,RHOX,RHOY	57
C *****	58
CALL IMPHF	59
C *****	60
WRITE(6,508)	61
DO 85 I=1,K1	62
LK=IK-1	63
WRITE(6,513)LK	64
WRITE(6,520)	65
XX=0.	66
DO 85 I1=1,NEQPT	67
WRITE(6,509)I1,XX,WZ(I1,IK),WZP(I1,IK),WZFP(I1,IK)	68
XX=XX+DELTA	69
85 CONTINUE	70
IF (LPRINT.NE.1) GO TO 39	71
WRITE(6,500)DELTA,AL1,GA1,AL2,BT2,GA2	72
WRITE(6,501)M11,M12,M22,Q11,Q12,Q22	73
WRITE(6,502)D11,D12,D22,D32,D33,D34	74
WRITE(6,503)DL1,DL2,DL3,DL4,DL5	75
WRITE(6,504)DA1,DA2,DA3,DA4	76
39 CONTINUE	77
DO 63 I1=1,NEQPT	78
DO 64 J1=1,K1	79
WM(I1,J1)=0.	80
ETH(I1,J1)=0.	81
WMP(I1,J1)=0.	82
64 CONTINUE	83
DO 65 J1=1,K2	84
FM(I1,J1)=0.	85
XFM(I1,J1)=0.	86
FMP(I1,J1)=0.	87
65 CONTINUE	88
63 CONTINUE	89
LP=0	
INXXPX=1	
READ(5,*)INXXP,LNXXPX,JPR,LPR,RW	
RW1=100.*RW	
WRITE(6,706)INXXP,LNXXPX,RW1	
706 FORMAT(//,2X,"INXXPX=",I5,5X,"LNXXPX=",I5//,2X,"THE INCREMENT OF	
1 W IS ",E12.4,2X,"PERCENT"/)	
READ(5,*)DLND,XNXX,XPRE,ONXX,ACCUR,RII,XNP1,XNP3	90
IRR=RII	91
IF(IRR.EQ.0)IRR=1	92
IOLND=DLND	93
ONX=ONXX	94
XPRES=XPRE	95
XFNX=XNXX	96
C XFNX=AXIAL COMPRESSION, XPRES=HYDROSTATIC PRESSURE, XNY= EITHER XFNX	97
C OR XPRES ACCORDING TO IOLND	98
GO TO(71,72,73),IOLND	99

71	WRITE(6,511)XFRES,XFNX,ONX,ACCUR	100
	XNX=XNXX	101
	XN11=XNXX	102
	GO TO 74	103
72	WRITE(6,512)XFMX,XPRES,ONX,ACCUR	104
	XNX=XPREL	105
	XN11=XFRES	106
	GO TO 74	107
73	WRITE(6,513)XNXX,XPRES,ONX,ACCUR	108
	IF(INXXP.EQ.1)GO TO 202	
	WRITE(6,203)INXXP.IDLND	
203	FORMAT(//,2X,"THE OPTION OF INXXPX=",I5,2X,"AND IDLND="	
	1,I5,2X,"IS NOT AVAILABLE YET"/)	
	STOP	
202	CONTINUE	
	TLMQX=XNXX	109
	XFNX=TLMQX*XPRES	110
	XNX=XPREL	111
	XN11=XFRES	112
74	TXNX=1000.*XNX	113
	READ(5,*)INON,INON1,INON2,INON3	114
	READ(5,*)NNN,LNNN,ILNW	115
	NWAVE=NNN	116
	IF(INXXP.NE.1)LNNN=0	
C	*****	117
	CALL COEFNN(NWAVE)	118
C	*****	119
	WRITE(6,505)NNN,INON,INON1,INON2,INON3	120
	IF(LPRINT.NE.1)GO TO 49	121
	WRITE(6,506)C1,C2,C3,C4,C5,C6	122
	WRITE(6,507)C7,C8,C9,C10,C11,C12	123
49	CONTINUE	124
	ILR=0	125
	LICON=1	126
	IPOTT=0	127
	CALL SECOND(TIM1)	128
	WRITE(6,743)TIM1	129
	TIM2=TIM1	130
	TIM4=TIM2	131
	IINN=0	132
	IF(INON2.EQ.2)WRITE(6,10)(TI(I1),I1=1,9)	
	IF(INXXP.NE.1.AND.INON3.EQ.2)GO TO 213	
	GO TO 555	
213	READ(5,214)((WM(I1,J1),I1=1,NEQPOT),J1=1,K1)	
	READ(5,214)((LTM(I1,J1),I1=1,NEQPOT),J1=1,K1)	
	READ(5,214)((WIF(I1,J1),I1=1,NEQPOT),J1=1,K1)	
	READ(5,214)((FM(I1,J1),I1=1,NEQPOT),J1=1,K2)	
	READ(5,214)((XFM(I1,J1),I1=1,NEQPOT),J1=1,K2)	
	READ(5,214)((FMP(I1,J1),I1=1,NEQPOT),J1=1,K2)	
214	FORMAT(5E16.3)	
	GO TO 815	
555	LN=1	133
	IF(IDLND.EQ.1)XFNX=XNX	134
	IF(IDLND.EQ.2.OR.IDLND.EQ.3)XPRES=XNX	135
	IF(IDLND.EQ.3)XFNX=TLMQX*XPRES	136
	IDET=IDDET	137
	CALL POTERS(IDET,NRHS,MAXN,AP,3P,CP,GP,PR,XP,CC,MT,T1,V1,MAX2,	138
	1IXPM,DETH,XFNX,LN,NJ,NH,NF,LP,DP)	139
	IF(LPRINT.NE.1)GO TO 101	140
	CALL SECOND(TIM3)	141
	TIM1=TIM3-TIM2	142
	TIM2=TIM3	143
	TIM4=TIM3	144
	WRITE(6,511)NWAVE,XFNX,XPRES,TIM1	145

101	CALL TRANSF(WF,XWF,FF,YFF,NW,NF,2,T1,MAXN,1,LPRINT,WW,XNP,LP)	146
444	IDET=IDDET	147
	IF (IDLND.EQ.1) XFN=XNX	148
	IF (IDLND.EQ.2.OR.IDLND.EQ.3) XPRES=XNX	149
	IF (IDLND.EQ.3) XFNX=TLMDX*XPRES	150
	IMAX=1	151
	WMAX=0.	152
	ITER=0	153
	DO 102 J1=1,K1	154
102	WMAX=WMAX+WM(1,J1)	155
	DO 103 I1=2,NPOT	156
	WM=0.	157
	DO 104 J1=1,K1	158
104	WM=WM+WM(I1,J1)	159
	IF (ABS(WM).LE.ABS(WMAX)) GO TO 103	160
	WMAX=WM	161
	IMAX=I1	162
103	CONTINUE	163
	JWMAX=1	164
	WM(1)=WM(IMAX,1)	165
	AWM=WM(1)	166
	IF (K1.EQ.1) GO TO 1051	167
	DO 105 J1=2,K1	168
	WM(J1)=WM(IMAX,J1)	169
	IF (ABS(WM(J1)).LE.ABS(AWM)) GO TO 105	170
	AWM=WM(J1)	171
	JWMAX=J1	172
105	CONTINUE	173
1051	JFMAX=1	174
	FFM(1)=FM(IMAX,1)	175
	AFFM=FFM(1)	176
	IF (K2.EQ.1) GO TO 333	177
	DO 106 J1=2,K2	178
	FFM(J1)=FM(IMAX,J1)	179
	IF (ABS(FFM(J1)).LE.ABS(AFFM)) GO TO 106	180
	AFFM=FFM(J1)	181
	JFMAX=J1	182
106	CONTINUE	183
333	LN=2	184
	ITER=ITER+1	185
	IF (ITER.LE.10) GO TO 113	186
	WRITE(6,114) ITER	187
	GO TO 9999	188
113	CALL POTERS(IDET,NRHS,MAXN,AP,BF,CP,GP,FR,XF,CC,MT,T1,V1,MAX2,	189
	1IXPM,DETH,XFNX,LN,NJ,NW,NF,LP,DP)	190
	IF (LPRINT.NE.1) GO TO 111	191
	CALL SECOND(TIM3)	192
	TIM1=TIM3-TIM2	193
	TIM2=TIM3	194
	WRITE(6,112) ITER,NWAVE,XFNX,XPRES,TIM1	195
111	CALL TRANSF(WF,XWF,FF,XFF,NW,NF,2,T1,MAXN,1,LPRINT,WW,XNP,LP)	196
	DO 115 J1=1,K1	197
	IF (WM(IMAX,J1).NE.0.) GO TO 57	198
	WCON(ITER,J1)=0.	199
	GO TO 115	200
57	CONTINUE	201
	WCON(ITER,J1)=ABS((WM(IMAX,J1)-WM(J1))/WM(IMAX,J1))	202
115	CONTINUE	203
	WCH=WCON(ITER,JWMAX)	204
	IWM=JWMAX	205
	DO 116 J1=1,K2	206
	IF (FM(IMAX,J1).NE.0.) GO TO 59	207
	FCON(ITER,J1)=0.	208
	GO TO 116	209

58	CONTINUE	210
	FCON(ITER,J1)=ABS((FM(IMAX,J1)-FFM(J1))/FM(IMAX,J1))	211
116	CONTINUE	212
	FCH=FCON(ITER,JFMAX)	213
	IFH=JFMAX	214
	IF(LPRINT.NE.1) GO TO 117	215
	WRITE(6,118)ITER,WCH,FCH	216
	WRITE(6,119)(J1,WCON(ITER,J1),J1=1,K1)	217
	WRITE(6,119)(J1,FCON(ITER,J1),J1=1,K2)	218
117	IF(WCH.GT.ECONV) GO TO 194	219
	IF(FCH.GT.ECONV) GO TO 194	220
	GO TO 195	221
194	IF(ITER.LE.2) GO TO 196	222
	IF(WCON(ITER,IWH).GT.WCON(ITER-1,IWH)) GO TO 197	223
	IF(FCON(ITER,IFH).GT.FCON(ITER-1,IFH)) GO TO 197	224
	GO TO 196	225
197	IF(XNX.NE.XN1) GO TO 198	226
	WRITE(6,991)XNX	227
	GO TO 999	228
198	DO 131 J1=1,K1	229
131	WHM(J1)=W(IMAX,J1)	230
	DO 132 J1=1,K2	231
132	FFM(J1)=FM(IMAX,J1)	232
	GO TO 333	233
195	IF(IOLND.EQ.1)XFNX=XNX	234
	IF(IOLND.EQ.2.OR.IOLND.EQ.3)XPRES=XNX	235
	IF(IOLND.EQ.3)XFNX=TLMDX*XPRES	236
	IVOUT=IVOUT+1	
	CALL PCTSN(POT,POTM,STRY,STRA,1,1,1,XFNX)	237
	CALL SECONO(TIM3)	238
	TIM1=TIM3-TIM4	239
	TIM2=TIM3	240
	TIM4=TIM3	241
	WRITE(6,241)XFNX,XPRES,NWAVE,ITER,TIM1	242
	WRITE(6,242)POT,POTM,STRY,STRA	243
	IF(ID=T.EQ.1) WRITE(6,243)DET,IXPH	244
	IF(LMOD.NE.1) GO TO 476	245
	CALL TRANSF(WF,XWF,FF,XFF,NW,NF,2,T1,MAXN,2,3,4W,XNP,LP)	246
476	CONTINUE	247
	IF(LNNH.EQ.2.AND.LICON.NE.10) GO TO 566	248
	IF(LICON.NE.10) GO TO 629	249
	ILR=1	250
	GO TO 777	251
629	XNX1=XNX	252
	IINN=IINN+1	253
	VOUT(1,IVOUT)=XFNX	
	VOUT(2,IVOUT)=XPRES	
	VOUT(3,IVOUT)=PCT	
	VOUT(4,IVOUT)=PCTM	
	VOUT(5,IVOUT)=STRY	
	VOUT(6,IVOUT)=STRA	
	VOUT(7,IVOUT)=0.	
	VOUT(9,IVOUT)=0.	
	IF(LF.EQ.0) GO TO 7311	
	VOUT(7,IVOUT)=WM(LP,1)	
	VOUT(9,IVOUT)=WM(LP,2)	
7311	NSHR=(NEQ(POT)+1)/2	
	VOUT(8,IVOUT)=WM(NSHR,1)	
	VOUT(10,IVOUT)=WM(NSHR,2)	
	VOUT(11,IVOUT)=ITER	
	VOUT(12,IVOUT)=NWAVE	
	IF(INXP.NE.1.AND.LNXPX.EQ.1)GO TO 615	
	IF(INXP.NE.1.AND.LNXPX.EQ.2.AND.IOVER.EQ.1)GO TO 615	
	IF(IINN.LE.IRR)GO TO 721	254

WRITE(6,722)IINN	255
GO TO 399	256
721 CONTINUE	257
XNX=XNX+DNX	258
IF(TXNX.GT.XNX) GO TO 244	259
DNX=DNX/2.	260
XNX=XNX-DNX	261
ADN=DNX*100/XNX	262
IINN=IINN-1	263
IF(ADN.GT.ACCUR) GO TO 244	264
XNX=XNX1	265
GO TO 819	266
244 IF(INON.EQ.1) GO TO 555	267
REWIND 20	268
WRITE(20)((WM(I1,J1),J1=1,K1),I1=1,NEQPOT),((ETH(I1,J1),J1=1,K1)	269
1,I1=1,NEQPOT),((WMP(I1,J1),J1=1,K1),I1=1,NEQPOT),((FM(I1,J1)	270
2,J1=1,K2),I1=1,NEQPCT),((XFM(I1,J1),J1=1,K2),I1=1,NEQPOT),	271
3((FMP(I1,J1),J1=1,K2),I1=1,NEQPCT)	272
GO TO 444	273
198 IF(LICON.NE.10) GO TO 429	274
ILR=0	275
GO TO 777	276
429 IF(LMNN.EQ.0) GO TO 249	277
IPOTT=IPCT+1	278
IF(IPOTT.GT.1) GO TO 249	279
POTT=PCT	280
PXNX=XNX-DNX	281
249 ADN=DNX*100./XNX	282
WRITE(6,545)NWAVE,XNX	283
IOVER=1	
TXNX=XNX	284
XNX=XNX-DNX	285
IINN=0	286
IF(ADN.LE.ACCUR) GO TO 819	287
DNX=DNX/2.	288
XNX=XNX-DNX	289
IF(INON.EQ.1) GO TO 555	290
REWIND 20	291
READ(20)((WM(I1,J1),J1=1,K1),I1=1,NEQPOT),((ETH(I1,J1),J1=1,K1)	292
1,I1=1,NEQPOT),((WMP(I1,J1),J1=1,K1),I1=1,NEQPOT),((FM(I1,J1)	293
2,J1=1,K2),I1=1,NEQPCT),((XFM(I1,J1),J1=1,K2),I1=1,NEQPOT),	294
2((FMP(I1,J1),J1=1,K2),I1=1,NEQPCT)	295
GO TO 444	296
819 IF(IDLND.EQ.1) XFNX=XNX	297
IF(IDLND.EQ.2) XPRES=XNX	298
IF(IDLND.EQ.3) XFNX=ILNDX*XPRES	299
WRITE(6,785)NWAVE,XFNX,XPRES,POT,PCTH,STRY,STRA	300
815 IF(INXXP.EQ.1) GO TO 816	
INXXPX=INXXP	
WH=0.	
IF(LPR.EQ.1) GO TO 944	
LP=LPR	
IF(JPR.EQ.0) GO TO 945	
JPS=JPR	
GO TO 946	
945 DO 947 J1=1,K1	
IF(ABS(WH).GE.ABS(WH(LP,J1))) GO TO 947	
WH=WH(LP,J1)	
JPS=J1	
947 CONTINUE	
GO TO 946	
944 IF(JPR.EQ.0) GO TO 941	
JPS=JPR	
DO 942 I1=1,NEQPOT	

IF (ABS(WW).GE.ABS(WM(I1,JPS)))GO TO 942	
WW=WM(I1,JPS)	
LP=I1	
942 CONTINUE	
GO TO 943	
941 CONTINUE	
DO 921 I1=1,NEQPOT	
DO 921 J1=1,K1	
IF (ABS(WW).GE.ABS(WM(I1,J1)))GO TO 921	
WW=WM(I1,J1)	
LP=I1	
JPS=J1	
921 CONTINUE	
943 CONTINUE	
IF (LP.LE.2)LP=3	
IF (LP.GE.NEQPOT-1)LP=NEQPOT-2	
946 WW=WM(LP,JPS)	
DWW=RW*WW	
CALL NONXP(XFNX,WW,DWW,LF,INON1,IODET,NRHS,MAXN,AP,BF,CP,	
1 DP,GP,PR,XP,CC,MT,T1,V1,MAX2,NJ,N4,NF,LPRINT,Wf,XWF,FF,XFF,	
2 ECONV,ECONM,NWAVE,LHOD,IRR,INON2,INOM3)	
GO TO 9999	
816 CONTINUE	
C CALCULATION OF CRITICAL WAVE NUMBER	301
566 WRITE(6,20)	302
IF (LNNN.EQ.0) GO TO 9999	303
WRITE(6,584)	304
ILR=1	305
NWPRIN=NWAVE	306
NWAVE=NWAVE+1	307
IF (LNNN.EQ.2) POTT=POT	308
POTMIN=POTT	309
NMIN=NNN	310
INWAVE=0	311
ISTCP=0	312
I9=C	313
POT=POTT	314
777 IF (IDLND.LQ.1)XFNX=XNX	315
IF (IDLND.LQ.2.OR.IDLND.EQ.3)XPRES=XNX	316
IF (IDLND.EQ.3)XFNX=TLHDX*XPRES	317
IF (ILR.EQ.1) GO TO 778	318
WRITE(6,582)NWAVE,XFNX,XPRES	319
GO TO 9999	320
778 INWAVE=INWAVE+1	321
IINN=0	322
IF (LNNN.EQ.2) FXNX=XNX	323
XNX=FXNX	324
LICON=10	325
IF (INWAVE.EQ.1) GO TO 391	326
NWPRIN=NWAVE	327
IF (I9.GE.1) GO TO 694	328
IF (POTMIN.LE.POT) GO TO 139	329
POTMIN=POT	330
NMIN=NWAVE	331
NWAVE=NWAVE+1	332
GO TO 391	333
139 IF (NWAVE.LE.NNN+1) GO TO 549	334
ISTCP=1	335
GO TO 185	336
549 I9=I9+1	337
IF (I9.GT.1) GO TO 694	338
NWAVE=NNN-1	339
GO TO 391	340
694 IF (POTMIN.LE.POT) GO TO 695	341

PCTMIN=0	342
NMIN=NWAVE	343
NWAVE=NWAVE-1	344
GO TO 391	345
695 ISTOP=1	346
GO TO 185	347
391 CALL COEFNN(NWAVE)	348
CALL SECOND(ITIM2)	349
185 WRITE(6,581)NWPRIN,PXHX,POT,TIM2	350
IF(NWAVE.LE.0) GO TO 9999	351
IF(ISTOP.NE.1) GO TO 798	352
WRITE(6,789)XNX,PCTMIN,NMIN	353
GO TO 9999	354
798 IF(INWAVE.GT.ILMW) GO TO 9999	355
GO TO 555	356
9999 READ(5,*) ILCONTN	357
WRITE(6,1021)	
1021 FORMAT(//,2X,"RESULTS FOR CONCLUSIONS"//,2X,	
1"RRRRRRRRRRRRRRRRRRRRRRRRRRRRRRRRR"//,2X,"AXIAL LOAD",2X,	
2"PRESSURE",3X,"POTENTIAL",3X,"MODIF. POT",2X,	
3"END-SHORTY=0",2X,"AVE ENDS",5X,"W(LP,0)",3X,"W(MID,0)",	
46X,"W(LP,1)",3X,"W(MID,1)",3X,"ITER NWAVE"/)	
WRITE(6,1022)(VOUT(I1,J1),I1=1,12),J1=1,IVOUT)	
1022 FORMAT(10E12.4,2F4.1)	
WRITE(6,1023)	
1023 FORMAT(//,2X,"MODIFICATION OF POTENTIAL ENERGY"//,	
13X,"POTENTIAL",4X,"MOD. POTENTIAL",5X,"PE1-F0",9X,	
2"PE2-F1",9X,"PE3-W1",8X,"PE4-NXXW",5X,"PE5-PW",6X,	
3"PE6-NXX",6X,"PE7-A2NXX"/)	
WRITE(6,1024)(VOUT(3,J1),VOUT(4,J1),(VPOT(I1,J1),I1=	
11,7),J1=1,IVOUT)	
1024 FORMAT(9E14.6)	
IF(LCONTN.EQ.1) GO TO 1111	358
20 FORMAT(1H1)	359
10 FORMAT(1H0,9A8)	360
60 FORMAT(//,25H BEGINNING OF NEXT CASE ///)	361
100 FORMAT(40I6)	362
200 FORMAT(6E12.4)	363
300 FORMAT(//,2X,"NO. OF POINTS=",I8,2X,"KFOUR=",I8,2X,"BOUND.CON OF	364
1POINT 1=",I8,2X,"BOUND.CON OF POINT NEQPOT=",I8)	365
400 FORMAT(//,2X,"R=",E12.4,2X,"XL=",E12.4,2X,"XH=",E12.4,2X,	366
1"ELAS=",E12.4,2X,"XNI=",E12.4,2X,"OO=",E12.4,2X,"EXXP=",E12.4)	367
500 FORMAT(//,2X,"THE IMPERFECTION FORM IN AXIAL DIRECTION IS"/)	368
510 FORMAT(//,2X,"THE IMPERFECTION FOR CIRCUMFERENTIAL WAVE ",I6/)	369
520 FORMAT(//,4X,"POINT",9X,"LENGTH",12X,"WZ",14X,"WZF",13X,"WZPP"/)	370
509 FORMAT(I10,4E16.6)	371
500 FORMAT(//,2X,"DELTA=",E12.4,2X,"AL1=",E12.4,2X,"GA1=",E12.4,2X,	372
1"AL2=",E12.4,2X,"PT2=",E12.4,2X,"GA2=",E12.4)	373
501 FORMAT(//,2X,"H11=",E12.4,2X,"H12=",E12.4,2X,"H22=",E12.4,2X,	374
1"Q11=",E12.4,2X,"Q12=",E12.4,2X,"Q22=",E12.4)	375
502 FORMAT(//,2X,"O11=",E12.4,2X,"O12=",E12.4,2X,"O22=",E12.4,2X,	376
1"OB2=",E12.4,2X,"OB3=",E12.4,2X,"OB4=",E12.4)	377
503 FORMAT(//,2X,"OL1=",E12.4,2X,"OL2=",E12.4,2X,"OL3=",E12.4,2X,	378
1"OL4=",E12.4,2X,"OL5=",E12.4)	379
504 FORMAT(//,2X,"DA1=",E12.4,2X,"DA2=",E12.4,2X,"DA3=",E12.4,2X,	380
1"DA4=",E12.4)	381
511 FORMAT(//,2X,"FOR FIXED PRESSURE OF ",E12.4,2X,"THE INITIAL AXIAL	382
LOAD IS ",E12.4,2X,"THE INCREMENT OF AXIAL LOAD IS ",E12.4/	383
12X,"AND THE ACCURACY (PERCENT) OF THE AXIAL LOAD IS ",E12.4)	384
512 FORMAT(//,2X,"FOR FIXED AXIAL LOAD OF ",E12.4,2X,"THE INITIAL HYDR	385
OSTATIC PRESSURE IS",E12.4/2X,"THE INCREMENT OF THE HYDROSTATIC PR	386
ESSURE IS",E12.4,2X,"AND THE ACCURACY (PERCENT) OF THE HYDROSTATIC	387
3 PRESSURE IS",E12.4)	388
505 FORMAT(//,2X,"THE CIRCUMFERENTIAL WAVE NUMBER=",I6)	389

166

WMAX=WHM	161
IMAX=I1	162
103 CONTINUE	163
IF (IMAX.EQ.LP.AND.IMAX.NE.NEQPOT) IMAX=IMAX+1	
JWMAX=1	164
WHM(1)=WM(IMAX,1)	165
AWHM=WHM(1)	166
IF (K1.EQ.1) GO TO 1051	167
DO 105 J1=2,K1	168
WHM(J1)=WM(IMAX,J1)	169
IF (ABS(WHM(J1)).LE.ABS(AWHM)) GO TO 105	170
AWHM=WHM(J1)	171
JWMAX=J1	172
105 CONTINUE	173
1051 JFMAY=1	174
FFM(1)=FM(IMAX,1)	175
AFFM=FFM(1)	176
IF (K2.EQ.1) GO TO 333	177
DO 106 J1=2,K2	178
FFM(J1)=FM(IMAX,J1)	179
IF (ABS(FFM(J1)).LE.ABS(AFFM)) GO TO 106	180
AFFM=FFM(J1)	181
JFMAY=J1	182
106 CONTINUE	183
333 LN=2	184
ITER=ITER+1	185
IF (ITER.LE.14) GO TO 113	186
WRITE(6,114) ITER	187
GO TO 403	188
114 FORMAT(//,2X,"END OF THIS CASE(NXXF) BECAUSE ITER GREATER 1THAN ",I8)	
113 CALL POTERS(IDET,NRHS,MAXN,AP,8P,CP,GP,PR,XP,CC,MT,T1,V1,MAX2, 1IXPM,DETH,XNXX,LN,NJ,NW,NF,LP,DF)	189
CALL TRANSF(WF,XWF,FF,XFF,NW,NF,2,T1,MAXN,1,LPRINT,WX,XNP,LP)	190
IF (INXXFX.EQ.4) XPRES=XNP	196
IF (INXXFX.NE.4) XNXX=XNP	
XCON(ITER)=ABS((XNP-XNN)/XNP)	
DO 115 J1=1,K1	197
IF (WM(IMAX,J1).NE.0.) GO TO 57	198
WCON(ITER,J1)=0.	199
GO TO 115	200
57 CONTINUE	201
WCON(ITER,J1)=ABS((WM(IMAX,J1)-WHM(J1))/WM(IMAX,J1))	202
115 CONTINUE	203
WCH=WCON(ITER,JWMAX)	204
IWH=JWMAX	205
DO 116 J1=1,K2	206
IF (FM(IMAX,J1).NE.0.) GO TO 58	207
FCON(ITER,J1)=0.	208
GO TO 116	209
58 CONTINUE	210
FCON(ITER,J1)=ABS((FM(IMAX,J1)-FFM(J1))/FM(IMAX,J1))	211
116 CONTINUE	212
FCH=FCON(ITER,JFMAY)	213
IFH=JFMAY	214
IF (LPRINT.NE.1) GO TO 117	215
WRITE(6,118) ITER,WCH,FCH,WX,XNP,XCON(ITER)	
WRITE(6,119) (J1,WCON(ITER,J1),J1=1,K1)	
WRITE(6,119) (J1,FCON(ITER,J1),J1=1,K2)	
118 FORMAT(//,2X,"ITER=",I5,2X,"WCH=",E15.5,2X,"FCH=",E15.5, 12X,"WX=",E15.5,2X,"XNP=",E15.5,2X,"XCON(ITER)=",E15.5/)	
119 FORMAT(//,2X,"(J1,WCON(ITER,J1),J1=1,K1)	
117 IF (XCON(ITER).GT.ECONV) GO TO 194	
IF (WCH.GT.ECONV) GO TO 194	219

```

IF (FCH.GT.1) GO TO 194
GO TO 195
194 IF (ITER.LE.4) GO TO 196
IF (XCON(ITER).GT.XCON(ITER-1)) GO TO 197
IF (WCON(ITER,IWH).GT.WCON(ITER-1,IWH)) GO TO 197
IF (FCON(ITER,IFH).GT.FCON(ITER-1,IFH)) GO TO 197
GO TO 196
197 WRITE (6,991) LP,JPS,WW,XNXX,XPRES,XNP
WRITE (6,992) IWH,IFH,ITER,IASF,CWW,DDWW
991 FORMAT (//,2X,"FOR W(",I5,2X,"",I5")=",E15.5,2X,"XNXX=",
1E15.5,2X,"XPRES=",E15.5,2X,"XNP=",E15.5/)
992 FORMAT (//,2X,"IWH=",I5,2X,"IFH=",I5,2X,"ITER=",I5//,4X,
1"ITER",3X,"XCON(ITER)",3X,"WCON(ITER,IWH)",3X,"FCON(ITER,IFH
2)",2X,"IASF=",I5,2X,"DDWW=",E12.4,2X,"DDWW=",E12.4/)
WRITE (6,993) (IK,XCON(IK),WCON(IK,IWH),FCON(IK,IFH),IK=1,
1ITER)
993 FORMAT (I8,3E15.5)
IASF=IASF+1
DDWW=DDWW/2.
WW=SWW
WW=WW+DDWW
IF (IASF.GT.4) GO TO 403
DO 216 I1=1,NLQ POT
DO 217 J1=1,K1
WM(I1,J1)=SWM(I1,J1)
ETM(I1,J1)=SETM(I1,J1)
217 WMP(I1,J1)=SWMP(I1,J1)
DO 218 J1=1,K2
FM(I1,J1)=SFM(I1,J1)
XFM(I1,J1)=EXFM(I1,J1)
218 FMP(I1,J1)=SFMP(I1,J1)
216 CONTINUE
XNP=SNXP
GO TO 444
196 XNN=XNP
DO 131 J1=1,K1
131 WWM(J1)=WM(IMAX,J1)
DO 132 J1=1,K2
132 FFM(J1)=FM(IMAX,J1)
GO TO 333
195 IVOUT=IVOUT+1
CALL PCTSN(POT,POTM,STRY,STRA,1,1,1,XNXX)
CALL SECOND(TIME)
TIM3=TIME-TIME1
TIME1=TIME
WRITE (6,141) LP,JPS,WW,XNXX,XPRES,NWAVE,ITER,TIM3
WRITE (6,142) POT,POTM,STRY,STRA
IF (IOUT.EQ.1) WRITE (6,143) DETM,IXFM
IF (LMOD.NE.1) GO TO 476
CALL TRANSF(WF,XWF,FF,XFF,NW,MF,2,T1,MAXN,2,3,WW,XNP,LP)
476 VOUT(1,IVOUT)=XNXX
VOUT(2,IVOUT)=XPRES
VOUT(3,IVOUT)=PCT
VOUT(4,IVOUT)=PCTM
VOUT(5,IVOUT)=STRY
VOUT(6,IVOUT)=STRA
VOUT(7,IVOUT)=WMP(LP,1)
VOUT(8,IVOUT)=WMP(LP,2)
NSHR=(NEQPOT+1)/2
VOUT(9,IVOUT)=WWM(NSHR,1)
VOUT(10,IVOUT)=WWM(NSHR,2)
VOUT(11,IVOUT)=ITER
VOUT(12,IVOUT)=NWAVE
241 FORMAT (//,2X,"NONLINEAR SOLUTION FOR W(",I5,2X,"",I5")=")

```



```

      A1=PI/XL
      A2=2.*A1
      XX=0.
      DO 10 I=1,NEQPOT
        WZ(I,1)=-AC1*COS(A2*XX)
        WZ(I,2)=AC2*IN(A1*XX)
        WZP(I,1)=AC1*A2*SIN(A2*XX)
        WZF(I,2)=AC2*A1*COS(A1*XX)
        WZPP(I,1)=AC1*A2*A2*COS(A2*XX)
        WZPP(I,2)=-AC2*A1*A1*SIN(A1*XX)
        IF(K1.LE.2) GO TO 50
        DO 11 J=3,K1
          WZ(I,J)=0.
          WZP(I,J)=0.
          WZPP(I,J)=0.
11      CONTINUE
50      CONTINUE
      XX=XX+DELTA
10     CONTINUE
      RETURN
      END
      SUBROUTINE TRANSF(WF,XWF,FF,XFF,NW,NF,NFF,T1,MAXN,IDER,IPRR,WM,XMS
1,L,P)
      COMMON/PRES1/WM(100,5),ETM(100,5),WMP(100,5)
      COMMON/PPLES3/FM(100,8),XFM(100,8),FMP(100,8)
      COMMON/FIDFR/DELTA,AL1,GA1,AL2,BT2,GA2
      COMMON/CDISK/I21(501),I22(501),I23(501)
      COMMON/DINTG/NEQPOT,MI(500)
      COMMON/FOUR1R/XFOUR,K6,K4,K3,K2,K1
      COMMON/NEWFT/JPS,INXXPX
      DIMENSION WF(NRF,NW),XWF(NRF,NW),FF(NRF,NF),XFF(NRF,NF),T1(MAXN)
      IF(IPRR.EQ.3) GO TO 278
      DO 10 I1=1,NEQPOT
        NL=MI(I1)
        CALL READ4S(22,T1,NL,I1)
        IF(I1.NE.1) GO TO 175
        DO 11 J1=1,K1
          WF(I1,J1)=T1(J1)
          WM(I1,J1)=T1(J1+K6)
          XWF(I1,J1)=T1(J1+K3-1)
          ETM(I1,J1)=T1(J1+K3+K6-1)
11      CONTINUE
        DO 12 J1=1,K2
          FF(I1,J1)=T1(J1+K1)
          FM(I1,J1)=T1(J1+K1+K6)
          XFF(I1,J1)=T1(J1+K4)
          XFM(I1,J1)=T1(J1+K4+K6)
12      CONTINUE
        GO TO 10
175     DO 13 J1=1,K1
          WM(I1,J1)=T1(J1)
          ETM(I1,J1)=T1(J1+K3-1)
13      CONTINUE
        DO 14 J1=1,K2
          FM(I1,J1)=T1(J1+K1)
          XFM(I1,J1)=T1(J1+K4)
14      CONTINUE
        IF(I1.NE.NEQPOT) GO TO 10
        DO 15 J1=1,K1
          WF(2,J1)=T1(J1+K6)
          XWF(2,J1)=T1(J1+K3+K6-1)
15      CONTINUE
        DO 16 J1=1,K2
          FF(2,J1)=T1(J1+K1+K6)

```

XFF(2,J1)=T1(J1*K4+K6)	511
16 CONTINUE	512
10 CONTINUE	513
IF(LP.EQ.8.OR.INXXPX.EQ.1)GO TO 176	
XNS=WM(LP,JP5)	
WM(LP,JP5)=WW	
176 CONTINUE	
IF(IDER.NE.1) GO TO 275	514
NEQP=NEQPOT-1	515
DO 20 I1=1,NEQP	516
DO 21 J1=1,K1	517
WMP(I1,J1)=AL1*WM(I1-1,J1)+GA1*WM(I1+1,J1)	518
21 CONTINUE	519
DO 22 J1=1,K2	520
FMP(I1,J1)=AL1*FM(I1-1,J1)+GA1*FM(I1+1,J1)	521
22 CONTINUE	522
20 CONTINUE	523
DO 23 J1=1,K1	524
WMP(1,J1)=AL1*WF(1,J1)+GA1*WM(2,J1)	525
WMP(NEQPOT,J1)=AL1*WM(NEQP,J1)+GA1*WF(2,J1)	526
23 CONTINUE	527
DO 24 J1=1,K2	528
FMP(1,J1)=AL1*FF(1,J1)+GA1*FM(2,J1)	529
FMP(NEQPOT,J1)=AL1*FM(NEQP,J1)+GA1*FF(2,J1)	530
24 CONTINUE	531
275 IF(IPRR.NE.1) RETURN	532
278 CONTINUE	533
J1=0	534
WRITE(6,400)J1	535
WRITE(6,500)	536
XX=0.	537
WRITE(6,600)WF(1,1),XWF(1,1)	538
DO 46 I1=1,NEQPOT	539
WRITE(6,509)I1,XX,WM(I1,1),WMP(I1,1),ETH(I1,1)	540
XX=XX+DELTA	541
46 CONTINUE	542
WRITE(6,600)WF(2,1),XWF(2,1)	543
DO 49 J1=1,KFOUR	544
WRITE(6,400)J1	545
WRITE(6,500)	546
WRITE(6,700)WF(1,J1+1),XWF(1,J1+1),FF(1,J1),XFF(1,J1)	547
DO 51 I1=1,NEQPOT	548
WRITE(6,609)I1,WM(I1,J1+1),WMP(I1,J1+1),ETH(I1,J1+1),FM(I1,J1),	549
1FMP(I1,J1),XFM(I1,J1)	550
51 CONTINUE	551
WRITE(6,700)WF(2,J1+1),XWF(2,J1+1),FF(2,J1),XFF(2,J1)	552
49 CONTINUE	553
DO 52 J1=K1,K2	554
WRITE(6,400)J1	555
WRITE(6,500)	556
WRITE(6,600)FF(1,J1),XFF(1,J1)	557
DO 53 I1=1,NEQPOT	558
WRITE(6,709)I1,FM(I1,J1),FMP(I1,J1),XFM(I1,J1)	559
53 CONTINUE	560
WRITE(6,800)FF(2,J1),XFF(2,J1)	561
52 CONTINUE	562
400 FORMAT(//,2X,"INTERMIDIAT RESULTS FOR KFOUR=",I8/2X,"*****	563
1*****")	564
500 FORMAT(//,2X,"POINT".4X,"LENGTH".13X,"W".14X,"WP".13X,"WPF".	565
112X,"F".14X,"FP".13X,"FPP"/2X,"*****	566
2*****")	567
3*****")	568
509 FORMAT(I8,E17.4,3E15.6)	569
600 FORMAT(//,4X,FICTIVE POINT E15.2,15X,E15.6//)	570

609	FORMAT (I1,10A,5T,5.6)	571
700	FORMAT (//20H FICTIVE POINT E15.6,15X,2E15.6,15X,2E15.6)	572
800	FORMAT (//65H FICTIVE POINT E15.6,15X,E15.6//)	573
1		574
769	FORMAT (I5,57X,5E15.6)	575
	RETURN	576
	END	577
	SUBROUTINE POTSN(POT,PCTH,STRY,STRA,IP,ISY,ISA,XNXX)	1263
C	POT - POTENTIAL ENERGY	1264
C	STRY - UNIT END SHORTENING FOR Y=0.	1265
C	STRA - AVERAGE UNIT END SHORTENING	1266
C	IP=1 FOR CALCULATE POT	1267
C	ISY=1 FOR CALCULATE STRY	1268
C	ISA=1 FOR CALCULATE STRA	1269
	COMMON/FOURIN/KFOUR,K6,K4,K3,K2,K1	1270
	COMMON/BOUNDO/LS1,LSN	7
	COMMON/SECH/RR,00,H11,H12,H22,Q11,Q12,Q22,O11,O12,O22	1271
	COMMON/PRES1/WM(100,5),ETM(100,5),WMP(100,5)	1272
	COMMON/PRES2/WZ(100,5),WZF(100,5),WZPP(100,5)	1273
	COMMON/PRES3/FM(100,5),XFM(100,8),FMP(100,8)	1274
	COMMON/FACTOR/C1,C2,C3,C4,C5,C6,C7,C8,C9,C10,C11,C12	1275
	COMMON/FACT2/DL1,DL2,DL3,DL4,DA1,DA2,DA3,DA4,DB1,DB3,DB4,XNI,EXXP	1276
	COMMON/FACT3/DL5,XL,XH	1277
	COMMON/CINTG/NEQPCT,MI(500)	1278
	COMMON/FIDFR/DELTA,AL1,GA1,AL2,BT2,GA2	1279
	COMMON/XXLOAD/XPRES	1280
	COMMON/SHEINN/VOUT(12,130),VPOT(7,130),IVOUT	
	DIMENSION PE(7),PEE(7)	
	CE1=C10/2.	1281
	CE2=C9**2/2.	1282
	CE3=C9/((1.-XNI)*EXXP)	1283
	CE4=C9*00*(1.-XNI)	1284
	POT=0.	1285
	DO 553 INA=1,7	
553	PEE(INA)=0.	
	STRY=0.	1286
	STRA=0.	1287
	DO 10 I1=1,NEQPOT	1288
	E7=1.	1289
	IF(I1.EQ...OR.I1.EQ.NEQPOT)E7=0.5	1290
	E1=-Q11*ETM(I1,1)-1./AR*WM(I1,1)+DA2*XNXX	1291
	E2=0.	1292
	DO 11 J1=1,KFOUR	1293
	JS=J1**2	1294
	E2=JS*WM(I1,J1+1)*(WM(I1,J1+1)+2.*WZ(I1,J1+1))+E2	1295
11	CONTINUE	1296
	E1=E1+CE1*E2	1297
	IF(IP.NE.1) GO TO 100	1298
	PE(1)=DB2/D11**2*E1**2	
	PE(3)=DL1*ETM(I1,1)**2	
	PE(4)=-XNXX*WMP(I1,1)*(WMP(I1,1)+2.*WZF(I1,1))+DA3*2.*ETM(I1,1)*XNXX	
1	I1,1)*XNXX	
	PE(5)=-2.*XPRES*WM(I1,1)	
	PE(7)=DB2/D11**2*DA2*DA2*XNXX*XNXX	
	PE(6)=0.	
100	E1=E1*DA2/D11+DA3*ETM(I1,1)	1302
	IF(ISY.NE.1) GO TO 120	1303
	PSY=E1	1304
110	IF(ISA.NE.1) GO TO 120	1305
	PSA=E1-WMP(I1,1)*(WMP(I1,1)+2.*WZF(I1,1))/2.	1306
120	IF(ISY.NE.1) GO TO 130	1307
	E1=0.	1308
	DO 16 J1=1,K1	1309
	DO 16 J2=1,K2	1310

E1=WM(I1,J1)*WMP(I1,J1)+2.*WZP(I1,J1)+C1	1311
10 CONTINUE	1312
PSY=PSY-E1/2.	1313
E1=0.	1314
E2=0.	1315
DO 12 J1=1,KFOUR	1316
JS=J1**2	1317
E1=ETM(I1,J1+1)*E1	1316
E2=E2+JS*WM(I1,J1+1)	1319
12 CONTINUE	1320
PSY=PSY+DA3*E1-DA4*C9*E2	1321
E1=0.	1322
E2=0.	1323
DO 13 J1=1,K2	1324
JS=J1**2	1325
E1=E1+XFM(I1,J1)	1326
E2=E2+JS*FM(I1,J1)	1327
13 CONTINUE	1328
PSY=PSY+DA2*E1-DA1*C9*E2	1329
STRY=STRY+PSY*E7	1330
130 IF(ISA.NE.1) GO TO 140	1331
E1=0.	1332
DO 14 J1=1,KFOUR	1333
14 E1=E1+WM(I1,J1+1)*(WMP(I1,J1+1)+2.*WZP(I1,J1+1))	1334
PSA=PSA-E1/4.	1335
STR=STR+PSA*E7	1336
140 IF(IP.NE.1) GO TO 10	1337
E1=0.	1338
E2=0.	1339
E3=0.	1340
E4=0.	1341
E5=0.	1342
DO 15 J1=1,KFOUR	1343
JS=J1**2	1344
JS2=JS**2	1345
E1=E1+WMP(I1,J1+1)*(WMP(I1,J1+1)+2.*WZP(I1,J1+1))	1346
E2=E2+JS2*WM(I1,J1+1)**2	1347
E3=E3+JS*WMP(I1,J1+1)**2	1348
E4=E4+ETM(I1,J1+1)**2	1349
E5=E5+JS*WM(I1,J1+1)*ETM(I1,J1+1)	1350
15 CONTINUE	1351
PE(3)=PE(3)+CE2*DL5*E2+CE4*E3+DL1*E4/2.-C9*DL2*E5	
PE(4)=PE(4)-XNXX*E1/2.	
E1=0.	1353
E2=0.	1354
E3=0.	1355
E4=0.	1356
DO 16 J1=1,K2	1357
JS=J1**2	1358
JS2=JS**2	1359
E1=JS2*FM(I1,J1)**2+E1	1360
E2=E2+JS*FMP(I1,J1)**2	1361
E3=E3+XFM(I1,J1)**2	1362
E4=E4+JS*FM(I1,J1)*XFM(I1,J1)	1363
16 CONTINUE	1364
PE(2)=CE2*DA1*E1+CE3*E2+DB2*E3/2.-DA2*C9*E4	
DO 143 INA=1,7	
143 PEE(INA)=PEE(INA)+PE(INA)*E7	
10 CONTINUE	1367
IF(IP.NE.1) GO TO 150	1368
DO 144 INA=1,7	
144 PEE(INA)=PEE(INA)*3.14159*RR*DELTA	
PEE(6)=-D22*3.14159*RA*XL*XNXX*XNXX	
POT=PEE(1)+PEE(2)+PEE(3)+PEE(4)+PEE(5)+PEE(6)	

POTM=POT+PEE(6)+PEE(7)	
PEES=J.	
IF(LSN.GT.4.AND.LSN.NE.9)GO TO 253	
PEES=-DL3*6.283185*RR*XXXX*WMP(1,1)	
253 IF(LSN.GT.4.AND.LSN.NE.9)GO TO 254	1370
PEES=PEES+DL3*6.283185*RR*XXXX*WMP(NEQPCT,1)	1371
254 PEE(3)=PEE(3)+PEES	1372
POT=POT+PEES	1373
PCTM=POTM+PEES	1374
DO 145 INA=1,7	1375
145 VPCT(INA,IVCUT)=PEE(INA)	1376
150 IF(ISY.NE.1) GO TO 160	578
STRY=DA1*XXXX-STRY/XL*DELTA	579
160 IF(ISA.NE.1) GO TO 170	580
STRA=DA1*XXXX-STRA/XL*DELTA	581
170 CONTINUE	
RETURN	
END	
SUBROUTINE ABCG(IEQ,M1,CF,BF,AF,GF,NRHS,XXXX,LN,NJ,NW,NF,LP,DF)	
COMMON/CINTG/NEQPOT,MI(SUC)	
COMMON/BOUND/LS1,LSN	
COMMON/FIDFR/DELTA,AL1,GA1,AL2,BT2,GA2	
COMMON/NE4PT/UPS,INXXPX	
COMMON/PRES1/WM(100,5),ETM(100,5),WMP(100,5)	
COMMON/FOURIR/KFOUR,K6,K4,K3,K2,K1	582
DIMENSION AF(M1,M1),BF(M1,M1),CF(M1,M1),GF(M1,NRHS),DF(M1,1)	583
C NEQPOT=NPOINT (EXCLUDING FICTIVES POINTS)	584
C LS1 -KIND OF BOUNDARY CONDITIONS OF POINT 1	585
C LSN -KIND OF BOUNDARY CONDITIONS OF POINT NP	586
C NW - MAXIMUM K+1 FOR DIMENSION WM(NJ,NW)	587
C NF - MAXIMUM 2*K FOR DIMENSION FM(NJ,NF)	588
IF(IEQ.GT.1) GO TO 10	589
CALL RSTG(BF,CF,AF,GF,1,XXXX,M1,NJ,NW,NF,LN,NRHS,LP,DF)	590
DO 2 I1=1,K6	591
GF(I1+K6,NRHS)=GF(I1,NRHS)	592
DF(I1+K6,1)=DF(I1,1)	
DO 2 J1=1,K6	593
BF(I1+K6,J1)=AL2*BF(I1,J1)+AL1*CF(I1,J1)	594
BF(I1+K6,J1+K6)=BT2*BF(I1,J1)+AF(I1,J1)	595
BF(I1,J1+K6)=GA2*BF(I1,J1)+GA1*CF(I1,J1)	596
2 CONTINUE	597
CALL BOUNDR(AF,CF,GF,1,XXXX,LS1,M1,NJ,NW,NF,LN,NRHS,DF)	598
DO 3 I1=1,K6	599
DO 3 J1=1,K6	600
BF(I1,J1)=AL1*AF(I1,J1)	601
AF(I1+K6,J1)=BF(I1,J1+K6)	602
BF(I1,J1+K6)=CF(I1,J1)	603
AF(I1,J1)=GA1*AF(I1,J1)	604
3 CONTINUE	605
RETURN	606
10 IF(IEQ.GT.2) GO TO 20	607
CALL RSTG(AF,CF,BF,GF,2,XXXX,M1,NJ,NW,NF,LN,NRHS,LP,DF)	608
DO 4 I1=1,K6	609
DO 4 J1=1,K6	610
BF(I1,J1)=BF(I1,J1)+BT2*AF(I1,J1)	611
CF(I1,J1+K6)=AL2*AF(I1,J1)+AL1*CF(I1,J1)	612
AF(I1,J1)=GA2*AF(I1,J1)+GA1*CF(I1,J1)	613
CF(I1,J1)=0.	614
4 CONTINUE	615
RETURN	616
20 IF(IEQ.GE.NEQPOT-1) GO TO 30	617
JP=IEQ	618
CALL RSTG(AF,CF,BF,GF,JP,XXXX,M1,NJ,NW,NF,LN,NRHS,LP,DF)	619
DO 5 I1=1,K6	620

DO 5 I1=1,K6	621
BF(I1,J1)=BF(I1,J1)+BT2*AF(I1,J1)	622
TEMP=GA2*AF(I1,J1)+GA1*CF(I1,J1)	623
CF(I1,J1)=AL2*AF(I1,J1)+AL1*CF(I1,J1)	624
AF(I1,J1)=TEMP	625
5 CONTINUE	626
IF(LP.EQ.J.CR.INXXPX.EQ.1)RETURN	
IF(IEQ.LT.LP-1.CR.IE.G.GT.LP+1)RETURN	
WWW=WM(LP,JPS)	
IF(IEQ.NE.LP-1)GO TO 51	
DO 53 I1=1,K6	
GF(I1,NRHS)=GF(I1,NRHS)-AF(I1,JPS)*WWW	
53 AF(I1,JPS)=DF(I1,1)	
RETURN	
51 IF(IEQ.NE.LP)GO TO 52	
DO 54 I1=1,K6	
GF(I1,NRHS)=GF(I1,NRHS)-BF(I1,JPS)*WWW	
54 BF(I1,JPS)=DF(I1,1)	
RETURN	
52 DO 55 I1=1,K6	
GF(I1,NRHS)=GF(I1,NRHS)-CF(I1,JPS)*WWW	
55 CF(I1,JPS)=DF(I1,1)	
RETURN	627
30 IF(IEQ.EQ.NEQPOT) GO TO 40	628
JP=IEQ	629
CALL RSTG(AF,CF,BF,GF,JP,XNXX,M1,NJ,NW,NF,LN,NRHS,LP,DF)	630
DO 6 I1=1,K6	631
DO 6 J1=1,K6	632
BF(I1,J1)=BF(I1,J1)+BT2*AF(I1,J1)	633
TEMP=GA2*AF(I1,J1)+GA1*CF(I1,J1)	634
CF(I1,J1)=AL2*AF(I1,J1)+AL1*CF(I1,J1)	635
AF(I1,J1)=TEMP	636
AF(I1,J1+K6)=U.	637
6 CONTINUE	638
RETURN	639
40 JP=IEQ	640
CALL RSTG(AF,CF,BF,GF,JP,XNXX,M1,NJ,NW,NF,LN,NRHS,LP,DF)	641
DO 7 I1=1,K6	642
GF(I1+K6,NRHS)=GF(I1,NRHS)	643
DF(I1+K6,1)=DF(I1,1)	
DO 7 J1=1,K6	644
BF(I1,J1)=BF(I1,J1)+BT2*AF(I1,J1)	645
BF(I1,J1+K6)=GA2*AF(I1,J1)+GA1*CF(I1,J1)	646
BF(I1+K6,J1)=AL2*AF(I1,J1)+AL1*CF(I1,J1)	647
7 CONTINUE	648
CALL BOUNDG(CF,AF,GF,JP,XNXX,LSN,M1,NJ,NW,NF,LN,NRHS,DF)	649
DO 8 I1=1,K6	650
TEMP=GF(I1,NRHS)	651
TEMPP=DF(I1,1)	
GF(I1,NRHS)=GF(I1+K6,NRHS)	652
GF(I1+K6,NRHS)=TEMP	653
DF(I1,1)=DF(I1+K6,1)	
DF(I1+K6,1)=TEMPP	
DO 8 J1=1,K6	654
BF(I1+K6,J1+K6)=GA1*CF(I1,J1)	655
CF(I1+K6,J1)=AL1*CF(I1,J1)	656
CF(I1,J1)=BF(I1+K6,J1)	657
BF(I1+K6,J1)=AF(I1,J1)	658
8 CONTINUE	659
RETURN	660
END	661
FUNCTION ALB(I,J,L,3,JP,N2,N3,N4,LL)	662
C N4=1 FOR B(JF,I+J) OR B(JP,I-J)	663
C N4=2 FOR B(JP,J)	664

C	LL=1 FOR H	LL=2 FOR F	665	
	COMMON/FOURIR/KFOUR,K6,K4,K3,K2,K1		666	
	DIMENSION B(N2,N3)		667	
	IF(L.GT.3) GO TO 10		668	
	I1=I+J		669	
	I2=I1		670	
	GO TO 20		671	
10	I1=IABS(I-J)		672	
	I2=I1		673	
20	IF(N4.EQ.1) GO TO 120		674	
	I2=J		675	
	GO TO 100		676	
120	IF(I1.LE.KFOUR) GO TO 100		677	
	ALB=0.		678	
	RETURN		679	
100	IF(L.LE.3) GO TO 110		680	
	ETA=1.		681	
	IF(I.EQ.J) ETA=0.		682	
110	GO TO(1,12,13,14,15,16),L		683	
11	R1=I1**2		684	
	GO TO 17		685	
12	R1=J**2		686	
	GO TO 17		687	
13	R1=2.*I1*J		688	
	GO TO 17		689	
14	R1=(2.-ETA)*I1**2		690	
	GO TO 17		691	
15	R1=(2.-ETA)*J**2		692	
	GO TO 17		693	
16	IF(I-J.LT.0) LTA=-1.		694	
	R1=-2.*ETA*J*I1		695	
17	IF(LL.EQ.1) I2=I2+1		696	
	ALB=R1*B(JP,I2)		697	
	RETURN		698	
	END		699	
	SUBROUTINE RSTG(R,S,T,G,JF,XNXX,M1,NJ,NW,NF,LN,NRHS,LP,DE)		700	
C	LN=1 FOR LINEAR	LN=2 FOR NONLINEAR	701	
C	NJ	MAXIMUM POINTS IN MERIDIONAL DIRECTION	702	
C	NW	MAXIMUM KFOUR+1	NF= MAXIMUM 2.*KFCUR	703
C	XNXX	AXIAL COMPRESSION LOAD	JP= THE POINT IN MERIDIONAL DIRECT	704
	COMMON/FOURIR/KFOUR,K6,K4,K3,K2,K1		705	
	COMMON/GEOM/RR,DD,M11,M12,M22,Q11,Q12,Q22,D11,D12,D22		706	
	COMMON/FACTCR/C1,C2,C3,C4,C5,C6,C7,C8,C9,C10,C11,C12		707	
	COMMON/FACT2/DL1,DL2,DL3,DL4,DA1,DA2,DA3,DA4,DB2,DB3,DB4,XNI,EXXP		888	
	COMMON/PRES1/WM(100,5),ETM(100,5),WMP(100,5)		708	
	COMMON/PRES2/WZ(100,5),WZF(100,5),WZPP(100,5)		709	
	COMMON/PRES3/FM(100,6),XFM(100,6),FMP(100,6)		710	
	COMMON/XXLOAD/XPRES		711	
	COMMON/NEWPT/JFS,INXXFX			
	DIMENSION R(M1,M1),S(M1,M1),T(M1,M1),G(M1,NRHS)		712	
	DIMENSION DE(M1,1)			
C	INXXPX=1 FOR NXX AND P AS KNOWN			
C	INXXPX=2 FOR NXX AS UNKNOWN, THE INITIAL SOLUTION IS NXX=0.			
C	INXXPX=3 SAME AS 2 BUT THE INITIAL SOLUTION IS A GIVEN NXX			
C	INXXPX=4 FOR P AS UNKNOWN			
C	K6=6*KFOUR+2		713	
C	K4=4*KFOUR+2		714	
C	K3=3*KFOUR+2		715	
C	K2=2*KFOUR		716	
C	K1=KFOUR+1		717	
C	C9=(NNN/RR)**2		718	
C	C1=CD*M11		719	
C	C2=2.*DD*M12*C9		720	
C	C3=2.*Q12*C9		721	

C	C4=00*H22+C9**2	722
C	C5=Q11/D11*C9	723
C	C6=1./(RR*D11)*C9	724
C	C7=C9**2/(2.*D11)	725
C	C8=Q22*C9**2	726
C	C10=C9/2.	727
C	C11=2.*C9*D12	728
C	C12=Q22*C9**2	729
	RCOR1=Q42/(RR*D11)	
	RCOR2=C9*Q42/D11	
	DO 1 I1=1,K6	730
	G(I1,NRHS)=0.	731
	DE(I1,1)=J.	
	DO 1 J1=1,K6	732
	R(I1,J1)=J.	733
	S(I1,J1)=0.	734
	T(I1,J1)=J.	735
1	CONTINUE	736
	J1=0	737
	DO 2 I1=K3,K6	738
	T(I1,I1)=1.	739
	J1=J1+1	740
	R(I1,J1)=-1.	741
2	CONTINUE	742
C	EQUILIBRIUM EQUATION FOR I=0	743
	R(1,K3)=J0*H11+Q11**2/D11	744
	T(1,K3)=2.*Q11/(RR*D11)	745
	T(1,1)=1./(RR**2*D11)	746
	GO TO(71,72,73,74),INXXFX	
71	T(1,K3)=T(1,K3)+XNXX	
	G(1,NRHS)=-XNXX*WZPP(JP,1)+XPRES+RCOR1*XNXX	
	GO TO 75	
72	DE(1,1)=WZPP(JP,1)-RCOR1	
	G(1,NRHS)=XPRES	
	IF(LN.EQ.1)GO TO 75	
	DE(1,1)=DE(1,1)+ETH(JP,1)	
	G(1,NRHS)=G(1,NRHS)+XNXX*ETH(JP,1)	
	T(1,K3)=T(1,K3)+XNXX	
	GO TO 75	
73	T(1,K3)=T(1,K3)+XNXX	
	DE(1,1)=WZPP(JP,1)-RCOR1	
	G(1,NRHS)=XPRES	
	IF(LN.EQ.1)GO TO 75	
	DE(1,1)=DE(1,1)+ETH(JP,1)	
	G(1,NRHS)=G(1,NRHS)+XNXX*ETH(JP,1)	
	GO TO 75	
74	T(1,K3)=T(1,K3)+XNXX	
	G(1,NRHS)=-XNXX*WZFP(JP,1)+FCOR1*XNXX	
	DE(1,1)=-1.	
75	DO 6 J=1,FOUR	749
	IS=J**2	750
	M=J+1	751
	T(1,K3+J)=T(1,K3+J)-C5/2.*IS*WZ(JP,M)	752
	S(1,J+1)=S(1,J+1)-C5*IS*WZP(JP,M)	753
	T(1,J+1)=T(1,J+1)-IS/2.*(C5*WZPP(JP,M)+C6*WZ(JP,M))	754
	T(1,K4+J)=T(1,K4+J)+C10*IS*WZ(JP,M)	755
	T(1,K1+J)=T(1,K1+J)+C10*IS*WZFP(JP,M)	756
	S(1,K1+J)=S(1,K1+J)+2.*C10*IS*WZP(JP,M)	757
	IF(LN.EQ.2.OR.INXXFX.EQ.1)GO TO 94	
	IF(JP.NE.LP.OR.JPS.NE.M)GO TO 94	
	T(1,K3+J)=T(1,K3+J)-C5/2.*IS*WM(JP,M)	
	T(1,J+1)=T(1,J+1)-IS/2.*C6*WM(JP,M)	
	T(1,K4+J)=T(1,K4+J)+C10*IS*WM(JP,M)	
	G(1,NRHS)=G(1,NRHS)-C6/4.*IS*WM(JP,M)**2	

94	IF (LN.EQ.1) GO TO 6	758
	T(1,K3+J)=T(1,K3+J)-C5/2.*IS*WM(JP,M)+C10*IS*FM(JP,J)	759
	T(1,J+1)=T(1,J+1)-IS/2.*(C5*ETM(JP,M)+C6*WM(JP,M))	760
	1 +C10*IS*XFM(JP,J)	761
	S(1,J+1)=S(1,J+1)-C5*IS*WMP(JP,M)+2.*C10*IS*FMP(JP,J)	762
	T(1,K4+J)=T(1,K4+J)+C10*IS*WM(JP,M)	763
	T(1,K1+J)=T(1,K1+J)+C10*IS*ETM(JP,M)	764
	S(1,K1+J)=S(1,K1+J)+2.*C10*IS*WMP(JP,M)	765
	G(1,NRHS)=G(1,NRHS)-C5/2.*IS*(WM(JP,M)*ETM(JP,M)+WMP(JP,M)**2)	766
	1-C6/4.*IS*(WM(JP,M)**2)+C10*IS*(WM(JP,M)*XFM(JP,J)+ETM(JP,M)*	767
	2FM(JP,J)+2.*WMP(JP,M)*FMP(JP,J))	768
	6 CONTINUE	769
C	EQUILIBRIUM EQUATIONS FOR I=1,2,.....,KFOUR	770
	DO 3 I1=2,K1	771
	I=I1-1	772
	IS=I**2	773
	IS2=IS**2	774
	T(I1,1)=-C6*IS*WZ(JP,I1)	775
	T(I1,K3)=-C5*IS*WZ(JP,I1)	776
	T(I1,I1)=C4*IS2	777
	T(I1,I1+K1-1)=-C6*IS2	778
	T(I1,I1+K2-1)=-C2*IS	779
	T(I1,I1+K4-1)=C3*IS-1./RR	780
	R(I1,I1+K3-1)=C1	781
	R(I1,I1+K4-1)=-Q11	782
	E1=C7*IS*WZ(JP,I1)	783
	GO TO (76,77,78,76), INXXPX	
76	T(I1,I1+K3-1)=T(I1,I1+K3-1)+XNXX	
	G(I1,NRHS)=-XNXX*WZFP(JP,I1)+RCOR2*IS*XNXX*WZ(JP,I1)	
	T(I1,I1)=T(I1,I1)+RCOR2*IS*XNXX	
	GO TO 831	
77	DE(I1,1)=WZFP(JP,I1)+RCOR2*IS*WZ(JP,I1)	
	IF (LN.EQ.1) GO TO 831	
	DE(I1,1)=DE(I1,1)+ETM(JP,I1)+RCOR2*IS*WM(JP,I1)	
	G(I1,NRHS)=G(I1,NRHS)+XNXX*ETM(JP,I1)+RCOR2*IS*WM(JP,I1)*XNXX	
	T(I1,I1+K3-1)=T(I1,I1+K3-1)+XNXX	
	T(I1,I1)=T(I1,I1)+RCOR2*IS*XNXX	
	GO TO 831	
78	T(I1,I1+K3-1)=T(I1,I1+K3-1)+XNXX	
	DE(I1,1)=WZFP(JP,I1)+RCOR2*IS*WZ(JP,I1)	
	T(I1,I1)=T(I1,I1)+RCOR2*IS*XNXX	
	IF (LN.EQ.1) GO TO 831	
	G(I1,NRHS)=G(I1,NRHS)+XNXX*ETM(JP,I1)+RCOR2*IS*XNXX*WM(JP,I1)	
	DE(I1,1)=DE(I1,1)+ETM(JP,I1)+RCOR2*IS*WM(JP,I1)	
831	CONTINUE	
	IF (LN.EQ.2.OR.INXXPX.EQ.1) GO TO 104	
	IF (JP.NE.LP.OR.JPS.NE.I1) GO TO 104	
	T(I1,1)=T(I1,1)-C6*IS*WM(JP,I1)	
	T(I1,K3)=T(I1,K3)-C5*IS*WM(JP,I1)	
	E1=C7*IS*(WM(JP,I1)+WZ(JP,I1))	
	E2=C7/2.*IS	
	E3=E2*WM(JP,I1)	
104	IF (LN.EQ.1) GO TO 60	785
	T(I1,1)=T(I1,1)-C6*IS*WM(JP,I1)	786
	T(I1,K3)=T(I1,K3)-C5*IS*WM(JP,I1)	787
	T(I1,I1)=T(I1,I1)-IS*(C5*ETM(JP,1)+C6*WM(JP,1))	788
	E1=C7*IS*(WM(JP,I1)+WZ(JP,I1))	789
	E2=C7/2.*IS	790
	E3=E2*WM(JP,I1)	791
	G(I1,NRHS)=G(I1,NRHS)-C5*IS*ETM(JP,1)*WM(JP,I1)	792
	1 -C6*IS*WM(JP,1)*WM(JP,I1)	793
60	DO 4 J=1,KFCUR	794
	JS=J**2	795
	M=J+1	796

T(I1,J+1)=T(I1,J+1)+E1*JS*WZ(JP,M)	797
IF(LN.EQ.1.AND.C.INXXPX.EQ.1)GO TO 6	
IF(LN.EQ.1.AND.JP.NE.LP)GC TO 4	
IF(LN.EQ.1.AND.JPS.NE.M)GC TO 4	
T(I1,J+1)=T(I1,J+1)+E1*JS*WM(JP,M)	799
T(I1,I1)=T(I1,I1)+E2*JS*WM(JP,M)*(WM(JP,M)+2.*WZ(JP,M))	800
G(I1,NRHS)=G(I1,NRHS)+E1/2.*JS*WM(JP,M)*2*E3*JS*WM(JP,M)	801
1*(WM(JP,M)+2.*WZ(JP,M))	802
4 CONTINUE	803
DO 5 J=1,K2	804
T(I1,K4+J)=T(I1,K4+J)+C10*(ALB(I,J,1,WZ,JP,NJ,NW,1,1)+	805
1ALB(I,J,4,WZ,JP,NJ,NW,1,1))	806
T(I1,K1+J)=T(I1,K1+J)+C10*(ALB(I,J,2,WZPP,JP,NJ,NW,1,1)+	807
1ALB(I,J,5,WZPP,JP,NJ,NW,1,1))	808
S(I1,K1+J)=S(I1,K1+J)+C10*(ALB(I,J,3,WZP,JP,NJ,NW,1,1)+	809
1ALB(I,J,6,WZP,JP,NJ,NW,1,1))	810
IF(LN.EQ.2.OR.INXXPX.EQ.1)GO TO 107	
IF(JP.NE.LP)GC TO 107	
IF(JFS.NE.I+J+1)GO TO 108	
T(I1,K4+J)=T(I1,K4+J)+C10*ALB(I,J,1,WM,JP,NJ,NW,1,1)	
108 IF(JFS.NE.IABS(I-J)+1)GO TO 107	
T(I1,K4+J)=T(I1,K4+J)+C10*ALB(I,J,4,WM,JP,NJ,NW,1,1)	
107 IF(LN.EQ.1)GO TO 5	811
T(I1,K4+J)=T(I1,K4+J)+C10*(ALB(I,J,1,WM,JP,NJ,NW,1,1)+	812
1ALB(I,J,4,WM,JP,NJ,NW,1,1))	813
T(I1,K1+J)=T(I1,K1+J)+C10*(ALB(I,J,2,ETM,JP,NJ,NW,1,1)+	814
1ALB(I,J,5,ETM,JP,NJ,NW,1,1))	815
S(I1,K1+J)=S(I1,K1+J)+C10*(ALB(I,J,3,WMP,JP,NJ,NW,1,1)+	816
1ALB(I,J,6,WMP,JP,NJ,NW,1,1))	817
G(I1,NRHS)=G(I1,NRHS)+C10*(ALB(I,J,1,WM,JP,NJ,NW,1,1)+	818
1ALB(I,J,4,WM,JP,NJ,NW,1,1))*XFM(JP,J)+(ALB(I,J,2,ETM,JP,NJ,NW,	819
21,1)+ALB(I,J,5,ETM,JP,NJ,NW,1,1))*FM(JP,J)+(ALB(I,J,3,WMP,JP,NJ,	820
3NW,1,1)+ALB(I,J,6,WMP,JP,NJ,NW,1,1))*FMP(JP,J))	821
IJ1=I+J	822
IF(IJ1.GT.KFOUR)GO TO 10	823
T(I1,IJ1+1)=T(I1,IJ1+1)+C10*(ALB(I,J,1,XFM,JP,NJ,NF,2,2))	824
T(I1,K3+IJ1)=T(I1,K3+IJ1)+C10*ALB(I,J,2,FM,JP,NJ,NF,2,2)	825
S(I1,IJ1+1)=S(I1,IJ1+1)+C10*ALB(I,J,3,FMP,JP,NJ,NF,2,2)	826
80 IJ2=IABS(I-J)	827
IF(IJ2.GT.KFOUR)GO TO 5	828
T(I1,IJ2+1)=T(I1,IJ2+1)+C10*ALB(I,J,4,XFM,JP,NJ,NF,2,2)	829
T(I1,K3+IJ2)=T(I1,K3+IJ2)+C10*ALB(I,J,5,FM,JP,NJ,NF,2,2)	830
S(I1,IJ2+1)=S(I1,IJ2+1)+C10*ALB(I,J,6,FMP,JP,NJ,NF,2,2)	831
5 CONTINUE	832
3 CONTINUE	833
C COMPATIBILITY EQUATIONS FOR I=1,2,...,2KFCUR	834
E1=C10/2.	835
I2=K1+1	836
I3=I2+K2-1	837
DO 7 I1=I2,I3	838
I=I1-K1	839
IS=I**2	840
R(I1,I1+K4-K1)=D11	841
T(I1,I1+K4-K1)=-IS*C11	842
T(I1,I1)=IS**2*C12	843
IF(I.GT.KFOUR)GO TO 82	844
R(I1,I1+K3-K1)=D11	845
T(I1,I1+K3-K1)=-IS*C3+1./AR	846
T(I1,I1-K1+1)=IS**2*C8	847
82 DO 9 J1=1,K1	848
J=J1-1	849
T(I1,J1+K3-J)=T(I1,J1+K3-J)+C10*(ALB(I,J,1,WZ,JP,NJ,NW,1,1)+	850
1ALB(I,J,4,WZ,JP,NJ,NW,1,1))	851
T(I1,J1)=T(I1,J1)+C10*(ALB(I,J,2,WZPP,JP,NJ,NW,1,1)+	852

1	ALB(I,J,5,WZP,JP,NJ,NW,1,1)	853
	S(I1,J1)=S(I1,J1)-C10*(ALB(I,J,3,WZP,JP,NJ,NW,1,1)+	854
1	ALB(I,J,6,WZP,JP,NJ,NW,1,1))	855
	IF(LN.EQ.2.OR.INXXPX.EQ.1)GO TO 109	
	IF(JP.NE.LP)GO TO 109	
	IF(JPS.NE.I+J+1)GO TO 111	
111	T(I1,J1+K3-1)=T(I1,J1+K3-1)-E1*ALB(I,J,1,WM,JP,NJ,NW,1,1)	
	IF(JPS.NE.IABS(I-J)+1)GO TO 112	
112	T(I1,J1+K3-1)=T(I1,J1+K3-1)-E1*ALB(I,J,4,WM,JP,NJ,NW,1,1)	
	IJ3=I+J	
	IF(IJ3.GT.KFOUR)GO TO 113	
	IF(JPS.NE.J+1)GO TO 113	
113	T(I1,K3+IJ3)=T(I1,K3+IJ3)-E1*ALB(I,J,2,WM,JP,NJ,NW,2,1)	
	IJ3=IABS(I-J)	
	IF(IJ3.GT.KFOUR)GO TO 109	
	IF(JPS.NE.J+1)GO TO 109	
	T(I1,K3+IJ3)=T(I1,K3+IJ3)-E1*ALB(I,J,5,WM,JP,NJ,NW,2,1)	
109	IF(LN.EQ.1)GO TO 9	856
	T(I1,J1+K3-1)=T(I1,J1+K3-1)-E1*(ALB(I,J,1,WM,JP,NJ,NW,1,1)+	857
1	ALB(I,J,4,WM,JP,NJ,NW,1,1))	858
	T(I1,J1)=T(I1,J1)-E1*(ALB(I,J,2,ETM,JP,NJ,NW,1,1)+	859
1	ALB(I,J,5,ETM,JP,NJ,NW,1,1))	860
	S(I1,J1)=S(I1,J1)-E1*(ALB(I,J,3,WMP,JP,NJ,NW,1,1)+	861
1	ALB(I,J,6,WMP,JP,NJ,NW,1,1))	862
	G(I1,NRHS)=G(I1,NRHS)-E1*((ALB(I,J,1,WM,JP,NJ,NW,1,1)	863
	+ALB(I,J,4,WM,JP,NJ,	864
	2NW,1,1)*ETM(JP,J1)+(ALB(I,J,2,ETM,JP,NJ,NW,1,1)+ALB(I,J,5,ETM,	865
	3JP,NJ,NW,1,1)*WM(JP,J1)+(ALB(I,J,3,WMP,JP,NJ,NW,1,1)+ALB(I,J,6,	866
	4WMP,JP,NJ,NW,1,1)*WMP(JP,J1))	867
	IJ1=I+J	868
	IF(IJ1.GT.KFOUR)GO TO 83	869
	T(I1,IJ1+1)=T(I1,IJ1+1)-E1*(ALB(I,J,1,ETM,JP,NJ,NW,2,1))	870
	T(I1,K3+IJ1)=T(I1,K3+IJ1)-E1*(ALB(I,J,2,WM,JP,NJ,NW,2,1))	871
	S(I1,IJ1+1)=S(I1,IJ1+1)-E1*ALB(I,J,3,WMP,JP,NJ,NW,2,1)	872
83	IJ2=IABS(I-J)	873
	IF(IJ2.GT.KFOUR)GO TO 9	874
	T(I1,IJ2+1)=T(I1,IJ2+1)-E1*ALB(I,J,4,ETM,JP,NJ,NW,2,1)	875
	T(I1,K3+IJ2)=T(I1,K3+IJ2)-E1*ALB(I,J,5,WM,JP,NJ,NW,2,1)	876
	S(I1,IJ2+1)=S(I1,IJ2+1)-E1*ALB(I,J,6,WMP,JP,NJ,NW,2,1)	877
9	CONTINUE	878
7	CONTINUE	879
	RETURN	880
	END	881
	SUBROUTINE EOUNDR(BS,BT,BG,IN,XXXX,LS,M1,NJ,NW,NF,LN,NRHS,DE)	882
	COMMON/PCURR/KFOUR,K4,K4,K3,K2,K1	883
	COMMON/PRLS1/WM(100,5),ETM(100,5),WMP(100,5)	884
	COMMON/PRLS2/WZ(100,5),WZP(100,5),WZPP(100,5)	885
	COMMON/PRLS3/XFM(100,5),XFM(100,5),FMP(100,5)	886
	COMMON/GEOM/AB,DD,H11,H12,H22,D11,D12,D22	887
	COMMON/FACT2/DL1,DL2,DL3,DL4,DA1,DA2,DA3,DA4,DB3,DB4,XNI,EXXP	888
	COMMON/FACT3/C1,C2,C3,C4,C5,C6,C7,C8,C9,C10,C11,C12	889
	COMMON/NEWPT/JPS,INXXPX	
	DIMENSION BS(M1,M1),BT(M1,M1),BG(M1,NRHS),DE(M1,1)	890
C	BOUNDARY CONDITIONS BS*Z1+BT*Z2=BG	891
C	LS=1 FOR SSC W=MX=NXY=NX=0.	892
C	LS=2 FOR SSC W=MX=NXY=U=0.	893
C	LS=3 FOR SSC W=MX=V=NX=0.	894
C	LS=4 FOR SSC W=MX=V=U=0.	895
C	LS=5 FOR CC1 W=W,X=NXY=NX=0.	896
C	LS=6 FOR CC2 W=W,X=NXY=U=0.	897
C	LS=7 FOR CC3 W=W,X=V=NX=0.	898
C	LS=8 FOR CC4 W=W,X=V=U=0.	899
C	LS=9 FOR CC5 NX=NXY=QX=MX=0.	900
C	LS=10 FOR SYMMETRY NXY=QX=W,X=U=0.	901

C	LS=1: FOR ANTILYMETRY NX=MX=H=V=0.	902
C	DALFA=(1.+XLAMD)*(1.+YLAMD)-XNI**2	903
C	DL1=DO*(1.+RHQX+EX**2*XLAMD*(1.+YLAMD-XNI**2)*12./(XH**2*DALFA))	904
C	DL2=DO*XNI*(1.+EX*EY*YLAMD*XLAMD*12./(XH**2*DALFA))	905
C	DL3=EX*XLAMD*(1.+YLAMD)/D-LFA	906
C	DL4=-XNI*EX*XLAMD/DALFA	907
C	DA1=(1.+YLAMD)/(DALFA*EXXP)	908
C	DA2=-XNI/(DALFA*EXXP)	909
C	DA3=- (1.+YLAMD)*EX*XLAMD/DALFA	910
C	DA4=XNI*EY*YLAMD/D-LFA	911
C	DB2=(1.+XLAMD)/(DALFA*EXXP)	912
C	DB3=XNI*EX*YLAMD/DALFA	913
C	DB4=- (1.+XLAMD)*EY*YLAMD/DALFA	914
C	K6=6*KFOUR+2	915
C	K4=4*KFOUR+2	916
C	K3=3*KFOUR+2	917
C	K2=2*KFOUR	918
C	K1=KFOUR+1	919
	RCK=1.	
	C80T=(1.-DL4*DA2/D11)/(DL1-DL4*Q11/D11)	
C	CORRECTED IN 1980 GA TACH	
	IF (LS.EQ.11) LS=3	920
	DO 4 I1=1,K6	921
	BG(I1,RHS)=0.	922
	DE(I1,1)=0.	
	DO 1 J1=1,K6	923
	BS(I1,J1)=0.	924
	BT(I1,J1)=0.	925
1	CONTINUE	926
	IF (LS.EQ.10) GO TO 866	927
	IF (LS.GT.8) GO TO 100	928
	DO 2 I1=1,K1	929
2	BT(I1,I1)=1.	930
	IF (LS.LE.4.OR.LS.GT.8) GO TO 100	931
866	J=0	932
	DO 3 I1=K3,K4	933
	J=J+1	934
3	BS(I1,J)=1.	935
100	IF (LS.GT.4) GO TO 200	936
	BT(K3,K3)=1.	937
	IF (INXXP.EQ.1.OR.INXXPX.EQ.4) GO TO 77	
	DE(K3,1)=-C80T*RCK	
	BG(K3,1)=0.	
	GO TO 78	
77	BG(K3,RHS)=C80T*INXXP*RCK	
78	CONTINUE	
	K31=K3+1	938
	DO 4 I1=K31,K4	939
	BT(I1,I1)=DL1	940
	BT(I1,I1+K4-K3)=DL4	941
	IF (LS.EQ.2.OR.LS.EQ.3) GO TO 4	942
	I=I1-K3	943
	BT(I1,I1+K1-K3)=BT(I1,I1+K1-K3)-I**2*C9*DL3	944
4	CONTINUE	945
200	IF (LS.NE.10) GO TO 300	946
	E1=DL4/D11*C10	947
	BS(1,K3)=DL1-DL4/D11*Q11	948
	DO 5 J1=1,KFOUR	949
	JS=J1**2	950
	BS(1,J1+1)=BS(1,J1+1)+E1*JS*WZ(IN,J1+1)	951
	BT(1,J1+1)=BT(1,J1+1)+E1*JS*WZP(IN,J1+1)	952
	BT(1,K1+J1)=BT(1,K1+J1)+C10*JS*WZP(IN,J1+1)	953
	IF (LS.EQ.1) GO TO 5	954
	BS(1,J1+1)=BS(1,J1+1)+E1*JS*WM(IN,J1+1)	955

BT(1,I1-1)=BT(1,J1+1)+E1*JS*WMP(IN,J1+1)	956
BG(1,NRHS)=BG(1,NRHS)+E1*JS*WM(IN,J1+1)*WMP(IN,J1+1)	957
5 CONTINUE	958
DO 12 I1=2,K1	959
I=I1-1	960
BS(I1,I1+K3-1)=BS(I1,I1+K3-1)+DL1	961
BS(I1,I1+K4-1)=BS(I1,I1+K4-1)+DL4	962
DO 12 J1=1,K2	963
BT(I1,K1+J1)=BT(I1,K1+J1)+Q10*(ALB(I,J1,2,WZP,IN,NJ,NW,1,1)+	964
1 ALB(I,J1,5,WZP,IN,NJ,NW,1,1))	965
12 CONTINUE	966
300 IF(LS.NE.9) GO TO 400	967
E1=DL4/D11*Q11	968
BT(1,K3)=DL1-E1	969
BS(K3,K3)=DL1-E1	970
E1=DL4/(D11*RR)	971
BT(1,1)=-E1	972
IF(INXXPX.EQ.1.OR.INXXPX.EQ.4)GO TO 87	
DE(1,1)=- (0.-DL4*DA2/D11)*RCK	
DE(K3,1)=WZP(IN,1)	
BS(K3,1)=-E1	
IF(INXXPX.EQ.3)BS(K3,1)=XNXX-E1	
IF(LN.EQ.2)GO TO 88	
BS(K3,1)=XNXX-E1	
DE(K3,1)=+WMP(IN,1)+DE(K3,1)	
BG(K3,1)=BG(K3,1)-WMP(IN,1)*XNXX	
GO TO 88	
87 BS(K3,1)=XNXX-E1	
BG(K3,NRHS)=-XNXX*WZP(IN,1)	974
BG(1,NRHS)=(0.-DL4*DA2/D11)*XNXX*RCK	
88 CONTINUE	
E1=DL4/D11*C10	975
DO 6 J1=1,KFOUR	976
JS=J1**2	977
BT(1,J1+1)=BT(1,J1+1)+E1*JS*WZ(IN,J1+1)	978
BT(K3,J1+1)=BT(K3,J1+1)+E1*JS*WZP(IN,J1+1)	979
BS(K3,J1+1)=BS(K3,J1+1)+E1*JS*WZ(IN,J1+1)	980
IF(LN.EQ.1)GO TO 6	981
BT(1,J1+1)=BT(1,J1+1)+E1*JS*WM(IN,J1+1)	982
BG(1,NRHS)=BG(1,NRHS)+E1/2.*JS*WM(IN,J1+1)**2	983
BT(K3,J1+1)=BT(K3,J1+1)+E1*JS*WMP(IN,J1+1)	984
BS(K3,J1+1)=BS(K3,J1+1)+E1*JS*WM(IN,J1+1)	985
BG(K3,NRHS)=BG(K3,NRHS)+E1*JS*WM(IN,J1+1)*WMP(IN,J1+1)	986
6 CONTINUE	987
DO 13 I1=2,K1	988
I=I1-1	989
IS=I**2	990
BT(I1,I1+K3-1)=DL1	991
BT(I1,I1)=-IS*C9*DL2	992
BT(I1,I1+K4-1)=DL4	993
BS(I1+K3-1,I1+K4-1)=DL4	994
BS(I1+K3-1,I1+K3-1)=DL1	995
IF(INXXPX.EQ.2.OR.INXXPX.EQ.3)GO TO 97	
BS(I1+K3-1,I1)=-IS*C9*(DL2+2.*DD*(1.-XNI))*XNXX	996
BG(I1+K3-1,NRHS)=-XNXX*WZP(IN,I1)	997
GO TO 13	
97 BS(I1+K3-1,I1)=-IS*C9*(DL2+2.*DD*(1.-XNI))	
IF(INXXPX.EQ.3)BS(I1+K3-1,I1)=BS(I1+K3-1,I1)+XNXX	
DE(I1+K3-1,1)=WZP(IN,I1)	
IF(LN.EQ.1)GO TO 13	
DE(I1+K3-1,1)=DE(I1+K3-1,1)+WMP(IN,I1)	
IF(INXXPX.EQ.2)BS(I1+K3-1,I1)=BS(I1+K3-1,I1)+XNXX	
BG(I1+K3-1,1)=BG(I1+K3-1,1)-XNXX*WMP(IN,I1)	
13 CONTINUE	998

400	I2=K2+1	999
	I3=I2+K2-1	1000
	I4=K3-1	1001
	DO 7 I1=I2,I3	1002
	I=I1-K1	1003
	IS=I+2	1004
	GO TO (21,22,23,24,21,26,27,28,21,30),LS	1005
21	BS(I1,K1+1)=1.	1006
	BT(I1+I4,K1+1)=1.	1007
	GO TO 7	1008
22	BS(I1,K1+1)=1.	1009
	BS(I1+I4,K4+1)=DB2	1010
	DO 8 J1=1,K1	1011
	J=J1-1	1012
	BS(I1+I4,J1)=BS(I1+I4,J1)-C10*(ALB(I,J,1,WZ,IN,NJ,NW,1,1)+	1013
	1ALB(I,J,4,WZ,IN,NJ,NW,1,1))	1014
8	CONTINUE	1015
	IF(I.GT.K-OUR) GO TO 7	1016
	BS(I1+I4,K3+1)=BS(I1+I4,K3+1)+DB3	1017
	BS(I1+I4,I+1)=BS(I1+I4,I+1)-IS*C9*DB4+1./RR	1018
	GO TO 7	1019
23	BT(I1,K1+1)=1.	1020
	BT(I1+I4,K4+1)=DB2	1021
	IF(I.GT.K-OUR) GO TO 7	1022
	BT(I1+I4,K3+1)=DB3	1023
	GO TO 7	1024
24	BT(I1,K1+1)=-IS*C9*DA2	1025
	BT(I1,K4+1)=DB2	1026
	BS(I1+I4,K1+1)=-IS*C9*(DA2+2./((1.-XNI)*E.XXP))	1027
	BS(I1+I4,K4+1)=DB2	1028
	DO 9 J1=1,K1	1029
	J=J1-1	1030
	BS(I1+I4,J1)=BS(I1+I4,J1)-C10*(ALB(I,J,1,WZ,IN,NJ,NW,1,1)+	1031
	1ALB(I,J,4,WZ,IN,NJ,NW,1,1))	1032
9	CONTINUE	1033
	IF(I.GT.K-OUR) GO TO 7	1034
	BT(I1,K3+1)=DB3	1035
	BS(I1+I4,K3+1)=DB3	1036
	BS(I1+I4,I+1)=BS(I1+I4,I+1)-IS*C9*DB4+1./RR	1037
	GO TO 7	1038
26	BS(I1,K1+1)=1.	1039
	BS(I1+I4,K4+1)=DB2	1040
	IF(I.GT.K-OUR) GO TO 7	1041
	BS(I1+I4,K3+1)=DB3	1042
	GO TO 7	1043
27	BT(I1,K1+1)=1.	1044
	BT(I1+I4,K4+1)=DB2	1045
	IF(I.GT.K-OUR) GO TO 7	1046
	BT(I1+I4,K3+1)=DB3	1047
	GO TO 7	1048
28	BT(I1,K1+1)=-IS*C9*DA2	1049
	BT(I1,K4+1)=DB2	1050
	BS(I1+I4,K1+1)=-IS*C9*(DA2+2./((1.-XNI)*E.XXP))	1051
	BS(I1+I4,K4+1)=DB2	1052
	IF(I.GT.K-OUR) GO TO 7	1053
	BT(I1,K3+1)=DB3	1054
	BS(I1+I4,K3+1)=DB3	1055
	GO TO 7	1056
30	BS(I1,K1+1)=1.	1057
	BS(I1+I4,K4+1)=DB2	1058
	DO 14 J1=1,K-OUR	1059
	BT(I1+I4,J1+1)=BT(I1+I4,J1+1)-C10*(ALB(I,J,2,WZP,IN,NJ,NW,1,1)+	1060
	1ALB(I1,J1,5,WZP,IN,NJ,NW,1,1))	1061
14	CONTINUE	1062

AD-A114 735

GEORGIA INST OF TECH. ATLANTA

F/G 20/11

DYNAMIC STABILITY OF STRUCTURES: APPLICATION TO FRAMES, CYLINDR--ETC(U)

FEB 82 G J SIMITSES, I SHEINMAN

F33615-79-C-3221

NL

UNCLASSIFIED

AFWAL-TR-81-3155

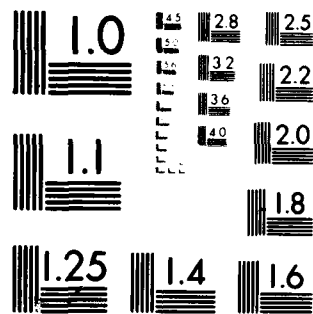
3-43

000

000



END
DATE
FILMED
6 82
DTIC



MICROCOPY RESOLUTION TEST CHART
NATIONAL BUREAU OF STANDARDS 1963-A

RS(I1+I4,K1) = RS(I1+I4,K1) + DB3	1063
7 CONTINUE	1064
666 RETURN	1065
END	1066
SUBROUTINE COEFF(EX,EY,XLAM,YLAM,RHOX,RHOY,ELAS)	1377
COMMON/GEOM/RR,DD,H11,H12,H22,Q11,Q12,Q22,Q11,Q12,Q22	1378
COMMON/FACT2/DL1,DL2,DL3,DL4,DA1,DA2,DA3,DA4,DB2,DB3,DB4,XNI,EXXP	1379
COMMON/CINTG/NEQPOT,MI(500)	1380
COMMON/FIDFR/DELTA,AL1,GA1,AL2,BT2,GA2	1381
COMMON/FIDFR/KFOUR,K6,K4,K3,K2,K1	1382
COMMON/FACT3/DL5,XL,XM	1383
K6=E*KFOUR+2	1384
K4=4*KFOUR+2	1385
K3=3*KFOUR+2	1386
K2=2*KFOUR	1387
K1=KFOUR+1	1388
XN2=XNI**2	1389
XN2=XN2**2	1390
DALFA=(1.+XLAM)*(1.+YLAM)-XN2	1391
DD=ELAS*XN2**3/(12.*(1.-XN2))	1392
EXXP=ELAS*XN/(1.-XN2)	1393
H11=1.+RHOX+12.*EX**2*XLAM*(1.+YLAM-XN2)/(XN2*DALFA)	1394
H22=1.+RHOY+12.*EY**2*YLAM*(1.+XLAM-XN2)/(XN2*DALFA)	1395
H12=1.+12.*XNI*EX*EY*XLAM*YLAM/(XN2*DALFA)	1396
Q11=XNI*EX*XLAM/DALFA	1397
Q22=XNI*EY*YLAM/DALFA	1398
Q12=-0.5*(1.+YLAM)*EX*XLAM+(1.+XLAM)*EY*YLAM/DALFA	1399
D11=(1.+XLAM)/(DALFA*EXXP)	1400
D22=(1.+YLAM)/(DALFA*EXXP)	1401
D12=((1.+XLAM)*(1.+YLAM)-XNI)/(DALFA*EXXP*(1.-XNI))	1402
DL1=DD*H11	1403
DL2=DD*XNI*(1.+(EX*EY*XLAM*YLAM*12.)/(XN2*DALFA))	1404
DL3=EX*XLAM*(1.+YLAM)/DALFA	1405
DL4=-XNI*EX*XLAM/DALFA	1406
DL5=DD*H22	1407
DA1=(1.+YLAM)/(DALFA*EXXP)	1408
DA2=-XNI/(DALFA*EXXP)	1409
DA3=-((1.+YLAM)*EX*XLAM/DALFA	1410
DA4=XNI*EY*YLAM/DALFA	1411
DB2=(1.+XLAM)/(DALFA*EXXP)	1412
DB3=XNI*EX*XLAM/DALFA	1413
DB4=-((1.+XLAM)*EY*YLAM/DALFA	1414
MI(1)=2*K6	1415
MI(NEQPOT)=2*K6	1416
NEQ1=NEQPOT-1	1417
DO 10 I1=2,NEQ1	1418
MI(I1)=K6	1419
10 CONTINUE	1420
DELTA=XL/(NEQPOT-1)	1421
AL1=-1./(2.*DELTA)	1422
GA1=1./(2.*DELTA)	1423
AL2=1./(DELTA**2)	1424
BT2=-2./DELTA**2	1425
GA2=1./DELTA**2	1426
RETURN	1427
END	1428
SUBROUTINE COEFFNN(NNN)	1429
COMMON/GEOM/RR,DD,H11,H12,H22,Q11,Q12,Q22,Q11,Q12,Q22	1430
COMMON/FACTOR/C1,C2,C3,C4,C5,C6,C7,C8,C9,C10,C11,C12	1431
C9=(NNN/RR)**2	1432
C1=DD*H11	1433
C2=2.*DD*H12*C9	1434
C3=2.*Q12*C9	1435
C4=DD*H22*C9**2	1436

C5=C11/(C9**2)	1437
C6=1./(P**0.11)*C9	1438
C7=C9**2/(C**0.11)	1439
C8=C22*C9**2	1440
C10=C9/2.	1441
C11=2.*09*012	1442
C12=022*C9**2	1443
RETURN	1444
END	1445
SUBROUTINE INVERT (NA,M,C,M,NM1,NM2,DET,IXP,IDET)	1067
DIMENSION A (NM1,NM1),C (NM2),M (NM2)	1068
DET=1.	1069
IXP=0	1070
NN=NA	1071
IF (NN.NE.1) GO TO 303	1072
DET=A(1,1)	1073
A(1,1)=1./A(1,1)	1074
GO TO 304	1075
303 DO 90 I=1,NN	1076
90 M(I)=-I	1077
DO 140 II=1,NN	1078
D=0.00	1079
DO 112 K=1,NN	1080
IF (M(K)) 100,100,112	1081
100 DO 110 L=1,NN	1082
IF (M(L)) 103,103,110	1083
103 IF (ABS(D)-ABS(A(K,L))) 105,105,110	1084
105 LD=L	1085
KD=K	1086
D=A(K,L)	1087
BIGA=D	1088
110 CONTINUE	1089
112 CONTINUE	1090
IF (D.EQ.0.00) GO TO 170	1091
GO TO 188	1092
170 WRITE(6,532)	1093
STOP	1094
502 FORMAT (1,5X,"DETERMINANT=0"/)	1095
188 NEMP=-M(LD)	1096
M(LD)=M(KD)	1097
M(KD)=NEMP	1098
DO 114 I=1,NN	1099
C(I)=A(I,LD)	1100
A(I,LD)=A(I,KD)	1101
114 A(I,KD)=0.00	1102
A(KD,KD)=1.00	1103
DO 115 J=1,NN	1104
115 A(KD,J)=A(KD,J)/D	1105
DO 135 I=1,NN	1106
IF (I.EQ.KD) GO TO 135	1107
DO 134 J=1,NN	1108
TEMP=C(I)*A(KD,J)	1109
134 A(I,J)=A(I,J)-TEMP	1110
135 CONTINUE	1111
IF (IDET.NE.1) GO TO 140	1112
DET=DET*BIGA	1113
IF (KD.NE.LD) DET=-DET	1114
629 IF (ABS(DLT).LT.1.E+10) GO TO 630	1115
DET=DET/1.E+10	1116
IXP=IXP+1	1117
GO TO 629	1118
630 IF (ABS(DET).GT.1.E+10) GO TO 140	1119
DET=DET*1.E+10	1120
IXP=IXP-10	1121

140	CONTINUE	1122
	DO 200 I=1,MN	1123
	L=0	1124
150	L=L+1	1125
	IF (M(L)-I) 150,160,150	1126
160	M(L)=M(I)	1127
	M(I)=1	1128
	DO 200 J=1,MN	1129
	TEMP=A(L,J)	1130
	A(L,J)=A(I,J)	1131
200	A(I,J)=TEMP	1132
304	RETURN	1133
	END	1134
	SUBROUTINE YMY(N1,A,B,C,N2,L1,L2,L3,T)	1135
	DIMENSION A(L1,L2),B(L1,L3),C(L1,L2),T(L3)	1136
	IF(N2.EQ.1) GO TO 100	1137
	DO 11 I=1,N1	1138
	DO 10 J=1,N2	1139
	TEMP=0.	1140
	DO 20 K=1,N1	1141
20	TEMP=TEMP+B(I,K)*C(K,J)	1142
10	T(J)=TEMP	1143
	DO 30 J=1,N2	1144
30	A(I,J)=T(J)	1145
11	CONTINUE	1146
	RETURN	1147
100	DO 111 I=1,N1	1148
	TEMP=0.	1149
	DO 120 K=1,N1	1150
120	TEMP=TEMP+B(I,K)*C(K,1)	1151
111	T(I)=TEMP	1152
	DO 130 I=1,N1	1153
130	A(I,1)=T(I)	1154
	RETURN	1155
	END	1156
	SUBROUTINE YSYHY(N2,M1,A,B,C,D,N3,L1,L2,L3,L4,T)	1157
	DIMENSION A(L1,L3),B(L1,L3),C(L1,L2),D(L2,L3),T(L4)	1158
	IF(N3.EQ.1) GO TO 100	1159
	DO 11 I=1,N1	1160
	DO 10 J=1,N3	1161
	TEMP=0.	1162
	DO 20 K=1,N2	1163
20	TEMP=TEMP+C(I,K)*D(K,J)	1164
10	T(J)=B(I,J)-TEMP	1165
	DO 30 J=1,N3	1166
30	A(I,J)=T(J)	1167
11	CONTINUE	1168
	RETURN	1169
100	DO 111 I=1,M1	1170
	TEMP=0.	1171
	DO 120 K=1,N2	1172
120	TEMP=TEMP+C(I,K)*D(K,1)	1173
111	T(I)=B(I,1)-TEMP	1174
	DO 130 I=1,M1	1175
130	A(I,1)=T(I)	1176
	RETURN	1177
	END	1178
	SUBROUTINE YMYN(V1,V2,A,M1,N2,M1,M2,M3,M4,T)	
C	V1(1,M2)=V2(1,M1)*A(M1,M2)	
	DIMENSION V1(1,M1),V2(1,M1),A(M2,M3),T(M4)	
	DO 10 J=1,M2	
	TEMP=0.	
	DO 20 K=1,M1	
20	TEMP=TEMP+V1(1,K)*A(K,J)	

```

10  T(J)=TEMP
    DO 30 J=1,N2
30  V1(1,J)=T(J)
    RETURN
    END
    SUBROUTINE POTERS(IDET,NRHS,MAXN,AP,BP,CP,GF,PR,XP,C,MT,T1,
1  V1,MAX2,IXPM,DETM,XNXX,LN,NJ,NH,NF,LP,DP)
C  MAX2=MAXN*MAXN
C  CHANGED BY SWEINMAN IN OCT 1980 FOR MARIX WITH DP
C  LP IS THE COLUMN OF DP
C  LP=0 FOR THE REGULAR FORM WITHCLT DP
C  LP SUPPOSE TO BE GT.2 AND LT NEQPOT-1
C  JPS IS THE COLUMN NO. OF DP ON WHICH THE TERMS ARE NONZERO
    COMMON/NEWPT/JPS,INXXPX
    COMMON/CINTG/NEQPOT,MI(500)
    COMMON/CDISK/I21(501),I22(501),I23(501)
    DIMENSION AP(MAXN,MAXN),BP(MAXN,MAXN),CP(MAXN,MAXN)
    DIMENSION PR(MAXN,MAXN),GF(MAXN,NRHS),XP(MAXN,NRHS)
    DIMENSION T1(MAXN),C(MAXN),MT(MAXN),V1(MAX2)
    DIMENSION DP(MAXN,1),EP(52,1),VB1(1,52),VB2(1,52)
C  EQUIVALENCE (AP(1,1),V1(1))
    IF (LP.NE.1.AND.LP.NE.2.AND.LP.LT.NEQPOT-1) GO TO 70
    WRITE(6,71) LP
71  FORMAT(//,2X,"LP=",I5,5X,"AND ITS SUPPOSE TO BE GT.2 AND LT
1.NEQPOT-1")
    STOP
70  CONTINUE
    R1=1.0
    IXPM=0
    DETM=1.
    DO 100 I=1,NEQPOT
    CALL ABCG(I,MAXN,CP,BP,AP,GF,NRHS,XNXX,LN,NJ,NH,NF,LP,DP)
    N=MI(I)
    IF (LP.EQ.0.OR.I.LT.LP+2) GO TO 80
    DO 4 K1=1,N
4    GP(K1,1)=GP(K1,1)-DP(K1,1)*VG1
80  IF (I.EQ.1) GO TO 888
    NMIN1=MI(I-1)
888  IF (I.EQ.NEQPOT) GO TO 999
    NPLUS1=MI(I+1)
999  CONTINUE
    IF (I.EQ.1) GO TO 12
    IF (LP.EQ.0.OR.I.LT.LP+2) GO TO 61
    DO 5 K1=1,N
    DO 5 K2=1,NMIN1
5    CP(K1,K2)=CP(K1,K2)-DP(K1,1)*VB1(1,K2)*R1
    R1=-R1
61  CALL YSYMY(NMIN1,N,BP,BP,CP,PR,N,MAXN,MAXN,MAXN,MAXN,T1)
12  CALL INVERT(N,BP,C,MT,MAXN,MAXN,DET,IXP,IDET)
    IF (IDET.NE.1) GO TO 640
    DETM=DET*DETM
    IXPM=IXP+IXPM
    IF (ABS(DETM).LT.2.E+10) GO TO 630
    DETM=DETM/1.E+10
    IXPM=IXPM+10
    GO TO 640
630  IF (ABS(DETM).GT.1.E-10) GO TO 640
    DETM=DETM*1.E+10
    IXPM=IXPM-10
640  CONTINUE
    IF (I.EQ.NEQPOT) GO TO 102
    IF (I.NE.LP-1) GO TO 77
    DO 37 K1=1,N
    DO 37 K2=1,NMIN1

```

```

37  AP(K1,JPS)=AP(K1,JPS)-CP(K1,K2)*LP(K1,1)
77  CONTINUE
    CALL YMY(N,PR,BF,AP,NPLUS1,MAXN,MAXN,MAXN,T1)
    CALL XWRITE(21,PR,N,NPLUS1,MAXN,MAXN,I,MAX2,V1)
    IF(LP.EQ.0.OR.I.LT.LP)GO TO 102
    IF(I.GE.LP+2)GO TO 360
    IF(I.EQ.LP+1)GO TO 290
    DO 6 K1=1,NPLUS1
6    VB1(1,K1)=PR(JPS,K1)
    GO TO 102
290  CALL YMYN(VB2,VB1,PR,N,NPLUS1,MAXN,MAXN,MAXN,MAXN,T1)
    KNS=NPLUS1
    GO TO 102
300  DO 7 K1=1,KNS
7    VB1(1,K1)=VB2(1,K1)
    IF(I.EQ.NEQPOT-1)GO TO 102
    CALL YMYN(VB2,VB1,PR,N,NPLUS1,MAXN,MAXN,MAXN,MAXN,T1)
    KNS=NPLUS1
102  IF(I.EQ.1) GO TO 32
    CALL YSYMY(NMIN1,N,XP,GF,CP,XP,NRHS,MAXN,MAXN,NRHS,MAXN,T1)
    CALL YMY(N,XP,BP,XP,NRHS,MAXN,NRHS,MAXN,T1)
    IF(I.EQ.NEQPOT) GO TO 42
    IF(LP.EQ.0.OR.I.LT.LP) GO TO 90
    IF(I.GE.LP+2)GO TO 350
    IF(I.EQ.LP+1)GO TO 360
    VG1=XP(JPS,1)
    VG2=VG1
    GO TO 90
360  DO 19 K1=1,N
19  VG2=VG2-VB1(1,K1)*XP(K1,1)
    GO TO 90
350  VG1=VG2
    IF(I.EQ.NEQPOT-1) GO TO 42
    DO 21 K1=1,N
21  VG2=VG2+VB1(1,K1)*XP(K1,1)*R1
90  IF(LP.EQ.0.OR.I.GT.LP-2)GO TO 42
    CALL YSYMY(NMIN1,N,EP,DP,CF,EP,NRHS,MAXN,MAXN,NRHS,MAXN,T1)
    CALL YMY(N,EP,BP,EP,NRHS,MAXN,NRHS,MAXN,T1)
    CALL XWRITE(23,EP,N,NRHS,MAXN,NRHS,I,MAXN,T1)
    GO TO 42
32  CALL YMY(N,XP,BP,GP,NRHS,MAXN,NRHS,MAXN,T1)
    IF(LP.EQ.0)GO TO 42
    CALL YMY(N,EP,BP,DP,NRHS,MAXN,NRHS,MAXN,T1)
    CALL XWRITE(23,EP,N,NRHS,MAXN,NRHS,I,MAXN,T1)
42  CALL XWRITE(22,XP,N,NRHS,MAXN,NRHS,I,MAXN,T1)
100 CONTINUE
    NEQPOT=NEQPOT-1
    DO 200 K=1,NEQPOT
    NK=NEQPOT-K
    NMIN1=MI(NK)
    N=MI(NK+1)
    CALL XREAD(21,PR,NMIN1,N,MAXN,MAXN,NK,MAX2,V1)
    CALL XREAD(22,GP,NMIN1,NRHS,MAXN,NRHS,NK,MAXN,T1)
    CALL YSYMY(N,NMIN1,XP,GP,PR,XP,NRHS,MAXN,MAXN,NRHS,MAXN,T1)
    IF(NK.EQ.LP) GO TO 74
    VG1=XP(JPS,1)
74  IF(LP.EQ.0.OR.NK.GT.LP-2)GO TO 92
    CALL XREAD(23,EP,NMIN1,NRHS,MAXN,NRHS,NK,MAXN,T1)
    DO 27 K1=1,NMIN1
27  XP(K1,1)=XP(K1,1)-EP(K1,1)*VG1
92  CALL XWRITE(22,XP,NMIN1,NRHS,MAXN,NRHS,NK,MAXN,T1)
200 CONTINUE
    RETURN
    END

```

SUBROUTINE XREAD(ND,A,L1,L2,M1,M2,IND,M3,VV)	1234
COMMON/CDISK/I21(501),I22(501),I23(501)	1235
DIMENSION A(M1,M2),VV(M3)	1236
C RECORD IND OF DIRECT ACCESS DATA SET NO IS READ AND ALLOCATED	1237
C BY ROWS INTO L1*L2 PORTION OF MATRIX A	1238
L3=L1*L2	1239
CALL READMS(ND,VV,L3,IND)	1240
KL=0	1241
DO 10 NROW=1,L1	1242
DO 10 NCOL=1,L2	1243
KL=KL+1	1244
A(NROW,NCOL)=VV(KL)	1245
10 CONTINUE	1246
RETURN	1247
END	1248
SUBROUTINE XWRITE(ND,A,L1,L2,M1,M2,IND,M3,VV)	1249
COMMON/CDISK/I21(501),I22(501),I23(501)	1250
DIMENSION A(M1,M2),VV(M3)	1251
C L1*L2 PORTION OF MATRIX A IS WRITTEN BY ROWS ON DIRECT ACCESS	1252
C DATA SET NO IN RECORD IND	1253
KL=0	1254
DO 10 NROW=1,L1	1255
DO 10 NCOL=1,L2	1256
KL=KL+1	1257
VV(KL)=A(NROW,NCOL)	1258
10 CONTINUE	1259
CALL WRITMS(ND,VV,KL,IND,-1)	1260
RETURN	1261
END	1262
/EOR	
EXAMPLE 1 R/H=500 L/R=1. N=5	
35,1,3,3,0,1,1	
4.,4.,0.000,105.000,0.3,1.0	
0.,0.,0.,0.,0.,0.	
2,2,2,10,1.	
1.,5.,0.,15.,5.,90.,300.,60.	
1,2,2,1	
5,0,1	
1	
EXAMPLE 1 R/H=500 L/R=1. N=6	
35,1,3,3,0,1,1	
4.,4.,0.000,105.000,0.3,1.0	
0.,0.,0.,0.,0.,0.	
2,2,2,10,1.	
1.,5.,0.,15.,5.,90.,300.,60.	
1,2,2,1	
6,0,1	
1	
EXAMPLE 1 R/H=500 L/R=1. N=7	
35,1,3,3,0,1,1	
4.,4.,0.000,105.000,0.3,1.0	
0.,0.,0.,0.,0.,0.	
2,2,2,10,1.	
1.,5.,0.,15.,5.,90.,300.,60.	
1,2,2,1	
7,0,1	
0	
/EOR	

REFERENCES

1. Simitzes, G. J. and Lazopoulos, C., "Dynamic Stability of Structures; Imperfection Sensitive Systems Acted upon by Step-Loads," AFWAL-TR-81-3040 Georgia Tech, Atlanta, Georgia, 1981.
2. Hoff, N. J., and Bruce, V. G., "Dynamic Analysis of the Buckling of Laterally Loaded Flat Arches," J. Math. and Phys., Vol. 32, pp. 276-288, 1954.
3. Budiansky, B., and Roth, R. S., "Axisymmetric Dynamic Buckling of Clamped Shallow Spherical Shells," Collected papers on Instability of Shell Structures, NASA TN D-1510, 1962.
4. Budiansky, B., and Hutchinson, J. W., "Dynamic Buckling of Imperfection-Sensitive Structures," Proceedings, XI International Congress of Applied Mechanics, Munich, 1964.
5. Budiansky, B., "Dynamic Buckling of Elastic Structures: Criteria and Estimates," Dynamic Stability of Structures, (edited by G. Herrmann), Pergamon Press, New York, 1967.
6. Hsu, C. S., "On the Dynamic Stability of Elastic Bodies with Prescribed Initial Conditions," Int. J. Engng, Sci., Vol. 4, pp. 1-21, 1966.
7. Hsu, C. S., "The Effects of Various Parameters on the Dynamic Stability of a Shallow Arch," J. Appl. Mech., Vol. 34, No. 2, pp. 349-356, 1967.
8. Hsu, C. S., "Stability of Shallow Arches Against Snap-Through Under Timewise Step Loads," J. Appl. Mech., Vol. 35, No. 1, pp. 31-39, 1968.
9. Hsu, C. S., "Equilibrium Configurations of a Shallow Arch of Arbitrary Shape and Their Dynamic Stability Character," Int. J. Nonlinear Mech., Vol. 3, pp. 113-136, June 1968.
10. Hsu, C. S., Kuo, C. T., and Lee, S. S., "On the Final States of Shallow Arches on Elastic Foundations Subjected to Dynamic Loads," J. Appl. Mech., Vol. 35, No. 4, pp. 713-723, December 1968.
11. Simitzes, G. J., "Dynamic Snap-Through Buckling of Low Arches and Shallow Spherical Shells," Ph.D. Dissertation, Department of Aeronautics and Astronautics, Stanford University, June 1965.
12. Simitzes G. J., "On the Dynamic Buckling of Shallow Spherical Shells," J. Appl. Mech., Vol. 41, No. 1, pp. 299-300, March 1974.
13. Simitzes, G. J., "Axisymmetric Dynamic Snap-Through Buckling of Shallow Spherical Caps," AIAA J., Vol. 5, pp. 1019-1021, May 1967.
14. Finlayson, B., The Method of Weighted Residuals and Variational Principles, Academic Press, New York, 1972.
15. Kounadis, A. N., Giri, J., and Simitzes, G. J., "Nonlinear Stability Analysis of an Eccentrically Loaded Two-Bar Frame," J. Appl. Mech., Vol. 44, Series E, No. 4, pp. 701-706, December 1977.

16. Simitses, G. J., Kounadis, A. N., and Giri, J., "Nonlinear Buckling Analysis of Imperfection Sensitive Simple Frames," Proceedings, International Colloquium on Stability of Structures Under Static and Dynamic Loads, ASCE Publication, New York, 1977, pp. 158-179.
17. Thompson, J. M. T., "Dynamic Buckling Under Step Loading," Dynamic Stability of Structures (edited by G. Herrmann), Pergamon Press, New York, 1967.
18. Fisher, C. A., and Bert, C. W., "Dynamic Buckling of an Axially Compressed Cylindrical Shell with Discrete Rings and Stringers," J. Appl. Mech., Vol. 40, No. 3, September 1973.
19. Almroth, B. O., Meller, E., and Brogan, F. A., "Computer Solutions for Static and Dynamic Buckling of Shells," Buckling of Structures, IUTAM Symposium, Cambridge, U.S.A., 1974, Springer-Verlag, Berlin, 1976.
20. Lakshmikantham, C., and Tsui, T., "Dynamic Stability of Axially-Stiffened Imperfect Cylindrical Shells under Axial Step Loading," AIAA J., Vol. 12, No. 2, 1974.
21. Tamura, Y. S., and Babcock, C. D., "Dynamic Stability of Cylindrical Shells Under Step Loading," J. Appl. Mech., Vol. 42, No. 1, March 1975, pp. 190-194.
22. Zimcik, D. G., and Tennyson, R. C., "Stability of Circular Cylindrical Shells Under Transient Axial Impulsive Loading," Proceedings, AIAA/ASME/ASCE/AHS 20th Structures, Structural Dynamics and Materials Conference, St. Louis, Missouri, 1979, pp. 275-284.
23. Simitses, G. J., and Ungbhakorn, V., "Minimum Weight Design of Stiffened Cylinders under Axial Compression," AIAA J., Vol. 13, No. 6, 1975, pp. 750-755.
24. Narasimham, K. Y., and Hoff, N. J., "Calculation of the Load Carrying Capacity of Initially Slightly Imperfect Thin Walled Circular Cylindrical Shells of Finite Length," SUDAER No. 329, School of Aeronautics and Astronautics, Stanford University, December 1967.
25. (a) Sheinman, I., and Simitses, G. J., "Buckling Analysis of Geometrically Imperfect Stiffened Cylinders under Axial Compression," AIAA J., Vol. 15, No. 3, March 1977. See also:

(b) Simitses G. J., and Sheinman, I., "The Effect of Initial Imperfections on Optimal Stiffened Cylinders under Axial Compression," AFOSR-TR-77-0639, Georgia Institute of Technology, Atlanta, Ga. 1977.
26. Sheinman, I., and Tene, Y., "Buckling in Segmented Shells of Revolution Subjected to Symmetric and Antisymmetric Loads," AIAA J., Vol. 12, No. 1, Jan. 1974, pp. 15-20.
27. Thurston, G. A., "Newton's Method Applied to Problems in Nonlinear Mechanics," J. Appl. Mech., Vol. 32, No. 2, June 1965, pp. 383-388.
28. Thurston, G. A., and Freeland, M. A., "Buckling of Imperfect Cylinders under Axial Compression," NASA CR-541, July 1966.

29. Tene, Y., Epstein, M. and Sheinman, I., "A Generalization of Potter's Method," Computers and Structures, Vol. 4, Dec. 1974, pp. 1099-1103.
30. Arbocz, J., and Sechler, E. E., "On the Buckling of Axially Compressed Imperfect Cylindrical Shells," J. Appl. Mech., Vol. 41, No. 3, Sept. 1974, pp. 737-743.
31. Simitzes, G. J., Sheinman, I., and Giri, J., "Nonlinear Stability Analysis of Pressure-Loaded Imperfect Stiffened Cylinders," J. Ship Research, Vol. 23, No. 2, June 1979, pp. 123-126.
32. Simitzes, G. J., An Introduction to the Elastic Stability of Structures, Prentice-Hall, Inc., Englewood Cliffs, N.J., 1976.
33. Cheung, M. C., and Babcock, C. D., Jr., "An Energy Approach to the Dynamic Stability of Arches," J. Appl. Mech., Vol. 37, No. 4., pp. 1012, 1018, December 1970.
34. Lo, D. L. C., and Masur, E. F., "Dynamic Buckling of Shallow Arches," J. Engng. Mech. Division, ASCE, EM5, pp. 901-917, October 1976.
35. Lazopoulos, C., "Dynamic Stability of Structural Elements Subjected to Step-Loads," Ph.D. Thesis, School of Engineering Science and Mechanics, Georgia Institute of Technology, Atlanta, Ga. 1980.
36. Clough, R. W. and Renzien, J., Dynamics of Structures, McGraw-Hill Kogakusha Ltd., Tokyo, 1975.
37. Thomson, W. T., Vibration Theory and Applications, Prentice-Hall, Inc. Englewood Cliffs, N.J. 1965.
38. Huffington, N. J., Jr., "Response of Elastic Columns to Axial Pulse Loading," AIAA J., Vol. 1, No. 9, 1963, pp. 2099-2104.
39. Ari-Gur, J., Weller, T., and Singer, J., "Experimental Studies of Columns under Axial Impact," TAE No. 346, December 1978, Dept. of Aeronautical Engineering, Technion-Israel Institute of Technology.
40. Koning, C., and Taub, J., "Impact Buckling of Thin Bars in the Elastic Range Hinged at Both Ends," Luftfahrtforschung, Vol. 10, No. 2, 1933, p. 55 (also translated as NACA TM 748 in 1934).
41. Gerard, G., and Becker, H., "Column Behavior under Conditions of Impact," J. Aero. Sci., Vol. 19, 1952, pp. 58-60.
42. Hoff, N. J., "The Dynamics of the Buckling of Elastic Columns," J. Appl. Mech., Vol. 18, No. 1, 1951, pp. 68-74.
43. Davidson, J. F., "Buckling of Struts under Dynamic Loading," J. Mech. Phys. Solids, Vol. 2, 1953, pp. 54-66.
44. Sevin, E., "On the Elastic Bending of Columns due to Dynamic Axial Forces Including Effects of Axial Inertia," J. Appl. Mech., Vol. 27, No. 1, 1960, pp. 125-131.

45. Housner, G. W., and Iso, W. K., "Dynamic Behavior of Supercritically Loaded Struts," J. Eng. Mech. Div., ASCE, Vol. 88, No. EM5, 1962, pp. 41-65.
46. Hayashi, T., and Sano, Y., "Dynamic Buckling of Elastic Bars, First Report, The Case of Low Velocity Impact," Bulletin of the ISME, Vol. 15, No. 88, 1972, pp. 1167-1175.
47. Hayashi, T., and Sano, Y., "Dynamic Buckling of Elastic Bars, Second Report, The Case of High Velocity Impact," Bulletin of the ISME, Vol. 15, No. 88, 1972, pp. 1176-1184.
48. McIvor, I. K., and Bernard, J. E., "The Dynamic Response of Columns under Short Duration Axial Loads," J. Appl. Mech., Vol. 40, No. 3, 1973, pp. 688-692.
49. Grybos, R., "Impact Stability of a Bar," Int. J. Eng. Sci., Vol. 13, No. 5, 1975, pp. 463-478.
50. Wauer, J., "Uber Kinetische Verzweigungs Probleme Elastischer Strukturen unter Stossbelastung," Ingenieur-Archiv, Vol. 49, 1980, pp. 227-233.

DATE
ILME
—8